A quantitative analysis of growth regulation by ppGpp in E. coli

Imholz, N.C.E.

DOI
10.4233/uuid:edef269a-610d-4304-b07d-58d3438b995f

Publication date
2020

Document Version
Final published version

Citation (APA)
Imholz, N. C. E. (2020). *A quantitative analysis of growth regulation by ppGpp in E. coli*. [Dissertation (TU Delft), Delft University of Technology]. https://doi.org/10.4233/uuid:edef269a-610d-4304-b07d-58d3438b995f

Important note
To cite this publication, please use the final published version (if applicable).
Please check the document version above.

A quantitative analysis of growth regulation by ppGpp in *E. coli*

A quantitative analysis of growth regulation by ppGpp in *E. coli*

Dissertation

for the purpose of obtaining the degree of doctor
at Delft University of Technology,
by the authority of the Rector Magnificus prof.dr.ir. T.H.J.J. van der Hagen,
chair of the Board of Doctorates,
to be defended publicly on
Friday 18 december 2020 at 12:30 o'clock

by

Nicole Charlotte Emma IMHOLZ

Master of Science in Biomolecular Engineering, KU Leuven, Belgium,
born in Voorburg, The Netherlands

This dissertation has been approved by the promoters.

Composition of the doctoral committee:

Rector Magnificus	chairperson
Prof.dr. M. Dogterom	Delft University of Technology, promoter
Dr. G.E. Bokinsky	Delft University of Technology, copromoter

Independent members:

Prof.dr. P.A.S. Daran-Lapujade	Delft University of Technology
Prof.dr. F.J. Bruggeman	VU Amsterdam
Prof.dr.ir. M. De Mey	Ghent University
Dr. S.M. Depken	Delft University of Technology
Prof.dr. G.H. Koenderink	Delft University of Technology, reserve member

Keywords: ppGpp, LC-MS, growth rate, translation, SpoT, ACP

Printed by: Ipskamp Printing

Cover: Nicole Imholz

ISBN 978-94-6421-154-2

An electronic version of this dissertation is available at
http://repository.tudelft.nl/.

To Chantal, Marcel and Maurice.

Contents

Summary

This thesis is about a little molecule called guanosine tetraphosphate. ppGpp. Consider it the bacterial brain, at the core of the coordination and regulation of bacterial growth. For over half a century, it has haunted microbiologists as it appears involved in every aspect of microbial physiology, yet incredibly difficult to study due to its fast dynamics, chemical instability and pleiotropic effects. Like the human brain, it cannot simply be removed to show its true nature.

In contrast to the pronunciation of its name, ppGpp is a rather simple molecule, and built from two of the most abundant substrates in the bacterial cell (ATP and GTP). The enzymes that make or break ppGpp are highly efficient, such that at any moment, the bacteria can decide to instantly 100-fold increase ppGpp concentrations, or virtually remove all of it. Thanks to this intelligent system, *E. coli* can decide to arrest growth, protecting itself against any threats, or to rapidly feast upon the sparse nutrients it may be tossed, within the order of minutes.

What does this mysterious molecule exactly *do* in bacteria? In **chapter 1**, a thing or two is explained about the regulatory network of ppGpp as it is currently understood. We know the exact nature of *some* of the environmental cues that are input information for this network. Similarly, quite a bit has been discovered about the exact intracellular targets of ppGpp: apparently it regulates synthesis of DNA, RNA, protein (or not?) and fatty acids. Importantly, ppGpp also influences the less appreciated functions of bacteria such as virulence, antibiotic resistance and interaction with the (human) host.

Yet, very fundamental questions remain unresolved. Progress in the field is hampered by the lack of (accurate) knowledge about the intracellular concentrations of ppGpp. Therefore, a new, sensitive method to absolutely quantify ppGpp in bacteria had to be developed. This is described in **chapter 2**.

This method was put into practice in **chapter 3** to investigate one of the most baffling observations regarding ppGpp: the concentration of ppGpp in the cell is inversely proportional to *how fast* that cell is growing. This (and some further substantiation) led to the prevailing theory that ppGpp is determining the growth rate of bacteria, by regulating the transcription of RNA. One might say ppGpp functions like the brake of a car: a bit more ppGpp and the bacteria reduce their growth rate, a bit less ppGpp and bacteria grow faster. Although a plausible theory in many circumstances, we have discovered that growth rate regulation by ppGpp is more complex than previously thought. *Escherichia coli* strains with subtle genetic differences display varying ppGpp versus growth rate trends. In addition, several

exceptions to this trend hint at the involvement of additional regulators of transcription besides ppGpp. In conclusion, ppGpp might not be at the apex of all genetic regulation in *E. coli*.

Chapter 4 focuses on one of the most debated functions of ppGpp: whether it directly regulates protein synthesis or not. The interest in this debate is instigated (for some) by the fact that proteins make up most of the actual mass of cells and also are the most energy-consuming cellular compound. For *E. coli*, a tight control on protein synthesis is simply smart economics. In this chapter, we have quantified the effect of ppGpp on protein synthesis. We show that indeed ppGpp helps *E. coli* to rapidly shut down protein synthesis in stressful conditions. Interestingly, it appears that at various concentrations of ppGpp, it shuts off different targets involved in protein synthesis.

Chapters 3 and 4 shed light on the functions of ppGpp, or the molecular changes it brings about inside bacteria. This is however only one part of the ppGpp regulatory network. The other part consists of what regulates the ppGpp level *itself*. There are two enzymes, RelA and SpoT, that based on environmental cues decide how much ppGpp will be made. SpoT is the only enzyme with the capacity to both synthesize or degrade ppGpp. In addition, SpoT appears to integrate information about the presence of sugars, iron, oxygen, and several other essential nutrients. Moreover, it also perceives heat, cold and osmotic stress. How does SpoT monitor all these parameters and change ppGpp concentrations accordingly?

It is currently believed SpoT interacts with multiple proteins to gain information about the cell. In **chapter 5**, I investigate the (presumed) interaction between SpoT and especially one of those, the acyl carrier protein or ACP. The experiments presented here confirm the interaction between SpoT and ACP, yet refute the current hypothesis that ACP activates SpoT to degrade ppGpp. On the contrary, it appears ACP inhibits SpoT's capacity to break down ppGpp. Unfortunately, this is only one small piece of a complicated puzzle, as there are many possible modifications to ACP and as several other proteins interact with SpoT as well. Future studies should finish this puzzle, hopefully with help of the methods developed in this chapter.

Samenvatting

Deze thesis gaat over een klein molecule genaamd guanosine tetrafosfaat, afgekort ppGpp. Beschouw het als 'het brein' van een bacterie, verantwoordelijk voor alle coördinatie en regulatie van bacteriële groei. Al ruim een halve eeuw achtervolgt ppGpp microbiologen omdat het betrokken lijkt bij elk aspect van microbiële fysiologie. Tegelijkertijd is het een ongelooflijk moeilijk studieobject vanwege ppGpp's snelle dynamiek, chemische instabiliteit en talrijke effecten. Zoals het menselijk brein kan het niet simpelweg verwijderd worden om te begrijpen hoe het werkt.

In tegenstelling tot de uitspraak van ppGpp, is het structureel gezien een relatief eenvoudig molecule, dat wordt gemaakt van twee bouwstenen die zeer abundant aanwezig zijn in de bacteriële cel (ATP en GTP). De enzymen die ppGpp maken of afbreken zijn zeer efficiënt zodat op ieder moment de bacterie kan beslissen om ineens de ppGpp concentratie 100 keer te verhogen of compleet te verwijderen. Dankzij dit intelligente systeem kan de bacterie *E. coli* zijn groei acuut stoppen, zichzelf beschermend tegen allerlei bedreigingen, of sneller groeien dankzij een plotse weelde aan voedingsstoffen in de darm, binnen slechts enkele minuten.

Wat *doet* ppGpp nou juist in een bacterie? In **hoofdstuk 1** wordt het een en ander uitgelegd over de heden ten daagse kennis omtrent het regulatienetwerk van ppGpp. Van *sommige* omgevingssignalen begrijpen we tot in de puntjes hoe ze als input-informatie dienen voor dit netwerk. Ook weten we aardig wat over de exacte intracellulaire doelwitten van ppGpp: blijkbaar reguleert ppGpp de synthese van DNA, RNA, eiwitten (of niet?) en vetzuren. Niet onbelangrijk, ppGpp heeft ook invloed op minder gewaardeerde eigenschappen van bacteriën, waaronder virulentie, antibioticaresistentie en interactie met de (menselijke) gastheer.

Toch zijn de meest fundamentele vragen nog onbeantwoord. De voortgang in het onderzoeksveld wordt belemmerd door een gebrek aan (accurate) kennis van de intracellulaire concentraties van ppGpp. Om deze reden was er nood aan een nieuwe, gevoelige methode om ppGpp absoluut te kwantificeren. Dit wordt beschreven in **hoofdstuk 2**.

In **hoofdstuk 3** wordt deze methode toegepast in een studie van een van de meest verbijsterende observaties omtrent ppGpp: de ppGpp concentratie in de cel is omgekeerd evenredig met *hoe snel* de cel groeit. Deze observatie (en bijkomend bewijs) heeft geleid tot de gangbare theorie dat ppGpp de groeisnelheid van bacteriën bepaalt, meer bepaald door de regulatie van RNA-transcriptie. ppGpp is als het ware de rem van een auto: wat meer ppGpp en de bacterie groeit trager, wat minder ppGpp en de bacterie groeit sneller. Hoewel deze theorie plausibel is

in veel groeiomstandigheden, hebben we ontdekt dat de regulatie van groeisnelheid door ppGpp meer complex is dan oorspronkelijk gedacht. *E. coli* stammen met subtiele genetische verschillen vertonen blijkbaar niet dezelfde trend in ppGpp versus groeisnelheid. Bovendien bestaan er meerdere uitzonderingen op de oorspronkelijke observatie die erop wijzen dat naast ppGpp er nog andere regulators van transcriptie moeten zijn. ppGpp staat vermoedelijk niet als enige aan de top van alle genregulatie in *E. coli*.

Hoofdstuk 4 richt zich op een van de meest controversiële functies van ppGpp: of het een direct effect heeft op eiwitsynthese of niet. De interesse in dit debat (voor sommigen) is gebaseerd op het feit dat eiwitten het grootste deel van de massa van een cel uitmaken en ook de meest energie vergende cellulaire component zijn. Een nauwgezette controle over eiwitsynthese is daarom economischer voor *E. coli*. In dit hoofdstuk hebben we het effect van ppGpp op eiwitsynthese gekwantificeerd. We tonen aan dat ppGpp wel degelijk eiwitsynthese een direct halt toeroept onder stress condities. Het blijkt echter dat afhankelijk van de ppGpp concentraties, verschillende doelwitten hierbij betrokken zijn.

Hoofdstukken 3 en 4 brengen nieuwe functies van ppGpp aan het licht, oftewel de moleculaire gevolgen van ppGpp binnen in de bacterie. Dit is slechts een deel van het regulatienetwerk van ppGpp. Het andere deel bestaat uit wat invloed heeft op ppGpp *zelf*. Er zijn twee enzymen, RelA en SpoT, die op basis van omgevingssignalen bepalen hoeveel ppGpp er aanwezig is in de cel. SpoT is het enige enzym dat zowel ppGpp kan aanmaken als afbreken. Bovendien integreert SpoT informatie over de aanwezigheid van suikers, ijzer, zuurstof en meerdere andere essentiële nutriënten. Ook neemt het hitte, koude en osmotische stress waar. Hoe kan SpoT al deze parameters monitoren en op basis van deze informatie de ppGpp concentratie aanpassen?

Momenteel gelooft men dat door interacties met andere eiwitten SpoT informatie inwint over de cel. In **hoofdstuk 5** onderzoek ik de (veronderstelde) interactie tussen SpoT en met name het eiwit Acyl Carrier Protein of ACP. De experimenten in dit hoofdstuk bevestigen de interactie tussen SpoT en ACP, maar weerleggen de huidige hypothese dat ACP de afbraak van ppGpp door SpoT activeert. Het blijkt daarentegen dat ACP voorkomt dat SpoT ppGpp afbreekt. Helaas is dit slechts een stukje van een gecompliceerde puzzel, aangezien er allerlei modificaties aan ACP bestaan die de interactie beïnvloeden en er ook andere eiwitten zijn die interageren met SpoT. Verdere studies zullen deze puzzel afmaken, hopelijk met hulp van de nieuwe methoden ontwikkeld in dit hoofdstuk.

1

Introduction

1.1. Bacterial metabolism is vast and well-coordinated

Bacteria represent about 15 % of all biomass on earth [1]. Together, they possess the most diverse metabolic pathways and are capable of building cells from virtually scratch [2]. They have the capability to grow on heavy metals, on light, under high (osmotic) pressure and in extreme temperatures [3]. Although in plants and animals the different metabolic functions are performed in specific organs, cells or cellular organelles, bacteria are basically little bags containing their whole metabolism as one big soup. How do bacteria perform an incomprehensible amount of reactions in a controlled manner, allowing them to multiply in virtually every habitat on earth?

Simply put, a (bacterial) cell consists of four compounds: DNA, RNA, protein and lipid. These compounds have to be synthesized in a coordinated way for the cell to grow. Hereto the cell has a machinery of enzymes that use the resources in the environment and perform reactions to assemble them into the four major compounds. For example, the cell builds proteins out of amino acids. There are 20 types of amino acids, each of which having a specific synthesis pathway involving several enzymes. The synthesis of each amino acid has to be balanced with the demand of protein synthesis. Summing up all the reactions to assemble the four major compounds creates a complex metabolic network of over 1000 reactions. How does the cell balance the rate of protein, lipid, RNA and DNA synthesis with each other and also with their precursors such as amino acids?

The cell is constrained by environmental conditions: most of the time there is no luxury in making more of a compound than is strictly necessary to grow. In addition, other (micro)organisms want to use the same resources, and the competition pushes bacteria to use their resources as efficiently as possible. Hence, the metabolic network needs to be well coordinated, which is done by 'signaling molecules'. These molecules have a communicative role and make sure that the right metabolic pathways are activated or repressed, depending on the environmental conditions.

1.2. The omnipresence of (p)ppGpp as a regulator of metabolism and growth

In the 1950's, microbiologists discovered that when bacteria are starved for amino acids, their RNA production arrests [4]. This was called the stringent response. Soon after, mutant strains were created that lacked this response of ceased RNA production, therefore called 'relaxed' mutants. The region of the chromosome responsible for the stringent or relaxed phenotype was named 'RC' (for RNA control) and the two alleles RC^{str} and RC^{rel} respectively [5], which later conformed to *relA+* and *relA-* [6]. In 1969, Mike Cashel and Jonathan Gallant discovered the actual products of the RC enzyme responsible for the inhibition of RNA synthesis and called them 'Magic Spot I' and 'Magic Spot II', after two unknown spots on TLC chromatograms of *E. coli* lysate [7]. These molecules were identified to be

guanosine tetraphosphate (ppGpp) and guanosine pentaphosphate (pppGpp) respectively, collectively called (p)ppGpp [8, 9] (**Figure 1.1**). Now over 50 years later, it is known (p)ppGpp affects nearly every aspect of bacterial physiology (section 1.4) and it is considered the major controller of bacterial growth rate [10].

In the 70's it became clear that the RC locus or RelA was not alone in synthesizing (p)ppGpp in *E. coli* and that a second system must be present for ppGpp synthesis, called PSII [12, 13]. Around the same time the major ppGpp hydrolase was discovered, SpoT [14, 15]. However, it took until 1991 to unveil SpoT is in fact a bifunctional enzyme, being also the mysterious effector of PSII activity [16, 17]. Knocking-out both SpoT and RelA showed that these enzymes together carry out all ppGpp synthesis in *E. coli* [16].

In many other organisms enzymes capable of synthesizing or degrading (p)ppGpp have been encountered. All these belong to the group of RelA/SpoT Homologue or RSH proteins, named after the two *E. coli* enzymes [18]. Rel, the ancestor of both SpoT and RelA, is present in nearly all major bacterial groups. Interestingly, many of the bacteria without any RSH are endosymbionts and pathogens.

Genomic and phylogenetic analysis has shown RSH genes are present across the tree of life, including in plants, fungi and animals [18]. The functions of (p)ppGpp in plants and algae are analogous to those of bacteria, managing the response to stress or damage (reviewed by [19]). In phototrophic cyanobacteria (p)ppGpp regulates the transition from light to dark, similar to the stringent response of heterotrophic bacteria [20]. In the algae *Synechococcus elongatus* it was demonstrated that as in *E. coli* basal ppGpp is vital for growth of the cell even in the absence of stress [21] (chapter sec: basalppGppchapter for more information about basal ppGpp in *E. coli*). Recently also in diatoms active RSH enzymes have been discovered [22]. In archaea, annotated RSH genes have not been investigated, but enzyme regulation by (p)ppGpp occurs *in vitro* [23]. Finally, deletion of the ppGpp hydrolase MeshI from *Drosophila melanogaster* impairs development and resistance to starvation [24]. This however does not demonstrate a role for (p)ppGpp in *D. melanogaster* as the exact catalytic function of MeshI *in vivo* is not known yet.

In most organisms the physiological roles of (p)ppGpp are not well studied, with exception of several bacterial species such as the model prokaryote *E. coli*. About (p)ppGpp regulation in *E. coli* currently most literature is available, with over 1700 hits when searching for ppGpp + *E. coli* in Web of Science!

1.3. RelA and SpoT: *E. coli* enzymes that make or break ppGpp

1.3.1. RelA and SpoT share a common ancestor and structure

RelA was the first enzyme discovered to be involved in synthesis of (p)ppGpp, even before (p)ppGpp itself was discovered [5]. Later, SpoT was identified as a bifunc-

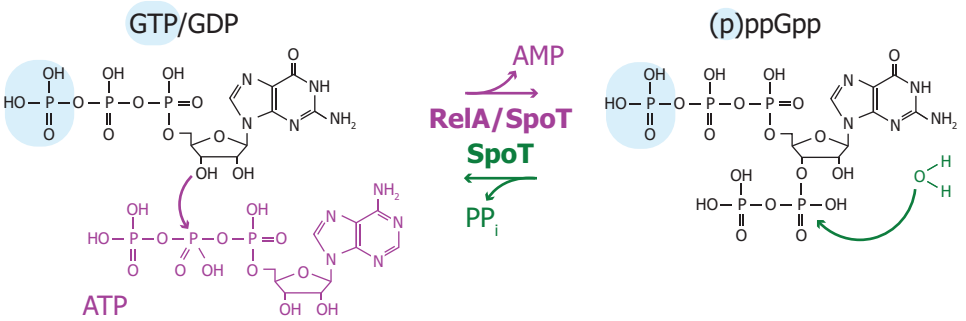

Figure 1.1: Synthesis and degradation of guanosine tetraphosphate and guanosine pentaphosphate by RelA and SpoT. Synthesis reaction of pppGpp (or ppGpp) from ATP and GTP (or GDP) is in purple. Degradation of pppGpp (or ppGpp) to GTP (or GDP) is colored green. The γ-phosphate moieties are highlighted in blue. These are only present in GTP and pppGpp, not in GDP and ppGpp. PP_i, pyrophosphate. Adapted from [11].

tional enzyme able to both synthesize and degrade (p)ppGpp in *E. coli* [25, 26]. RelA and SpoT are present in γ and β-proteobacteria and are believed to have arisen from the duplication of a common ancestral Rel enzyme present in many bacteria [27]. The RSH proteins RelA, SpoT and Rel belong to what are called 'long RSH' proteins [18]. The N-terminal half of these proteins contains both a sometimes-inactive hydrolysis domain and a synthesis domain (**Figure 1.2A**). The hydrolysis domain is responsible for the degradation of (p)ppGpp to GTP or GDP and PP_i and the synthesis domain for the transfer of pyrophosphate from ATP to GTP or GDP. The C-terminal half of long RSH proteins consists out of a TGS, alpha-helical, CC and ACT domain [18]. TGS stands for threonyl-tRNA synthetase, GTPase and SpoT, representing the three protein groups in which the domain was discovered [28]. The alpha-helical domain is entirely composed out of alpha-helices and the CC domain contains three conserved cysteines [18]. The ACT domain is named after aspartokinase, chorismate mutase and prephenate dehydrogenase (TyrA), although it is found in many other enzymes regulated by amino acids [29]. Although the structure and function of these C-terminal domains have been determined for RelA [30, 31], this is still unknown in other RSH proteins, including SpoT [18]. TGS is presumed to be (nucleotide) ligand binding [28] and ACT to be amino acid binding, based on homology to enzymes allosterically inhibited by amino acids [29]. Indeed, the ACT domain of Rel of *Rhodobacter capsulatus* and other α-protobacteria binds to valine and isoleucine, whereas Rel of some Gram-positive species binds leucine [32].

Structural studies of Rel from *Mycobacterium tuberculosis*, *Mycobacterium smegmatis* and *Streptococcus dysgalactiae* subsp. *equisimilis* have shown the N-terminal half (NTH) with the hydrolysis and synthesis domains is regulated by the C-terminal half (CTH) [33, 34]. The NTH of Rel exists as two conformations: hydrolase ON/ synthetase OFF or hydrolase OFF/ synthetase ON. The two catalytic domains are coupled such that when one changes in conformation this is communicated to the

other domain. ppGpp binding in the hydrolysis site initiates a signaling cascade all the way to and inactivating the synthesis domain [34, 35]. In addition, deacylated tRNA binding to the CTH induces a more compact conformation of Rel, whereas free Rel is more open. pppGpp binding to the CTH causes a more unstructured conformation and reduces synthesis [34]. It is believed the binding of pppGpp to the CTH creates a negative feedback arresting ppGpp synthesis to maintain a specific level of ppGpp [36].

Most structural studies of RSH proteins have been performed on Rel enzymes from other bacteria than *E. coli*, which due to their homology also provide insight about RelA and SpoT. However, in these other bacteria Rel is the single long RSH enzyme, whereas *E. coli* possesses two. Bacteria with a single RSH instead of two use different signals to regulate the catalytic activities of Rel [18]. Therefore, it is possible that SpoT and RelA have evolved to use different intramolecular signals compared to Rel to integrate information about the environment.

1.3.2. RelA mechanism of action

In vitro RelA can synthesize both pppGpp and ppGpp from GTP and GDP respectively via a pyrophosphatase of ATP to 3' of GTP and GDP [9, 37]. The affinity for GTP is higher and the intracellular concentration of GTP is much higher than GDP, hence pppGpp synthesis is probably the most important pathway [37]. pppGpp 5'-phosphohydrolase rapidly degrades pppGpp to ppGpp *in vivo* [38]. ppGpp is about 10-fold more potent as an inhibitor than pppGpp, indicating it is the main regulator of the two [39].

What activates or inhibits the hydrolysis activity of RelA *in vivo*? Early on it was clear that RelA is ribosome associated [9], which was corroborated by the finding that specific ribosomal mutations abolished the activation of RelA [40]. Eventually deacylated tRNA (tRNA not carrying an amino acid) in the ribosomal acceptor-site was identified as the trigger for (p)ppGpp synthesis by RelA [41]. Deacylated tRNA is a good universal signal for an inability of metabolism to supply amino acids as there is no need for 20 separate signals for the 20 amino acids. This illustrates how simple signals can report the status of a complex metabolic network.

Studies of the RelA-ribosome diffusive behaviour to determine whether RelA is active while attached to the ribosome and/or not were contradictive [42, 43]. Yet recently a cryo-EM study determined the structure of RelA while attached to the ribosome and its mechanism of activation [30] (**Figure 1.2B** and **C**). A penultimate C-terminal domain interacts with the 70S ribosome (hence coined RIS or ribosome-intersubunit domain), which adopts a CCHC-type zinc-finger fold therefore also called zinc-finger domain (ZFD) [44]. The ACT domain contains an RNA recognition motif (RRM) which binds to the rRNA. Together the RIS/ZFD and ACT/RRM domains anchor RelA to the ribosome. The deacylated tRNA interacts with the TGS domain [45]. The alpha-helical and TGS domains form a sort of flexible hinge between the anchoring C-terminus and the N-terminal domains. These domains only become stable and

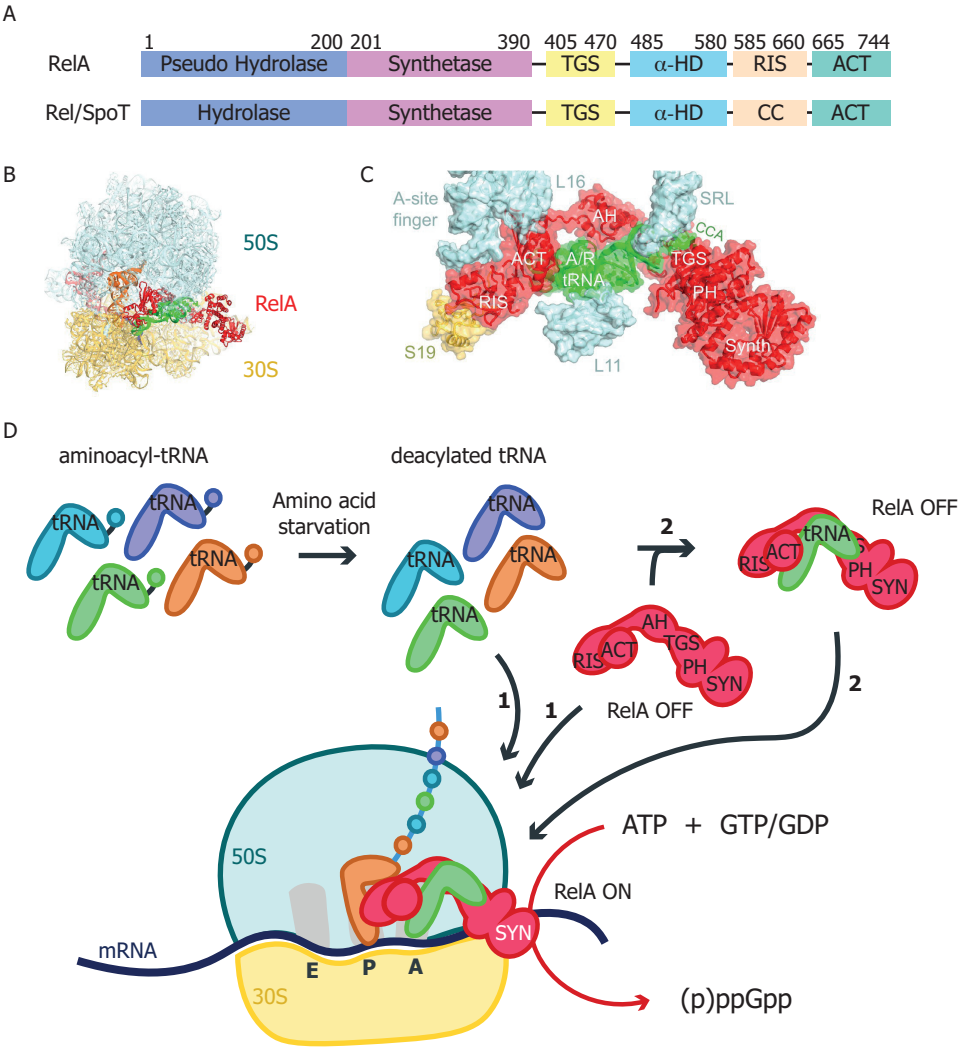

Figure 1.2: Structure of long-RSH proteins and regulation of RelA activity in *E. coli*. A) Domain overview of Rel, RelA and SpoT. See main text for explanation. B) The cryo-EM structure of RelA and deacylated tRNA attached to the ribosome. Picture taken from [30]. C) Cryo-EM structure showing the interaction between the various domains of RelA, the ribosome and deacylated tRNA. RIS: ribosome-intersubunit domain, AH: alpha-helical domain, PH: pseudohydrolase, Synth: synthetase. Picture taken from [30]. D) Model for the activation of (p)ppGpp synthesis by RelA. So far two routes for RelA binding to the ribosome have been reported. The first holds that RelA and deacylated tRNA both individually bind the ribosome (indicated by arrows numbered '1'). The second holds that RelA forms a complex with deacylated tRNA, which then binds the ribosome (indicated by arrows numbered '2').

the synthetase activated when cognate deacylated tRNA has bound. Thus, RelA can bind the ribosome while it has an empty A-site but is only active while bound to a ribosome carrying a cognate deacylated tRNA in its A-site [30] (**Figure 1.2D**, route 1). Using an *in vivo* crosslinking approach it was demonstrated that RelA can bind with deacylated tRNA as a prior formed complex before binding to the ribosome [45]. Due to steric clashing with elongation factors, it seems unlikely that the RelA-deacyl-tRNA complex binds during active translation. Combined with the high abundance of ternary complexes and their higher affinity for the ribosome, RelA-deacyl-tRNA would probably only bind during amino acid starvation, when the ribosome is stalled. This would activate (p)ppGpp synthesis as long as it remains stably bound to the ribosome (**Figure 1.2D**, route 2). The potential existence of a RelA-deacyl-tRNA complex however does not mean that deacyl-tRNA can only bind the ribosome as a complex with RelA, nor that this is the major route for RelA binding to the ribosome.

As for Rel [33, 46], several studies observed RelA can form dimers via disulphide bridges between C-termini [47, 48]. However, recently it was shown RelA does not activate or inhibit itself, indicating it does not form dimers and if so it is not relevant for its regulation [49].

1.3.3. SpoT mechanism of action

As RelA, SpoT was discovered in the ribosomal fraction of cellular extracts. *In vitro* analyses of SpoT catalytic activity have used these to characterize SpoT [14, 15, 50–52], with exception of Mechold *et al.* [53], who were the first and only to completely purify SpoT. Together these studies have shown that SpoT is responsible for ppGpp (pppGpp) hydrolysis to GDP (GTP) and PP_i in *E. coli*, without a strong preference for ppGpp or pppGpp [53]. PP_i inhibits the decay of ppGpp [52]. Just as RelA, SpoT also catalyzes pppGpp synthesis from ATP and GTP, yet no synthesis has been observed *in vitro* [53].

Although for RelA it is well known which exact intracellular events regulate its catalytic activity, for SpoT this is mostly still a mystery (**Figure 1.3**). SpoT is ribosome-associated but is not dependent on ribosomes for hydrolysis activity [15]. As Rel and RelA, SpoT has been reported to be sensitive to deacylated tRNA (*in vitro*), yet only its 3'-pyrophosphohydrolase activity is inhibited [54]. It is unknown what the effect is on (p)ppGpp synthesis. Furthermore, in contrast with some species Rel, *E. coli* SpoT is not responsive to valine, isoleucine or leucine [32].

Numerous studies have sought for proteins interacting with SpoT which lead to the discovery of many potential interactions. Here an overview will be provided of the reported interactions. These and the proposed models for SpoT regulation will be discussed further in chapter 5.

One study used mass spectrometry to analyze all proteins pulled down with SpoT [55], which included large and small ribosomal subunits, RNA helicases (*deaD*, *csdA*,

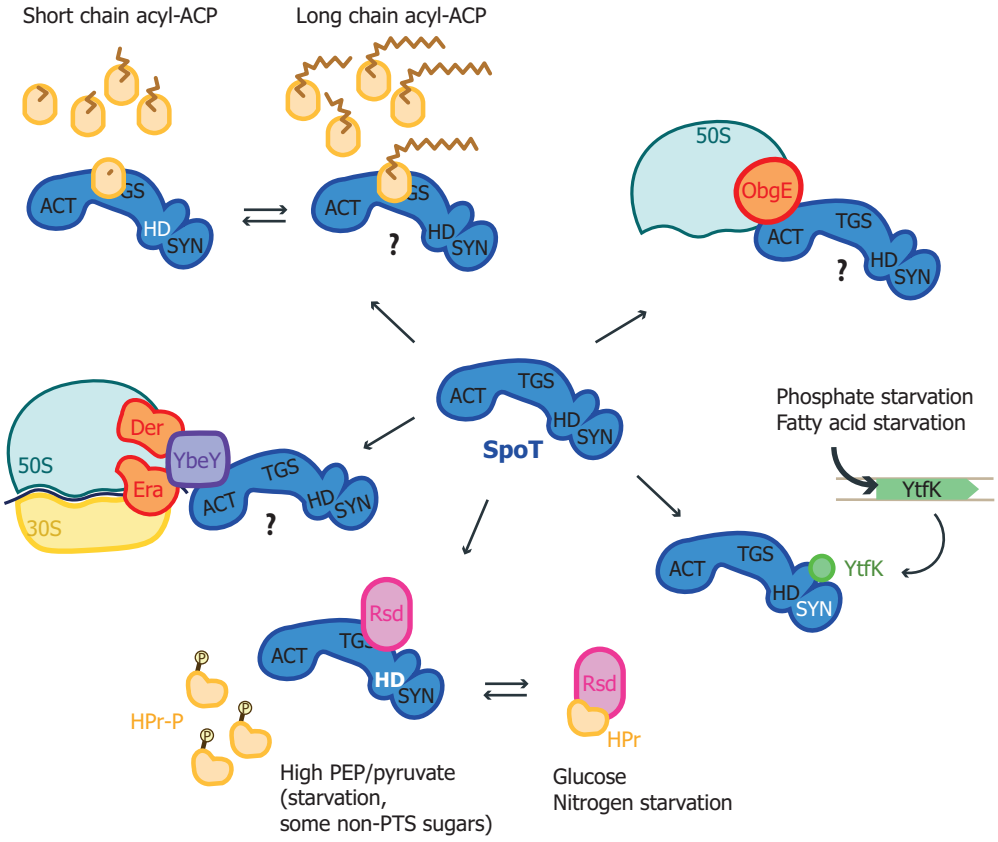

Figure 1.3: Regulation of SpoT activity in *E. coli*. If a catalytic domain is activated by an interaction it is shown in white letters. Question marks indicate for which interactions it is unknown what catalytic activity of SpoT they promote or inhibit.

srmB), DNA binding proteins such as *hupA* and *mukB*, inner membrane protein TolR which accumulates at constriction sites of dividing cells, 23S rRNA modification enzymes *yciL*, *yceC* and *yfgB*, putative transcription factor *yihL*, RNA pyrophosphohydrolase *rppH* involved in mRNA degradation, translation elongation factor EF-Tu (*tufA*), NAD kinase *yfjB*, SpoU involved in methylation of rRNA and acyl carrier protein (ACP). Consistent with SpoT residing in the ribosomal fraction, many of these are part of the ribosome assembly or translation machinery. The only protein of this list that has been reported in other studies is **ACP**, a 9 kDa protein that functions as cofactor in fatty acid, lipid A and lipoic aid synthesis [56]. It therefore can carry various acyl-groups with various chemical properties. Several studies have demonstrated the interaction [57, 58], which occurs via the TGS domain of SpoT [58, 59]. The current model proposes that SpoT binds ACP by default, which maintains SpoT in a basal hydrolysis state. During carbon or fatty acid starvation, the abundance of specific acyl-ACPs would change, which would cause a transition from hydrolysis to synthesis state in SpoT [58].

Another protein that has been reported to interact with SpoT in several bacterial species is **ObgE or CgtA** [60, 61]. ObgE is a mysterious GTP hydrolase, which supposedly plays a role in DNA replication [62–64], ribosome maturation [65], stress response and ppGpp signaling [66]. Both ObgE and SpoT bind 30S and 50S ribosomes, although ObgE has a higher affinity for 50S. However, the ribosomal binding patterns of ObgE and SpoT do not completely overlap during starvation or stationary phase, indicating ObgE and SpoT do not interact in all conditions [61, 67].

The last few years three new binding partners have been discovered and more thoroughly studied. A first is **YbeY**, a conserved endoribonuclease [68]. YbeY presumably interacts with the 30S ribosomal subunit to process 16S rRNA. It also binds proteins involved in ribosome maturation and stress regulation, including ribosomal protein S11, Era, Der and *ybeZ*. Interestingly, Rel from *S. aureus* is believed to form a complex with Era, YbeY and YbeZ, which is hypothesized to assure the maturation of 16S rRNA [69]. Further studies will need to elucidate whether this complex involving SpoT really occurs *in vivo* and how it affects the activity of SpoT.

Second, the anti-sigma^{70} factor **Rsd** can bind SpoT and the TGS domain is necessary for the interaction [70]. Interaction between Rsd and SpoT leads to an increased hydrolysis activity of SpoT. Rsd also binds to HPr, a protein of the phosphoenolpyruvate:sugar phosphotransferase system (PTS) that phosphorylates and imports carbohydrates into the cell. When Rsd is bound to HPr, Rsd can no longer stimulate SpoT. HPr can however be phosphorylated, which impedes its binding to Rsd and thus promotes Rsd-SpoT interaction [70]. The phosphorylation state of HPr is influenced by three factors [71]. First, the phosphoenolpyruvate (PEP)/pyruvate ratio, which depends on the metabolic state of the cell. Under starvation, the PEP/pyruvate ratio is high, so PTS proteins are phosphorylated. Growth on non-PTS sugars can lower the PEP-pyruvate ratio and thus also the phosphorylation state. Second, when PTS sugars (glucose) are abundant in the environment, the PTS proteins are general unphosphorylated. Third, α-ketoglutarate inhibits PTS

protein phosphorylation. During nitrogen limitation, α-ketoglutarate increases in concentration which inhibits carbohydrate uptake. In short, during steady state growth in glucose or unlimited growth, HPr binds Rsd and ppGpp hydrolysis by SpoT is not stimulated. When glucose becomes limiting, phosphorylated HPr sets free Rsd to stimulate hydrolysis in SpoT. This would function to suppress an overdose of ppGpp synthesis by RelA [70]. This regulatory mechanism promotes ppGpp hydrolysis during a carbon source downshift, presumably to resume growth after the growth arrest installed by elevated ppGpp levels [70].

A last protein discovered to bind SpoT is **YtfK**, an 8 kDa, not well characterized protein present in specific orders of γ-proteobacteria [72]. During phosphate and fatty acid limitation, YtfK interacts with the N-terminus of SpoT, flipping the switch to hydrolase OFF/ synthetase ON. Overexpression of YtfK causes an increased ppGpp level, indicating that the absolute YtfK levels matter.

Further evidence about the external or internal clues that affect SpoT activity is indirect and based on comparison of a wild-type strain with a RelA knock-out. An interesting study was performed by Roghanian *et al.* [73], who show that suppression of specific genes in *E. coli* is sensed by SpoT. These include LpxA, which catalyzes the first reaction of lipid A synthesis, part of LPS, and LptA, which transports LPS monomers to the outer membrane. How SpoT senses these internal imbalances is not clear.

1.3.4. Other enzymes potentially affecting (p)ppGpp levels

There also exist short RSHs which contain only one of the hydrolysis or synthesis domains, such as MeshI [18]. These have not been discovered in *E. coli*, with exception of one study. Zhang *et al.* [74] brought to light 4 novel (p)ppGpp hydrolyzing proteins: MutT, NudG, TrmE, NadR. Probably MutT and NudG have cleavage activities *in vivo*, yet could only reduce the stringent response or complement SpoT deletion when overexpressed. This indicates their ppGpp degradation might not be physiologically relevant at their normal expression levels. Finally, although it is not clear how, ObgE affects the pppGpp/ppGpp ratio in the cell and could therefore be involved in conversion of pppGpp to ppGpp [66].

1.4. The widespread effects of (p)ppGpp on bacterial metabolism

The extensive regulation of SpoT and RelA activities are understandable given the widespread effects (p)ppGpp exerts on bacterial metabolism. Before diving into the physiological roles appointed to (p)ppGpp, it must be noted that (p)ppGpp can exist at a spectrum of intracellular concentrations ranging from the low µM regime to a few mM (see Supplementary note 1). The upper end of the concentration range is called 'stringent', which is observed in conditions of starvation or stress,

such as the stringent response (**Figure 1.4**). Most of the effects of (p)ppGpp have been observed at stringent levels and serve to cope with the stress applied. The role of (p)ppGpp at lower or 'basal' concentrations, which occur during steady-state growth, is less clear. In this paragraph, all reported possible interactions of (p)ppGpp with intracellular targets are discussed. At which concentration of (p)ppGpp they take place (if at all) is often not known. What the role is of basal ppGpp is one of the key questions of this thesis and will be expanded upon in chapter 3.

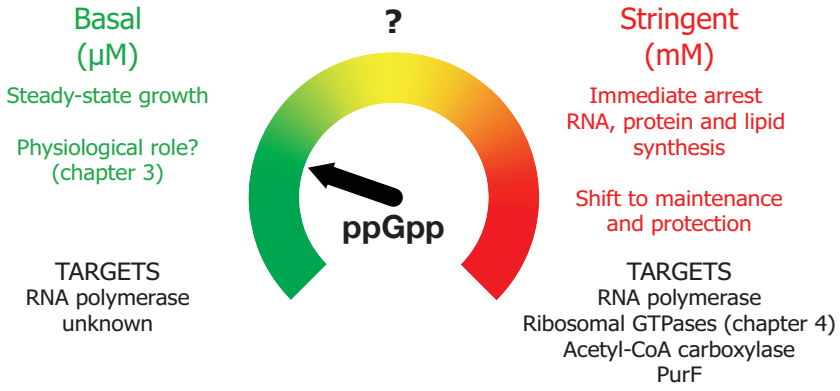

Figure 1.4: (p)ppGpp effects on cellular physiology are concentration dependent, with 'basal' and 'stringent' regimes as its extremes. The stringent targets mentioned are not exhaustive (see section 1.4.2).

1.4.1. Transcriptional regulation by (p)ppGpp

One major target regulated by (p)ppGpp - and historically the most known and studied - is RNA polymerase. Combined with the so far elusive regulation of sigma factors, nearly all promoters in the cell are affected by (p)ppGpp [75].

The interaction between ppGpp, DksA and RNA polymerase

In *E. coli* ppGpp implements a spectrum of changes in the cell by binding RNA polymerase (RNAP) on two sites [76]. Only mutations in both sites abolish any effect of ppGpp on transcription initiation *in vitro* [76]. Site 1 is at the interface of β and ω peptides. A single-molecule analysis of holo-RNAP (with σ^{70}) by Duchi *et al.* [77] reported that by binding to site 1, ppGpp decreases the RNAP clamp opening rates and promotes the partly closed state. Clamp opening is necessary for the melting of the promoter region and hence for the formation of the RNAP open complex. Therefore, this study provides a first mechanism by which ppGpp can inhibit RNAP open complex formation on certain promoters.

Site 2 is created by the regulatory protein DksA and RNAP [76]. ppGpp binding initiates a conformational change in DksA which promotes its activity, indicating ppGpp can be considered an allosteric regulator of DksA on RNAP [78]. In contrast with Duchi *et al.* [77], site 2 is believed to be the site responsible for the inhibition of ribosomal promoters during the stringent response. In a DksA knock-out mutant the stringent response does not occur, indicating DksA is necessary to potentiate ppGpp's inhibition of promoters during the stringent response [79]. Mechanistically, DksA reduces the half-life of the open complex of RNAP on DNA to the range where ppGpp can affect transcription initiation [79].

Other transcription factors such as GreA, GreB, TraR and Rnk are also involved as they can compete with or complement DksA for RNAP binding, depending on the growth conditions [78, 80, 81]. What the physiological role is of these interactions is not clear yet.

(p)ppGpp affects sigma factor competition

To initiate transcription, RNAP needs to interact with a sigma factor that guides RNAP to specific promoters. Osterberg, del Peso-Santos, and Shingler [82] have reviewed the different sigma factors and their regulation. There are 7 sigma factors in *E. coli*. The housekeeping sigma factor σ^{70} interacts with the majority of promoters. Examples of other sigma factors are σ^{S} (RpoS) and σ^{E}, which are involved during stress response and extracytoplasmatic signals respectively. Different sigma factors compete for binding RNAP and transcription initiation of different gene sets. Not only by direct binding to RNAP and DksA, but also by affecting sigma factor amount and activity, ppGpp is believed to regulate transcription initiation. ppGpp affects somehow which sigma factor interacts with RNAP, promoting the alternative sigma factors over σ^{70} [82].

There are two theories on the mechanism of sigma factor regulation by ppGpp. In summary, one proposes that the interaction between ppGpp and RNAP (+DksA) influences also the activity of the bound sigma factor, and that this regulation is sigma factor specific. Gopalkrishnan, Nicoloff, and Ades [83] showed that depending on the condition (amino acid or phosphate starvation, entry into stationary phase), ppGpp and DksA are not always both required to affect RNAP-σ^{E}. However, DksA and ppGpp are both required to increase σ^{S} activity. Probably together with other transcription factors and anti-sigma factors, ppGpp regulates the different sigma factors in distinct ways depending on the external conditions. Structural studies of sigma factors also support this theory [78], as it is specifically the structure of σ^{70} that enables the destabilization of RNAP on rRNA promoters by ppGpp and DksA [84]. Mutations in σ^{70} can change the stability of the open complex.

The other theory proposes that the upregulation of alternative sigma factors in conditions with elevated ppGpp is a consequence of the inhibition of rRNA synthesis. As ppGpp inhibits transcription from *rrn* promoters, it sets free RNAP available for alternative sigma factors. Hence, the second theory assumes one passive role

for ppGpp in sigma factor selection. This is supported by studies that showed that overexpression [85] or underexpression [86] of σ^{70} leads to a respectively increased or decreased expression of the protein synthesizing system, as well as mathematical modeling [87].

Likely a combination of the two describes the actual scenario in *E. coli*. According to Girard *et al.* [88], DksA and ppGpp promote the amount and activity of σ^{S} in three ways : 1) by directly promoting transcription of σ^{S} (by promoting transcription of the small regulatory RNA DsrA), 2) by improving transcription of anti-adaptor protein IraP, which prevents degradation of σ^{S} and 3) indirectly by reducing transcription from rRNA promoters with σ^{70}, setting free more RNAP for other sigma factors.

DNA repair

Errors in the DNA can be detected and repaired during transcription coupled DNA repair [89]. Pausing of RNA polymerase signals to specialized transcription-repair coupling factors the presence of DNA lesions. Therefore, the transcription elongation rate of RNA polymerase affects the ability of these factors to repair the DNA. Besides deciding which genes are transcribed, ppGpp binding to RNAP could also affect the transcriptional *elongation* rate [90, 91] and play an important role in DNA damage repair [92], which is reviewed in [93].

Physiological role of transcriptional regulation by (p)ppGpp

The best-known consequence of transcriptional regulation by (p)ppGpp is the arrest of stable RNA synthesis during the stringent response [7, 94]. Specifically, transcription of all **ribosomal RNA and proteins** is inhibited by ppGpp [95], although ribosomal proteins are not transcriptionally regulated by ppGpp in stationary phase [96]. However, also at basal levels ppGpp appears to limit RNA polymerase, as there is an inverse correlation between ppGpp concentration and ribosomal RNA levels during steady-state growth [12]. By determining the amount of ribosomes the cell synthesizes, ppGpp determines the amount of translation the cell can perform, and hence has a vast influence on the potential growth rate of the cell (more in chapter 3).

Over the last 20 years, it has become clear that the physiological effects of ppGpp are beyond ribosomes. (p)ppGpp dramatically alters the whole transcriptome [75, 97–99]. Already 5 min after RelA induction, 757 genes have a different transcription profile due to the binding of ppGpp to RNAP Sanchez-Vazquez *et al.* [75]. Two studies performed transcriptomics analysis of *E. coli* starved for an amino acid (Traxler *et al.* [98]) or overexpressing RelA (Sanchez-Vazquez *et al.* [75]), both leading to a dramatic increase in ppGpp concentration. The reported changes in transcriptome induced by ppGpp are however similar:

- **Amino acid biosynthesis** genes are induced [98], already by the presence of basal ppGpp [75]. Also when all amino acids are present in the media, ppGpp does not induce all amino acid biosynthesis pathways to the same degree, and not all genes within a pathway [75].
- Genes involved in **nucleotide biosynthesis and salvage** pathways are repressed, already at basal ppGpp levels [75], and genes involved in **nucleotide catabolism** are activated [75, 98].
- Genes involved in **fatty acid or phospholipid biosynthesis** are mainly repressed and in **fatty acid β-oxidation** activated [75, 98]. According to Wahl *et al.* [100], the transcriptional regulation of PlsB by ppGpp couples phospholipid synthesis to the growth rate.
- Many genes in **central metabolism** are induced, including in the pentose phosphate pathway, glyoxylate shunt and TCA cycle [75, 98]. In [98] three glycolysis genes were also induced, although [75] did not detect a change in glycolysis genes expression. The increased tricarboxylic acid (TCA) cycle, glycolysis, glyoxylate shunt and β-oxidation of fatty acids promotes an increased flux to pyruvate and α-ketoglutarate [98]. Finally, [75] also observed increased expression of genes involved in fermentation and aerobic respiration.

  Many genes involved in the **breakdown** of amino acids, alcohols, amines, aromatics, carbohydrates and nucleotides are activated [75]. The transcriptional changes indicate ppGpp is responsible for restructuring *E. coli* metabolism not only at specific metabolic branches (e.g. synthesis of the limiting amino acid), but recycling macromolecules and redirecting central metabolism to produce the necessary precursors [98] .
- Genes involved in **DNA replication and repair** are mainly repressed. Genes involved in **cell division** are either repressed or activated [98]
- Several genes in **LPS and plasma membrane synthesis, peptidoglycan biosynthesis** [75, 98] and **transport** proteins are repressed [75].
- Genes in **glycogen metabolism** are activated [98].
- Genes to cope with all kinds of **stress** (DNA damage, osmotic stress, oxidants, heat, pH stress) mostly increased in expression [75].
- About a third of genes involved in **translation** are inhibited (ribosomal proteins, rRNA processing, ribosome maturation, modification and assembly, initiation factors, elongation factors, termination factors, tRNA maturation enzymes) [75].

Together, these changes in gene expression allow the cell to restructure its metabolism to replenish necessary metabolites and to protect cellular compounds threatened by stressful conditions. The state of the cell switches from active growth to maintenance or dormancy. This massive adjustment of bacterial metabolism has been

observed in conditions with stringent ppGpp, while comparing a wild type to a strain that lacks ppGpp [98], lacks RelA [97] or regulation of RNAP by ppGpp [75]. What happens at ppGpp concentrations between basal and stringent is still not clear. One study by Traxler *et al.* [99] argues that different ppGpp levels activate different regulons depending on the degree of the applied starvation of stress. Intermediate ppGpp levels will activate the transcription factor Lrp to drive expression of amino acid biosynthesis enzymes. The subsequent increase in amino acids causes a decrease in ppGpp and resumption of growth. However, a high ppGpp activates the RpoS stress response. Thus, the concentration of ppGpp determines which genes are activated or repressed, as a rheostat rather than an on/off stringent response.

1.4.2. Post-translational regulation by (p)ppGpp

On top of transcriptional regulation, (p)ppGpp has been reported to be involved in the post-translational regulation of multiple metabolic pathways or enzymes. The effects of (p)ppGpp on various intracellular targets has been reviewed by Kanjee, Ogata, and Houry [101] and Hauryliuk *et al.* [11], and are represented in **Figure 1.5**. The last few years, new techniques have allowed a high-throughput identification of (p)ppGpp targets [74, 102, 103], which identified over 50 potential (p)ppGpp-protein interactions. Only detailed *in vitro* and *in vivo* analysis can however verify whether these are physiologically relevant. The difficulty of *in vivo* analyses however is to disentangle the transcriptional from the post-translational effects of (p)ppGpp.

Regulation of translation

There are many ribosome-associated GTPases, involved in the assembly of ribosomes and their translation activity. As they use hydrolysis of GTP to GDP for their catalytic functions, they are possibly bound by (p)ppGpp based on the structural similarity between GTP/GDP and (p)ppGpp. Hence, it is not surprising many of these GTPases have been reported to interact with (p)ppGpp, which is summarized below.

Ribosome assembly

The subclass of GTPases involved in the correct assembly of ribosomal proteins onto the rRNA, which guarantees the correct folding and accuracy of 30S and 50S and eventual 70S ribosomes, is called TRAFAC (translation factor association) GTPases [109]. Basically, ribosomal assembly of subunits occurs while the rRNA is transcribed which immediately serves as a guide for assembly. The TRAFAC GTPases ascertain correct folding by binding the assembling rRNA as long as it is not folded properly, thereby preventing premature binding of ribosomal proteins [109].

Recently, two studies used genome-wide nucleotide-protein interaction screens to identify potential interactions between (p)ppGpp and proteins in *E. coli* [74] and *S.*

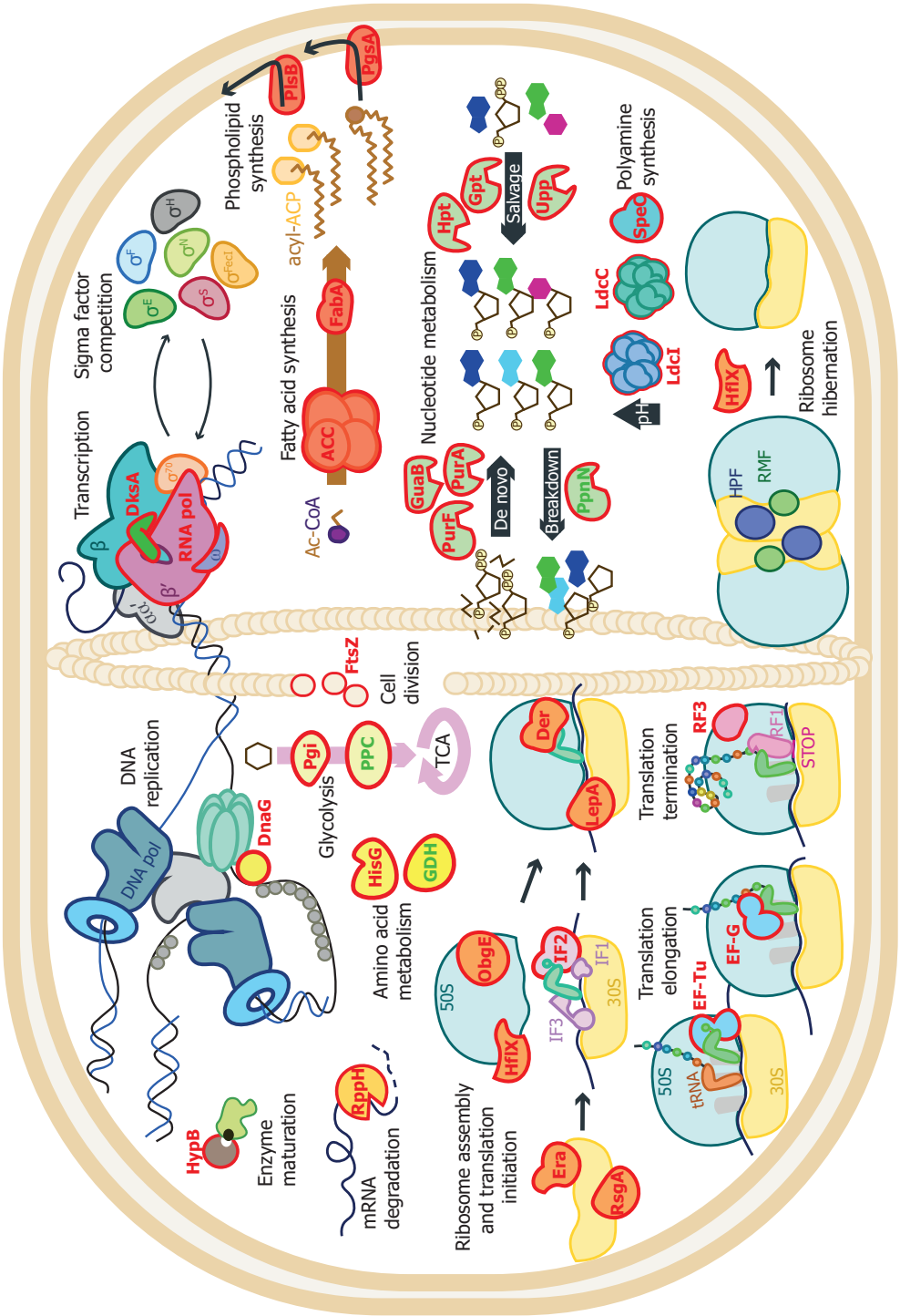
Transcription
Sigma factor competition
Phospholipid synthesis
Fatty acid synthesis
acyl-ACP
Ac-CoA
Nucleotide metabolism
Salvage
De novo
Breakdown
Polyamine synthesis
pH
Ribosome hibernation
DNA replication
Glycolysis
Cell division
TCA
Amino acid metabolism
Translation termination
Translation elongation
Ribosome assembly and translation initiation
Enzyme maturation
mRNA degradation
DksA
RNA pol
FabA
ACC
PlsB
PgsA
Hpt
Gpt
Upp
GuaB
PurF
PurA
PpnN
SpeC
LdcC
LdcI
HflX
HPF
RMF
DNA pol
DnaG
Pgi
PPC
FtsZ
HisG
GDH
Der
LepA
RF3
RF1
STOP
ObgE
IF2
IF1
IF3
EF-G
EF-Tu
tRNA
50S
30S
HypB
RppH
Era
RsgA

Figure 1.5: The various effects of (p)ppGpp. The proteins to which (p)ppGpp binds directly are named in red (inhibition) or green (activation). Inspiration for parts of this figure was provided by [76, 104–108].

aureus [102]. Both identified a number of ribosome-associated GTPases as targets for (p)ppGpp. In *E. coli*, these were **RsgA, HflX, Der (EngA), ObgE, Era** and **LepA**. GDP and ppGpp have similar affinities for these GTPases, and higher affinities than GTP or pppGpp. The binding affinities imply that ppGpp can compete with GTP (and GDP) in stressful conditions [74]. The individual effects of these interactions are believed to depend on the specific GTPase and reviewed by Bennison, Irving, and Corrigan [109]. RsgA, HflX, ObgE and Era belong to a group of Era/Obg GTPases that are involved in the maturation of 50S and 30S ribosomal subunits. RsgA and LepA are involved in 30S assembly [110, 111]. Probably (p)ppGpp binding to HflX it will prevent the splitting of 70S. ObgE becomes more associated with 50S during stringent response, consistent with the notion of being an anti-association factor, preventing further ribosomal assembly. Overall, it appears that the stringent response serves to reduce the pool of 70S ribosome to adjust growth rate and increase degradation under stress conditions [109]. There is currently no evidence that any inhibition would occur at (p)ppGpp concentrations in non-stress conditions. A quantitative analysis of this is made in paragraph 1.4.3.

When prokaryotes undergo nutritional stress or are in stationary phase, translation is halted by hibernation of ribosomes, which is the dimerization of 70S ribosomes to 100S ribosomes [112]. In this state, ribosomes are not mRNA-bound and not able to perform translation. The formation of 100S ribosomes is concerted by ribosome modulation factor (RMF) and hibernation promoting factor (HPF) [112]. The release of 100S to individual 70S is presumably effected by HflX [108]. Given that (p)ppGpp promotes transcription of RMF, HPF and can bind to HflX, it is believed (p)ppGpp also regulates ribosome hibernation, although the exact net effect is unknown. It has been hypothesized that action of (p)ppGpp on inactivating ribosomes also plays a role in governing persistence [108].

Overall translation activity

There is substantial evidence that (p)ppGpp suppresses translation at stringent concentrations, yet the exact target of (p)ppGpp is still not clear after decades of research. In addition, it is not clear whether there is inhibition at basal (p)ppGpp levels as well. Some studies have proposed that (p)ppGpp does not affect translation directly, but via its effect on transcription [90, 113, 114]. They argue that by inhibiting mRNA synthesis, ppGpp prevents mistranslation [90] or adjusts the number of active ribosomes to the availability of resources [113]. However, the number of studies proposing targets of ppGpp amongst the ribosome associated factors is still increasing.

Translation can be divided into three phases: initiation, elongation and termination (more in chapter 4). For each phase, potential (p)ppGpp targets have been

identified. Several *in vitro* studies showed ppGpp could inhibit translation initiation by binding initiation factor 2 (**IF2**) [115, 116]. The elongation factors **EF-Tu** and **EF-G** could also be inhibited by ppGpp [116, 117], although not all studies agree [118]. The slowing down of translation elongation coincided with a decrease in translational errors, giving rise to the hypothesis that ppGpp's arrest on translation serves to improve translation fidelity [119–121]. However, the affinity of ppGpp for IF2 is higher than that of GTP and GDP and the affinity of EF-G for ppGpp is lower than that for GTP and similar to GDP [115, 116]. This indicates that *in vivo* translation initiation is relatively more inhibited than elongation [116], which was confirmed by a quantitative evaluation (paragraph 1.4.3).

Translation termination involves the action of several release factors (RF). **RF3** is potentially inhibited by stringent ppGpp levels, as RF3 is inhibited 3.3-fold by 1 mM ppGpp *in vitro* [122]. RF3 helps release RF1 and RF2 from the ribosome to promote a next elongation round. Hence, RF3-ppGpp binding would reduce the translation rate. In their genome-wide study Zhang *et al.* [74] have confirmed (p)ppGpp interacting with IF2, EF-G and RF3.

It should be noted that some genes have an increased transcription and translation during the stringent response, which seems paradoxical regarding the widespread inhibition of translation by stringent (p)ppGpp. Vinogradova *et al.* [123] observed that specific mRNA sequences form hairpin structures that impose a different sensitivity for GTP and ppGpp on 30S-bound IF2. These mRNA sequences allow translation initiation even in the presence of ppGpp. Furthermore, pppGpp-bound IF2 still initiates translation. This is consistent with the observation that pppGpp actually has an activating effect on IF2 and EF-Tu *in vitro* [124]. Additionally, the stabilization of mRNA could promote translation of some mRNAs during the stringent response despite high (p)ppGpp concentrations. *E. coli* Nudix hydrolase **RppH** hydrolyzes (pyro)phosphoryl groups from the 5' end of RNA to initialize its degradation. It was recently shown to bind ppGpp with an IC_{50} of 50-200 µM suggesting RppH could be inhibited *in vivo* and limit the degradation of RNA [125].

Central metabolism during stress conditions

Phosphoenolpyruvate (PEP) carboxylase (***ppc***) catalyzes the synthesis of oxaloacetate from PEP and vice versa and is an important bridge between glycolysis/ gluconeogenesis and the TCA cycle. ppGpp allosterically activates the synthesis of oxaloacetate by PEP carboxylase, increasing the flux in the TCA cycle presumably to provide more amino acid precursors [126–128]. However, given the many allosteric regulators of PEP carboxylase, it is not certain what the exact net effect is *in vivo*. Also glucose-6'-phosphate isomerase (***pgi***) was shown to be inhibited by (p)ppGpp, causing the intracellular levels of several glycolysis intermediates to drop during the stringent response [127].

Amino acid metabolism during stress conditions

To cope with low pH stress, the cell uses decarboxylases to protect the intracellular pH. Ornithine decarboxylase (**SpeC**) was reported to be inhibited by ppGpp during the stringent response [129], although this could not be repeated in a K^+ requiring *E. coli* strain [130]. Recent publications settled the debate with the discovery that ppGpp binds and inhibits several decarboxylases: both the constitutive and inducible lysine decarboxylase (**LdcC** and **LdcI**) [131, 132] as well as ornithine decarboxylase SpeC [103, 131]. Constitutive decarboxylases have various intracellular roles such as DNA replication, transcription, protein synthesis, membrane permeability and biofilm formation. The lysine decarboxylases are likely regulated by ppGpp to prevent overconsumption of lysine in environments with both low pH and nutrient limitation.

Also biosynthesis of histidine is prevented when amino acids – but not histidine – are scarce. Although only studied in *Salmonella typhimurium*, ppGpp inhibits the first reaction in the biosynthesis of histidine (ATP phosphoribosyltransferase, **HisG**) in synergy with inhibition by histidine. Without histidine, ppGpp cannot inhibit the enzyme [133].

Finally, *E. coli* has two systems to assimilate nitrogen from ammonia into amino acids, glutamate dehydrogenase (GDH) and glutamine synthetase (GS). Although GS has a higher affinity for NH_3 [134], which is useful in nitrogen limiting conditions, the degradation of **GDH** could be reduced by ppGpp binding to GDH [135].

Fatty acid, phospholipid and peptidoglycan synthesis

Merlie and Pizer [136] reported based on *in vitro* and *in vivo* data that ppGpp inhibits phospholipid synthesis at 2 steps: glycerol-3-phosphate acyltransferase (**PlsB**) and phosphatidylglycerophosphate synthase (**PgsA**) at stringent levels. The *in vitro* applied ppGpp concentrations however range from 1 to 5 mM, which could explain why others did not observe an inhibitory effect of ppGpp on PlsB [137]. Later, a quantitative correlation between ppGpp levels and the rate of phospholipid synthesis was found at basal and stringent levels [138]. However, the basal trend was based on only two measurements in strains with different genetic background with several pleiotropic mutations. Therefore, the concomitant difference between basal ppGpp and phospholipid synthesis rate does not guarantee a causal relationship. Finally, Heath, Jackowski, and Rock [139] confirmed PlsB is post-translationally inhibited by ppGpp. Specifically, induction of RelA lead to a build-up of long chain acyl-ACPs as well as an arrest of phospholipid synthesis, which indicated that the PlsB step is inhibited by ppGpp, although not necessarily directly. The *de novo* fatty acid synthesis (FAS) rate was also reduced, suggesting that ppGpp might mildly inhibit FAS as well. Indeed, already in the '70s, it was brought to light that stringent ppGpp inhibits the initial committed step catalyzed by acetyl-coA carboxylase (**ACC**) by 50-60% *in vitro* and *in vivo* [140]. This is consistent with the observation that beta-hydroxy, free hydroxy, saturated and unsaturated fatty acids are all inhibited to the

same degree during amino acid starvation, insinuating inhibition of FAS happens early in the pathway [141]. In addition, the synthesis of unsaturated fatty acids is inhibited by about 40% during the stringent response by direct binding to 3-hydroxydecanoyl dehydratase (**FabA**) [142]. Overall, there is very little known about ppGpp and fatty acid or lipid biosynthesis. In these studies inhibition was at above 1 mM ppGpp and not complete, suggesting that any inhibition *in vivo* would occur only in stringent conditions. Further *in vivo* evidence did not decipher by which exact interactions ppGpp would inhibit these pathways and cannot exclude effects of other regulators.

Several studies have pointed at an inhibition of peptidoglycan synthesis by ppGpp [143–145]. However, the effect on peptidoglycan synthesis might be a consequence of reduced phospholipid synthesis, although the exact mechanism is unknown [146].

Cell division

ppGpp can compete with GTP for the binding to **FtsZ**, which forms filaments part of the Z-ring necessary for cell division. It was hypothesized that high (stress) ppGpp levels inhibit the formation of these filaments and prevent cell division [147]. However, the observation that RelA induction prevents Z-ring formation *in vivo*, is no evidence for a direct inhibition of FtsZ by (p)ppGpp.

DNA replication

Active transcription of rRNA is believed to promote the initiation of DNA replication. The origin of replication is close to *rrn* operons on the chromosome and their transcription introduces negative supercoiling, which unwinds the origin and hence promotes binding of DnaA and other factors involved in replication. When RNA polymerase activity is inhibited by ppGpp, the origin remains more supercoiled, so ppGpp indirectly regulates DNA replication [148]. Also the subsequent replication elongation phase is inhibited by ppGpp in a dose dependent manner in both *E. coli* and *B. subtilis* [149], although another study did not confirm this for *E. coli* [150]. Based on *in vitro* experiments the target is likely DNA primase (**DnaG**) [151, 152].

Enzymes involved in nucleotide metabolism

Several steps in the uptake, salvage and *de novo* synthesis pathways of nucleotides are inhibited by ppGpp. The first steps of GMP and AMP synthesis are catalyzed by IMP dehydrogenase (**GuaB**) and adenylosuccinate synthetase (**PurA**) respectively. For GuaB, the inhibition is competitive with IMP with a K_i of 30-48 µM, which actively inhibits GuaB during the stringent response [128, 153]. PurA is competitively inhibited by GMP, GDP and by ppGpp, although for the latter it is not certain whether the inhibition is GTP-competitive [153] or non-competitive [128, 154]. The

inhibition should be relevant *in vivo* during the stringent response [128, 153] and is estimated to be about 40% [154]. Recently, Wang *et al.* [103] measured that the inhibition of 1 mM ppGpp on GuaB and PurA is less than 20% *in vitro*. Also the screening of [74] did not detect GuaB or PurA as ppGpp binding proteins. The majority of experiments however points at an inhibitory effect, which is very likely influenced by various factors *in vivo*, such as the concentrations of IMP, GMP, GDP, GTP and other potential regulators of these enzymes. Wang *et al.* [103] identified other targets with <20% (pyrH, Ndk, PK-LDH), 50% (GpmA) and more than 75% inhibition (Gsk and **PurF**) *in vitro*, and the latter was confirmed *in vivo*. After RelA induction in medium without nucleotides or bases, ATP and GTP synthesis rates drop by 65%, again confirming that ppGpp inhibits *de novo* purine synthesis.

Other steps of nucleotide metabolism include the salvage reactions of nucleobases with phosphoribosyl pyrophosphate (PRPP) to form nucleoside monophosphates. These include the purine phosphoribosyltransferases Gpt and Hpt, the adenine phosphoribosyltransferase Apt and uracil phosphoribosyltransferase Upp. The degrees of inhibition by ppGpp however vary amongst studies. **Gpt** and **Hpt** are inhibited by ppGpp [155] and bind ppGpp with a K_d of 5 and 6 µM respectively. The inhibition is competitive for PRPP [74]. According to Wang *et al.* [103] the inhibition of 1 mM ppGpp on Gpt is however less than 20% and for Hpt more than 75% *in vitro*. Only Hochstadt-Ozer and Cashel [155] observed Apt inhibition *in vivo* albeit less than inhibition of Gpt and Hpt. However, Fast and Skold [156] do not observe adenine uptake inhibition during stringent response *in vivo* and Wang *et al.* [103] did not detect ppGpp binding to Apt. Both Fast and Skold [156] and Hochstadt-Ozer and Cashel [155] observed an allosteric inhibition of **Upp** by ppGpp during the stringent response. As for Gpt, Wang *et al.* [103] measured a mild inhibition of Upp by 20% at 1 mM ppGpp *in vitro*. Paradoxically, Jensen and Mygind [157] reported that ppGpp activates Upp. They suggested that there are other parameters such as the amount of metal ions that might cloud the effect of ppGpp on Upp.

Not only in the synthesis but also in the degradation of nucleotides (p)ppGpp is involved. **PpnN**, a nucleosidase that cleaves purine nucleoside monophosphates to nucleobases and ribose-5'-phosphate, was shown to be allosterically activated by ppGpp [74, 158]. The combined activation and inhibition of enzymes in purine metabolism causes a rapid decrease in biosynthesis and increase in degradation and reuse, promoting a fast recovery from stress or starvation.

The presence of many potential targets in nucleotide metabolism is what makes it difficult to elucidate the exact effect of ppGpp on each enzyme involved. Future studies with metabolic flux analysis combined with ectopic overexpression and comparison with mutant enzymes will show how exactly ppGpp directs nucleotide metabolism.

Other targets

HypB is a GTPase responsible for the maturation of dehydrogenases by conferring a nickel ion. It has similar affinity for GTP and (p)ppGpp [74], both binding in the HypB active site. This interaction supposedly functions to prevent the activation of unnecessary dehydrogenases during oxidative stress.

There have been mixed results about an inhibitory effect of (p)ppGpp on ADP-glucose synthetase activity, the rate-limiting step in glycogen synthesis [159, 160]. It is not clear what the role is of (p)ppGpp in glycogen metabolism [161].

Finally, there are many effects of (p)ppGpp observed, where there is little known about a possible mechanism, and the discovery is based on a comparison of a specific trait between a wild-type strain and an isogenic RelA SpoT double knock-out, which does not contain ppGpp (abbreviated as $ppGpp^0$). For example, it was shown that contrary to previous results, ppGpp is not necessary for polyphosphate synthesis in *E. coli*, yet DksA is [162]. Smirnova *et al.* [163] show that stringent ppGpp concentrations inhibit respiratory metabolism, presumably directly ATP synthase, thereby preventing electron transport and proton transfer. This is supposed to coordinate energy generation with other metabolic changes in the cell. Although these studies might shed light on connections between certain metabolic pathways or physiological properties, it must be kept in mind that (p)ppGpp not necessarily directly influences these traits. Some phenotypic traits are the consequence of a complex interplay between many factors regulated by (p)ppGpp, such as resistance to bacteriophages [164] and antibiotics [165], gut colonization [166], virulence [167] and persistence [108], making it difficult to decipher the exact role of (p)ppGpp in these phenomena.

1.4.3. A critical evaluation of post-translational regulation

Many of the reported interactions with ppGpp are based on observations *in vitro*. Can this be translated to an *in vivo* function? What does a binding constant of e.g. 150 µM mean? Michaelis-Menten kinetics describe enzymatic activity as a function of substrate concentration and the Michaelis-Menten constant K_M. If inhibitors affect the enzymatic rate, the degree of inhibition as a function of inhibitor concentration can also be determined if the mode of inhibition and inhibition constant K_i are known. For competitive inhibition (inhibitor competes with substrate for binding the catalytic site) this is described by equation 1.1 [168]:

$$\frac{V}{V_{\text{max}}} = \frac{S}{S + K_M(1 + \frac{I}{K_i})} \tag{1.1}$$

V is the reaction rate, V_{max} the theoretical maximal reaction rate with saturating substrate concentration and S and I the substrate and inhibitor concentrations respectively. For many of the ppGpp targets, it is known (or assumed) ppGpp inhibits

in competition with regard to GDP, GTP, IMP or PRPP. If the intracellular concentrations of these compounds, the K_M and K_i are known, the concentration of I necessary to reduce the reaction rate by 50% can be derived from equation 1.1:

$$I_{V/V\text{max}=0.5} = (\frac{S}{K_M} - 1) * K_i \quad (1.2)$$

Equation 1.2 translates an *in vitro* measured parameter (K_i) to an *in vivo* ppGpp concentration, which can be compared to ppGpp concentrations measured in a range of conditions. The highest basal ppGpp levels occurring during steady-state growth was measured to be about 200 µM ([90], Supplementary note 1). ppGpp concentrations during stress and starvation responses reach up to several millimolar depending on the type of stress of starvation (Supplementary note 1).

For all of the post-translational targets mentioned above an overview was made of the currently presumed inhibition mechanism, the K_M, K_i and S (**Table S1.2**). This allowed for a number of targets to determine whether basal or stringent ppGpp concentrations affect the target *in vivo* (**Table 1.1**). As a reference for basal ppGpp a concentration of 40 µM was used, based on *E. coli* grown in glucose minimal medium measured by Varik *et al.* [169].

Table 1.1 shows that some of the small GTPases involved in ribosome biogenesis are unlikely to be significantly regulated by ppGpp in the basal regime. If only considering competitive inhibition by ppGpp, Der might be inhibited for about 20%. However, these GTPases generally have an equally high affinity for GDP as ppGpp, and given that the intracellular concentration of GDP is 0.68 mM [170] the inhibition by GDP will be much stronger than any inhibition exerted by ppGpp. During a stringent response, however, ppGpp would significantly inhibit Der, ObgE and to a lesser extent Era. Interestingly, due to a very low K_M, EF-G does not appear to be inhibited by ppGpp *in vivo*, whereas IF-2 could already be mildly inhibited at basal levels.

For enzymes in nucleotide metabolism, for which there have been several reports of competitive inhibition by ppGpp, the calculated levels of *in vivo* inhibition vary. For Gpt, three studies observed affinities for ppGpp that suggest 10 µM ppGpp can inhibit Gpt by 70% and 40 µM by 80-90%. In other words, from 10 µM to 40 µM intracellular ppGpp, the activity of Gpt decreases by at least 50%. Similarly, Hpt is inhibited by 22-49% at 40 µM ppGpp. Also PurF, although only studied once, would be inhibited by 86% at 40 µM ppGpp. It seems at first impression counterintuitive that at low basal ppGpp, which reflects good growth conditions, some enzymes would be operating significantly below their maximal rate. Especially PurF seems unlikely to be nearly completely inhibited during steady state growth as it catalyzes the committed step for ATP and GTP *de novo* synthesis. However, enzymes operating below optimum efficiency creates the option of regulating the enzyme. For many enzymes, the cost of inhibition is worth the cost of producing more of these

enzymes, as it enables the adjustment of metabolic fluxes to environmental conditions and prevents unneeded biosynthetic overproduction [171]. It might be ppGpp creates the possibility for these enzymes to be activated by other regulators.

For some enzymes such as SpeC, LdcC, LdcI, DnaG, Upp and PurA, various inhibition mechanisms by ppGpp have been reported (**Table S1.2**). As illustrated for DnaG, whether ppGpp inhibits competitively or as a mixed competitor dramatically affects the inhibitory concentration. In addition, some of these enzymes have several potential inhibitors and activators besides ppGpp and the information is lacking to precisely decipher the *in vivo* inhibition mechanism.

In conclusion, many enzymes that were reported to be significantly inhibited by ppGpp *in vitro* are not necessarily inhibited by basal levels *in vivo*. Here, ppGpp serves as a 'hand brake' during severe stress to adjust the whole cellular metabolism from active growth to rescue mode. Few enzymes could be inhibited by ppGpp during steady state growth. Ultimately, a statement such as "enzyme X is inhibited by Y% at Z mM ppGpp" does not provide physiologically relevant information unless there is a rough estimate available about the inhibitory mechanism, the K_M and the concentration of enzyme substrate. The elongation factor EF-G illustrates that if an enzyme operates at substrate concentrations far above its K_M, competitive inhibition can become negligible. It must be kept in mind that other still unknown regulators could be involved that have counteracting or synergistic effects. Naturally, this interpretation depends on the availability of accurate biochemical parameters. For most enzymes this analysis cannot even be made given there is insufficient data regarding the inhibition mechanism and parameters, or accurate intracellular concentration of substrates.

1.5. Thesis outline

As demonstrated in the previous paragraphs, the importance of (p)ppGpp for bacterial growth cannot be overestimated. This is why researchers are currently looking into potential antibiotics that hijack or attack ppGpp regulatory networks [173,

Table 1.1: Biochemical data available in literature regarding inhibition of enzymes by ppGpp. K_M values were obtained from BRENDA or Uniprot databases. *K_M value of EF-G was obtained from [172]. Intracellular concentrations were obtained from [170]. For all V/V_{max} calculations and 50% inhibitory ppGpp concentrations equations 1.1 and 1.2 were used, with exception of the data by Rymer *et al.* [152]. In this study DnaG was inhibited in a both GTP-competitive and non-competitive manner. Under the assumption of simple mixed inhibition $IC_{50}=K_i$ and equation 1.1 becomes $\frac{S}{(S+K_M)(1+\frac{I}{K_i})}$ [168]. It should be noted that for both DnaG and GuaB there were studies that did not observe an interaction with ppGpp ([150] for DnaG and [74, 103] for GuaB).

Study	Inhibition constant	Target	Km	Intracellular concentration (mM)	V/Vmax at 40 µM ppGpp	V/Vmax at 1 mM ppGpp	[ppGpp] for 50% inhibition (mM)
Zhang et al 2018	Kd 1.77 µM for ppGpp, 13.7 for GTP, 1.3 for GDP	Der	59.2 µM	GTP 4.9	0.78	0.13	0.14
Bharat et al 2014	Ki 6 µM for GTP, 2 µM for GDP/ppGpp	Der	59.2 µM	GTP 4.9	0.80	0.14	0.16
Zhang et al 2018	Kd 1.8 µM for ppGpp	ObgE	18 µM	GTP 4.9	0.92	0.33	0.49
Zhang et al 2018	Kd 4.3 µM for ppGpp	Era	9-15.4 µM	GTP 4.9	0.97	0.63	1.72
Mitkevich et al 2010	Kd for ppGpp is 9.1-13.9 µM and similar to GTP and GDP	EF-G	0.22 µM*	GTP 4.9	1.00	1.00	278.4
Mitkevich et al 2010	Kd for ppGpp is similar to GDP (1.7-2.8 µM) and about 2.5-5 fold lower than GTP	IF2	30 µM	GTP 4.9	0.87	0.22	0.28
Rymer et al 2012	50% inhibition above 1 mM ppGpp without GTP. At 100-700 µM GTP, 1 mM ppGpp inhibits by about 60%	DnaG	0.012 mM	GTP 4.9	0.96	0.50	1.00
Maciag et al 2010	50% inhibitory concentration of DnaG in the presence of DnaB helicase was 0.3 mM ppGpp	DnaG	0.012 mM	GTP 4.9	0.99	0.87	6.92
Maciag et al 2013	DNA replication 50% inhibited by 0.2-0.3 mM ppGpp	DnaG	0.012 mM				
Pao et al 1981	Ki 0.048 mM	GuaB	0.013 mM	IMP 0.27	0.92	0.49	0.95
Gallant et al 1971	GMP (Ki 80 µM) and ppGpp (Ki 30 µM)	GuaB	0.013 mM	IMP 0.27	0.89	0.37	0.59
Wang et al 2018	Kd 1.6 µM. Activity inhibited by 92%	PurF	0.053-0.067 mM	PRPP 0.26	0.14	0.01	0.01
Wang et al 2018	Kd 3.2 µM. 87% inhibition of activity	Gpt	0.139 mM	PRPP 0.26	0.12	0.01	0.003
Hochstadt-Ozer and Cashel 1972	50% inhibition at 1 mM PRPP and 200 µM ppGpp for Gpt. Ki = IC50/(1+S/Km) = 0,0244	Gpt	0.139 mM	PRPP 0.26	0.10	0.005	0.002
Zhang et al 2018	Kd 5.2 µM for ppGpp	Gpt	0.139 mM	PRPP 0.26	0.18	0.01	0.005
Zhang et al 2018	Kd 6.1 µM for ppGpp	Hpt	0.033 mM	PRPP 0.26	0.51	0.05	0.04
Wang et al 2018	Kd 32 µM and 96% inhibition	Hpt, GuaB	0.033 mM	PRPP 0.26	0.78	0.20	0.02

174]. However, there are many gaps in the knowledge about the ppGpp signaling network. This thesis aimed at addressing one of the central questions related to (p)ppGpp and metabolism: what is the physiological role of ppGpp during steady-state growth? Transcriptional regulation is clearly vital for the cell in all conditions, but how important is post-translational regulation by ppGpp during steady-state growth? In order to answer this question, it is necessary to

1. accurately quantify ppGpp;
2. critically evaluate the literature for what is known about ppGpp during steady-state growth;
3. determine the role of basal ppGpp on translation;
4. understand how basal ppGpp levels are set by SpoT.

These four topics are explained in chapters 2-5.

- In chapter 2, **an LC-MS method is described to accurately quantify ppGpp and other compounds in *E. coli***. This method provided the basis for much of the research in this thesis.
- Chapter 3 is about one of the earliest, central, yet unexplained observations about ppGpp: that low intracellular ppGpp concentrations correlate linearly with growth rate. It is still not completely understood today why this happens (what adjusts ppGpp levels to the growth rate) and **what the effects are of these very low (basal) ppGpp levels**.
- Protein synthesis is the costliest process of the cell. In chapter 4, the potential effect of (basal) ppGpp on translation is investigated. That ppGpp might inhibit translation is heavily debated due to (amongst others) inconsistencies between *in vitro* and *in vivo* data. Here both types of experiments were performed ultimately showing that **ppGpp inhibits translation, independently of transcriptional regulation**.
- Another one of the central questions about (p)ppGpp, is how it is synthesized and degraded according to environmental conditions. It is known that the enzymes RelA and SpoT are responsible for this, and for RelA the molecular mechanism is well understood. However, for SpoT, the enzyme that is responsible for the correlation with growth rate, it is still a mystery what activates it to synthesize or degrade (p)ppGpp. In chapter 5, it is investigated **whether SpoT activity might be regulated by acyl carrier protein (ACP)**.

1.6. Supplementary information

1.6.1. Supplementary note 1: intracellular ppGpp concentrations

Intracellular ppGpp concentrations have been measured in various units (see also chapter 2). Most of the absolute data is given in units of pmol OD^{-1}, which has to be translated to molarity to use equations 1.1 and 1.2. Units of mol OD^{-1} can be converted to molarity if the number of cells per OD (in OD^{-1}) and the volume of a single cell (in L) are known. Both Volkmer and Heinemann [175] and Varik *et al.* [169] have characterized how these two parameters vary as a function of growth media [175] and growth phase [169]. Results of both papers were used to convert a list of *in vivo* ppGpp concentrations from mol OD^{-1} to mol L^{-1}. This is represented in **Table S1.1**. It can be seen that the concentration based on the Varik *et al.* [169] conversion reaches intracellular concentrations up to 1.5 mM whereas the concentrations based on the Volkmer and Heinemann [175] conversion not even 300 µM. The few molarity concentrations available in literature report a ppGpp concentration of 1 until 4 mM during stress response or RelA overexpression. Given that the conversion based on [169] is more consistent with literature values, this was used to calculate concentrations in molarity. The basal ppGpp levels in literature, which range from 10 to 130 pmol OD^{-1}, then correspond to a concentration of 15 to 200 µM (**Table S1.1**). It should be noted the list of data in this table is not exhaustive, but rather to provide an estimate of intracellular concentrations occurring during stress and steady state growth.

Table S1.1: Intracellular ppGpp concentrations and unit conversions. A) Studies used to calculate the conversion of mol OD^{-1} to mol L^{-1}. B) Literature data used to estimate the concentration range of basal and stress conditions. Data was taken from the original graphs, which could not always be estimated exactly. Literature data was converted into molarity based on A. C) Studies that reported ppGpp concentration in molarity to compare with the calculated concentrations in B.

A

Study	Single cell volume (fL)	Number of cells per OD	Volume of cells of 1 OD (µL/OD)
Bennett et al 2009	0.69		
Varik et al 2017	1.22	1.4*10^8	0.63 (a)
Volkmer et al 2011	3.2	8-11*10^8	3.6 (b)

B

Study	Before stress (pmol/ OD)	Peak of stress (pmol/ OD)	Ratio stress/ basal	Growth conditions	Basal based on (a) (µM)	Peak of stress based on (a) (µM)	Peak of stress based on (b) (µM)
Sorensen et al 1994	130	800	6	valine addition	206	1270	222
Cashel et al 1969	50	800	16	valine addition	79	1270	222
Ryals et al 1982	20	800	40	pseudomonic acid	32	1270	222
Harshman and Yamazaki 1969	10	600	60	phenylalanine starvation	16	952	167
Harshman and Yamazaki 1972	30	675	23	arginine starvation	48	1071	188
Lazzarini et al 1971	80	950	12	methionine starvation	127	1508	264
Winslow 1971	35	175	5	glucose-lactate downshift	56	278	49
Metzger et al 1989			7	glucose starvation			
Gentry and Cashel 1996			12	glucose starvation			
Lazzarini et al 1971	80	850	11	glucose starvation	127	1349	236
Lazzarini et al 1971	80	430	5	glucose-succinate diauxic shift	127	683	119
Harshman and Yamazaki 1969	10	225	23	glucose-succinate diauxic shift	16	357	63
Seyzfadeh et al 1993			3	cerulenin (FA starvation)			
Harshman and Yamazaki 1972	10	225	23	NaCl stress	16	357	63
Lazzarini et al 1971	20	135	7	phosphate starvation	32	214	38
Schreiber et al 1991	50	1000	20	RelA overexpression	79	1587	278
Wang et al 2018		1000		RelA overexpression		1587	278
Harshman and Yamazaki 1971	50	250	5	Levallophan	79	397	69

C

Study	Before stress (mM)	Peak of stress (mM)	Ratio stress/ basal	Growth conditions
Cashel 1975		4	5-20	amino acid starvation
Varik et al 2017	0.04	0.91		stationary phase entry
Wang et al 2018		1.5		RelA overexpression
Ross et al 2016	0.01-0.1	1		stringent levels vs. basal
Kanjee et al 2011		1-2		

Table S1.2: Biochemical literature data of enzymes reported to be post-translationally regulated by (p)ppGpp.

Enzyme function	Enzyme	*in vivo* or *in vitro*	Measured inhibition by (p)ppGpp	[ppGpp] used	GTP or other molecules in assay	Type of regulation	Km	V/Vmax at 10 µM ppGpp	V/Vmax at 1 mM ppGpp	Formula V/Vmax	Study
ribosome biogenesis	Der	vitro	Kd 1.77 µM for ppGpp, 13.7+- 7 for GTP, 6.9 for pppGpp, 1.3 for GDP	2 nM	100 µM for GDP and GTP	competitive for GDP and GTP	59.2 µM for GTP	0.93	0.13	v/Vmax= [GTP]/([GTP]+Km*(1 +[GDP]/Ki,gdp + [ppGpp]/Ki,ppGpp))	Zhang et al 2018
	Der	vitro	Ki 6 µM for GTP and 2 µM for GDP and for ppGpp	2 nM		competitive for GDP and GTP	59.2 µM for GTP	0.93	0.14	v/Vmax= [GTP]/([GTP]+Km*(1 +[GDP]/Ki,gdp + [ppGpp]/Ki,ppGpp))	Bharat et al 2014
	LepA	vitro	binding to ppGpp	2 nM	100 µM for GDP and GTP	competitive for GDP and GTP	32 µM for GTP				Zhang et al 2018
	ObgE	vitro	Kd 1.8 µM for ppGpp and 6.6 µM for pppGpp	2 nM	100 µM for GDP and GTP	competitive for GDP and GTP	18 µM for GTP	0.98	0.33	[GTP]/([GTP]+Km*(1 +[ppGpp]/kd))	Zhang et al 2018
	HflX	vitro	binding to ppGpp	2 nM	100 µM for GDP and GTP	competitive for GDP and GTP					Zhang et al 2018
	RsgA	vitro	binding to ppGpp	2 nM	100 µM for GDP and GTP						Zhang et al 2018
	Era	vitro	Kd 4.3 µM for ppGpp and 21.4 for pppGpp	2 nM	100 µM for GDP and GTP	competitive for GDP and GTP	9- 15.4 µM for GTP	0.99	0.63	[GTP]/([GTP]+Km*(1 +[ppGpp]/Kd))	Zhang et al 2018
translation	EF-G	vitro	Kd for ppGpp is 9.1-13.9 µM and similar to GTP and GDP			competitive for GDP and GTP	NA	1.00	1.00	v/Vmax= [GTP]/([GTP]+Km*(1 +[GDP]/Ki,gdp + [ppGpp]/Ki,ppGpp))	Mitkevich et al 2010
	EF-G	vitro	binding to ppGpp	2 nM	100 µM for GDP and GTP	competitive for GDP and GTP	NA				Zhang et al 2018
	RF3	vitro	Kd 0.82 µM for ppGpp and 29+-10 µM for GTP and 15 µM+- 5 for pppGpp	2 nM	100 µM for GDP and GTP	competitive for GDP and GTP	NA				Zhang et al 2018
	RF3	vitro	RF3 60% less active	1 mM	1 mM GDP	GDP competitive	NA				Kihira et al 2012
	IF2	vitro	binding to ppGpp	2 nM	100 µM for GDP and GTP	competitive for GDP and GTP	30 µM for GTP				Zhang et al 2018
	IF2	vitro	Kd for ppGpp is similar to GDP (1.7-2.8 µM) and about 2.5-5 fold lower (so higher affinity) than GTP			competitive for GDP and GTP	30 µM for GTP	0.96	0.22	v/Vmax= [GTP]/([GTP]+Km*(1 +[GDP]/Ki,gdp + [ppGpp]/Ki,ppGpp))	Mitkevich et al 2010
	IF2	vitro	1:1 ppGpp:GTP inhibits IF-2 reaction by 45-60%,1:10 ppGpp:GTP inhibits IF-2 by about 14%			competitive for GDP and GTP (and pppGpp)	30 µM for GTP				Hamel and Cashel 1974
	EF-Tu	vitro	1:1 ppGpp:GTP inhibits IF-2 reaction by 45-60%, EF-Tu by 20-40%.			competitive for GDP and GTP (and pppGpp)	Km 0,84 µM for GTP				Hamel and Cashel 1974

Table S1.2: Biochemical literature data of enzymes reported to be post-translationally regulated by (p)ppGpp.

Enzyme function	Enzyme	*in vivo* or *in vitro*	Measured inhibition by (p)ppGpp	[ppGpp] used	GTP or other molecules in assay	Type of regulation	Km	V/Vmax at 10 µM ppGpp	V/Vmax at 1 mM ppGpp	Formula V/Vmax	Study
translation	IF2, EF-Tu	vitro	pppGpp supposedly a substrate								Hamel and Cashel 1974
mRNA degradation	RppH	vitro	GPD IC50 of 32 and 59 µM. (p)ppGpp IC50 54-190 µM. IC50 GTP 1.6-4.1 mM	0.1-5 mM	0.1-5 mM of GDP or GTP (not combined)	competitive for RNA	NA				Gao et al 2020
glycolysis	PEP carbo-xylase	vitro	0.1 mM ppGpp inhibits 31%, 1 mM increases activity by 76% (so less than Taguchi1977) 1 mM GDP and GTP increased the activity with 90% and 43% respectively.	0.1 and 1 mM	1 mM GDP and 1 mM GTP (not combined)	activation					Pao et al 1981
	PEP carbo-xylase	vitro	about 2-fold increase in activity	1 mM	1 mM GTP and other regulators	allosteric activation					Tagushi et al 1977
	gpi	vitro	1 mM ppGpp: 39% inhibited activity; 2 mM ppGpp: 61%	1 and 2 mM		allosteric inhibition					Tagushi et al 1978
polyamine metabolism	SpeC	vitro	Partially purified enzyme with 1 mM GTP: 0.5 mM ppGpp nhibits by about 49% and 2 mM ppGpp about 75%.	0.5 and 2 mM	1 mM GTP	inhibition					Hölttä et al 1974
	SpeC	vitro	1:2 ppGpp: GTP, more than 50-60% reduced activity, 1:1 ppGpp: GTP about 75% inhibition (ppGpp alone: 50% reduced activity, but without GTP baseline activity is lower) Both GTP and GDP stimulate the enyme by about 50%.	0-1000 µM	0-1000 µM GTP	allosteric inhibition					Kanjee et al 2011 (Biochemistry)
	SpeC	vitro	Kd 1.6 µM,activity inhibited bt 98%.	1 mM		presumably allosterically (like LdcI and LdcC)	3.3 mM ornithine	0.14	0.00	Vapp/Vmax=1/(1+[ppGpp]/Ki)	Wang et al 2018
	LdcC	vitro	No effect by GTP or GDP. Ki for ppGpp is 100-500 nM range. 4-6 fold reduction in activity by 100 µM ppGpp.	100 µM	100 µM GTP or GDP (not together with ppGpp)	non competitive allosteric inhibition	NA				Kanjee et al 2011 (Biochemistry)
	LdcI	vitro	No effect by GTP or GDP. Kd for ppGpp is 13 nM and 685 nM (10 binding sites in a decamer, 5 with lower and 5 with higher affinity). Ki values in the nM to 2.5 µM.	100 µM	100 µM GTP or GDP (not together with ppGpp)	allosteric inhibition	2 mM for Lys	0.03	0.00	[S]/(([S]+Km)(1+[ppGpp]/Ki))	Kanjee et al 2011 (EMBO journal)
amino acid metabolism	HisG	vitro	Inhibition constant is 139 µM at 50 µM His and 76 µM at 100 µM His	0-0.6 mM	various concentrations of histidine	allosteric inhibition, (cooperative with His)					Morton and Parsons, 1977

Table S1.2: Biochemical literature data of enzymes reported to be post-translationally regulated by (p)ppGpp.

Enzyme function	Enzyme	*in vivo* or *in vitro*	Measured inhibition by (p)ppGpp	[ppGpp] used	GTP or other molecules in assay	Type of regulation	Km	V/Vmax at 10 µM ppGpp	V/Vmax at 1 mM ppGpp	Formula V/Vmax	Study
amino acid metabolism	GDH	vitro	for GTP and ppGpp Kd is 40 and 30 µM resp.	1 mM	1 mM GTP (not together with ppGpp)	allosteric activation (might be GTP competitive). Prevents degradation.					Morton and Parsons, 1977
lipid synthesis	lipid synthesis after glycerol-3-phosphate	vivo	In CP78 guaA-: compare different ppGpp levels with lipid synthesis and observe that when ppGpp has stringent levels, lipid synthesis arrests. Compare with relA- strain (CP79), which does not have lipid arrest under amino acid starvation.	starvation + basal							Merlie and Pizer, 1973
	PlsB	vitro	Cell free extracts: inhibition of glycerol-3-phosphate transferase was independent of the presence of ATP/GTP (3.3 mM) inhibited 50% by 3.9 mM ppGpp. At 1 mM ppGpp there was 15% inhibition.	3.9 mM	3.3 mM GTP	allosteric noncompetitive inhibtion					Merlie and Pizer, 1973
	PgsA	vitro	Glycerol-3-phosphate CMP phosphatidyltransferase was inhibted 50% by 5 mM ppGpp.	5 mM							Merlie and Pizer, 1973
	phospho-lipid synthesis (PlsB)	vivo	Overexpression of RelA decreases phospholipid synthesis from exogenous fatty acids. Acyl-ACP response is similar to having a defective PlsB suggesting that enzyme is the target of ppGpp. Overexpression of PlsB reverses the inhibition.	stringent		inhibition					Heath et al 1994
	phospho-lipid synthesis	vivo	During amino acid starvation, compare several SpoT/RelA mutant isogenic pairs. Only when (p)ppGpp is stringent, phospholipid synthesis is inhibited, and resumes when stringent response is over. During balanced growth, the relA- or spoT mutant with lower ppGpp had higher phospholipid synthesis rate.	stringent		inhibition					Nunn and Cronan 1976 Biochemistry

Table S1.2: Biochemical literature data of enzymes reported to be post-translationally regulated by (p)ppGpp.

Enzyme function	Enzyme	*in vivo* or *in vitro*	Measured inhibition by (p)ppGpp	[ppGpp] used	GTP or other molecules in assay	Type of regulation	Km	V/Vmax at 10 µM ppGpp	V/Vmax at 1 mM ppGpp	Formula V/Vmax	Study
fatty acid synthesis (FAS)	FAS	vivo	Amino acid starvation and link with lipid synthesis in relA+ and -. Stringent ppGpp inhibits fatty acid synthesis by 60%.	stringent		inhibition					Polakis et al 1973
	ACC	vitro	1 mM ppGpp inhibits about 50% in vitro activity. Higher ppGpp does not inhibit more.	0-2.5 mM		inhibition					Polakis et al 1973
	FAS	vivo	FAS, incorporation of FA into LipidA and phospholipid synthesis are all inhibited during amino acid starvation of relA+ but not of relA-.	stringent		inhibition					Spencer et al 1977
	FabA	vitro	FabA is inhibited about 40% at 1 mM ppGpp. 60% at 2.5 mM. GDP no effect.	0-2.5 mM	GDP 0-2.5 mM (not together with ppGpp)	inhibition					Stein and Bloch 1976
cell division	FtsZ	vivo	RelA expression and fluorescence staining of FtsZ. ppGpp levels is supposedly 15 µmol/OD (without induction ppGpp levels is 5 µmol/OD).	stringent			0.042 mM for GTP				Yamaguchi et al 2015
	FtsZ	vitro	1 mM ppGpp and 1 mM GTP (separately) induce different FtsZ assemblies, but the one with ppGpp are aberrant. When both are added at same time ratio 2:1 (1 mM ppGpp and 0.5 mM GTP) they look normal, indicating GTP has a higher affinity than ppGpp. When GTP and ppGpp are added sequentially, the first one determines the type of FtsZ assembly, suggesting they bind competitively and the binding is irreversible.	1 mM	1 mM GTP both together with ppGpp and in separate assay	possible competitive inhibtion with GTP	0.042 mM for GTP				Yamaguchi et al 2015
DNA replication	DnaG	vitro	ppGpp binds at the active site. Inhibition is competitive for GTP, but mix-type. 50% inhibition above 1 mM ppGpp (without GTP). At 100-700 µM GTP, 1 mM ppGpp inhibits by about 60%	0-1 mM	0-700 µM GTP (both separate and combined with ppGpp)	mixed GTP competitive noncompetitive inhibition	0.012 mM	0.99	0.50	Assume simple mixed inhibition, then IC50=Ki, so roughly 1 mM. [GTP]/((GTP+Km)(1+[ppGpp]/Ki))	Rymer et al 2012

Table S1.2: Biochemical literature data of enzymes reported to be post-translationally regulated by (p)ppGpp.

Enzyme function	Enzyme	*in vivo* or *in vitro*	Measured inhibition by (p)ppGpp	[ppGpp] used	GTP or other molecules in assay	Type of regulation	Km	V/Vmax at 10 µM ppGpp	V/Vmax at 1 mM ppGpp	Formula V/Vmax	Study
DNA replication (DNA rep)	DnaG	vitro	50% inhibitory concentration of DnaG in the presence of DnaB helicase was 0.3 mM ppGpp. Without DnaB, GDP also inhibits with 0.5 mM IC50 and ppGpp 0.2 mM.	0-1 mM	0.2 mM GTP	(competitive?) inhibition	0.012 mM	1.00	0.87	[GTP]/([GTP]+Km*(1+[ppGpp]/Ki))	Maciag et al 2010
	DnaG	vitro	DNA replication 50% inhibited by 0.2-0.3 mM ppGpp.	0-1 mM	0.2 mM GTP	(competitive?) inhibition					Maciag et al 2013
	DnaG	vitro	no binding								Zhang et al 2018
	DNA rep	vivo	The DNA synthesis rate is the same in WT, WT + valine, ppGpp0 and ppGpp0 + valine.								Maciag et al 2013
	DNA rep	vivo	SHX treatment or RelA induction reduce transcription elongation rate by 15%.								DeNapoli et al 2013
nucleotide synthesis	IMP to GMP synthesis	vivo	During valine addition (AA starvation) in relA+ but not relA- the synthesis of GTP, GDP, GMP but little AXP arrests.	stringent							Gallant et al 1971
	PurA	vitro	Competitively inhibited by GMP and GDP with Ki 33 and 67 µM resp. Inhibition by ppGpp is non-competitive with a Ki of 130 µM for GTP binding. However, for IMP binding, ppGpp does inhibit competitively with a Ki of 33 µM.		GTP, IMP	GTP competitive, IMP non competitive inhibition					Gallant et al 1971
	PurA	vitro	Ki of ppGpp estimated at 50-65 µM.	0-0.2 mM	GTP 11-99 µM, IMP 0.099 mM and aspartate 0.987 mM	GTP competitive inhibition	0.042 mM for GTP	0.99	0.86	[GTP]/([GTP]+Km*(1+[ppGpp]/Ki))	Stayton and Fromm 1979
	PurA, Ndk, PK-LDH	vitro	Kd 61 µM and 25% inhibition	1 mM	2 mM L-aspartate, 1 mM IMP, 2 mM ATP						Wang et al 2018
	purA	vitro	no binding								Zhang et al 2018

Table S1.2: Biochemical literature data of enzymes reported to be post-translationally regulated by (p)ppGpp.

Enzyme function	Enzyme	*in vivo* or *in vitro*	Measured inhibition by (p)ppGpp	[ppGpp] used	GTP or other molecules in assay	Type of regulation	Km	V/Vmax at 10 µM ppGpp	V/Vmax at 1 mM ppGpp	Formula V/Vmax	Study
nucleotide synthesis	PurA	vitro	Ki 0.143 mM for competitive inhibition with IMP (0.15 mM GTP, 0.2 mM ppGpp), and Ki 0.045 mM for non-competitive inhibition with GTP (0.15 mM IMP, 0.067 mM ppGpp).	0.2 mM with IMP, and 0.067 mM with GTP	GTP 0.15 mM (and IMP varied) or IMP 0.15 mM (and GTP varied)	IMP competitive, GTP non-competitive inhibition	0.01-0.048 mM (IMP), 0.02-0.0596 (GTP), 0.023-0.308 (Asp)				Pao et al 1981
	GuaB	vitro	Ki 0.048 mM	0.4 mM	IMP (substrate) at various concentrations	competitive inhibition	Km 0.013 mM for IMP	0.95	0.49	[IMP]/([IMP]+Km*(1+[ppGpp]/Ki))	Pao et al 1981
	GuaB	vitro	IMP dehyd is inhibited by GMP (Ki 80 µM) and ppGpp (Ki 30 µM)		GMP (separately, not combined)	competitive inhibition	Km 0.013 mM for IMP	0.93	0.37	[IMP]/([IMP]+Km*(1+[GMP]/Ki,gmp+[ppGpp]/Ki,ppGpp))	Gallant et al 1971
	GuaB	vitro	no inhibition	1 mM							Wang et al 2018
	GuaB	vitro	no binding								Zhang et al 2018
	PurF	vitro	Kd 1.6 µM. Activity inhibited by 92%	1 mM	5 mM glutamine, 5 mM ATP, 5 mM glycine	PRPP competitive inhibition	0.053-0.067 mM for PRPP	0.37	0.01	[PRPP]/([PRPP]+Km*(1+[ppGpp]/Kd))	Wang et al 2018
	PurF	vivo	In strain with mutant purF (not binding ppGpp anymore but catalytically active): RelA induction now does not decrease GTP, GDP and GMP but still IMP levels.	about 1 mM		PRPP competitive inhibition					Wang et al 2018
	de novo purine synthesis	vivo	RelA induction causes decrease in GTP, GDP, GMP. Rate of ATP and GTP synthesis reduced 65%.	about 1 mM							Wang et al 2018
	Gpt, Gmk, Ndk, PK-LDH	vitro	Kd 3.2 µM. 87% inhibition at 1 mM ppGpp	1 mM	PRPP concentration used not clear.		0.139 mM (for PRPP)	0.31	0.01	[PRPP]/([PRPP]+Km*(1+[ppGpp]/Kd))	Wang et al 2018
	Gpt	vitro	50% inhibition at 1 mM PRPP and 200 µM ppGpp for Gpt.	0-2 mM	1 mM PRPP	competitive inhibition	0.139 mM (for PRPP)	0.27	0.00	[PRPP]/([PRPP]+Km*(1+[ppGpp]/Kd))	Hochstadt-Ozer and Cashel 1972
	Gpt	vitro	Kd 5.2 µM and 6.7 µM for ppGpp and pppGpp.	2 nM	100 µM PRPP	competitive for PRPP	0.139 mM (for PRPP)	0.39	0.01	[PRPP]/([PRPP]+Km*(1+[ppGpp]/Kd))	Zhang et al 2018
	Hpt	vitro	Kd 6.1 µM and 6.2 µM for ppGpp and pppGpp.	2 nM	100 µM PRPP	competitive for PRPP	0.033 mM (for PRPP)	0.75	0.05	[PRPP]/([PRPP]+Km*(1+[ppGpp]/Kd))	Zhang et al 2018

Table S1.2: Biochemical literature data of enzymes reported to be post-translationally regulated by (p)ppGpp.

Enzyme function	Enzyme	*in vivo* or *in vitro*	Measured inhibition by (p)ppGpp	[ppGpp] used	GTP or other molecules in assay	Type of regulation	Km	V/Vmax at 10 µM ppGpp	V/Vmax at 1 mM ppGpp	Formula V/Vmax	Study
nucleotide synthesis	Hpt, GuaB	vitro	Kd 32 µM and 96% inhibition.	1 mM	PRPP concentration used not clear.		0.033 mM (for PRPP)	0.86	0.20	[PRPP]/([PRPP]+Km*(1+[ppGpp]/Kd))	Wang et al 2018
	ApT	vitro	50% inhibition at 1 mM PRPP and 1.5 mM ppGpp for Apt (soluble enzyme fractions)	0-2 mM	1 mM PRPP	inhibition	NA				Hochstadt-Ozer and Cashel 1972
	Apt	vitro	no binding				NA				Zhang et al 2018
	Upp, PyrH, Ndk, PK-LDH	vitro	Kd 47 µM and 24% inhibition	1 mM	0.2 mM uracil, 1 mM pRpp, 5 mM ATP						Wang et al 2018
	Upp	vitro	1mM ppGpp inhibits Upp activity in vitro by 60% at concentrations above 0.5 mM GTP and 0.2 mM PRPP.	1 mM	0.2 mM PRPP. 0.5-0.8 mM GTP	competitive inhibition for PRPP (substrate) and GTP (activator)					Fast and Skold 1977
	Upp	vitro	Mild activation (not even 10%) at all GTP (0-1mM) concentrations at 30 µM, 130 µM and 1.2 mM PRPP. GTP itself does not activate above 0.5 mM.	0.375 mM ppGpp + 0.625 mM pppGpp	Mg2+, GTP and PRPP varied.	no inhibition, low activation					Jensen and Mygind 1996
nucleotide degradation	YgdH (ppnN)	vitro	Kd 24.4 and 37.2 µM for ppGpp and pppGpp.	2 nM	100 µM for GDP and GTP	allosteric activation	NA				Zhang et al 2018, 2019
enzyme maturation Nickel incorporation	HypB	vitro	Kd 12.4 µM for ppGpp, 14.5 µM for pppGpp, 9 µM for GTP.	2 nM	100 µM for GDP and GTP	competitive for GDP and GTP	NA				Zhang et al 2018

references

[1] Y. M. Bar-On, R. Phillips, and R. Milo. "The biomass distribution on Earth". In: *Proceedings of the National Academy of Sciences* 115.25 (2018), pp. 6506–6511.

[2] P. J. Jurtshuk. *Medical Microbiology*. Ed. by S. Baron. 4th ed. University of Texas Medical Branch at Galveston, 1996. Chap. Bacterial Metabolism. url: https://www.ncbi.nlm.nih.gov/books/NBK7919/.

[3] N. Merino, H. S. Aronson, D. P. Bojanova, J. Feyhl-Buska, M. L. Wong, S. Zhang, and D. Giovannelli. "Living at the Extremes: Extremophiles and the Limits of Life in a Planetary Context". In: *Frontiers in Microbiology* 10 (2019), pp. 1–25.

[4] M. Cashel and J. Gallant. "Control of RNA Synthesis in *Escherichia coli* I. Amino Acid Dependence of the Synthesis of the Substrates of RNA Polymerase". In: *Journal of Molecular Biology* 34 (1968), pp. 317–330.

[5] G. S. Stent and S. Brenner. "A genetic locus for the regulation of ribonucleic acid synthesis". In: *Biochemistry* 47 (1961), pp. 2005–2014.

[6] M. Cashel. "Regulation of bacterial ppGpp and pppGpp". In: *Annual Review of Microbiology* 29 (1975), pp. 301–318.

[7] M. Cashel and J. Gallant. "Two Compounds implicated in the Function of the RC Gene of *Escherichia coli*". In: *Nature* 221 (1969), pp. 838–841.

[8] M. Cashel and B. Kalbacher. "The control of ribonucleic acid synthesis in *Escherichica coli*. V. Characterization of a nucleotide associated with the stringent response". In: *The Journal of Biological Chemistry* 245.9 (1970), pp. 2309–2318.

[9] W. A. Haseltine and R. Block. "MSI and MSII made on ribosome in idling step of protein synthesis". In: *Nature* 238 (1972), pp. 381–384.

[10] K. Potrykus, H. Murphy, N. Philippe, and M. Cashel. "ppGpp is the major source of growth rate control in *E. coli*". In: *Environmental Microbiology* 13.3 (2011), pp. 563–575.

[11] V. Hauryliuk, G. C. Atkinson, K. S. Murakami, T. Tenson, and K. Gerdes. "Recent functional insights into the role of (p)ppGpp in bacterial physiology". In: *Nature Reviews Microbiology* 13.5 (2015), pp. 298–309.

[12] R. Lazzarini, M. Cashel, and J. Gallant. "On the Regulation of Guanosine Tetraphosphate Levels in Stringent and Relaxed Strains of *Escherichia coli*". In: *Journal of Biological Chemistry* 246.14 (1971), pp. 4381–4385.

[13] S. Metzger, G. Schreiber, E. Aizenman, M. Cashel, and G. Glaser. "Characterization of the *relA1* mutation and a comparison of *relA1* with new *relA* null alleles in *Escherichia coli*". In: *Journal of Biological Chemistry* 264.35 (1989), pp. 21146–21152.

[14] J. Sy. "*In vitro* degradation of guanosine 5'-diphosphate, 3'-diphosphate". In: *Proceedings of the National Academy of Sciences* 74.12 (1977), pp. 5529–5533.

[15] E. Heinemeyer and D. Richter. "*In vitro* degradation of guanosine tetraphosphate (ppGpp) by an enzyme associated with the ribosomal fraction from *Escherichia coli*". In: *FEBS letters* 84.2 (1977), pp. 357–361.

[16] H. Xiao, M. Kalman, K. Ikehara, S. Zemel, G. Glaser, and M. Cashel. "Residual guanosine3',5'-bispyrophosphate synthetic activity of *relA* null mutants can be eliminated by *spoT* null mutations". In: *Journal of Biological Chemistry* 266.9 (1991), pp. 5980–5990.

[17] F. J. Hernandez and H. Bremer. "*Escherichia coli* ppGpp synthetase II activity requires SpoT". In: *Journal of Biological Chemistry* 266.9 (1991), pp. 5991–5999.

[18] G. C. Atkinson, T. Tenson, and V. Hauryliuk. "The RelA/SpoT Homolog (RSH) superfamily: Distribution and functional evolution of ppgpp synthetases and hydrolases across the tree of life". In: *PLoS ONE* 6.8 (2011), pp. 1–21.

[19] B. Field. "Green magic: Regulation of the chloroplast stress response by (p)ppGpp in plants and algae". In: *Journal of Experimental Botany* 69 (11 2018), pp. 2979–2807.

[20] R. D. Hood, S. A. Higgins, A. Flamholz, R. J. Nichols, and D. F. Savage. "The stringent response regulates adaptation to darkness in the cyanobacterium *Synechococcus elongatus*". In: *Proceedings of the National Academy of Sciences* (2016), E4867–E4876.

[21] A. Puszynska and E. Oshea. "ppGpp Controls Global Gene Expression in Light and in Darkness in *S. elongatus*". In: *Cell Reports* 21 (11 2017), pp. 3155–3165.

[22] L. Avilan, C. Puppo, A. Villain, E. Bouveret, B. Menand, B. Field, and B. Gontero. "RSH enzyme diversity for (p)ppGpp metabolism in *Phaeodactylum tricornutum* and other diatoms". In: *Scientific Reports* 9.1 (2019), pp. 1–11.

[23] N. M. Martucci, A. Lamberti, L. Vitagliano, P. Cantiello, I. Ruggiero, P. Arcari, and M. Masullo. "The magic spot ppGpp influences *in vitro* the molecular and functional properties of the elongation factor 1α from the archaeon *Sulfolobus solfataricus*". In: *Extremophiles* 16.5 (2012), pp. 743–749.

[24] D. Sun, G. Lee, J. H. Lee, H.-Y. Kim, H.-W. Rhee, S.-Y. Park, K.-J. Kim, Y. Kim, B. Y. Kim, J.-I. Hong, C. Park, H. E. Choy, J. H. Kim, Y. H. Jeon, and J. Chung. "A metazoan ortholog of SpoT hydrolyzes ppGpp and functions in starvation responses." In: *Nature structural & molecular biology* 17.10 (2010), pp. 1188–94.

[25] T. Laffler and J. Gallant. "*spoT*, a new genetic locus involved in the stringent response in *E. coli*". In: *Cell* 1.1 (1974), pp. 27–30.

[26] G. Stamminger and R. A. Lazzarini. "Altered metabolism of the guanosine tetraphosphate, ppGpp, in mutants of *E. coli*". In: *Cell* 1.2 (1974), pp. 85–90.

[27] G. Mittenhuber. "Comparative genomics and evolution of genes encoding bacterial (p)ppGpp synthetases/hydrolases (the Rel, RelA and SpoT proteins)". In: *Journal of Molecular Microbiology and Biotechnology* 3.4 (2001), pp. 585–600.

[28] Y. I. Wolf, L. Aravind, N. V. Grishin, and E. V. Koonin. "Evolution of aminoacyl-tRNA synthetases – analysis of unique domain architectures and phylogenetic trees reveals a complex history of horizontal gene transfer events". In: *Genome Research* 9 (1999), pp. 689–710.

[29] L. Aravind and E. V. Koonin. "Gleaning non-trivial structural, functional and evolutionary information about proteins by iterative database searches". In: *Journal of Molecular Biology* 287.5 (1999), pp. 1023–1040.

[30] A. B. Loveland, E. Bah, R. Madireddy, Y. Zhang, A. F. Brilot, N. Grigorieff, and A. A. Korostelev. "Ribosome-RelA structures reveal the mechanism of stringent response activation". In: *eLife* 5 (2016), pp. 1–23.

[31] S. Arenz, M. Abdelshahid, D. Sohmen, R. Payoe, A. L. Starosta, O. Berninghausen, V. Hauryliuk, R. Beckmann, and D. N. Wilson. "The stringent factor RelA adopts an open conformation on the ribosome to stimulate ppGpp synthesis". In: *Nucleic Acids Research* 44.13 (2016), pp. 6471–6481.

[32] M. Fang and C. E. Bauer. "Regulation of stringent factor by branched-chain amino acids". In: *Proceedings of the National Academy of Sciences* 115.25 (2018), pp. 6446–6451.

[33] A. Avarbock, D. Avarbock, J.-S. Teh, M. Buckstein, Z.-m. Wang, and H. Rubin. "Functional regulation of the opposing (p)ppGpp synthetase/hydrolase activities of Rel_{Mtb} from *Mycobacterium tuberculosis*". In: *Biochemistry* 44.29 (2005), pp. 9913–9923.

[34] V. Jain, R. Saleem-Batcha, and D. Chatterji. "Synthesis and hydrolysis of pppGpp in mycobacteria: A ligand mediated conformational switch in Rel". In: *Biophysical Chemistry* 127 (2007), pp. 41–50.

[35] T. Hogg, U. Mechold, H. Malke, M. Cashel, and R. Hilgenfeld. "Conformational antagonism between opposing active sites in a bifunctional RelA/SpoT homolog modulates (p)ppGpp metabolism during the stringent response". In: *Cell* 117.1 (2004), pp. 57–68.

[36] K. Syal, H. Joshi, D. Chatterji, and V. Jain. "Novel pppGpp binding site at the C-terminal region of the Rel enzyme from *Mycobacterium smegmatis*". In: *FEBS journal* 282.19 (2015), pp. 3773–3785.

[37] J. Justesen, T. Lund, F. Skou Pedersen, and N. O. Kjeldgaard. "The physiology of stringent factor (ATP: GTP 3′-diphosphotransferase) in *Escherichia coli*". In: *Biochimie* 68.5 (1986), pp. 715–722.

[38] A. Hara and J. Sy. "Guanosine 5′-triphosphate, 3-diphosphate 5′-phosphorylase: Purification and substrate specificity". In: *Journal of Biological Chemistry* 258.3 (1983), pp. 1678–1683.

[39] U. Mechold, K. Potrykus, H. Murphy, K. S. Murakami, and M. Cashel. "Differential regulation by ppGpp versus pppGpp in *Escherichia coli*". In: *Nucleic Acids Research* 41.12 (2013), pp. 6175–89.

[40] J. D. Friesen, N. P. Fill, J. M. Parker, and W. A. Haseltine. "A new relaxed mutant of *Escherichia coli* with an altered 50S ribosomal subunit". In: *Proceedings of the National Academy of Sciences* 71.9 (1974), pp. 3465–3469.

[41] W. A. Haseltine and R. Block. "Synthesis of guanosine tetra- and pentaphosphate requires the presence of a codon-specific, uncharged transfer ribonucleic acid in the acceptor site of ribosomes". In: *Proceedings of the National Academy of Sciences* 70.5 (1973), pp. 1564–1568.

[42] B. P. English, V. Hauryliuk, A. Sanamrad, S. Tankov, N. H. Dekker, and J. Elf. "Single-molecule investigations of the stringent response machinery in living bacterial cells". In: *Proceedings of the National Academy of Sciences* 108.31 (2011), E365–E373.

[43] W. Li, E. Bouveret, Y. Zhang, K. Liu, J. D. Wang, and J. C. Weisshaar. "Effects of amino acid starvation on RelA diffusive behavior in live *Escherichia coli*". In: *Molecular Microbiology* 99.3 (2015), pp. 571–585.

[44] A. Brown, I. S. Fernández, Y. Gordiyenko, and V. Ramakrishnan. "Ribosome-dependent activation of stringent control". In: *Nature* 534 (2016), pp. 277–280.

[45] K. S. Winther, M. Roghanian, and K. Gerdes. "Activation of the Stringent Response by Loading of RelA-tRNA Complexes at the Ribosomal A-Site". In: *Molecular Cell* 70.1 (2018), pp. 95–105.

[46] V. Jain, R. Saleem-Batcha, A. China, and D. Chatterji. "Molecular dissection of the mycobacterial stringent response protein Rel". In: *Protein Science* 15.6 (2006), pp. 1449–1464.

[47] X. Yang and E. E. Ishiguro. "Dimerization of the RelA protein of *Escherichia coli*". In: *Biochemistry and Cell Biology* 79.6 (2001), pp. 729–736.

[48] M. Gropp, Y. Strausz, M. Gross, and G. Glaser. "Regulation of *Escherichia coli* RelA requires oligomerization of the C-terminal domain". In: *Journal of Bacteriology* 183.2 (2001), pp. 570–579.

[49] K. J. Turnbull, I. Dzhygyr, S. Lindemose, V. Hauryliuk, and M. Roghanian. "Intramolecular interactions dominate the autoregulation of *Escherichia coli* stringent factor RelA". In: *Frontiers in Microbiology* 10 (2019), pp. 1–12. doi: doi:10.3389/fmicb.2019.01966.

[50] E.-A. Heinemeyer, M. Geis, and D. Richter. "Degradation of guanosine 3′-diphosphate 5′-diphosphate *in vitro* by the *spoT* gene product of *Escherichia coli*". In: *European Journal of Biochemistry* 89 (1978), p. 1.

[51] E.-A. Heinemeyer and D. Richter. "Characterization of the guanosine 5′-triphosphate 3′-diphosphate and guanosine 5′-diphosphate 3′-diphosphate degradation reaction catalyzed by a specific pyrophosphorylase from *Escherichia coli*". In: *Biochemistry* 17.25 (1978), pp. 5368–5372.

[52] E.-A. Heinemeyer and D. Richter. "Mehcanism of the *in vitro* breakdown of guanosine 5′-diphosphate 3′-diphosphate in *Escherichia coli*". In: *Proceedings of the National Academy of Sciences* 75.9 (1978), pp. 4180–4183.

[53] U. Mechold, M. Cashel, K. Steiner, D. Gentry, and H. Malke. "Functional analysis of a *relA/spoT* gene homolog from *Streptococcus equisimilis*". In: *Journal of Bacteriology* 178.5 (1996), pp. 1401–1411.

[54] D. Richter. "Uncharged tRNA inhibits guanosine 3′,5′-bis (diphosphate) 3′-pyrophosphohydrolase [ppGppase], the *spoT* gene product, from *Escherichia coli*". In: *Molecular and General Genetics* 178.2 (1980), pp. 325–327.

[55] G. Butland, J. M. Peregrin-Alvarez, J. Li, W. Yang, X. Yang, V. Canadien, A. Starostine, D. Richards, B. Beattie, N. Krogan, M. Davey, J. Parkinson, J. Greenblatt, and A. Emili. "Interaction network containing conserved and essential protein complexes in *Escherichia coli*". In: *Nature* 433.7025 (2005), pp. 531–537. doi: 10.1038/nature03239.

[56] D. I. Chan and H. J. Vogel. "Current understanding of fatty acid biosynthesis and the acyl carrier protein". In: *The Biochemical journal* 430.1 (2010), pp. 1–19. doi: 10.1042/BJ20100462.

[57] D. Gully, D. Moinier, L. Loiseau, and E. Bouveret. "New partners of acyl carrier protein detected in *Escherichia coli* by tandem affinity purification". In: *FEBS Letters* 548.1-3 (2003), pp. 90–96. doi: 10.1016/S0014-5793(03)00746-4.

[58] A. Battesti and E. Bouveret. "Acyl carrier protein/SpoT interaction, the switch linking SpoT-dependent stress response to fatty acid metabolism". In: *Molecular Microbiology* 62.4 (2006), pp. 1048–1063. doi: 10.1111/j.1365-2958.2006.05442.x.

[59] S. Angelini, L. My, and E. Bouveret. "Disrupting the acyl carrier protein/SpoT interaction *in vivo*: Identification of ACP residues involved in the interaction and consequence on growth". In: *PLoS ONE* 7.4 (2012). doi: 10.1371/journal.pone.0036111.

[60] P. Wout, K. Pu, S. M. Sullivan, V. Reese, S. Zhou, B. Lin, and J. R. Maddock. "The *Escherichia coli* GTPase CgtAE cofractionates with the 50S ribosomal subunit and interacts with SpoT, a ppGpp synthetase/hydrolase". In: *Journal of Bacteriology* 186.16 (2004), pp. 5249–5257.

[61] M. Jiang, S. M. Sullivan, P. K. Wout, and J. R. Maddock. "G-protein control of the ribosome-associated stress response protein SpoT". In: *Journal of Bacteriology* 189.17 (2007), pp. 6140–6147.

[62] R. Dutkiewicz, M. Slominska, G. Wegrzyn, and A. Czyz. "Overexpression of the cgtA (yhbZ, obgE) gene, coding for an essential GTP-binding protein, impairs the regulation of chromosomal functions in *Escherichia coli*". In: *Current Microbiology* 45.6 (2002), pp. 440–445.

[63] J. J. Foti, J. Schienda, V. A. Sutera, and S. T. Lovett. "A bacterial G protein-mediated response to replication arrest". In: *Molecular Cell* 17.4 (2005), pp. 549–560.

[64] G. Kobayashi, S. Moriya, and C. Wada. "Deficiency of essential GTP-binding protein ObgE in *Escherichia coli* inhibits chromosome partition". In: *Molecular Microbiology* 41.5 (2001), pp. 1037–1051.

[65] A. Sato, G. Kobayashi, H. Hayashi, H. Yoshida, A. Wada, M. Maeda, S. Hiraga, K. Takeyasu, and C. Wada. "The GTP binding protein Obg homolog ObgE is involved in ribosome maturation". In: *Genes to Cells* 10.5 (2005), pp. 393–408.

[66] N. S. Persky, D. J. Ferullo, D. L. Cooper, H. R. Moore, and S. T. Lovett. "The ObgE/CgtA GTPase influences the stringent response to amino acid starvation in *Escherichia coli*". In: *Molecular Microbiology* 73.2 (2009), pp. 253–266.

[67] M. Jiang, K. Datta, A. Walker, J. Strahler, P. Bagamasbad, P. C. Andrews, and J. R. Maddock. "The *Escherichia coli* GTPase CgtAE is involved in late steps of large ribosome assembly". In: *Journal of Bacteriology* 188.19 (2006), pp. 6757–6770.

[68] M. Vercruysse, C. Kohrer, Y. Shen, S. Proulx, A. Ghosal, B. W. Davies, U. L. RajBhandary, and G. C. Walker. "Identification of YbeY-Protein Interactions Involved in 16S rRNA Maturation and Stress Regulation in *Escherichia coli*". In: *mBio* 7.6 (2016), pp. 1–13.

[69] A. Wood, S. E. Irving, D. J. Bennison, and R. M. Corrigan. "The (p)ppGpp-binding GTPase Era promotes rRNA processing and cold adaption in *Staphylococcus aureus*". In: *PLoS Genetics* 15 (8 2019), pp. 1–23.

[70] J.-W. Lee, Y.-H. Park, and Y.-J. Seok. "Rsd balances (p)ppGpp level by stimulating the hydrolase activity of SpoT during carbon source downshift in *Escherichia coli*". In: *Proceedings of the National Academy of Sciences* 115.29 (2018), pp. 6845–6854.

[71] J. Deutscher, F. M. D. Aké, M. Derkaoui, A. C. Zébré, T. N. Cao, H. Bouraoui, T. Kentache, A. Mokhtari, E. Milohanic, and P. Joyet. "The Bacterial Phosphoenolpyruvate:Carbohydrate Phosphotransferase System: Regulation by Protein Phosphorylation and Phosphorylation-Dependent Protein-Protein Interactions". In: *Microbiology and Molecular Biology Reviews* 78.2 (2014), pp. 231–256.

[72] E. Germain, P. Guiraud, D. Byrne, B. Douzi, M. Djendli, and E. Maisonneuve. "YtfK activates the stringent response by triggering the alarmone synthetase SpoT in *Escherichia coli*". In: *Nature Communications* 10.1 (2019), pp. 1–12.

[73] M. Roghanian, S. Semsey, A. Løbner-olesen, and F. Jalalvand. "(p)ppGpp-mediated stress response induced by defects in outer membrane biogenesis and ATP production promotes survival in *Escherichia coli*". In: 9 (2019), pp. 1–11.

[74] Y. Zhang, E. Zbornikova, D. Rejman, and K. Gerdes. "Novel (p)ppGpp Binding and Metabolizing Proteins of *Escherichia coli*". In: *mBio* 9.2 (2018), pp. 1–20.

[75] P. Sanchez-Vazquez, C. N. Dewey, N. Kitten, W. Ross, and R. L. Gourse. "Genome-wide effects on *Escherichia coli* transcription from ppGpp binding to its two sites on RNA polymerase". In: *Proceedings of the National Academy of Sciences* (2019).

[76] W. Ross, P. Sanchez-Vazquez, A. Y. Chen, J. H. Lee, H. L. Burgos, and R. L. Gourse. "ppGpp binding to a site at the RNAP-DksA interface accounts for its dramatic effects on transcription initiation during the stringent response". In: *Molecular Cell* 62.6 (2016), pp. 811–823. doi: 10.1016/j.molcel.2016.04.029.

[77] D. Duchi, A. Mazumder, A. M. Malinen, R. H. Ebright, and A. N. Kapanidis. "The RNA polymerase clamp interconverts dynamically among three states and is stabilized in a partly closed state by ppGpp". In: *Nucleic Acids Research* 46.14 (2018), pp. 7284–7295.

[78] V. Molodtsov, E. Sineva, L. Zhang, X. Huang, M. Cashel, S. E. Ades, and K. S. Murakami. "Allosteric effector ppGpp potentiates the inhibition of transcript initiation by DksA". In: *Molecular Cell* 69.5 (2018), pp. 828–839.

[79] B. J. Paul, M. M. Barker, W. Ross, D. A. Schneider, C. Webb, J. W. Foster, and R. L. Gourse. "DksA: A Critical Component of the Transcription Initiation Machinery that Potentiates the Regulation of rRNA Promoters by ppGpp and the Initiating NTP". In: *Cell* 118 (2004), pp. 311–322.

[80] D. Vinella, K. Potrykus, H. Murphy, and M. Cashel. "Effects on growth by changes of the balance between GreA, GreB, and DksA suggest mutual competition and functional redundancy in *Escherichia coli*". In: *Journal of Bacteriology* 194.2 (2012), pp. 261–273.

[81] L. Fernández-Coll and M. Cashel. "Contributions of SpoT hydrolase, SpoT synthetase, and RelA synthetase to carbon source diauxic growth transitions in *Escherichia coli*". In: *Frontiers in Microbiology* 9.AUG (2018), pp. 1–13.

[82] S. Osterberg, T. del Peso-Santos, and V. Shingler. "Regulation of alternative sigma factor use". In: *Annual Review of Microbiology* 65 (2011), pp. 37–55.

[83] S. Gopalkrishnan, H. Nicoloff, and S. E. Ades. "Co-ordinated regulation of the extracytoplasmic stress factor, sigmaE, with other *Escherichia coli* sigma factors by (p)ppGpp and DksA may be achieved by specific regulation of individual holoenzymes". In: *Molecular Microbiology* 93 (3 2014), pp. 479–493.

[84] D. Pupov, I. Petushkov, D. Esyunina, K. S. Murakami, and A. Kulbachinskiy. "Region 3.2 of the σ factor controls the stability of rRNA promoter complexes and potentiates their repression by DksA". In: *Nucleic Acids Research* 46.21 (2018), pp. 11477–11487.

[85] B. Gummesson, L. U. Magnusson, M. Lovmar, K. Kvint, O. Persson, M. Ballesteros, A. Farewell, and T. Nystrom. "Increased RNA polymerase availability directs resources towards growth at the expense of maintenance". In: 28.15 (2009), pp. 2209–2219.

[86] L. U. Magnusson, T. Nystrom, and A. Farewell. "Underproduction of σ^{70} mimics a stringent response". In: *Journal of Biological Chemistry* 278.2 (2003), pp. 968–973.

[87] M. Mauri and S. Klumpp. "A model for sigma factor competition in bacterial cells". In: *PLoS Computation Biology* 10 (10 2014), pp. 1–16.

[88] M. E. Girard, S. Gopalkrishnan, E. D. Grace, J. A. Halliday, R. L. Gourse, and C. Herman. "DksA and ppGpp regulate the σ^S stress response by activating promoters for the small RNA DsrA and the anti-adaptor protein IraP". In: *Journal of Bacteriology* 200 (2 2017), pp. 1–12.

[89] V. Kamarthapu and E. Nudler. "Rethinking transcription coupled DNA repair". In: *Current Opinion in Microbiology* 24 (2015), pp. 15–20.

[90] M. A. Sorensen, K. F. Jensen, and S. Pedersen. "High Concentrations of ppGpp Decrease the RNA Chain Growth Rate: Implications for Protein Synthesis and Translational Fidelity During Amino Acid Starvation in *Escherichia coli*". In: *Journal of Molecular Biology* 236 (1994), pp. 441–454.

[91] S. Iyer, D. Le, B. R. Park, and M. Kim. "Distinct mechanisms coordinate transcription and translation under carbon and nitrogen starvation in *Escherichia coli*". In: *Nature Microbiology* 3.6 (2018), pp. 741–748. doi: 10.1038/s41564-018-0161-3.

[92] V. Kamarthapu, V. Epshtein, B. Benjamin, S. Proshkin, A. Mironov, M. Cashel, and E. Nudler. "ppGpp couples transcription to DNA repair in *E. coli*". In: *Science* 352.6288 (2016), pp. 993–996.

[93] A. Rasouly, B. Pani, and E. Nudler. "A Magic Spot in Genome Maintenance". In: *Cell Trends in Genetics* 33.1 (2017), pp. 58–67.

[94] J. Ryals, R. Little, and H. Bremer. "Control of ribosomal-RNA and transfer-RNA syntheses in *Escherichia coli* by guanosine tetraphosphate". In: *Journal of Bacteriology* 151.3 (1982), pp. 1261–1268.

[95] J. J. Lemke, P. Sanchez-Vazquez, H. L. Burgos, G. Hedberg, W. Ross, and R. L. Gourse. "Direct regulation of *Escherichia coli* ribosomal protein promoters by the transcription factors ppGpp and DksA". In: *Proceedings of the National Academy of Sciences* 108.14 (2011), pp. 5712–5717.

[96] H. L. Burgos, K. O'Connor, P. Sanchez-Vazquez, and R. L. Gourse. "Roles of Transcriptional and Translational Control Mechanisms in Regulation of Ribosomal Protein Synthesis in *Escherichia coli*". In: *Journal of Bacteriology* 199.21 (2017), e00407–17.

[97] M. F. Traxler, D.-E. Chang, and T. Conway. "Guanosine 3',5'-bipyrophosphate coordinates global gene expression during glucose-lactose diauxie in *Escherichia coli*". In: *Proceedings of the National Academy of Sciences* 103.7 (2006), pp. 2374–2379.

[98] M. F. Traxler, S. M. Summers, H. T. Nguyen, V. M. Zacharia, G. A. Hightower, J. T. Smith, and T. Conway. "The global, ppGpp-mediated stringent response to amino acid starvation in *Escherichia coli*". In: *Molecular Microbiology* 68.5 (2008), pp. 1128–1148.

[99] M. F. Traxler, V. M. Zacharia, S. Marquardt, S. M. Summers, H.-T. Nguyen, S. E. Stark, and T. Conway. "Discretely calibrated regulatory loops controlled by ppGpp partition gene induction across the 'feast to famine' gradient in *Escherichia coli*". In: *Molecular microbiology* 79.4 (2011), pp. 830–45.

[100] A. Wahl, L. My, R. Dumoulin, J. N. Sturgis, and E. Bouveret. "Antagonistic regulation of *dgkA* and *plsB* genes of phospholipid synthesis by multiple stress responses in *Escherichia coli*". In: *Molecular Microbiology* 80.5 (2011), pp. 1260–1275.

[101] U. Kanjee, K. Ogata, and W. A. Houry. "Direct binding targets of the stringent response alarmone (p)ppGpp". In: *Molecular Microbiology* 85.6 (2012), pp. 1029–1043.

[102] R. M. Corrigan, L. E. Bellows, A. Wood, and A. Gründling. "ppGpp negatively impacts ribosome assembly affecting growth and antimicrobial tolerance in Gram-positive bacteria". In: *Proceedings of the National Academy of Sciences* 113.12 (2016), pp. 1710–1719.

[103] B. Wang, P. Dai, D. Ding, A. D. Rosario, R. A. Grant, B. L. Pentelute, and M. T. Laub. "Affinity-based capture and identification of protein effectors of the growth regulator ppGpp". In: *Nature Chemical Biology* (2018). doi: 10.1038/s41589-018-0183-4.

[104] T. J. Santangelo and I. Artsimovitch. "Termination and antitermination: RNA polymerase runs a stop sign". In: *Nature Reviews Microbiology* 9.5 (2011), pp. 319–329.

[105] K. S. Murakami. "Structural Biology of Bacterial RNA Polymerase". In: *Biomolecules* 5.2 (2015), pp. 848–864.

[106] Y.-M. Zhang and C. O. Rock. "Glycerolipids Acyltransferases in bacterial glycerophospholipid synthesis". In: *Journal of Lipid Research* 49.9 (2008), pp. 1867–1874.

[107] M. V. Rodnina. "The ribosome in action: Tuning of translational efficiency and protein folding". In: *Protein Science* 25.8 (2016), pp. 1390–1406. doi: 10.1002/pro.2950.

[108] T. K. Wood and S. Song. "Forming and waking dormant cells: The ppGpp ribosome dimerization persister model". In: *Biofilm* 2 (2020), pp. 1–6.

[109] D. J. Bennison, S. E. Irving, and R. M. Corrigan. "The Impact of the Stringent Response on TRAFAC GTPases and Prokaryotic Ribosome Assembly". In: *Cells* 8.11 (2019), pp. 1–24.

[110] M. R. Gibbs, K.-M. Moon, M. Chen, R. Balakrishnan, L. J. Foster, and K. Fredrick. "Conserved GTPase LepA (Elongation Factor 4) functions in biogenesis of the 30S subunit of the 70S ribosome". In: *Proceedings of the National Academy of Sciences* 114.5 (2017), pp. 980–985.

[111] A. Bharat and E. D. Brown. "Phenotypic investigations of the depletion of EngA in *Escherichia coli* are consistent with a role in ribosome biogenesis". In: *FEMS Microbiology Letters* 353.1 (2014), pp. 26–32.

[112] R. Troesch and F. Willmund. "The conserved theme of ribosome hibernation: from bacteria to chloroplasts of plants". In: *Biological Chemistry* 400.7 (2019), pp. 879–893.

[113] K. Johnsen, S. Molin, O. Karlstrom, and O. Maaloe. "Control of protein synthesis in *Escherichia coli*: analysis of an energy source shift-down". In: *Journal of Bacteriology* 131.1 (1977), pp. 18–29.

[114] U. Vogel and K. F. Jensen. "Effects of guanosine 3',5'-bisdiphosphate (ppGpp) on rate of transcription elongation in isoleucine-starved Escherichia coli". In: *Journal of Biological Chemistry* 269.23 (1994), pp. 16236–16241. issn: 00219258.

[115] P. Milon, E. Tischenko, J. Tomsic, E. Caserta, G. Folkers, A. La Teana, M. V. Rodnina, C. L. Pon, R. Boelens, and C. O. Gualerzi. "The nucleotide-binding site of bacterial translation initiation factor 2 (IF2) as a metabolic sensor". In: *Proceedings of the National Academy of Sciences* 103.38 (2006), pp. 13962–13967.

[116] V. A. Mitkevich, A. Ermakov, A. A. Kulikova, S. Tankov, V. Shyp, A. Soosaar, T. Tenson, A. A. Makarov, M. Ehrenberg, and V. Hauryliuk. "Thermodynamic Characterization of ppGpp Binding to EF-G or IF2 and of Initiator tRNA Binding to Free IF2 in the Presence of GDP, GTP or ppGpp". In: *Journal of Molecular Biology* 402.5 (2010), pp. 838–846. doi: 10.1016/j.jmb.2010.08.016.

[117] D. B. Dix and R. C. Thompson. "Elongation factor Tu-guanosine 3′-diphosphate 5′-diphosphate complex increases the fidelity of proofreading in protein biosynthesis: Mechanism for reducing translational errors induced by amino acid starvation". In: *Proceedings of the National Academy of Sciences* 83 (1986), pp. 2027–2031.

[118] A. M. Rojas and M. Ehrenberg. "How does ppGpp affect translational accuracy in the stringent response?" In: *Biochimie* 73.5 (1991), pp. 599–605. doi: 10.1016/0300-9084(91)90028-Y.

[119] J. A. Gallant and D. Foley. "Stringent control of translational accuracy". In: *Regulation of macromolucular synthesis by low molecular weight mediators*. 1979.

[120] P. Edelmann and J. Gallant. "Mistranslation in *E. coli*". In: *Cell* 10.1 (1977), pp. 131–137. doi: 10.1016/0092-8674(77)90147-7.

[121] P. H. OFarrell. "The suppression of defective translation by ppGpp and its role in the stringent response". In: *Cell* 14.3 (1978), pp. 545–557. doi: 10.1016/0092-8674(78)90241-6.

[122] K. Kihira, Y. Shimizu, Y. Shomura, N. Shibata, M. Kitamura, A. Nakagawa, T. Ueda, K. Ochi, and Y. Higuchi. "Crystal structure analysis of the translation factor RF3 (release factor 3)". In: *FEBS Letters* 586.20 (2012), pp. 3705–3709.

[123] D. S. Vinogradova, V. Zegarra, E. Maksimova, J. A. Nakamoto, P. Kasatsky, A. Paleskava, A. L. Konevega, and P. Milón. "How the initiating ribosome copes with ppGpp to translate mRNAs". In: *PLOS Biology* 18.1 (2020), pp. 1–25.

[124] E. Hamel and M. Cashel. "Guanine nucleotides in protein synthesis". In: *Archives of Biochemistry and Biophysics* 162.1 (1974), pp. 293–300.

[125] A. Gao, N. Vasilyev, A. Kaushik, W. Duan, and A. Serganov. "Principles of RNA and nucleotide discrimination by the RNA processing enzyme RppH". In: *Nucleic Acids Research* (2020). doi: https://doi.org/10.1093/nar/gkaa024.

[126] M. Taguchi, K. Izui, and H. Katsuki. "Activation of *Escherichia coli* phosphoenolpyruvate carboxylase by guanosine-5′-diphosphate-3′-diphosphate". In: *FEBS Letters* 77.2 (), pp. 270–272.

[127] M. Taguchi, K. Izui, and H. Katsuki. "Stringent control of glycolysis in *Escherichia coli*". In: *Biochemical and Biophysical Research Communications* 84.1 (1978), pp. 195–201.

[128] C. C. Pao and B. T. Dyess. "Effect of unusual guanosine nucleotides on the activities of some *Escherichia coli* cellular enzymes". In: *Biochimica et Biophysica Acta* 677 (1981), pp. 358–362.

[129] E. Hölttä, J. Jänne, and J. Pispa. "The regulation of polyamine synthesis during the stringent control in *Escherichia coli*". In: *Biochemical and Biophysical Research Communications* 59.3 (1974), pp. 1104–1111.

[130] T. T. Sakai and S. S. Cohen. "Regulation of ornithine decarboxylase activity by guanine nucleotides: *in vivo* test in potassium-depleted *Escherichia coli*". In: *Proceedings of the National Academy of Sciences* 73.10 (1976), pp. 3502–3505.

[131] U. Kanjee, I. Gutsche, S. Ramachandran, and W. A. Houry. "The enzymatic activities of the *Escherichia coli* basic aliphatic amino acid decarboxylases exhibit a pH zone of inhibition". In: *Biochemistry* 50 (2011), pp. 9388–9398.

[132] U. Kanjee, I. Gutsche, E. Alexopoulos, B. Zhao, M. El Bakkouri, G. Thibault, K. Liu, S. Ramachandran, J. Snider, E. F. Pai, and W. A. Houry. "Linkage between the bacterial acid stress and stringent responses: the structure of the inducible lysine decarboxylase". In: *EMBO Journal* 30.5 (2011), pp. 931–944.

[133] D. P. Morton and S. M. Parsons. "Synergistic inhibition of ATP phosphoribosyltransferase by guanosine tetraphosphate and histidine". In: *Biochemical and Biophysical Research Communications* 74.1 (1977), pp. 172–177.

[134] J. Yuan, C. D. Doucette, W. U. Fowler, X.-j. Feng, M. Piazza, H. A. Rabitz, N. S. Wingreen, and J. D. Rabinowitz. "Metabolomics-driven quantitative analysis of ammonia assimilation in *E . coli*". In: *Molecular Systems Biology* 5.302 (2009), pp. 1–16. doi: 10.1038/msb.2009.60.

[135] M. R. Maurizi and F. Rasulova. "Degradation of Glutamate Dehydrogenase from *Escherichia coli*: Allosteric Regulation of Enzyme Stability". In: *Archives of Biochemistry and Biophysics* 397.2 (2002), pp. 206–216.

[136] J. P. Merlie and L. I. Pizer. "Regulation of Phospholipid Synthesis in *Escherichia coli* by Guanosine Tetraphosphate". In: *Journal of Bacteriology* 116.1 (1973), pp. 355–366.

[137] D. R. Lueking and H. Goldfine. "The involvement of guanosine 5-diphosphate-3-diphosphate in the regulation of phospholipid biosynthesis in *Escherichia coli*. Lack of ppGpp inhibition of acyltransfer from acyl-ACP to sn-glycerol 3-phosphate". In: *Journal of Biological Chemistry* 250 (1975), pp. 4911–4917.

[138] W. D. Nunn and J. E. Cronan. "Regulation of membrane phospholipid synthesis by the *relA* gene: dependence on ppGpp levels". In: *Biochemistry* 15.12 (1976), pp. 2546–2550.

[139] R. J. Heath, S. Jackowski, and C. O. Rock. "Guanosine tetraphosphate inhibition of fatty acid and phospholipid synthesis in *Escherichia coli* is relieved by overexpression of glycerol-3-phosphate acyltransferase (*plsB*)". In: *Journal of Bacteriology* 269.42 (1994), pp. 26584–26590.

[140] S. E. Polakis, R. B. Guchhait, and M. D. Lane. "Stringent control of fatty acid synthesis in *Escherichia coli*". In: *Journal of Biological Chemistry* 248.22 (1973), pp. 7957–7966.

[141] A. Spencer, E. Muller, J. E. Cronan, and T. A. Gross. "*relA* gene control of the synthesis of lipid A fatty acyl moieties". In: *Journal of Bacteriology* 130.1 (1977), pp. 114–117.

[142] J. P. Stein and K. E. Bloch. "Inhibition of *E.coli* β-hydroxydecanoyl thioester dehydrase by ppGpp". In: *Biochemical and Biophysical Research Communications* 73.4 (1976), pp. 881–884.

[143] E. E. Ishiguro and W. D. Ramey. "Stringent control of peptidoglycan biosynthesis in *Escherichia coli* K-12". In: *Journal of Bacteriology* 127.3 (1976), pp. 1119–1126.

[144] E. E. Ishiguro and W. D. Ramey. "Involvement of the *relA* gene product and feedback inhibition in the regulation of DUP-N-acetylmuramyl-peptide synthesis in *Escherichia coli*". In: *Journal of Bacteriology* 135.3 (1978), pp. 766–774.

[145] W. D. Ramey and E. E. Ishiguro. "Site of Inhibition of Peptidoglycan Biosynthesis During the Stringent Response in *Escherichia coli*". In: *Journal of Bacteriology* 135.1 (1978), pp. 71–11.

[146] E. E. Ishiguro, D. Mirelman, and R. E. Harkness. "Regulation of the terminal streps in peptidoglycan biosynthesis in ether-treated cells of *Escherichia coli*". In: *FEBS Letters* 120.2 (1980), pp. 175–178.

[147] T. Yamaguchi, K. I. Iida, S. Shiota, H. Nakayama, and S. I. Yoshida. "Elevated guanosine 5′-diphosphate 3′-diphosphate level inhibits bacterial growth and interferes with FtsZ assembly". In: *FEMS microbiology letters* 362.23 (2015).

[148] J. Kraemer, A. Sanderlin, and M. Laub. "The stringent response inhibits DNA replication initiation in *E. coli* by modulating supercoiling of *oriC*". In: *mBio* 10 (4 2019), pp. 1–18.

[149] J. DeNapoli, A. K. Tehranchi, and J. D. Wang. "Dose-dependent reduction of replication elongation rate by (p)ppGpp in *Escherichia coli* and *Bacillus subtilis*". In: *Molecular Microbiology* 88.1 (2013), pp. 93–104.

[150] M. Maciąg-Dorszyńska, A. Szalewska-Pałasz, and G. Węgrzyn. "Different effects of ppGpp on *Escherichia coli* DNA replication *in vivo* and *in vitro*." In: *FEBS open bio* 3 (2013), pp. 161–4.

[151] M. Maciag, M. Kochanowska, R. Lyzen, G. Wegrzyn, and A. Szalewska-Palasz. "ppGpp inhibits the activity of *Escherichia coli* DnaG primase". In: *Plasmid* 63 (1 2010), pp. 61–67.

[152] R. U. Rymer, F. A. Solorio, A. K. Tehranchi, C. Chu, J. E. Corn, J. L. Keck, J. D. Wang, and J. M. Berger. "Binding Mechanism of Metal·NTP Substrates and Stringent-Response Alarmones to Bacterial DnaG-Type Primases". In: *Cell* 20.9 (2012), pp. 1478–1489.

[153] J. Gallant, J. Irr, and M. Cashel. "The mechanism of amino acid control of guanylate and adenylate biosynthesis". In: *Journal of Biological Chemistry* 246.18 (1971), pp. 5812–5816.

[154] M. M. Stayton and H. J. Fromm. "Guanosine 5'-diphosphate-3'-diphosphate inhibition of adenylosuccinate synthetase". In: *Journal of Biological Chemistry* 254 (1979), pp. 2579–2581.

[155] J. Hochstadt-Ozer and M. Cashel. "The Regulation of Purine Utilization in Bacteria. V. Inhibition of purine phosphoribosyltransferase activities and purine uptake in isolated membrane vesicles by guanosine tetraphosphate". In: *Journal of Biological Chemistry* 247 (1972), pp. 7067–7072.

[156] R. Fast and O. Skold. "Biochemical mechanism of uracil uptake regulation in *Escherichia coli* B". In: *Journal of Biological Chemistry* 252.21 (1977), pp. 7620–7624.

[157] K. F. Jensen and B. Mygind. "Different Oligomeric States are Involved in the Allosteric Behavior of Uracil Phosphoribosyltransferase from *Escherichia coli*". In: *European Journal of Biochemistry* 240.3 (1996), pp. 637–645.

[158] Y. E. Zhang, R. L. Baerentsen, T. Fuhrer, U. Sauer, K. Gerdes, and D. E. Brodersen. "(p)ppGpp Regulates a Bacterial Nucleosidase by an Allosteric Two-Domain Switch". In: *Molecular Cell* 74.6 (2019), pp. 1239–1249.

[159] D. N. Dietzler and M. P. Leckie. "Regulation of ADP-glucose synthetase, the rate-limiting enzyme of bacterial glycogen synthesis, by the pleiotropic nucleotides ppGpp and pppGpp". In: *Biochemical and Biophysical Research Communications* 77.4 (1977), pp. 1459–1467.

[160] M. P. Leckie, V. L. Tieber, S. E. Porter, and D. N. Dietzler. "The *relA* gene is not required for glycogen accumulation during NH4+ starvation of *Escherichia coli*". In: *Biochemical and Biophysical Research Communications* 95.3 (1980), pp. 924–931.

[161] J. Preiss. "Bacterial glycogen synthesis and its regulation". In: *Annual Review of Microbiology* 38 (1984), pp. 419–458.

[162] M. J. Gray. "Inorganic Polyphosphate Accumulation in *Escherichia coli* Is Regulated by DksA but Not by (p)ppGpp". In: *Journal of Bacteriology* 201.9 (2019), pp. 1–20.

[163] G. V. Smirnova, A. V. Tyulenev, N. G. Muzyka, and O. N. Oktyabrsky. "The sharp phase of respiratory inhibition during amino acid starvation in *Escherichia coli* is RelA-dependent and associated with regulation of ATP synthase activity". In: *Research in Microbiology* 169.3 (2018), pp. 157–165.

[164] D. Nowicki, M. Maciąg-Dorszyńska, W. Kobiela, A. Herman-Antosiewicz, A. Węgrzyn, A. Szalewska-Pałasz, and G. Węgrzyn. "Phenethyl isothiocyanate inhibits shiga toxin production in enterohemorrhagic *Escherichia coli* by stringent response induction". In: *Antimicrobial agents and chemotherapy* 58.4 (2014), pp. 2304–2315.

[165] J. K. Hobbs and A. B. Boraston. "(p)ppGpp and the Stringent Response: An Emerging Threat to Antibiotic Therapy". In: *ACS Infectious Diseases* 5.9 (2019), pp. 1505–1517.

[166] W. B. Schofield, M. Zimmermann-Kogadeeva, M. Zimmermann, N. A. Barry, and A. L. Goodman. "The Stringent Response Determines the Ability of a Commensal Bacterium to Survive Starvation and to Persist in the Gut". In: *Cell Host & Microbe* 24.1 (2018), pp. 120–132.

[167] Z. D. Dalebroux, S. L. Svensson, E. C. Gaynor, and M. S. Swanson. "ppGpp Conjures Bacterial Virulence". In: *Microbiology and Molecular Biology Reviews* 74.2 (2010), pp. 171–199.

[168] B. T. Burlingham and T. S. Widlanski. "An intuitive look at the relationship of Ki and IC50: a more general use for the dixon plot". In: *Concepts in Biochemistry* 80.2 (2003), p. 2.

[169] V. Varik, S. R. A. Oliveira, V. Hauryliuk, and T. Tenson. "HPLC-based quantification of bacterial housekeeping nucleotides and alarmone messengers ppGpp and pppGpp". In: *Scientific Reports* 7.1 (2017), pp. 1–12. doi: 10.1038/s41598-017-10988-6.

[170] B. D. Bennett, E. H. Kimball, M. Goa, R. Osterhout, S. J. Van Dien, and J. D. Rabinowitz. "Absolute metabolite concentrations and implied enzyme active site occupancy in *Escherichia coli*". In: *Nature Chemical Biology* 5.8 (2009), pp. 593–599.

[171] E. Reznik, D. Christodoulou, J. E. Goldford, E. Briars, U. Sauer, D. Segrè, and E. Noor. "Genome-Scale Architecture of Small Molecule Regulatory Networks and the Fundamental Trade-Off between Regulation and Enzymatic Activity". In: *Cell Reports* 20.11 (2017), pp. 2666–2677.

[172] W. Mohr D. adn Wintermeyer and M. V. Rodnina. "Arginines 29 and 59 of elongation factor G are important for GTP hydrolysis or translocation on the ribosome". In: *The EMBO Journal* 19.13 (2000), pp. 3458–3464.

[173] J. Beljantseva, S. Kudrin P. andJimmy, M. Ehn, R. Pohl, V. Varik, Y. Tozawa, V. Shingler, T. Tenson, D. Rejman, and V. Hauryliuk. "Molecular mutagenesis of ppGpp: turning a RelA activator into an inhibitor". In: *Scientific Reports* 7.1 (2017), pp. 1–10.

[174] G. S. Kushwaha, B. F. Oyeyemi, and N. S. Bhavesh. "Stringent response protein as a potential target to intervene persistent bacterial infection". In: *Biochimie* 165 (2019), pp. 67–75.

[175] B. Volkmer and M. Heinemann. "Condition-dependent cell volume and concentration of *Escherichia coli* to facilitate data conversion for systems biology modeling". In: *PLoS ONE* 6.7 (2011), pp. 1–6.

2

Development of an LC-MS method for measurement of ppGpp and other metabolites in *E. coli*

The signaling molecule guanosine tetraphosphate (ppGpp), present in nearly all bacteria, is known to be key to the regulation of bacterial growth rate. ppGpp likely balances the various metabolic fluxes in the cell, optimizing the growth rate in a given environment. How the ppGpp signaling network achieves this is still a mystery. To completely understand what ppGpp does in the cell, it is vital to accurately quantify it, which is impeded by ppGpp's fast dynamics and instability, and still today a limiting factor in ppGpp research. Here, we developed a LC-MS method to quantify ppGpp in E. coli, ranging from basal to stringent levels. Several other important metabolites and signaling molecules such as ATP, GTP, acetyl-CoA and cAMP were included to investigate the physiological state of the cell, or to understand the link between ppGpp and its substrates or degradation products. The LC-MS method was assessed in situations with well-known fluctuations in ppGpp levels, namely amino acid starvation, diauxic shift and RelA induction, as well as basal growth in various carbon sources.

Part of this chapter has been published as: N. C. E. Imholz, M. J. Noga, N. J. F. van den Broek, and G. Bokinsky. "Calibrating the bacterial growth rate speedometer: a re-evaluation of the relationship between basal ppGpp, growth, and RNA synthesis in *Escherichia coli*". In: *Frontiers in Microbiology* (2020). doi: 10.3389/fmicb.2020.574872

2.1. Introduction

The current literature suggests that the effect of ppGpp on cellular processes depends on its intracellular concentration. Slight differences of a few pmol OD^{-1} appear to dramatically affect *E. coli*'s growth rate [2, 3]. In addition, potential ppGpp levels span a range of less than 10 to over 1000 pmol OD^{-1}. In order to understand the role of ppGpp in *E. coli* in both stress conditions as well as steady state growth, it needs to be accurately quantified. Moreover, absolute quantitation is vital as it allows a better comparison of data between research groups as well as quantitative modelling, which helps to understand biological systems.

The main challenges in measuring ppGpp levels *in vivo* are 1) its low abundance during steady state growth compared to other nucleotides; 2) the chemical instability of the two diphosphate groups prone to hydrolysis and 3) the presence of intracellular enzymes that rapidly hydrolyze and synthesize ppGpp depending on environmental conditions. This means the analytical method to measure intracellular ppGpp levels in a certain condition at a specific time needs to be sensitive, maintain ppGpp stability and immediately denature enzymes that could bias the actual ppGpp levels. Moreover, to study ppGpp dynamics, it is required to sample frequently with a high time resolution (for example few seconds), which reduces the possible sample volume that can be used.

Several methods have been used to measure (p)ppGpp, including radiolabeling combined with thin layer chromatography (TLC) [3–5], high performance liquid chromatography (HPLC) [6–10] and liquid chromatography mass spectrometry (LC-MS) [11, 12]. These and their corresponding benefits and shortcomings are summarized in **Table 2.1**. An excellent detailed overview of current nucleotide analytical methods was made by Varik *et al.* [9].

In short, TLC is the oldest yet still used method because of its simplicity. It consists of spotting cellular extracts on a membrane, which are separated chromatographically based on charge in one dimension and subsequently based on hydrophobicity in a second perpendicular dimension [4]. Detection is based on autoradiography and determining the activity in a given spot with scintillation counting. Hence, the culture must be grown in ^{32}P phosphate with a constant phosphate uptake rate. This unfortunately creates a bias in measuring intracellular nucleotide concentrations under conditions with varying ppGpp levels, as ppGpp affects the uptake of phosphate [13].

HPLC consists of the separation of nucleotides by applying the sample on a column existing of a solid phase. The column is continuously rinsed with a liquid mobile phase, and depending on the preferred interaction with solid or mobile phase, the different compounds (in this case nucleotides) will travel through the column with different velocities. The separated nucleotides are detected by UV light absorption at the end of the column. Standards of the compounds of interest are necessary to determine the exact time it takes each compound to travel through the column

Table 2.1: Comparison of current analytical methods for ppGpp quantification.

Separation + detection method	Equipment needed (excl. sample preparation)	Studies with exemplary methods	Basal ppGpp reported?	Culture volume required (at OD ± 0.5)	Advantages	Disadvantages
TLC + autoradiography	TLC development tank, UV- imager of nucleotide spots, X-ray film cassette and intensifying screens, scintillation counter or imaginer.	[3-5]	Many studies, for broad range of conditions, e.g. [5,35,37].	20 µL [5], 200 µL [3], 1-2 mL [35]	- Small culture volume; - Broad scope of nucleotides detectable with a single method	- Low phosphate concentration in medium (e.g. 0.2 mM vs. 4 mM [4]); - Need radioactivity safety certificate of both lab and scientist (The Netherlands).
HPLC + UV	HPLC with UV-detector, HPLC column	[6,-9]	Yes, e.g. [6-9].	5-10 mL [6], 50 mL at OD 1 [7], 10-40 mL [9]	- Mobile phases can contain (high concentrations of) non-volatile salts, improved separation.	- Large sample volume; - Unspecific identification; - Baseline separation of compounds is necessary for quantitation; - difficult to find a single chromatographic method for both NTP and (p)ppGpp [9]
HPLC + MS	HPLC, HPLC column, mass spectrometer	[11,12]	Twice for one condition [11,12].	Not mentioned [11], 2.8 mL [12]	- High sensitivity; - More accurate identification; - Generally no baseline separation needed. - Isotope-labeled internal standards reduce errors. - Broad scope of nucleotides detectable in a single method.	- Cannot use (standard concentrations) of non-volatile salts for the mobile phase buffer; - Expensive; - Sensitive to sample matrix; - Need internal standard for accurate quantitation.

(called the retention time) and also to make a calibration curve for absolute quantitation of the compound.

LC-MS uses HPLC to separate different compounds, followed by detection via MS instead of UV light. This has several advantages. First, MS is more sensitive [14]. Secondly, MS allows to detect numerous different compounds at the same time as it rapidly scans for specific masses, whereas with UV light any compound that absorbs at the specified wavelength will give a signal. This means that with HPLC baseline separation of different compounds is vital, as overlapping peaks do not allow quantitation. For the same reason, MS provides more certainty of quantifying a specific compound, while UV detection does not identify exactly the compounds it detects. A disadvantage of MS compared to UV detection is that it is a more expensive, complex and less robust system, more prone to technical issues.

Although current methods have successfully characterized (p)ppGpp levels in bacteria in multiple conditions, they have several limitations: 1) they require large sample volumes (10 mL up to 30 mL for exponentially growing cells) which limits the sample number and time resolution; 2) in most cases they lack absolute quantitation enabling only relative quantitation and 3) they use UV light for detection which is inherently less specific than MS. Ihara, Ohta, and Masuda [11] have developed an ion pairing reverse phase ESI QQQ MS/MS method for quantification of ppGpp in plants and *E. coli*. However, the ppGpp concentration in *E. coli* growing in M9 glucose with casamino acids was reported to be about 200 pmol OD^{-1}, which is significantly higher than others have measured, possibly caused by insufficiently fast quenching.

Recently Jin *et al.* [10] have developed the first UHPLC-HILIC method to separate nucleotides including ppGpp with a limit of detection of 50 nM. This method was tested on algae, which have lower ppGpp levels compared to bacteria (3 pmol g^{-1} algae). The method was however not tested on bacteria, which would be promising. Interestingly, through the use of ion chromatography high resolution MS with double isotopic labeling, Patacq, Chaudet, and Letisse [12] could measure ppGpp as well as pppGpp with correction for degradation of pppGpp into ppGpp during sample preparation. Unfortunately, this method was only used to test the response of *E. coli* to serine hydroxamate. Other analytical methods rely on the interaction between Cu^{2+} ions and ppGpp in a colorimetric assay based on modified gold nanoparticles [15] or fluorescent silver nanoclusters [16]. The ease, low price, lack of complex equipment and speed make these assays very attractive. However, they lack the sensitivity to detect basal ppGpp levels in *B. subtilis* [15] or have not been used in a biological matrix [16].

Clearly analytical methods for (p)ppGpp are still being developed and are promising, yet have not been tested in various conditions and concentration ranges. Many questions remain unanswered because of these technical limitations. What is the behaviour of ppGpp in different exponential growth or non-stress conditions? What are the dynamics of ppGpp and other nucleotides in changing environmental conditions? Do discrepancies in ppGpp data have a technical or biological (strain-related)

origin? As described in this chapter, the current challenges were overcome with a LC-MS method that allows more sensitive, specific and absolute quantitation than reported so far, with a time resolution of up to 30 s.

2.2. Materials and methods

Chemicals

All chemicals for LC-MS purpose (glacial acetic acid, acetonitrile, methanol, formic acid, ammonium acetate) were ULC/MS grade and obtained from Biosolve. Ammonium hydroxide (28-30 %) was obtained from Honeywell and acetylacetone (AnalaR Normapur) from VWR. $^{15}NH_4Cl$ was obtained from CortecNet. UTP, UDP, UMP, CDP and CMP were obtained from VWR. All other chemicals were obtained from Sigma.

Strains and plasmids

An overview of strains, plasmids and their sources is given in **Table S2.1**. The reader is referred to chapter 4 for construction of plasmid pJEx-RelA*.

Growth media and conditions

The media used were MOPS-based minimal media [17] (**Table S2.2**) with 0.2 % w/v glucose, glycerol, succinate or acetate, and if mentioned all amino acids (**Table S2.3**). The medium for diauxic shift was MOPS-based with 0.03 % glucose and 0.1 % lactose, based on Zaslaver *et al.* [18]. LB was obtained from Sigma. All media were filtered after preparation and before use (0.2 µm pore size). The antibiotics kanamycin (25 µg mL^{-1}) and ampicillin (50 µg mL^{-1}) were added when needed.

Overnight cultures of single colonies were prepared by inoculating a single colony from a freshly streaked LB plate in 5 mL of the medium of choice. After overnight incubation at 37 °C and 250 rpm, these were diluted to OD 0.05 in a total volume of 20 mL and grown in a 250 mL culture flask with a 12 mm magnetic stir bar (VWR). The flasks were placed in a water bath (Grant Instruments Sub Aqua Pro) set at 37 °C on top of a magnetic stir plate (2 mag MIXdrive 1 Eco and MIXcontrol 20) set at 1200 rpm. This set-up allowed to pipette a volume out of the flask without disturbing the conditions. Optical density was measured at 600 nm using an Ultrospec 10 Cell Density Meter (GE Healthcare) to monitor growth.

Sampling *E. coli* cultures

An overview of the sampling and sample preparation is presented in **Figure 2.1** and is based on Bennett *et al.* [19]. Extra detailed recommendation for the rest of the protocol are given in Supplementary section 2.6.1 for those interested.

At the time or OD of choice, 1 mL of the culture was pipetted on top of a prewetted filter (0.2 µm pores, 25 mm, Sartorius), placed on a filter manifold under vacuum. The filter with cells was immediately transferred to a 6-well plate containing 1 mL ice cold 2 M formic acid with the cells facing down to make sure the filter was immediately wetted. Right before sampling, a known amount of ^{14}N internal standard was added to the 1 mL 2 M formic acid solution, as this is necessary for absolute quantitation. The composition of the standard mix is shown in **Table S2.4**. For cells growing in not isotopically labeled medium (^{14}N), a culture grown on ^{15}N medium was used as an internal standard. This ^{15}N labeled culture was grown in parallel with the experiment of interest, filtered and resuspended in ice cold 2 M formic acid solution. This 2 M formic acid solution was subsequently used as quenching solution for the unlabeled ^{14}N culture. Alternatively, the ^{15}N internal standard culture could be neutralized with 27.8 µL 28 % NH_4OH per ml culture, lyophilized and kept at −80 °C. On the day of use, the ^{15}N cell extract would be redissolved in 2 M ice cold formic acid right before use.

Sample preparation

After staying 30 min to 1 h on ice to extract metabolites from the cells, the filters were washed by holding them with a tweezer and pipetting the quenching solution repeatedly over them. The rest of the protocol was based on Ihara, Ohta, and Masuda [11]. The samples were transferred to tubes and neutralized by adding 27.8 µL of 28 % NH_4OH and briefly vortexed. Neutralization is necessary because ppGpp is extra labile in acid [20]. The samples were stored at −80 °C. The samples were thawed in a water bath at 37 °C for 2 min and subsequently sonicated for 10 min on ice. Then, the samples were centrifuged at 15000 g and 4 °C for 10 min to remove any cellular debris.

Hereafter, solid phase extraction (SPE) was performed to remove sample compounds that might cause so called matrix effects [21]. Matrix effects include all potential effects of sample molecules that change the chromatographic separation or ionization of a specific analyte of interest [22]. The most important matrix effect (in our case) was ion suppression: specific matrix compounds suppressing the ionization of the analyte of interest, which decreases sensitivity. Briefly, during electrospray ionization (ESI), the sample is 'sprayed' into tiny charged droplets, in which water and volatile compounds evaporate to leave ionized molecules in the gas phase, which subsequently can be detected by the MS. In various ways, the matrix compounds can deteriorate this process [22]. For example, due to semi-volatile matrix compounds the analyte could precipitate and never reach the gas phase. Matrix compounds can also compete with the analyte to gain charge, preventing

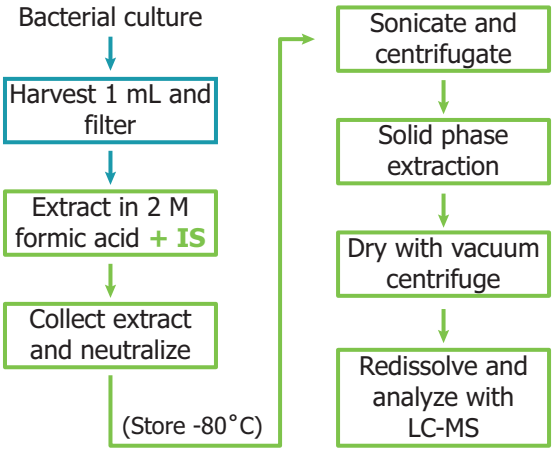

Figure 2.1: Overview of the analytical method to measure ppGpp and nucleotides in *E. coli*. The bacterial culture was growing on $^{15}NH_4Cl$ as only nitrogen source. The steps in green are the ones for which variability is corrected for by the presence of ^{14}N labeled internal standard (IS). In case nitrogen source was more complex (e.g. amino acids medium), the labeling was reversed, and the internal standard was an extract of another culture grown on $^{15}NH_4Cl$.

its detection. Matrix components that increase the surface tension of the droplets might prevent the droplet break into smaller droplets necessary for reaching the gas phase. Therefore, removal of matrix compounds can greatly improve sensitivity.

Hereto, SPE with a weak anion exchanging capacity was used given that all our compounds of interest (nucleotides) possess acidic phosphate groups (pKa = 0.7-1) [23]. The anion exchange occurred at pH 4.5, such that all nucleotides were negatively charged and retained by the column, which is in this range positively charged, whereas all compounds that are neutral or positively charged at this pH (which is the majority of metabolites) would be separated out of the sample [24]. The retained nucleotides can be removed from the column by applying a basic solution that renders the solid phase neutral and thereby breaks the electrostatic interaction.

Using SPE presumably also removes metallic cations from the sample. These are of particular interest because these may form a complex with ppGpp, such as Mg^{2+}-ppGpp, which are not detected by MS (unless included in the transitions). We verified with MS that these adducts were in fact not present after SPE.

In practice, Oasis Wax SPE cartridges (Waters, product number 186002489) were equilibrated with first 1 mL methanol and then 1 mL 50 mM ammonium acetate at pH 4.5. After applying the samples, the SPE cartridges were washed with 1 mL 50 mM ammonium acetate pH 4.5, 1 mL methanol, and dried under vacuum for about 5 min. The sample was eluted with 200 µL 5:3:1:1 of methanol:acetonitrile:water: 28 % NH_4OH. To this 10 µL 5 % trehalose was added. The trehalose was added under

the assumption that it would form hydrogen bonds with ppGpp during the drying [25], which should prevent losses from ppGpp sticking to the tube wall. However, no significant improvement in sensitivity was observed due to trehalose, so this step could be omitted, which was not done for comparability to other data sets acquired within the lab.

After brief vortexing and centrifuging the samples were dried in a vacuum centrifuge for 1 h without heating. No clear or a small transparent pellet was visible. The dried sample was dissolved in 20 µL 5:3:2 methanol:acetonitrile:water. This was centrifuged for 10 min at 15 000 g and 4 °C after which 18 µL of supernatant was transferred to a vial.

LC-MS method

The LC/MS system (Agilent) consisted of a binary pump (G1312B), autosampler (G7167A), temperature-controlled column compartment (G1316A) and triple quadrupole mass spectrometer (G6460C) equipped with a standard ESI source, all operated using MassHunter data acquisition software (version 7.0). 2 µL of the sample was injected onto a iHILIC-fusion column (Hilicon AB, 100 mm length and 2.1 mm internal diameter, 3.5 µm particle size and 100 Å pore diameter) or 3 µL onto a ZIC-cHILIC column (Merck, 100 mm length and 2.1 mm internal diameter, 3 µm particle size and 100 Å pore diameter). For iHILIC the column compartment was set at 20 °C and for cHILIC at 30 °C. Both iHILIC and cHILIC columns were used, but although initial iHILIC columns performed well, batches obtained later from the manufacturer tended to clog easily. Whether this was due to changes to our LC-MS system or due to the manufacturer was not known, but for this reason eventually cHILIC was preferred over iHILIC. Mobile phase A consisted of 3.75 mM ammonium acetate, 1.25 mM acetic acid and 2 mM acetylacetone and mobile phase B of 11.25 mM ammonium acetate, 3.75 mM acetic acid and 2 mM acetylacetone in 80 % acetonitrile. The used gradients and flow rates can be found in **Table S2.5**. Mass spectrometer operated in dynamic MRM mode (EMV+400) set to unit resolution with 1000 ms cycle time and cell accelerator voltage 4, using transitions defined in **Table S2.4**. An example chromatogram of separation of standards within a biological sample can be found in **Figure S2.1**.

LC-MS peak areas were integrated using MassHunter (Agilent). Equation 2.1 was used to calculate the concentration of compound X in the sample (in pmol OD^{-1}), with $^{15N}area_x$ the ^{15}N peak area of compound X, IS_x the amount of compound X in the internal standard in pmol and OD the OD of the sample.

$$[X] = \frac{^{15N}area_x * IS_x}{^{14N}area_x * OD} \tag{2.1}$$

Remark on units used to quantify ppGpp

Depending on the used analytical method, ppGpp amounts or concentrations have been reported as counts per minute (cpm), peak areas and number of moles, which can be divided by OD, dried cell mass or cell volume, or as ratios of other nucleotides (e.g. ppGpp/ppGpp+GTP). Due to the various units, comparison is sometimes difficult. Volkmer and Heinemann [26] addressed this by quantifying both the cell size and the number of cells per OD at various growth rates. They observed that the total intracellular volume of all cells for 1 OD unit in 1 mL culture is more or less constant amongst cells in different growth rates and about 3.6 µL. This way mol OD^{-1} data can be calculated from molarity data and vice versa. Varik *et al.* [9] however did not observe this and calculate molarity from OD data with a different factor. See also section 1.6.1.

2.3. Results and discussion

To validate the developed method, it was tested on *E. coli* growing in various conditions corresponding with a broad range of and dynamic ppGpp levels: 1) amino acid starvation, 2) a glucose to lactose diauxic shift, 3) expression of a (p)ppGpp synthetase RelA and 4) during exponential growth on different carbon sources. For these conditions, it is known from previous studies what the expected range of ppGpp concentrations is. However, amongst these studies there often exist considerable variation in the used method, bacterial strain and measured ppGpp concentration, rendering a direct comparison not necessarily meaningful. This is why multiple different biological conditions were used to validate the method.

2.3.1. Amino acid starvation or stringent response

Excessive valine addition to *E. coli* MG1655 has been known for decades to cause a starvation of isoleucine due to a shared biosynthesis pathway of isoleucine and valine, combined with feedback inhibition of valine upstream of this pathway. The isoleucine starvation ultimately triggers RelA to synthesize ppGpp, resulting in ppGpp levels reported to peak at 800 pmol OD^{-1} [27, 28] (**Figure 2.2A**). We added valine to an exponentially growing culture of *E. coli* MG1655, which leads to rapid growth arrest (**Figure 2.2B**). As shown in **Figure 2.2C**, we observe a ppGpp response that closely matches those reported previously: there is a rapid increase in ppGpp concentration within the first minutes after valine addition, followed by a decrease to a level much higher than the initial basal level. The different strain, media and detection method (radiolabeling) might explain the small difference as here ppGpp peaks at 500 pmol OD^{-1}. Interestingly, the concentrations of all other nucleotides decrease, although at different rates (**Figure 2.2D**). The adenine nucleotide levels decrease linearly, whereas the guanine nucleotide levels decrease exponentially, mirroring the initial decrease in ppGpp concentration.

As a quality control for sampling, extraction and storage it is standard to determine the adenylate energy charge (AEC) [9]:

$$AEC = \frac{ATP + 0.5ADP}{ATP + ADP + AMP} \tag{2.2}$$

The AEC should be between 0.8-0.9 for bacteria [29, 30]. Due to the high intracellular turnover rate of ATP and its unstable phosphoanhydride bond, this ratio is a good measure to verify whether metabolism was quenched rapidly, and whether there were no losses during the acid extraction. In this experiment the AEC was on average 0.94 ± 0.004, which demonstrates the quenching of metabolism was adequate and there were no significant losses of ATP during extraction and storage.

2.3.2. ppGpp levels during diauxic adaptation

When bacteria grow in the presence of several carbon sources, their consumption is sequential, as bacteria will first consume their preferred carbon source (e.g. glucose), followed by the less preferred one (e.g. lactose). As soon as the level of the preferred carbon source no longer supports growth, gene expression is adjusted to metabolize the second source. The phase of arrested growth and adaptation to a different carbon source is what Monod called 'diauxic adaptation' [31] (see growth curves in **Figure 2.3A-B**). During this phase, the sigma factor RpoS initiates the general stress response and the transcription factor CRP (cAMP-responsive protein) orchestrates the increased transcription of enzymes and transporters to metabolize the second carbon source [32]. A sudden rise in ppGpp concentration at the onset of the diauxic shift is necessary for the timely response of both RpoS and CRP regulons [32] (observe ppGpp curve in **Figure 2.3A**).

The ppGpp dynamics of diauxic shifts have been quantified in several studies [5, 33–36], with rather varying outcomes regarding absolute concentrations. The ppGpp peak during glucose-succinate transitions has been reported to be 225 pmol OD^{-1} [34], 430 pmol OD^{-1} [35] and 650 pmol OD^{-1} [36], and 175 pmol OD^{-1} during a glucose-lactate transition [33] (**Figure 2.3A**). Interestingly, the lower reported values of [34] and [33] are both derived from *E. coli* CP78, whereas the higher reported values of [35] and [36] were both measured in *E. coli* NF161. *E. coli* NF161 also displayed higher basal ppGpp levels before the diauxic shift, which has also been confirmed in a study that directly compared basal ppGpp levels in both strains [37]. Given that the basal level of our strain MG1655 - before the shift 37 pmol OD^{-1} - corresponds more with strain CP78, the CP78 data offers a more suited validation for our method. In our data (**Figure 2.3C**), ppGpp peaks at an average of 177 pmol OD^{-1}, which overlaps nicely with the CP78 data [33, 34].

The reported trends however are consistent amongst the reference studies [33–36], with a sudden increase in ppGpp at the onset of growth arrest, followed by a gradual decrease during the diauxic transition. The duration of the diauxic shift and

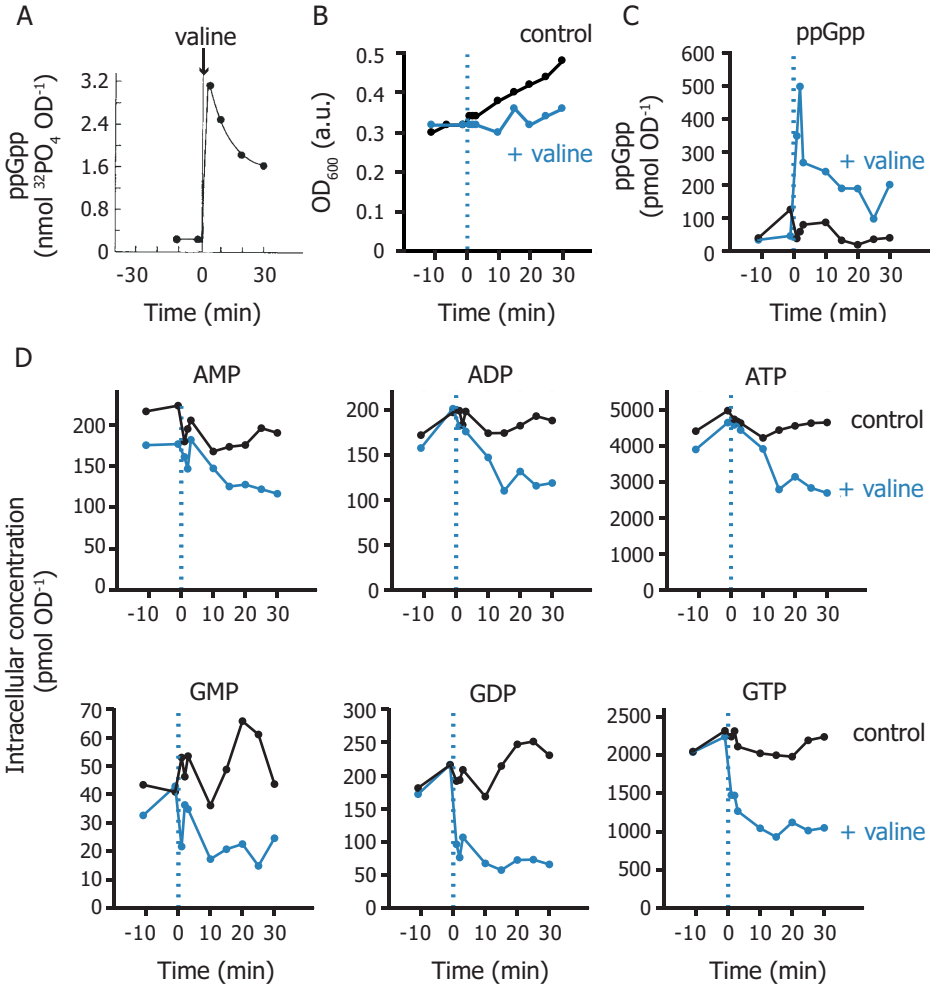

Figure 2.2: Valine addition to *E. coli* causes an increase in ppGpp as reported in literature, and concomitant decrease in other nucleotides. A) Data from Cashel and Gallant [27]: in *E. coli* CP78 ppGpp increases to 3.2 nmol $^{32}PO_4$ OD^{-1} or 0.8 nmol ppGpp OD^{-1} within 5 min after valine addition. Data acquired with TLC. B-D) Data collected to validate LC-MS analytical method. Valine was added at 0 min to an *E. coli* MG1655 culture growing on 0.2 % glucose minimal MOPS medium. B) Growth arrests after valine addition at 0 min. C) Response of ppGpp levels and D) the purine nucleotides to valine addition. Points indicate single samples. Data collected with iHILIC column.

the growth rate afterwards vary, presumably due to the different strains and carbon sources used. The moment cells resume growth on the second carbon source, the ppGpp level is still on average about 2-fold the pre-shift basal level [33–35]. In addition, our measured trend in ppGpp increase and decrease are perfectly in line with previous studies (**Figure 2.3C**).

One exception to these studies is Fernández-Coll and Cashel [5], the only to investigate a glucose-lactose transition. They however do not observe the peak of ppGpp (reported as a ratio of ppGpp/((p)ppGpp+GTP), but rather a plateau that only decreases after growth has resumed. Their diauxic transition phase is in fact 75 min whereas in our case only 35 min. The difference in diauxic lag might be due to the difference between growth in batch culture (this chapter) and 96-well plates [5].

Another important signaling molecule that is involved in the adaptation to different carbon sources is cAMP, which regulates the activity of CRP [38]. There are few studies available that have absolutely quantified the intracellular concentration of cAMP during a glucose-lactose diauxic shift [39]. According to Inada, Kimata, and Aiba [40], the intracellular cAMP concentration increases from 2.5 µM to 15 µM, a six-fold increase, which decreases again concomitantly with growth resumption (**Figure 2.3B**). **Figure 2.3C** shows that our data are similar to their observation, as there is an 8 to 9-fold increase in cAMP at the onset of the diauxic shift, which decreases again as the cells recommence growth.

Finally, **Figure 2.3C** shows that ATP, GTP and GDP concentrations nearly instantly decrease about 30 %, 60 % and 40 % respectively, trends also observed by Winslow [33]. Interestingly the ADP concentration quickly doubles, presumably due to a sudden augmented hydrolysis rate of ATP to ADP. AMP and GMP were not quantifiable in this experiment.

2.3.3. ppGpp dynamics after RelA induction

In search of a way to control ppGpp levels in *E. coli*, Schreiber *et al.* [41] decided to ectopically overexpress the ppGpp synthetase RelA. They observed that although RelA overexpression causes an increase in ppGpp, overexpression of a truncated RelA leads to even higher levels. Moreover, this truncated RelA, which contains only the first 455 amino acids (henceforth called RelA*), does not require interaction with a ribosome-deacyl-tRNA complex to be active. Overexpression of RelA* caused an increase of ppGpp, regardless of medium conditions, yet dependent on the inducer level. This discovery became a valuable tool to physiological studies of ppGpp, as it allows the researcher to artificially increase the intracellular ppGpp level.

Several studies [41–43] used this strategy and observed that within 5 min ppGpp increases, followed by a plateau reached at 10-15 min (**Figure 2.4A-B**). The height of the plateau varies, probably due to differences in analytical method, strain, induction system or growth media used.

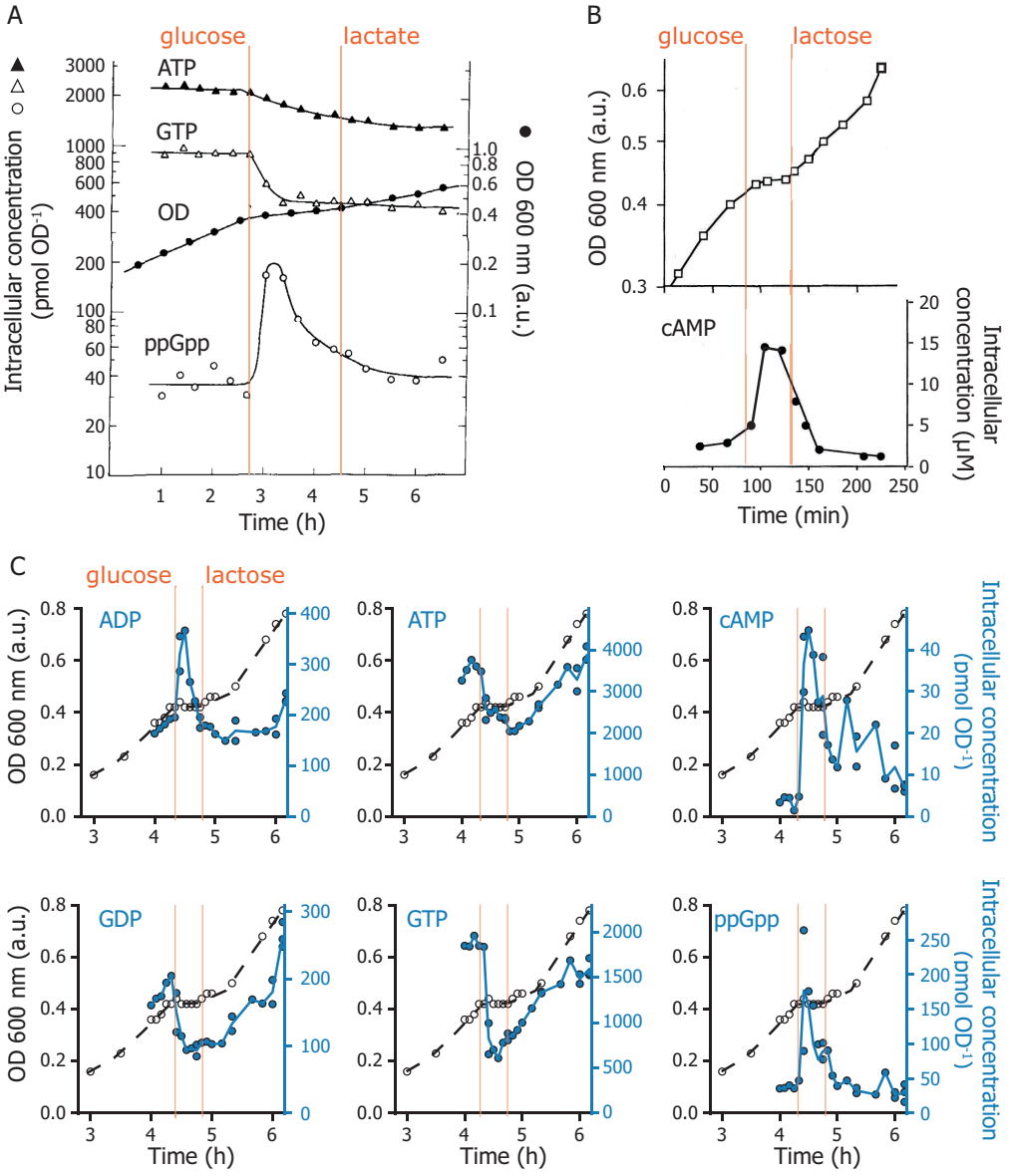

Figure 2.3: Dynamics of ppGpp, cAMP and nucleotides during diauxic shift are consistent with previous studies. A) Nucleotide concentrations and growth during a glucose (0.025 %)-lactate (0.25 %) diauxic shift of *E. coli* CP78. Data from Winslow [33]. B) Growth curve and cAMP concentration of *E. coli* W3110 during glucose (0.02 %) - lactose (0.04 %) diauxic shift. C) Data obtained in this chapter. *E. coli* MG1655 was grown on 0.03 % glucose and 0.1 % lactose minimal MOPS medium. During the diauxic shift between 4 and 5 h cells were sampled every 5 min for LC-MS analysis (iHILIC) (blue data) and $OD_{600\,nm}$ (black data). The individual data points are shown, and the curves go through the average.

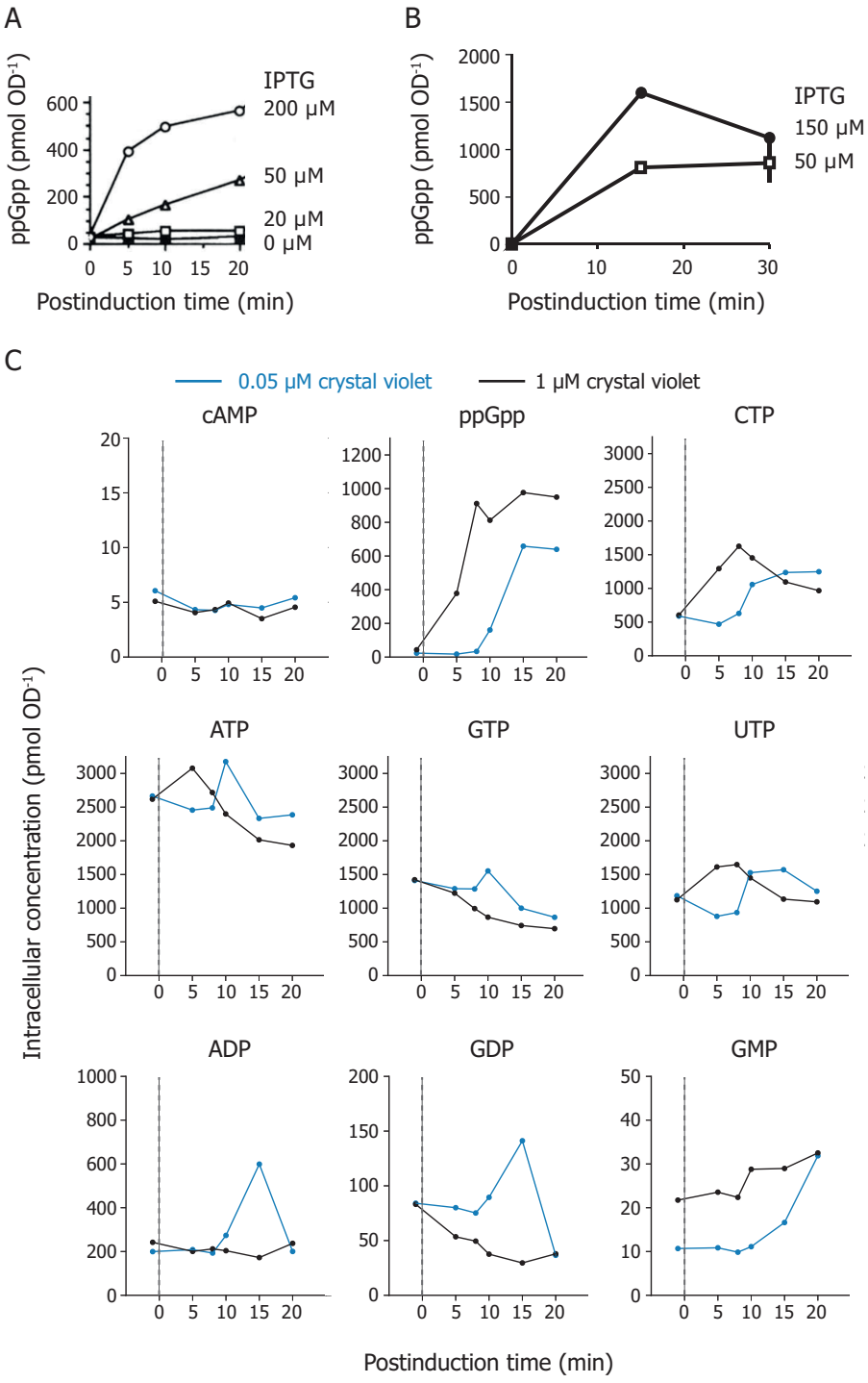
A
ppGpp (pmol OD-1)
IPTG
200 μM
50 μM
20 μM
0 μM
Postinduction time (min)
B
ppGpp (pmol OD-1)
IPTG
150 μM
50 μM
Postinduction time (min)
C
0.05 μM crystal violet
1 μM crystal violet
cAMP
ppGpp
CTP
ATP
GTP
UTP
ADP
GDP
GMP
Intracellular concentration (pmol OD-1)
Postinduction time (min)

Figure 2.4: RelA* induction in *E. coli* causes rapid changes in nucleotide levels that are induction level dependent. A) ppGpp response upon induction of RelA* in *E. coli* JM109 (glucose minimal medium) using the *tac* promoter system. Data from Schreiber *et al.* [41]. B) ppGpp response upon induction of RelA* in *E. coli* NCM3722 (M9 + glucose + amino acids + vitamins medium), using the same plasmid as A, but including a C-terminal octahistidine tag to RelA*. Data from Wang *et al.* [42]. C) Data generated using the LC-MS method described in this chapter (cHILIC). *E. coli* NCM3722 growing in 0.2 % glucose minimal medium was induced with 0.05 µM (blue) or 1 µM (black) crystal violet at 0 min (indicated with a dashed line) (at that corresponding to an OD of 0.3).

RelA* was expressed in *E. coli* NCM3722 using the Jungle Express system, in which the promoter is induced with crystal violet [44]. RelA* rapidly produces ppGpp in the cell, which augments its level to about 650 and 1000 pmol OD^{-1} for 0.05 and 1 µM crystal violet respectively (**Figure 2.4C**) in glucose minimal medium. cAMP concentration remains constant. ATP levels only significantly decrease at 1 µM induction. ADP levels remain more or less constant. Both GTP and GDP levels decrease for nearly 50 %. The GTP decrease at 0.05 µM appears to lag behind on the 1 µM induction, similar to the difference in ppGpp increase between the two induction levels. The correlation between the decrease in ATP, GTP and GDP and RelA* induction level suggests that the decrease in these nucleotide levels is due to their consumption for synthesis of ppGpp. Interestingly both UTP and CTP start increase in concentration once a ppGpp threshold of about 200 pmol OD^{-1} is reached.

Wang *et al.* [42] measured ppGpp in the same strain before and after saturating RelA induction, but in synthetic rich medium (containing glucose, amino acids and vitamins). They report a ppGpp concentration of 1 nmol OD^{-1}, which confirms our result. They also measured the relative increase or decrease in purines after RelA induction, all consistent with our results, apart from that we observe an increase in GMP, whereas they observed a 50% decrease. The difference in GMP dynamics might be a consequence of the different media used.

In this chapter and chapter 4 two different induction systems were used to express RelA* to various degrees (**Figure 2.4** and **2.6B**).

2.3.4. A decrease in ppGpp due to light activation of MeshI

So far ppGpp was measured in situations where ppGpp levels increase. More difficult to detect is a decrease in low ppGpp levels. In our laboratory Ferhat Buke has developed a light-activated enzyme for degradation of ppGpp by fusing a light-sensitive domain (AsLov) to MeshI, a ppGpp hydrolase (**Figure 2.5A**). To test whether MeshI would really be more active in the presence of light, ppGpp levels were measured in *E. coli* expressing AsLov-MeshI before and after exposure to

blue light (**Figure 2.5B-E**). After 3 min of blue light irradiation, ppGpp levels had dropped from 65 pmol OD^{-1} to 50 pmol OD^{-1}, confirming AsLov-MeshI is responsive to light.

2.3.5. ppGpp levels during steady state growth in various media: assessment of sensitivity

Finally, the LC-MS method was assessed (and used in chapter 3) to measure ppGpp levels during steady state growth, as this requires the highest sensitivity compared to other growth or stress conditions (**Figure 2.6A**). The reported levels correspond with the range of previously measured basal ppGpp levels [35, 37, 45–47].

2.3.6. Evaluation of the error of the method

The sample preparation and LC-MS measurement entail many steps that can create sample and/or signal losses. These include for example the decomposition of ppGpp during the extraction in 2 M formic acid, residues on the filter, incomplete recovery of the SPE, pipetting errors, incomplete redissolving after drying, and so on. These losses can vary amongst different samples and hence increase the technical error of the method. Most of these losses are corrected for by the use of an internal standard that undergoes the exact same treatment as the sample, such that the ratio of analyte to standard remains constant throughout the protocol. Nevertheless, with the internal standard the remaining sources of technical variation are the internal standard mix itself (composition as well as the volume), variation in sampling volume and speed of sampling (which might cause that cells already sense oxygen or temperature stress and produce ppGpp) and the error of the OD measurement (**Figure 2.1**).

A culture growing at steady-state should have a constant ppGpp value (no biological variation), which is why repeated sampling of the same culture provides a measure of the technical error. For the data in **Figure 2.5** (iHILIC), the standard deviation is on average 13 % of the average measured value for each point (e.g. a measured value of 50 pmol OD^{-1} would have a standard deviation of 6.5 pmol OD^{-1}). For the data presented in **Figure 2.6A** (cHILIC), this is on average 23 %. The difference lies in the fact that the wild-type data actually also includes biological replicates (different cultures). Although the two data sets were analyzed with different columns, the cHILIC data generally had higher signal and better peak shapes, hence this cannot explain the higher variation.

As a comparison, the RelA induction data (**Figure 2.6B**, iHILIC - same as used in Figure 4.3) exhibited on average a standard deviation of 32 % of the mean measured value of 3 biological replicates. The higher variability likely comes from biological variation, in particular due to small differences in RelA* expression and/or the exact timing of ppGpp increase. Overall, the data show that the developed method can

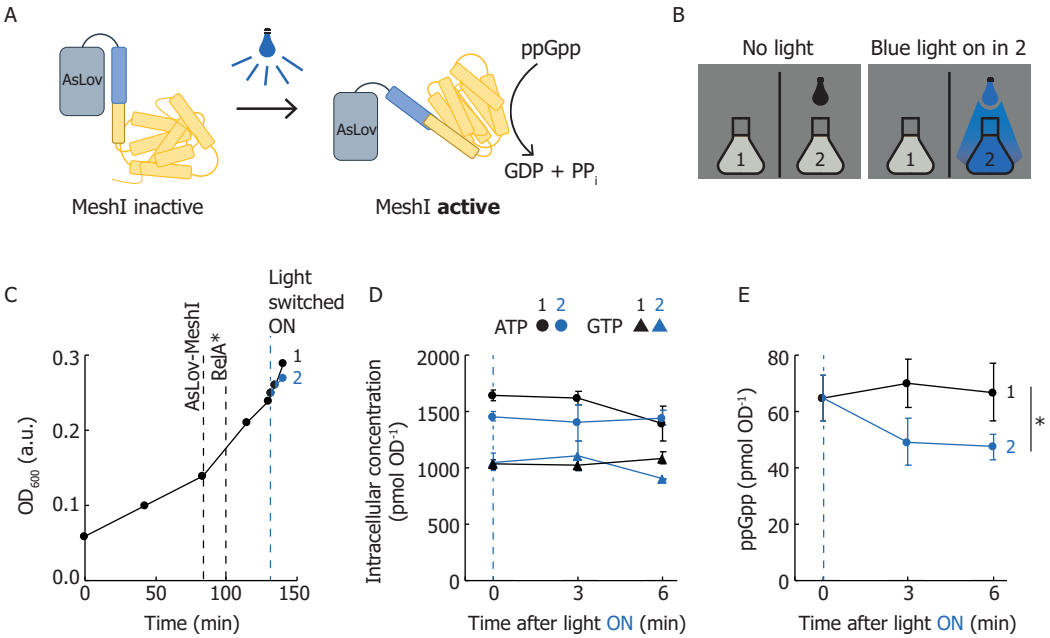

Figure 2.5: The LC-MS method allows to detect variation in basal ppGpp levels caused by light-activated MeshI. A) Mechanism of AsLov-MeshI activation by light. B) Experimental set-up: 2 cultures expressing AsLov-MeshI are growing in the dark and at a certain time number 2 is exposed to blue light. C) Growth curve of both cultures. MG1655 cells harboring the pSC101**-RelA* and pAsLov-MeshI plasmids were growing in the dark in 0.2 % glucose minimal medium, supplemented with 100 µM $MnCl_2$ and 20 µg mL^{-1} uracil. At 86 min (OD 0.14), AsLov-MeshI was induced with 250 µM IPTG. At 100 min (OD about 0.17) RelA* was induced with 40 ng mL^{-1} doxycycline. At 130 min cells were sampled for LC-MS analysis (iHILIC). Right after, culture 2 was exposed to blue light. D) ATP and GTP concentrations do not change significantly after blue light exposure. E) ppGpp levels decrease only during exposure to blue light, suggesting that the blue light activated MeshI. *P-value of a two-tailed t-test after 3 min is 0.026 and after 6 min is 0.065. Errors bars represent the standard deviation from three samples from 1 culture.

reproducibly quantify low levels of ppGpp with an error that allows detection of variation in basal levels.

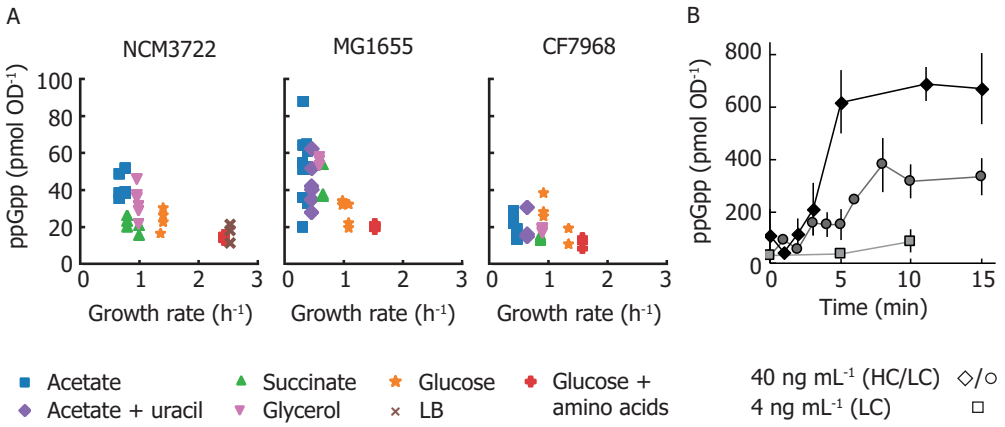

Figure 2.6: The sensitivity and variability of the method was assessed by measuring basal ppGpp levels (cHILIC) and RelA induction (iHILIC). A) Basal ppGpp levels of *E. coli* NCM3722, MG1655 and CF7869 grown in various carbon sources were measured in triplicate (technical replicates) from either one or two cultures (biological replicates) at OD 0.3. B) ppGpp was measured at various timepoints after induction of RelA* at OD 0.3 with 4 or 40 ng mL^{-1} anhydrous tetracycline, from a low-copy (LC) or high-copy (HC) number plasmid. Error bars represent the standard deviation of three biological replicates (3 cultures).

2.4. Conclusion

In order to understand the ppGpp signaling network, a LC-MS method was developed to quantify ppGpp, as well as various nucleotides, acetyl-coenzyme A and cAMP. LC-MS detection enabled sensitive, absolute quantitation due to the use of internal standards, and omitted the need for high phosphate concentrations in the media as is the case for radiolabeling. The method allowed to sample a cell amount of only 0.3 OD mL^{-1} (or depending on growth conditions 1 ml culture), which enabled repeated sampling of small culture volumes, a great improvement over former sampling volumes of up to 50 ml.

The experimental data in this chapter is consistent with trends reported in literature. Often a quantitative comparison is not possible due to the different units, strains or experimental conditions used, exemplifying the need for a universal, accurate analytical method for ppGpp, such as the one developed in this chapter.

2.5. Acknowledgements

We would like to thank Michael Cashel for strain CF7968 and Nicole Scherer and Flora Yang for technical support with the LC-MS.

2.6. Supplementary information

2.6.1. Tips and tricks for measuring ppGpp

What follows are a few more detailed recommendations to optimally execute the method as described above.

1. **The accuracy of internal standards determines the accuracy of the final result.** For each compound, make a dissolved stock from the whole vial of the compound (no weighing using inaccurate or dirty scales), aliquot these and store in the freezer. When making the final internal standard mix, prepare a large volume (some mL) such that you can use it for at least 100 measurements (or according to your scientific goals). Make the solution such that you use (close to) maximal accuracy of your pipette. Pipette carefully, no rush. Aliquot the stock into single-use aliquots. For each experiment, keep what is left of the used internal standard aliquots, such that you can verify afterwards whether the internal standard was fine.

2. **Keep internal standards on ice.** When using the internal standard aliquots, thaw them right before (e.g. 15 min) usage and leave them on ice. Add the IS solution to the 2 M formic acid solution as placing a tiny droplet next to a big drop of 1 mL. Make sure they do not mix yet! Only when the filter containing the cells is placed into the well holding both IS and extraction solutions, these will mix. This assures that the internal standard is not degraded by the formic acid solution before the sample touches the formic acid.

3. **Practice the sampling multiple times before sampling.** The key to this protocol is calm yet fast removal of 1 mL culture that is being vigorously stirred, pipetting this on top of a small filter at adequate speed and quickly placing the filter top-down into a 6-well plate holding 1 mL extraction solution. Ideally this step can be done in 5 s. Hereto, make sure

   - the pump is set to minimal pressure (or maximal vacuum) and is functioning. Make sure all the tubing connections are air tight. Check with some water if the filtration happens in 1-2 s.
   - all tools (filters, pipette, pipette tips, tweezers, waste bag, 6-well plate, OD meter) are arranged around you such that you can immediately and easily reach them all. Put filters in a rack such that you can instantly grab them with the tweezers. Put already a pipette tip on the pipette. Grab a second 1 mL pipette to measure OD and sample right after one another.

- not to pipette too fast. Due to the aeration of the culture, it is easy to suck up air. Therefore, pay close attention that there are no bubbles in the pipette tip. You can tilt the flask a bit (without affecting the stirring bar) to reach deeper into the culture medium. Regarding pipetting the 1 mL culture onto the filter, this ideally happens at the same pace as the pull from the vacuum, such that there is no build-up of liquid on top of the filter.
- to not be afraid to tear the filter. You can tear the filter a bit, you will not lose cells over it. The easiest way to remove the filter from the filter manifold (while under vacuum) is to put the tweezers under roughly a 30° angle on top of the filter and then firmly squeeze the ends of the tweezer together. You should be instantly holding the filter.

4. **In each step, try to recover as much sample as possible.** There is an internal standard to correct for losses, but for a nice peak, the LS-MS needs a nice amount of sample. Therefore,

- do not leave the sample in the extraction solution for longer than ideally 30 min up to 1 h.
- when the extraction solution (with the precious sample) is removed from the 6-well plate, try to recover as much as possible. Squeeze out the filter with tweezers.
- try to work fast. Do not leave samples unnecessarily waiting on ice. Plan and book all equipment ahead.

5. **MAINTENANCE OF THE LC-MS IS VITAL!** In my personal experience, the most challenging part is stability of the column, LC-MS system and ionization efficiency. Although some of these are only possible in a perfect world, still aspire to

- have a personal chromatography column. Clean it after each use, and keep track of the number of runs.
- extensively rinse the whole LC-MS system before usage. Ideally use it right after the source has been thoroughly cleaned. I sometimes observed a clear drop in signal depending on the used method before my run.
- use clean mobile phase flasks each run and prepare buffers fresh. Always use the exact same order for buffer preparations.

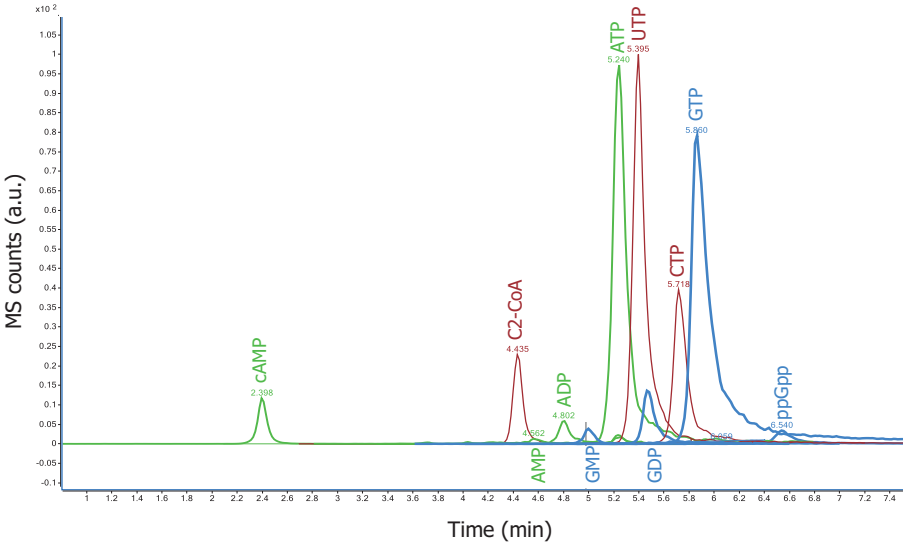

Figure S2.1: Chromatogram of internal standards (the quantifier ions) from a biological sample run on cHILIC. The amount of internal standard present in the sample is as in Table S2.4, with 25 pmol ppGpp.

Table S2.1: Strains and plasmids used in this chapter.

Strain	Description	Source
E. coli DH5α	Used for cloning and plasmid amplification	Invitrogen
E. coli NCM3722	Wild type	CGSC 12355
E. coli MG1655	Wild type	DSMZ 18039
E. coli CF7968	MG1655 *rph*+	Michael Cashel
Plasmid		
p15A-AsLov-MeshI	Expression of AsLov-MeshI from *lacUV5* promoter, ampicillin resistant	Ferhat Buke [**Buke2020**]
pTR_sJExA1-RFP	Backbone containing SC101 origin and crystal violet inducible promoter.	[44]
pJEx-RelA*	pTR_sJExA1-RFP with RFP replaced by $RelA_{1-455}$-Gly-Ser-mVenus	This work

Table S2.2: MOPS buffer components

Components	Concentration
MOPS	40 mM
Tricine	4 mM
$FeSO_4$	10 µM
NH_4Cl	9.5 mM
MgCl	523 µM
$CaCl_2$	0.5 µM
K_2HPO_4	1.32 mM
K_2SO_4	276 µM
NaCl	50 mM
micronutrients stock	20 µL L^{-1}
KOH	until pH 7.2

Table S2.3: Amino acid concentrations for defined amino acids medium

Components	Concentration [mM]
L-alanine	0.8
L-arginine	5.2
L-asparagine	0.4
L-aspartic acid, potassium salt	0.4
L-glutamic acid, potassium salt	0.66
L-glutamine	0.6
L-glycine	0.8
L-histidine	0.2
L-isoleucine	0.4
L-proline	0.4
L-serine	10
L-threonine	0.4
L-tryptophan	0.1
L-valine	0.6
L-leucine	0.8
L-lysine	0.4
L-methionine	0.2
L-phenylalanine	0.4
L-cysteine	0.1
L-tyrosine	0.2

Table S2.4: Amount of internal standard used for the corresponding compounds added to each *E. coli* sample for quantitation.

Compound	Amount (pmol)	Compound	Amount (pmol)
ATP	750	UTP	500
ADP	50	UDP	50
AMP	50	UMP	50
GTP	500	CTP	500
GDP	50	CDP	50
GMP	50	CMP	50
ppGpp	25 or 150	cAMP	50

Table S2.5: Used gradients of the LC-MS methods developed in this chapter for both iHILIC and cHILIC columns.

iHILIC			cHILIC		
Time (min)	% Mobile phase B	Flow rate ($mL\,min^{-1}$)	Time (min)	% Mobile phase B	Flow rate ($mL\,min^{-1}$)
0.0	100	0.3	0.0	100	0.4
0.5	100	0.3	1.0	90	0.4
1.5	85	0.3	15.0	80	0.4
10.0	85	0.3	16.0	80	0.4
10.5	85	0.25	18.0	100	0.4
13.0	30	0.25	19.0	100	0.5
15.0	30	0.25	22.0	100	0.5
17.5	100	0.25	22.5	100	0.4
20.5	100	0.25	26.5	100	0.4
21.5	100	0.3			
25.5	100	0.3			

Table S2.6: Transitions and retention times of LC-MS method (cHILIC) for analysis of nucleotides and signaling molecules in *E. coli*. In blue are quantifier ions, in white the qualifier ions. The settings for pppGpp are not complete as pppGpp was not included in the optimization of the final method.

Compound	Precursor ion	Product ion	Retention time (min)	Fragmentor	Collision energy
ADP	428	136,1	4,8	90	40
ADP	428	348,1	4,8	90	10
AMP	348,1	136,1	4,3	100	20
AMP	348,1	119	4,3	100	40
ATP	508	136,1	5,3	100	20
ATP	508	410	5,3	100	10
C2-CoA	810,1	303	4,2	120	29
C2-CoA	810,1	136,1	4,2	120	29
cAMP	330,1	136,3	2,3	96	35
cAMP	330,1	119,1	2,3	96	35
CTP	484	112	6,1	100	10
CTP	484	97	6,1	100	30
GDP	444	152,1	5,5	96	17
GDP	444	135	5,5	96	69
GMP	364,1	152,1	5,1	96	5
GMP	364,1	135	5,1	96	40
GTP	524	152,1	6,3	122	25
GTP	524	135	6,3	122	77
ppGpp	604	152,1	6,9	142	40
ppGpp	604	506	6,9	142	20
pppGpp	638,9	152,1			
pppGpp	638,9	506			
UTP	485	97	5,7	100	30
UTP	485	227,1	5,7	100	10
U-15N-ADP	433	141	4,8	90	20
U-15N-ADP	433	353	4,8	90	10
U-15N-AMP	353,1	141	4,3	100	20
U-15N-AMP	353,1	123	4,3	100	40
U-15N-ATP	513	141	5,3	100	20
U-15N-ATP	513	415	5,3	100	10
U-15N-C2-CoA	817,1	305,1	4,2	120	29
U-15N-C2-CoA	817,1	141	4,2	120	29
U-15N-cAMP	335	141	2,3	96	35
U-15N-cAMP	335	124	2,3	96	35
U-15N-CTP	487	115	6,1	100	10
U-15N-CTP	487	97	6,1	100	30
U-15N-GDP	449	157	5,5	96	17
U-15N-GDP	449	139	5,5	96	69
U-15N-GMP	369,1	157	5,1	96	5
U-15N-GMP	369,1	139	5,1	96	40
U-15N-GTP	529	157	6,3	122	25
U-15N-GTP	529	139	6,3	122	77

Table S2.4: Transitions and retention times of LC-MS method (cHILIC) for analysis of nucleotides and signaling molecules in *E. coli* (continued).

Compound	Precursor ion	Product ion	Retention time (min)	Fragmentor	Collision energy
U-15N-ppGpp	608,9	157	6,9	142	40
U-15N-ppGpp	608,9	511	6,9	142	20
U-15N-UTP	487	97	5,7	100	30
U-15N-UTP	487	229,1	5,7	100	10
U-13C-ADP	438,1	141,1	4,8	90	20
U-13C-ADP	438,1	124,1	4,8	90	
U-13C-ATP	518	141,1	5,3	100	20
U-13C-ATP	518	420,1	5,3	100	10
U-13C-GMP	374,1	157,1	5,1	96	5
U-13C-GMP	374,1	140	5,1	96	40
U-13C-GDP	454,1	157,1	5,5	96	17
U-13C-GDP	454,1	140	5,5	96	69
U-13C-GTP	534	157,1	6,3	122	25
U-13C-GTP	534	140	6,3	122	77
U-13C-ppGpp	614	157,1	6,9	142	40
U-13C-ppGpp	614	516	6,9	142	20
U-13C-pppGpp	694	157,1			
U-13C-pppGpp	694	516			

references

[1] N. C. E. Imholz, M. J. Noga, N. J. F. van den Broek, and G. Bokinsky. "Calibrating the bacterial growth rate speedometer: a re-evaluation of the relationship between basal ppGpp, growth, and RNA synthesis in *Escherichia coli*". In: *Frontiers in Microbiology* (2020). doi: 10.3389/fmicb.2020.574872.

[2] M. Zhu, M. Mori, T. Hwa, and X. Dai. "Disruption of transcription–translation coordination in *Escherichia coli* leads to premature transcriptional termination". In: *Nature Microbiology* (2019). doi: 10.1038/s41564-019-0543-1.

[3] E. Sarubbi, K. E. Rudd, and M. Cashel. "Basal ppGpp level adjustment shown by new SpoT mutants affect steady state growth rates and *rrnA* ribosomal promoter regulation in *Escherichia coli*". In: *MGG Molecular & General Genetics* 213.2-3 (1988), pp. 214–222. doi: 10.1007/BF00339584.

[4] B. R. Bochners and B. N. Ames. "Complete Analysis of Cellular Nucleotides by Two-dimensional Thin Layer Chromatography". In: *Journal of Biological Chemistry* 257.16 (1982), pp. 9759–9769.

[5] L. Fernández-Coll and M. Cashel. "Contributions of SpoT hydrolase, SpoT synthetase, and RelA synthetase to carbon source diauxic growth transitions in *Escherichia coli*". In: *Frontiers in Microbiology* 9.AUG (2018), pp. 1–13.

[6] J. Ryals, R. Little, and H. Bremer. "Control of RNA Synthesis in *Escherichia coli* After a Shift to Higher Temperature". In: 151.3 (1982), pp. 1425–1432.

[7] M. H. Buckstein, J. He, and H. Rubin. "Characterization of nucleotide pools as a function of physiological state in *Escherichia coli*". In: *Journal of Bacteriology* 190.2 (2008), pp. 718–726.

[8] G. Bokinsky, E. E. K. Baidoo, S. Akella, H. Burd, D. Weaver, J. Alonso-Gutierrez, H. García-Martín, T. S. Lee, and J. D. Keasling. "HipA-triggered growth arrest and β-lactam tolerance in *Escherichia coli* are mediated by RelA-dependent ppGpp synthesis". In: *Journal of Bacteriology* 195.14 (2013), pp. 3173–82.

[9] V. Varik, S. R. A. Oliveira, V. Hauryliuk, and T. Tenson. "HPLC-based quantification of bacterial housekeeping nucleotides and alarmone messengers ppGpp and pppGpp". In: *Scientific Reports* 7.1 (2017), pp. 1–12. doi: 10.1038/s41598-017-10988-6.

[10] H. Jin, Y. M. Lao, J. Zhou, H. J. Zhang, and Z. H. Cai. "A rapid UHPLC-HILIC method for algal guanosine 5′-diphosphate 3′-diphosphate (ppGpp) and the potential separation mechanism". In: *Journal of Chromatography B: Analytical Technologies in the Biomedical and Life Sciences* 1096.February (2018), pp. 143–153. doi: 10.1016/j.jchromb.2018.08.009.

[11] Y. Ihara, H. Ohta, and S. Masuda. "A highly sensitive quantification method for the accumulation of alarmone ppGpp in *Arabidopsis thaliana* using UPLC-ESI-qMS/MS". In: *Journal of Plant Research* 128.3 (2015), pp. 511–518. doi: 10.1007/s10265-015-0711-1.

[12] C. Patacq, N. Chaudet, and F. Letisse. "Absolute Quantification of ppGpp and pppGpp by Double-Spike Isotope Dilution Ion Chromatography-High-Resolution Mass Spectrometry". In: *Analytical Chemistry* 90.18 (2018), pp. 10715–10723. doi: 10.1021/acs.analchem.8b00829.

[13] J. Irr and J. Gallant. "The control of RNA synthesis in *Escherichia coli*. II. Stringent control of energy metabolism." In: *Journal of Biological Chemistry* 244.8 (1969), pp. 2233–2239.

[14] W. Lu, X. Su, M. S. Klein, I. A. Lewis, O. Fiehn, and J. D. Rabinowitz. "Metabolite Measurement: Pitfalls to Avoid and Practices to Follow". In: *Annual Review of Biochemistry* 86.1 (2017), pp. 277–304. doi: 10.1146/annurev-biochem-061516-044952.

[15] J. Chen, Y. Huang, X. Yang, H. Zhang, Z. Li, B. Qin, X. Chen, and H. Qiu. "Highly sensitive and visual detection of guanosine 3′-diphosphate-5′-di(tri)phosphate (ppGpp) in bacteria based on copper ions-mediated 4-mercaptobenzoic acid modified gold nanoparticles". In: *Analytica Chimica Acta* 1023 (2018), pp. 89–95. doi: 10.1016/j.aca.2018.02.082.

[16] P. Zhang, Y. Wang, Y. Chang, Z. H. Xiong, and C. Z. Huang. "Highly selective detection of bacterial alarmone ppGpp with an off-on fluorescent probe of copper-mediated silver nanoclusters". In: *Biosensors and Bioelectronics* 49 (2013), pp. 433–437. doi: 10.1016/j.bios.2013.05.056.

[17] F. C. Neidhardt, P. L. Bloch, and D. F. Smith. "Culture Medium for Enterobacteria". In: *Journal of Bacteriology* 119.3 (1974), pp. 736–747.

[18] A. Zaslaver, A. Bren, M. Ronen, S. Itzkovitz, I. Kikoin, S. Shavit, W. Liebermeister, M. G. Surette, and U. Alon. "A comprehensive library of fluorescent transcriptional reporters for *Escherichia coli*". In: *Nature methods* 3.8 (2006), pp. 623–628. doi: 10.1038/nmeth895.

[19] B. D. Bennett, J. Yuan, E. H. Kimball, and J. D. Rabinowitz. "Absolute quantitation of intracellular metabolite concentrations by an isotope ratio-based approach". In: *Nature protocols* 3.8 (2008), pp. 1299–1312. doi: 10.1038/nprot.2008.107.

[20] M. Cashel and B. Kalbacher. "The control of ribonucleic acid synthesis in *Escherichica coli*. V. Characterization of a nucleotide associated with the stringent response". In: *The Journal of Biological Chemistry* 245.9 (1970), pp. 2309–2318.

[21] R. Dams, M. A. Huestis, W. E. Lambert, and C. M. Murphy. "Matrix effect in bio-analysis of illicit drugs with LC-MS/MS: Influence of ionization type, sample preparation, and biofluid". In: *Journal of the American Society for Mass Spectrometry* 14.11 (2003), pp. 1290–1294.

[22] P. Panuwet, R. E. Hunter, P. E. D'Souza, X. Chen, S. A. Radford, J. R. Cohen, M. E. Marder, K. Kartavenka, P. B. Ryan, and D. B. Barr. "Biological Matrix Effects in Quantitative Tandem Mass Spectrometry-Based Analytical Methods: Advancing Biomonitoring". In: *Critical Reviews in Analytical Chemistry* 46.2 (2015), pp. 93–105.

[23] Z. Shabarova and A. Bogdanov. "Structure of Nucleotides". In: *Advanced Organic Chemistry of Nucleic Acids*. Wiley-VCH Verlag GmbH, 2007, pp. 71–92.

[24] S. Cohen, M. Megherbi, L. P. Jordheim, I. Lefebvre, C. Perigaud, and J. Dumontet C.and Guitton. "Simultaneous analysis of eight nucleoside triphosphates in cell lines by liquid chromatography coupled with tandem mass spectrometry". In: *Journal of Chromatography B* 877.30 (2009), pp. 3831–3840.

[25] L. M. Crowe, D. S. Reid, and J. H. Crowe. "Is Trehalose Special for Preserving Dry Biomaterials?" In: *Biophysical Journal* 71 (1996), pp. 2087–2093.

[26] B. Volkmer and M. Heinemann. "Condition-dependent cell volume and concentration of *Escherichia coli* to facilitate data conversion for systems biology modeling". In: *PLoS ONE* 6.7 (2011), pp. 1–6.

[27] M. Cashel and J. Gallant. "Two Compounds implicated in the Function of the RC Gene of *Escherichia coli*". In: *Nature* 221 (1969), pp. 838–841.

[28] M. A. Sorensen, K. F. Jensen, and S. Pedersen. "High Concentrations of ppGpp Decrease the RNA Chain Growth Rate: Implications for Protein Synthesis and Translational Fidelity During Amino Acid Starvation in *Escherichia coli*". In: *Journal of Molecular Biology* 236 (1994), pp. 441–454.

[29] A. G. Chapman, L. Fall, and D. E. Atkinson. "Adenylate Energy Charge in *Escherichia coli* During Growth and Starvation". In: *Journal of Bacteriology* 108.3 (1971), pp. 1072–1086.

[30] M. Faijes, A. E. Mars, and E. J. Smid. "Comparison of quenching and extraction methodologies for metabolome analysis of *Lactobacillus plantarum*". In: *Microbial Cell Factories* 6.1 (2007), pp. 1–8. doi: 10.1186/1475-2859-6-27.

[31] J. Monod. *Selected Papers in Molecular Biology by Jacques Monod*. Ed. by A. Lwoff and A. Ullmann. Academic Press, Inc., 1978. Chap. The phenomenon of enzymatic adaptation, pp. 68–134.

[32] M. F. Traxler, D.-E. Chang, and T. Conway. "Guanosine 3',5'-bipyrophosphate coordinates global gene expression during glucose-lactose diauxie in *Escherichia coli*". In: *Proceedings of the National Academy of Sciences* 103.7 (2006), pp. 2374–2379.

[33] R. M. Winslow. "A consequence of the *rel* gene during a glucose to lactate downshift in *Escherichia coli*. The rates of ribonucleic acid synthesis." In: *The Journal of Biological Chemistry* 246.15 (1971), pp. 4872–4877.

[34] R. B. Harshman and H. Yamazaki. "Formation of ppGpp in a relaxed and stringent strain of *Escherichia coli* during diauxie lag". In: *Biochemistry* 10.21 (1971), pp. 3980–3982.

[35] R. Lazzarini, M. Cashel, and J. Gallant. "On the Regulation of Guanosine Tetraphosphate Levels in Stringent and Relaxed Strains of *Escherichia coli*". In: *Journal of Biological Chemistry* 246.14 (1971), pp. 4381–4385.

[36] G. Braedt and J. Gallant. "Role of the *rel* gene product in the control of cyclic adenosine 3',5'-monophosphate accumulation". In: *Journal of Bacteriology* 129.1 (1977), pp. 564–566.

[37] Y. Sokawa, J. Sokawa, and Y. Kaziro. "Regulation of stable RNA synthesis and ppGpp levels in growing cells of *Escherichia coli*". In: *Cell* 5.1 (1975), pp. 69–74.

[38] V. Chubukov, L. Gerosa, K. Kochanowski, and U. Sauer. "Coordination of microbial metabolism". In: *Nature Reviews Microbiology* 12.5 (2014), pp. 327–340.

[39] A. Narang. "Quantitative effect and regulatory function of cyclic adenosine 5′-phosphate in *Escherichia coli*". In: *Journal of Biosciences* 34.3 (2009), pp. 445–463.

[40] T. Inada, K. Kimata, and H. Aiba. "Mechanism responsible for glucose-lactose diauxie in *Escherichia coli*: challenge to the cAMP model". In: *Genes to Cells* 1.3 (1996), pp. 293–301.

[41] G. Schreiber, S. Metzgers, E. Aizenman, S. Roza, M. Cashel, and G. Glaser. "Overexpression of the *relA* gene in *Escherichia coli*". In: *Journal of Biological Chemistry* 266.6 (1991), pp. 3760–3767.

[42] B. Wang, P. Dai, D. Ding, A. D. Rosario, R. A. Grant, B. L. Pentelute, and M. T. Laub. "Affinity-based capture and identification of protein effectors of the growth regulator ppGpp". In: *Nature Chemical Biology* (2018). doi: 10.1038/s41589-018-0183-4.

[43] A. L. Svitil, M. Cashel, and J. W. Zyskind. "Guanosine tetraphosphate inhibits protein synthesis *in vivo*". In: *The Journal of Biological Chemistry* 268.4 (1993), pp. 2307–2311. issn: 0021-9258.

[44] T. L. Ruegg, J. H. Pereira, J. C. Chen, A. DeGiovanni, P. Novichkov, V. K. Mutalik, G. P. Tomaleri, S. W. Singer, N. J. Hillson, B. A. Simmons, P. D. Adams, and M. P. Thelen. "Jungle Express is a versatile repressor system for tight transcriptional control". In: *Nature Communications* 9.1 (2018), pp. 1–13. doi: 10.1038/s41467-018-05857-3.

[45] S. R. Khan and H. Yamazaki. "Inapparent correlation between guanosine tetraphosphate levels and RNA contents in *Escherichia coli*". In: *Biochemical and Biophysical Research Communications* 59.I (1974), pp. 125–132.

[46] J. Ryals, R. Little, and H. Bremer. "Control of ribosomal-RNA and transfer-RNA syntheses in *Escherichia coli* by guanosine tetraphosphate". In: *Journal of Bacteriology* 151.3 (1982), pp. 1261–1268.

[47] E. Baracchini, R. Glass, and H. Bremer. "Studies *in vivo* on *Escherichia coli* RNA polymerase mutants altered in the stringent response". In: *Molecular & General Genetics* 213 (1988), pp. 379–387.

3

A re-evaluation of trends in basal ppGpp in *E. coli*

The molecule guanosine tetraphophosphate (ppGpp) is perhaps most commonly understood as an alarmone produced during times of acute stress. However, concentrations of ppGpp also play a role during steady-state growth. For decades, it has been demonstrated that ppGpp is present at levels inversely related with the growth rate. Evidence suggests that these so-called basal ppGpp concentrations are necessary to regulate transcription of ribosomal RNA in response to nutrient conditions via interactions involving RNA polymerase and the protein DksA. Although RNA polymerase is sensitive to small variations in basal ppGpp concentration, several studies indicate conditions in which RNA polymerase apparently is less sensitive to ppGpp. In addition, recent studies reveal potential roles for transcription factors competing with DksA and ppGpp regarding control over RNA polymerase. Unfortunately, studies to understand the role of basal ppGpp are limited by difficulties in analytical methods able to consistently quantify basal ppGpp. Therefore, it is unclear if RNA polymerase sensitivity to ppGpp varies in different biological conditions, or whether discrepancies can be explained by different analytical methods used. In this study we have carefully examined current literature of basal ppGpp concentrations in E. coli, including strain genotype, growth conditions and analytical method. This was compared with new experimental data of several strains obtained with a recently developed analytical method. In addition, we investigated a commonly used mutation that effects ppGpp insensitivity to RNA polymerase. In conclusion, our analysis suggests that steady-state rRNA synthesis and growth rate are not completely regulated by the concerted action of DksA and ppGpp alone.

This chapter has been published as: N. C. E. Imholz, M. J. Noga, N. J. F. van den Broek, and G. Bokinsky. "Calibrating the bacterial growth rate speedometer: a re-evaluation of the relationship between basal ppGpp, growth, and RNA synthesis in *Escherichia coli*". In: *Frontiers in Microbiology* (2020). doi: 10.3389/fmicb.2020.574872

3.1. Introduction

In bacteria ppGpp is the major signaling molecule to direct metabolism and growth, responsible for the regulation of transcription [2–5], ribosome synthesis [6] and translation [7–13]. It also post-translationally directs numerous enzymes involved in nucleotide metabolism [14–20], amino acid and polyamine biosynthesis [21–23], central metabolism [17, 24, 25], ribosome assembly [19], fatty acid [26–28] and phospholipid synthesis [29] and DNA replication [30–32]. ppGpp also plays a role in responses to nutritional stress [33], osmotic stress [34] and temperature shifts [35], and is involved in virulence [36], antibiotic resistance [37] and persistence [38]. The currently known physiological effects of ppGpp are reviewed by Hauryliuk *et al.* [39]. These functions are mainly ascribed to ppGpp based on conditions in which intracellular ppGpp levels are very high (or stringent). It is clear that high ppGpp levels help the cell to overcome stressful conditions.

In fact, ppGpp levels can span a range of less than 10 to over 1000 pmol OD^{-1}, In steady-state growth, ppGpp varies between 10 to 90 pmol OD^{-1} and correlates with the growth rate [40–42]. In this regime, slight differences of a few pmol OD^{-1} appear to dramatically affect the growth rate [43–45]. The correlation between ppGpp and growth rate suggests ppGpp is necessary to establish a specific growth rate in a specific environment. How does basal ppGpp regulate growth rate?

Several studies have shown a correlation between basal ppGpp levels and inhibition of ribosomal RNA synthesis [40–42]. Combined with the discovery that ppGpp directly binds to RNA polymerase [46], these studies have led to the prevailing theory that basal ppGpp controls growth rate by controlling the amount of ribosomal RNA or ribosomes [47–50]. In other words, the function of basal ppGpp is to make sure the cell does not waste resources on synthesizing ribosomes it cannot use. Many studies have since shown that ppGpp regulates transcription of numerous genes besides rRNA, including promoting transcription of biosynthesis operons [5, 51]. Zhu *et al.* [45] were the first to demonstrate that *E. coli* actually produces an optimal level in the cell, because both artificial higher and lower levels reduce the growth rate. Mechanistically, higher ppGpp levels would impede ribosome synthesis, and lower levels would hinder precursor biosynthesis.

However, other studies have observed that the number of ribosomes is not always growth rate-limiting, as in many conditions more ribosomes could be active or they could synthesize proteins faster [52–55]. Keeping a reserve potential for protein production might allow cells to rapidly take advantage of nutrient spikes, typical for environments such as the intestine. How ppGpp determines the growth rate is clearly not completely explained by transcriptional control of rRNA.

The uncertainty about the exact physiological role of basal ppGpp levels is partially because of a lack of consistent basal ppGpp data. Several methods have been used to measure (p)ppGpp, including radiolabeling combined with thin layer chromatography (TLC), high performance liquid chromatography (HPLC) [56, 57] and liquid chromatography mass spectrometry (LC-MS) [58, 59]. An excellent overview of

current nucleotide analytical methods was made by Varik *et al.* [56]. Although current methods have successfully characterized (p)ppGpp levels in bacteria in several conditions, they have several limitations: 1) ^{32}P labeling requires a constant phosphate uptake rate, which makes it hard to compare conditions with different ppGpp level as ppGpp affects the uptake of phosphate [60] and local regulations can make radiolabeling experiments inconvenient; 2) they require large sample volumes up to 50 mL which limits the sample number and time resolution; 3) in most cases they lack absolute quantitation enabling only relative quantitation; 4) they use UV light for detection which is inherently less specific than MS. Besides the detection method, also the sampling method needs to be adapted to ppGpp. ppGpp is unstable, including in acidic solutions widely used to quench cell metabolism. In addition, the enzymes that synthesize and degrade ppGpp are highly sensitive to changes in the environment. It is hence necessary to rapidly quench cellular metabolism, which excludes collecting cells by centrifugation prior to quenching.

Many questions remain unanswered because of these technical limitations. We reexamined all published measurements of basal ppGpp, performed using many different techniques and in many different *E. coli* strains, to evaluate the widely-held notion that ppGpp is inversely proportional to growth rate. Do discrepancies in ppGpp data have a technical or biological (strain-related) origin? We have focused on studies that absolutely quantified basal ppGpp concentrations in *E. coli* strains grown at 37 °C. The deduction of universal trends from this large data set is complicated by the variety in growth conditions, strain genotypes and used analytical methods. We introduce our own measurements of basal ppGpp with a new, sensitive LC-MS method (chapter 2). The combination of former and new data suggests that absolute ppGpp concentrations are not the same across different strains in the same medium, indicating ppGpp calibration to growth conditions is strain specific. In addition, although the correlation between basal ppGpp and growth rate is quite robust, multiple exceptions exist. These offer interesting new insights into the physiological role of basal ppGpp.

3.2. Materials and methods

3.2.1. Strains and growth conditions

The used strains and their sources are presented in **Table S3.1**. Construction of the *rpoC* mutant is explained in chapter 4. Growth conditions are as explained in chapter 2.

3.2.2. Absolute quantification of ppGpp

The LC-MS method to measure basal ppGpp levels in *E. coli* is described in chapter 2.

3.2.3. Total RNA measurements

Cells were sampled and lysed according to the protocol of Potrykus *et al.* [48]. Subsequent RNA quantitation of the lysates was performed using the Quant-iT^{TM} RNA Assay Kit (Thermo Fisher Scientific) according to manufacturer's instructions.

3.3. The basal ppGpp vs. growth rate relationship is strain dependent

First, an overview of steady-state ppGpp basal levels of wild-type strains was made. All data presented in this paragraph are presented in **Figure 3.1**. All the data can also be found in **Table S2.2**.

3.3.1. Basal ppGpp in wild-type strains supporting the correlation between growth rate and ppGpp

The first who measured basal ppGpp levels in various growth media were Lazzarini, Cashel, and Gallant [40]. In an *E. coli* K12 derivative, they observed a clear correlation between ppGpp levels and growth rate (**Figure 3.1A**), as well as RNA/DNA ratios, measured in minimal medium with alanine, succinate, glucose or glucose and casamino acids. Other K12 derivates were studied by Sokawa, Sokawa, and Kaziro [41], who measured basal levels ranging from 20 to 90 pmol OD^{-1} in glucose with amino acids, glucose and succinate media (**Figure 3.1B**), which also inversely correlated with growth rate and RNA levels. Ryals, Little, and Bremer [42] studied the correlation between ppGpp levels and growth rate in an *E. coli* B derivative (**Figure 3.1C**). A linear correlation between ppGpp and growth rate was found based on growth in alanine, succinate, glycerol, glucose and glucose with casamino acids medium. ppGpp levels varied from 15 to 80 pmol OD^{-1}, corresponding nicely with the Lazzarini data and Sokawa data.

In 1988, Baracchini, Glass, and Bremer [61] measured in yet another K12 derivative a range of basal levels (**Figure 3.1D**). They also observe a correlation ppGpp with growth rate, yet the ppGpp levels are lower. This could be related to the different ppGpp analytical methods used: Baracchini, Glass, and Bremer [61] used formaldehyde quenching, lysis with KOH and HPLC quantification of ppGpp, whereas Lazzarini, Cashel, and Gallant [40] used the more common ^{32}P radiolabeling, extraction with formic acid and TLC quantification.

More recently, Buckstein, He, and Rubin [62] measured ppGpp of *E. coli* MG1655 in glycerol, glucose and glucose amino acids medium, with a concentration of respectively 180, 100 and 48 pmol OD^{-1} (estimated from their figure, **Figure 3.1E**). Their values are slightly higher than reported before, which could be due to the large sample volume (50 mL) that cooled down in 30 s. Given that stressed cells

increase from basal to stringent ppGpp regime in a few minutes [63], cooling down for 0.5 min could cause a significant increase in ppGpp level. Therefore, for optimal ppGpp measurement, cells should be quenched within a few seconds.

Given the abundance of studies using *E. coli* MG1655, we measured basal levels in this strain (**Figure 3.1E**), which should be comparable to [62]. We observe a similar trend, but our values are lower, comparable to reports in other strains. This is likely because our sample volume is only 1 mL, allowing quenching times of less than 5 s.

We also included basal level measurements of other common strains, *E. coli* NCM3722 and CF7968 (which is MG1655 *rph*+) (**Figure 3.1G-H**). To our knowledge no other labs have performed prior studies about basal ppGpp in various media on these strains. The basal levels of MG1655, NCM3722 and CF7968 measured here with the same method and same conditions confirm that the correlation between ppGpp and growth rate is quite robust, although quantitative differences might be present.

3.3.2. Certain carbon sources do not follow the ppGpp vs. growth rate trend, in certain strains

All measurements described have been performed in laboratory-adapted strains. Khan and Yamazaki [64] were the only ones to measure ppGpp levels, growth rate and RNA/DNA ratios in an *E. coli* K12 isolated from a patient. In this particular wild-type strain ppGpp levels were determined for an extensive set of carbon sources (glucose with amino acids, glucose, succinate, lactate, pyruvate, acetate, alanine and aspartate) (**Figure 3.1I**). Although a trend is visible between growth rate and several carbon sources (glucose amino acids, glucose, acetate and alanine) others do not align (succinate, pyruvate, lactate, aspartate). Yet RNA/DNA ratios formed a perfect linear trend with growth rate. Unfortunately, the off-trend carbon sources have to our knowledge not been used in any other study.

It is interesting to speculate why certain carbon sources such as succinate, pyruvate, lactate and aspartate do not follow the ppGpp-growth rate trend, yet still display the correlation between RNA level and growth rate [64]. Given that they all have less ppGpp than expected, it seems that RNA synthesis in these cases is limited by something else, potentially NTP substrates (see below). Whatever exactly is limiting growth rate, it appears to not trigger ppGpp synthesis (or decreased ppGpp hydrolysis) by SpoT as much as other carbon sources allowing similar or higher growth rates, such as glycerol and glucose.

3.3.3. Basal ppGpp in *relA*- strains

Of the studies mentioned above, three worked with isogenic *relA*+ and *relA*- strains [40–42]. The data is shown in **Figure 3.1J**. All three observed no significant difference in ppGpp levels and growth rates in *relA*+ and *relA*-, suggesting that SpoT is

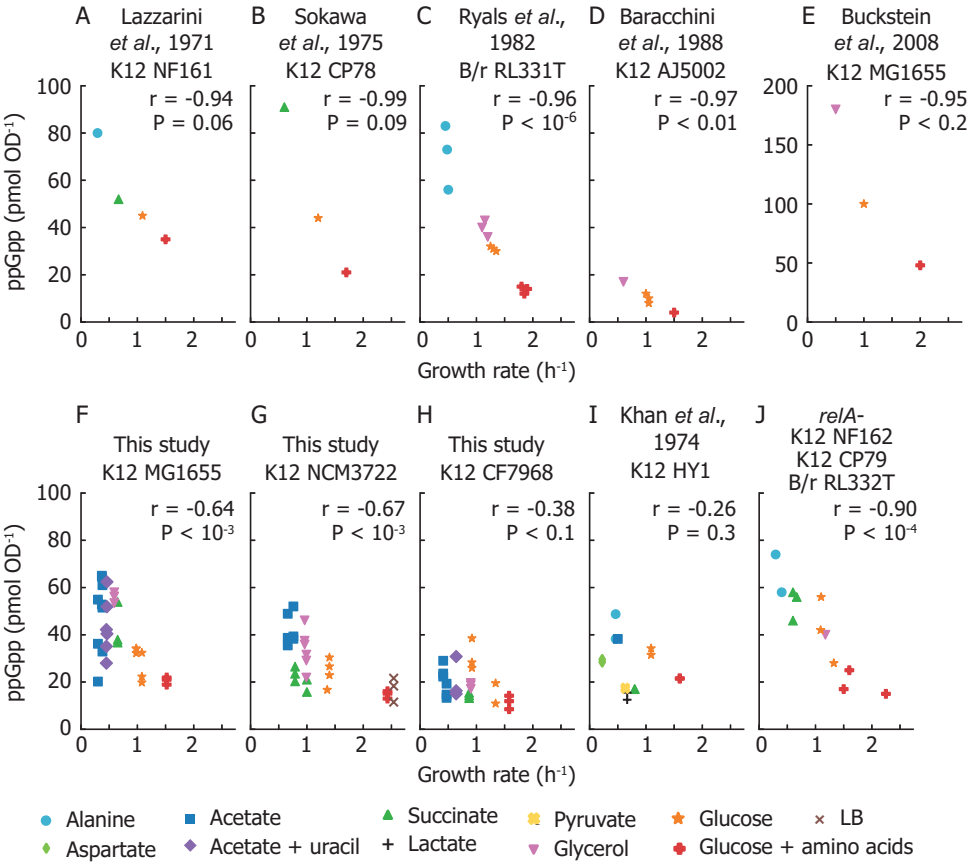

Figure 3.1: Basal ppGpp data from literature and new data showing the correlation between ppGpp and growth rate is quite robust. Data taken from [40–42, 63, 64] and data obtained with new LC-MS method developed in chapter 3. For *relA*- strains, basal ppGpp versus growth rate data was obtained from [40–42]. Data points represent individual replicates. The Pearson correlation coefficient *r* and significance figure P (from a two-tailed significance test) are shown. An overview of all growth conditions, strain genotypes and analytical methods used is presented in Table S3.2.

responsible for the ppGpp levels. It does not necessarily mean that RelA is normally inactive during steady state growth, as it is possible that SpoT activity is not the same in *relA*+ and *relA*- strains.

3.4. Artificial increase of basal ppGpp leads to a steeper ppGpp vs. growth rate trendline

In order to understand how basal ppGpp affects growth rate, scientists have found ways to artificially increase or decrease basal ppGpp in *E. coli*. This allows to titrate ppGpp, without changing any conditions such as the carbon source of the medium.

3.4.1. Increasing basal ppGpp by mutating RelA and SpoT

Some studies used chromosomal SpoT and RelA mutations to achieve different growth rates [43, 44] (**Figure 3.2A**). With this approach, Sarubbi, Rudd, and Cashel [43] varied basal ppGpp levels and observed a decreased activity of *rrnA* promoters. The SpoT mutant strains (CF953-CF956) were derived from *E. coli* NF952 which has a complex genotype with various auxotrophies and a mutation in *relA* (Table S3.2). Hernandez and Bremer [44] also studied ppGpp basal levels in various RelA SpoT mutants, also forming a linear correlation between growth rate (0.55-0.95 h^{-1}) and ppGpp levels (80-10 pmol OD^{-1}) (growing in glucose minimal medium). These mutants were all derivatives of *E. coli* N99, a strain without auxotrophies (Table S3.2).

Changing the activity of SpoT or RelA clearly affects the basal level, which then appears to affect the growth rate. The trend in both studies however is steeper than the correlation between basal levels and growth rate in various carbon sources.

3.4.2. Ectopic overexpression of RelA

Three studies measured ppGpp levels and growth rates in response to overexpression of RelA. This artificially elevates the ppGpp concentration for a given medium. The data of these studies are compared to basal ppGpp vs. growth rate trend obtained by varying carbon sources in **Figure 3.2B**.

Schreiber *et al.* [65] were probably the first to overexpress RelA to titrate ppGpp levels *in vivo*. RelA induction decreased *rrn* P1 activity, but mainly at high levels, below 100 pmol OD^{-1} there was no significant effect. The authors noted that their strain JM109 with a plasmid overexpressing RelA (a growth rate of 0.6 h^{-1} at 200 pmol OD^{-1}) is apparently 10 fold less sensitive to ppGpp than the strain used by Sarubbi, Rudd, and Cashel [43], which has a growth rate of 0.6 h^{-1} at 22 pmol/OD.

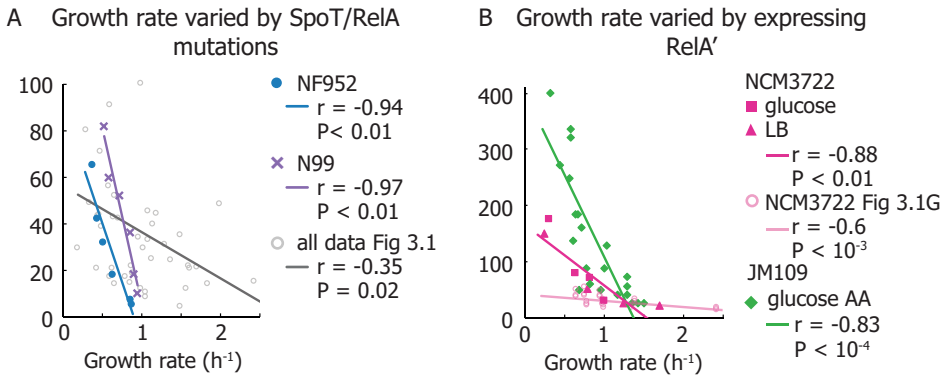

Figure 3.2: ppGpp vs. growth rate trends obtained by varying the numbers or catalytic activity of RelA and SpoT in a constant medium, as compared to varying the carbon source. A) Trends obtained by several *E. coli* strains bearing various mutations in ppGpp synthase/hydrolase enzyme SpoT grown in glucose minimal medium. Each point represents values obtained from one strain (genotypes available in Table S3.2). This is compared to compiled data from Figure 3.1. Data from Sarubbi, Rudd, and Cashel [43] and Hernandez and Bremer [44]. B) Overexpression of RelA in *E. coli* JM109 (in glucose amino acids without Gln, Glu) from Schreiber *et al.* [65] and in *E. coli* NCM3722 in LB (Zhu *et al.* [45]) and glucose minimal medium (Noga *et al.* [66]).

They explain the difference between the two studies as a difference between steady state versus induced ppGpp dynamics. This means that a steady-state ppGpp concentrations has a different effect than the same ppGpp level that is changing over time. It should be noted that the study of Schreiber used glucose medium with most amino acids (all but glutamate and glutamine), whereas Sarubbi used glucose minimal medium.

The RelA overexpression data of Zhu *et al.* [45] (in LB medium) overlap partially with the basal level data of NCM3722 at high growth rates, consistent with the notion that ppGpp controls growth rate in a concentration dependent manner (**Figure 3.2B**). However, at lower growth rates, the ppGpp values are higher than observed in the ppGpp vs. growth rate trend based on different carbon sources. Our lab (Noga *et al.* [66]) also measured the relation between ppGpp and growth rate in NCM3722 with RelA induction (in glucose minimal medium), observing similarly that at lower growth rates, basal ppGpp is higher than expected. The overlap between the Zhu and Noga data suggests that in LB and glucose minimal medium NCM3722 is equally sensitive for ppGpp.

The difference between Schreiber *et al.* [65] and Noga *et al.* [66] or Zhu *et al.* [45] could be due to the different strain used by Schreiber *et al.* [65], or analytical method. Nevertheless, in all studies, overexpression of RelA leads to a ppGpp level higher than expected for a given growth rate. For example, a level of 100 pmol/OD in glucose medium does not reduce growth rate as much as a level of 80 pmol/OD

in acetate medium.

The inhibition of stable RNA synthesis by basal ppGpp has been estimated to be 50 to over 70% at 75 pmol/OD [42, 67], and maximal at 100 pmol/OD [47, 63]. It seems odd that the increased ppGpp due to overexpression of RelA does not reduce growth rate as much. The study of Zhu *et al.* [45] observed however a perfect overlap between RNA/protein vs. growth rate of RelA overexpressed cells and cells that grow in different carbon sources. This suggests that the inhibitory concentration of ppGpp towards RNA polymerase or RNA polymerase 'sensitivity' for ppGpp varies according to the growth conditions.

Given that it is known DksA modulates the sensitivity of RNA polymerase for ppGpp and this way adjusts rRNA synthesis and growth rate, we hypothesize that additional transcription factors or regulators must be present to either regulate DksA, to compete with DksA or to act in parallel with DksA. This is in lign with recent studies showing DksA activity itself is regulated according to pH [68] and oxidative stress in *Salmonella* [69] and that several transcription factors such as GreA, GreB and TraR compete with DksA [70–72].

3.5. Defective nucleotide metabolism leads to a positive correlation between growth rate and ppGpp

Interestingly, some studies of nucleotide metabolism discovered a positive instead of inverse correlation between ppGpp and growth rate. Poulsen and Jensen [73] varied growth rate of *E. coli* (*carAB*-, *guaB*(ts) – uncapable of *de novo* pyrimidine or guanosine synthesis) by varying the pyrimidine and purine source, while monitoring basal ppGpp levels (**Figure 3.3**). Strikingly they discovered that the lower the growth rate is due to limitation of UTP and CTP, the *lower* the level is of basal ppGpp.

A similar study was performed by Vogel, Pedersen, and Jensen [3] with *E. coli* B AS18 (*leu*-) *pyrB*5, a strain also uncapable of *de novo* pyrimidine synthesis. By providing the cells with orotate, the step catalyzed by *pyrBI* is skipped and cells can grow. The growth rate increases with increasing concentrations of orotate in the medium indicating that orotate uptake and pyrimidine synthesis are the growth rate limiting steps in these conditions in this strain. Also here, ppGpp levels increased with increasing growth rate, from 15 to 44 pmol OD^{-1} (**Figure 3.3A**). Total RNA levels increased with increasing growth rate as well, in contrast to the usual decrease of RNA with ppGpp concentration. It appears under these circumstances that ppGpp is not limiting RNA synthesis, but the availability of the substrate, NTP.

Why are ppGpp levels here positively correlated with growth rate? First, it has been observed before that ppGpp does not increase in case of uracil limitation [74]. This appears logical as very low levels of nucleotides will anyway lead to reduced RNA synthesis, omitting the need for ppGpp-mediated arrest. Secondly, the low levels

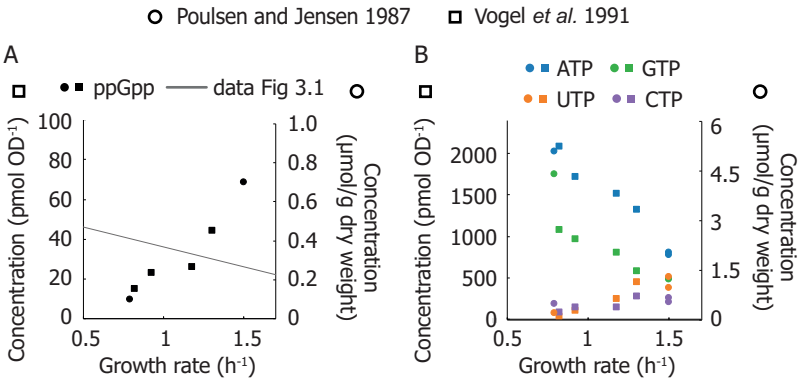

Figure 3.3: Pools of ribonucleotides in *E. coli* with varying degrees of pyrimidine starvation. Data from Poulsen and Jensen [73] and Vogel, Pedersen, and Jensen [3]. A) ppGpp levels overlaid with the ppGpp vs. growth rate trend of Figure 3.1, and B) intracellular ATP, GTP, UTP and CTP levels as a function of growth rate.

of UTP and CTP at slower growth likely represent that they are growth-rate limiting. The fact that their concentrations increase at higher growth rates could mean that they become less and less limiting, and other compounds become more limiting for growth (**Figure 3.3B**). The increased ppGpp levels with growth rate would then be a consequence of another coupled limitation, such as amino acids.

3.6. Growth rate and RNA content do not strictly follow ppGpp concentrations during out-of-steady-state growth transitions

There have been reports of conditions in which (wild-type) RNA polymerase has virtually become insensitive to basal ppGpp. In 1988, Baracchi and Bremer adjusted basal ppGpp levels by addition of varying levels of chloramphenicol or pseudomonic acid to cells growing in glucose medium [63]. Interestingly, very low levels of antibiotics could change ppGpp levels dramatically, with peaks of 20 to 60 pmol OD^{-1}, without a significant effect on the growth rate.

In another study, cells growing in acetate medium were shifted to or glucose medium or a mix of 5 amino acids, both media supporting the same final growth rate, and same RNA/protein ratio [75]. Although the starting and final growth rate are the same, in both situation the ppGpp dynamics and final levels are radically different.

Finally, Hansen *et al.* [76] studied the relief of glucose starvation in *relA*- cells. When glucose was added, ppGpp would increase from 50 pmol to 100 pmol/OD, but RNA

synthesis resumed. When glucose and amino acids mix were added, ppGpp would decrease, yet RNA synthesis resumed in a similar manner as when only glucose was added. Here, the ppGpp level, either virtually 0 or 100 pmol/OD, does not appear to affect RNA synthesis.

Apparently temporal fluctuations of basal ppGpp levels do not affect the cell's response much. However, we know that consistent adjustment of basal ppGpp does affect growth rate and stable RNA levels. Therefore it seems that limited exposure to decreases or increases of ppGpp within the basal regime are not sufficient to elicit a response from RNA polymerase to ppGpp.

3.7. Measurements of basal ppGpp reveal that disruption of ppGpp binding sites on RNA polymerase does not abolish correlation between basal ppGpp, RNA, and growth rate

To determine whether RNA polymerase (RNAP) retains regulation by basal ppGpp if its two ppGpp binding sites are disrupted, we measured basal ppGpp levels, growth rates and cellular RNA in *E. coli* strains expressing RNAP mutants [46, 77]. Although we did not test a strain bearing both mutations together, we reasoned that mutations in either individual binding site might nevertheless strongly affect RNA synthesis control by basal ppGpp and exhibit a weaker relationship between RNA and growth rate, as observed in a $ppGpp^0$ strain by Potrykus *et al.* [48].

We transferred mutations that disrupt ppGpp binding site 1 (*rpoZ*(wt) *rpoC* R362A R417A K615A [77]) or that disrupt ppGpp binding site 2 (*rpoC* N680A K681A [46]) from *E. coli* MG1655 to *E. coli* NCM3722. We confirmed that the stringent response does not arrest RNA synthesis in our mutant strains as strongly as in wild-type (**Figure S3.1**), qualitatively consistent with results previously observed [46]). We sampled cultures that had been grown directly from fresh colonies (i.e. without dilution from overnight cultures) to reduce the outgrowth of cells bearing additional RNAP mutations [78].

ppGpp concentrations remain inversely correlated with growth rate in both mutants. However, both mutants grow more slowly and have correspondingly higher ppGpp concentrations in most growth media than wild-type NCM3722 (**Figure 3.4A,B**). Furthermore, the RNA content of both mutants correlates positively with growth rate, as it does for the wild-type strain (**Figure 3.4C**), with exception of the lower RNA concentration for the *rpoC*2- mutant in LB medium. At first glance, this is consistent with the notion that the RNAP mutants are less sensitive to ppGpp, as apparent from the slopes of cellular RNA content versus ppGpp (**Figure 3.4D**). A chi-squared goodness-of-fit test verified that the mutants do not fit the wild-type pattern ($P<10^{-6}$). In other words, higher ppGpp concentrations may be required

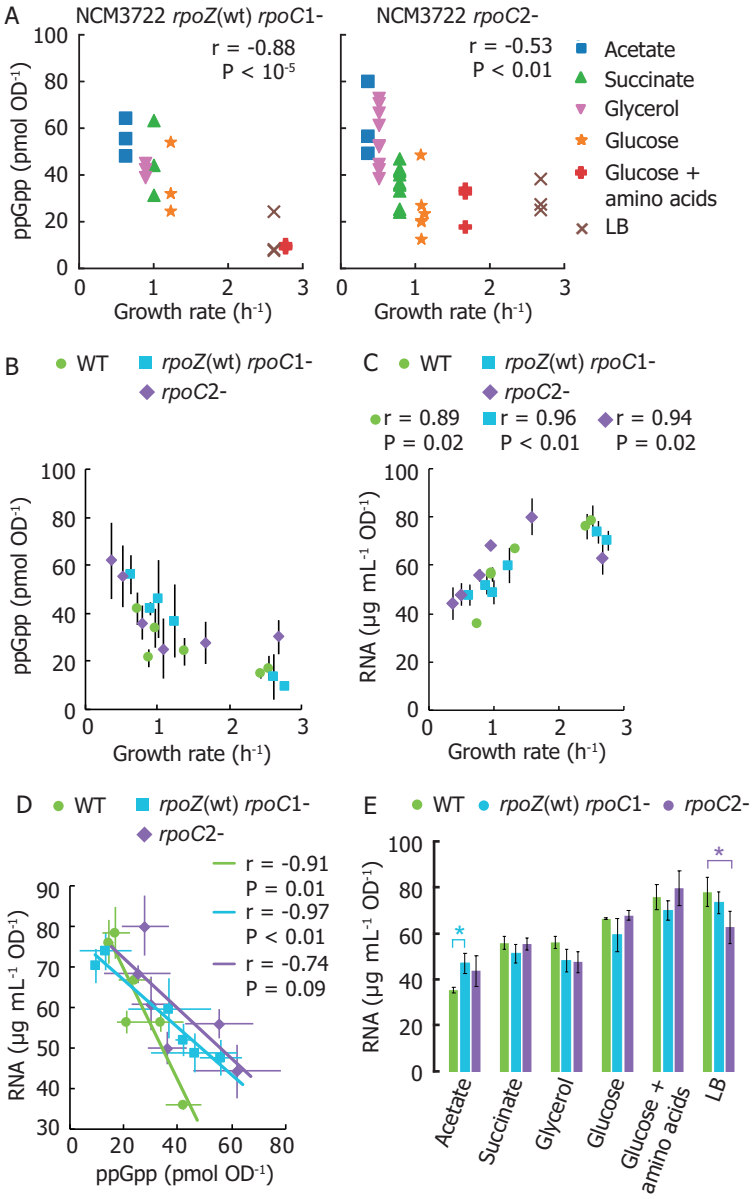

Figure 3.4: RNA polymerase mutants without ppGpp binding site 1 or 2 still exhibit the typical ppGpp and RNA vs. growth rate trends. A) Basal ppGpp in NCM3722 *rpoZ*(wt) and in NCM3722 *rpoC*2- (showing technical replicates, 3 per culture). B) Averaged data of A and B overlapped with average NCM3722 wild-type data from Figure 3.1G. C-E) The total RNA concentration of NCM3722 wild type and rpoC mutants in various growth media. Error bars represent standard deviations. C) Total RNA concentration plotted as a function of growth rate. D) Data of C plotted as a function of ppGpp concentrations with a linear fit. The average or each condition is shown. E) Data of C plotted to compare RNA content between strains grown in identical media. Bars represent the average of three technical replicates of one culture, with exception of *rpoC*2- in glycerol (2 cultures, 6 replicates) and succinate (3 cultures, 9 replicates). *P<0.05 for a two-tailed student's t-test. For A, C and D, the Pearson correlation coefficient *r* and significance figure P (from a two-tailed significance test) is shown.

to inhibit RNA synthesis in these strains. While it might be expected that the cultures expressing ppGpp-insensitive RNAP thus contain a higher RNA abundance than wild-type, we found that for every medium aside from MOPS/acetate, both mutant strains exhibit equivalent or even less RNA per OD unit than does the wild-type (**Figure 3.4E**). This is inconsistent with the abolition of growth rate control of RNA content observed in ppGpp^0 strains [48]. While our results indicate that neither ppGpp binding site on RNAP is individually sufficient to mediating ppGpp control over RNA content, we cannot exclude the possibility that the simultaneous removal of both ppGpp binding sites is required to fully eliminate the ppGpp-RNA content relationship. Other factors may also be implicated in the NCM3722 strain, such as TraR, a transcription factor expressed on the F plasmid (carried by NCM3722) known to mimic the action of DksA and ppGpp [71].

3.8. Conclusion

There is no doubt that basal ppGpp functions as a vital transcriptional regulator, limiting the overproduction of ribosomal RNA and stimulating expression of biosynthetic operons. Our analysis shows however, that the exact concentrations at which ppGpp operates are strain dependent. Given that both the proteins that (potentially) interact with RelA and SpoT, as well as the targets of ppGpp can show extensive genetic variation amongst different strains, it seems plausible the ppGpp signaling network is slightly different amongst different strains. For example the transcription factor TraR is encoded by the F plasmid, which is present in *E. coli* NCM3722, but not MG1655. Compared to MG1655, NCM3722 also carries mutations in *rpoS*, *rpoD* and *rpsG* [79, 80]. In addition, strains can vary in their metabolic capacities. For example, auxotrophies have been reported to confound with the ppGpp signaling network as it forces the use of specific metabolic pathways. This highlights the need of reference strains to be able to compare data from different studies. Also apparent from our analysis, is the importance of keeping in mind the used analytical methods to measure ppGpp, as these can create a bias.

We have presented several conditions in which it appears basal ppGpp has no tight grip on growth rate or RNA levels. Basal ppGpp can easily double in the basal regime below 100 pmol/OD without a decrease in growth rate as expected based on the typical ppGpp vs. growth rate trend in different carbon sources. In addition, brief ups or downs within the basal regime do not appear to have dramatic effects on RNA levels or growth rate.

In line with recent analyses [72], we believe that other factors could be involved in the regulation of RNA polymerase and particular adjusting its sensitivity to ppGpp in various conditions. Although speculative, we hypothesize two in particular. First, we believe additional (unknown) transcription factors such as TraR might play a role [71]. We have observed that even without the DksA-ppGpp binding site on RNA polymerase, RNA levels still correlate with growth rate, suggesting additional factors besides DksA are also involved. Also the activities of these transcription factors

themselves might be regulated according to envionmental conditions, which was recently shown for DksA [68, 69]. Second, when growth rate and RNA synthesis are limited by impaired nucleotide biosynthesis, ppGpp is probably not involved. Possibly NTP shortage is a blind spot for RelA and SpoT.

3.9. Acknowledgements

We thank Michael Cashel and Richard L. Gourse for providing strains.

3.10. Supplementary information

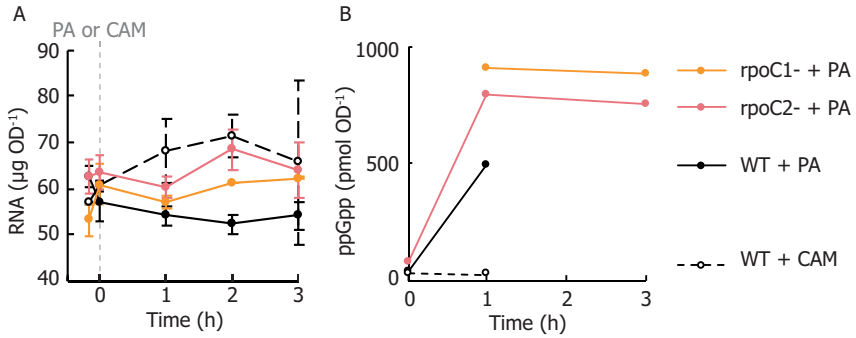

Figure S3.1: Reduced stringent response in the *rpoC* mutants. A) After induction of stringent response by addition of pseudomonic acid (PA) at 100 µg mL^{-1}, the total RNA levels stay more or less constant in the wild-type, whereas they mildly increase in the *rpoC*2- mutant. As a control, chloramphenicol (CAM) was added at 200 µg mL^{-1} to wild type as this shows the increase in RNA when growth is arrested witout an increase with ppGpp. Error bars represent standard deviation of 2 biological replicates. B) ppGpp levels increase in both the wild-type and mutant.

Table S3.1: Strains and plasmids used in this chapter.

Strain	Description	Source
E. coli NCM3722	Wild type	CGSC 12355
E. coli NCM3722 *rpoC*1-	NCM3722 *rpoC* R362A R417A K615A *tetAR*	This work
E. coli NCM3722 *rpoC*2-	NCM3722 *rpoC* N680A K681A *tetAR* (1+2-)	This work
E. coli MG1655	Wild type	DSMZ 18039
E. coli CF7968	MG1655 *rph*+	Mike Cashel

Table S3.2: Data overview of basal ppGpp concentrations used in this chapter.

Figure	Study	Parent strain	Strain	Growth medium	Carbon source	Growth rate (1/h)	ppGpp (pmol/OD)	ppGpp quantification
3.1	Baracchini *et al* 1988	K12 AJ1 (Hayman et al 1974)	AJ5002 (argG metB lacZ53(Am) rpsL(str^r) recA1)	Helmstetter medium C, arginine, methionine	glycerol	0.60	17	10 ml sample, formaldehyde incubation (lysis), KOH extraction, neutralize, HPLC
					glucose	1.00	12	
						1.05	10	
						1.05	8	
					glucose + amino acids	1.50	4	
	Khan and Yamazaki 1974	K12 (patient)	HY1	1 mM phosphate	aspartate	0.19	28.75	radiolabeling, formic acid extraction, TLC
						0.19	29.75	
					alanine	0.46	48.75	
						0.46	38.25	
					acetate	0.50	38.25	
					pyruvate	0.63	17	
						0.63	17.75	
					lactate	0.67	15.5	
						0.67	12.5	
					succinate	0.80	17	
						0.80	17	
					glucose	1.09	34.25	
						1.09	31.5	
					glucose + amino acids	1.60	21.5	
						1.60	21.5	
	Lazzarini *et al* 1971	K12 (W1655 F-)Fiil *et al* 1977	NF161 (meth arg spoT1?)	methionine, arginine, 1 mM KH2PO4	alanine	0.29	80	radiolabeling, formic acid extraction, TLC
					succinate	0.67	52	
					glucose	1.09	45	
					glucose + amino acids	1.50	35	
			NF162 (meth arg spoT1? relA)		alanine	0.29	74	
					succinate	0.67	56	
					glucose	1.09	42	
					glucose + amino acids	1.50	17	

Table S3.2: Data overview of basal ppGpp concentrations used in this chapter.

Figure	Study	Parent strain	Strain	Growth medium	Carbon source	Growth rate (1/h)	ppGpp (pmol/OD)	ppGpp quantification
3.1	Ryals *et al* 1982	B/r ATCC 12407	RL331T (phe)	medium C (Helmstetter, 1967), phenylalanine	alanine	0.45	83	5 ml sample, formaldehyde incubation (lysis), KOH extraction, neutralize, HPLC
						0.48	73	
						0.50	56	
					glycerol	1.10	40	
						1.15	43	
						1.20	36	
					glucose	1.25	32	
						1.30	31	
						1.35	30	
					glucose + amino acids	1.80	15	
						1.85	12	
						1.90	14	
			RL332T (phe relA)		alanine	0.40	58	
					succinate	0.60	46	
					glycerol	1.18	40	
					glucose	1.33	28	
					glucose + amino acids	2.25	15	
	Sokawa *et al* 1975	K12 W677 (Fiil and Friesen 1968)	CP78 (thr leu arg his thi)	threonine, leucine, histidine, arginine, thiamine, 0.1 mM phosphate.	succinate	0.60	91	radiolabeling, formic acid extraction, TLC
					glucose	1.20	44	
					glucose + amino acids	1.70	21	
			CP79 (thr leu arg his thi relA)		succinate	0.60	58	
					glucose	1.10	56	
					glucose + amino acids	1.60	25	
	This thesis	K12 MG1655	CF7968 (lacZ, rph+) (Cashel lab)	1.32 mM phosphate	acetate	0.41	23.6	1 ml sample, formic acid extraction, SPE, LCMS
						0.41	22.3	
						0.41	29.0	
						0.47	19.3	
						0.47	13.3	
						0.47	14.7	

Table S3.2: Data overview of basal ppGpp concentrations used in this chapter.

Figure	Study	Parent strain	Strain	Growth medium	Carbon source	Growth rate (1/h)	ppGpp (pmol/OD)	ppGpp quantification
3.1	This thesis	K12 MG1655	CF7968 (lacZ, rph+) (Cashel lab)	1.32 mM phosphate	acetate + uracil	0.64	16.3	1 ml sample, formic acid extraction, SPE, LCMS
						0.64	30.8	
						0.64	15.0	
					succinate	0.87	14.3	
						0.87	13.2	
						0.87	15.4	
					glycerol	0.90	18.7	
						0.90	19.6	
						0.90	17.1	
					glucose	0.92	26.0	
						0.92	38.5	
						0.92	28.3	
						1.34	19.5	
						1.34	10.9	
					glucose + uracil	1.20	25.8	
						1.20	24.7	
						1.20	21.2	
					glucose + amino acids	1.58	14.2	
						1.58	8.5	
						1.58	11.9	
		K12	MG1655		acetate	0.30	36.2	
						0.30	54.9	
						0.30	20.2	
						0.37	65.0	
						0.37	64.6	
						0.37	52.8	
						0.38	61.0	
						0.38	32.9	
						0.38	51.5	

Table S3.2: Data overview of basal ppGpp concentrations used in this chapter.

Figure	Study	Parent strain	Strain	Growth medium	Carbon source	Growth rate (1/h)	ppGpp (pmol/OD)	ppGpp quantification
3.1	This thesis	K12	MG1655	1.32 mM phosphate	acetate + uracil	0.45	28.0	1 ml sample, formic acid extraction, SPE, LCMS
						0.45	42.2	
						0.45	35.1	
						0.46	40.4	
						0.46	51.9	
						0.46	62.4	
					glycerol	0.59	58.0	
						0.59	53.4	
						0.59	56.2	
					succinate	0.65	37.9	
						0.65	53.9	
						0.65	36.7	
					glucose	0.98	34.2	
						0.98	34.1	
						0.98	32.2	
						1.08	32.4	
						1.08	19.8	
						1.08	22.3	
					glucose + uracil	0.90	88.6	
						0.90	91.4	
						0.90	135.2	
						1.39	38.2	
						1.39	36.5	
						1.39	55.4	
					glucose + amino acids	1.52	18.9	
						1.52	21.0	
						1.52	21.9	

Table S3.2: Data overview of basal ppGpp concentrations used in this chapter.

Figure	Study	Parent strain	Strain	Growth medium	Carbon source	Growth rate (1/h)	ppGpp (pmol/OD)	ppGpp quantification
3.4	This thesis	K12	NCM3722 rpoC1-	1.32 mM phosphate	acetate	0.62	48.1	1 ml sample, formic acid extraction, SPE, LCMS
						0.62	64.3	
						0.62	55.6	
					glycerol	0.89	44.9	
						0.89	38.8	
						0.89	42.2	
					succinate	1.00	31.3	
						1.00	63.3	
						1.00	44.1	
					glucose	1.23	32.0	
						1.23	53.4	
						1.23	24.5	
					glucose + amino acids	2.77	9.4	
						2.77	8.9	
						2.77	10.2	
					LB	2.61	8.1	
						2.61	7.6	
						2.61	24.3	
			NCM3722 rpoC2-		acetate	0.36	49.3	
						0.36	5.6	
						0.36	80.1	
					succinate	0.79	24.1	
						0.79	25.3	
						0.79	33.2	
						0.79	35.7	
						0.79	36.5	
						0.79	40.1	
						0.79	41.7	
						0.79	42.5	
						0.79	46.9	

Table S3.2: Data overview of basal ppGpp concentrations used in this chapter.

Figure	Study	Parent strain	Strain	Growth medium	Carbon source	Growth rate (1/h)	ppGpp (pmol/OD)	ppGpp quantification
3.4	This thesis	K12	NCM3722 rpoC2-	1.32 mM phosphate	glycerol	0.51	38.4	1 ml sample, formic acid extraction, SPE, LCMS
						0.51	42.2	
						0.51	44.5	
						0.51	52.1	
						0.51	52.5	
						0.51	61.2	
						0.51	66.4	
						0.51	70.5	
						0.51	72.7	
					glucose	1.08	12.5	
						1.08	20.0	
						1.08	20.5	
						1.13	23.4	
						1.08	26.9	
						1.07	48.5	
					glucose + amino acids	1.67	17.7	
						1.67	32.3	
						1.67	33.9	
					LB	2.68	25.0	
						2.68	27.4	
						2.68	38.3	
3.1+3.4			NCM3722		acetate	0.76	39.3	
						0.76	38.3	
						0.76	52.0	
						0.66	48.9	
						0.66	38.7	
						0.66	35.5	
					succinate	1.00	21.0	
						1.00	15.8	
						0.79	20.3	

Table S3.2: Data overview of basal ppGpp concentrations used in this chapter.

Figure	Study	Parent strain	Strain	Growth medium	Carbon source	Growth rate (1/h)	ppGpp (pmol/OD)	ppGpp quantification
3.1+3.4	This thesis	K12	NCM3722	1.32 mM phosphate	succinate	0.79	23.5	1 ml sample, formic acid extraction, SPE, LCMS
						0.79	26.5	
					glycerol	0.99	31.6	
						0.99	21.9	
						0.99	29.1	
						0.96	46.1	
						0.96	37.5	
						0.96	35.9	
					glucose	1.36	16.7	
						1.40	26.6	
						1.40	22.9	
						1.40	30.4	
					glucose + amino acids	2.43	15.1	
						2.43	13.0	
						2.43	16.1	
					LB	2.54	21.6	
						2.54	18.3	
						2.54	11.5	
3.2	Hernandez and Bremer 1990	N99: F- galK2 rpsL200 IN(rrnD-rrnE) from K. Rudd/ M.Cashel	CF931 (relA1 spoT204)	Helmstetter medium C	glucose	0.52	82	10 ml sample, formaldehyde incubation (lysis), KOH extraction, neutralize, HPLC
			CF930 (relA1 spoT203)			0.58	60	
			CF929 (relA1 spoT202)			0.72	52	
			CF967 (spoT201)			0.85	36	
			CF927 (relA1)			0.90	18	
			CF926			0.95	10	

Table S3.2: Data overview of basal ppGpp concentrations used in this chapter.

Figure	Study	Parent strain	Strain	Growth medium	Carbon source	Growth rate (1/h)	ppGpp (pmol/OD)	ppGpp quantification
3.2	Sarubbi *et al* 1988	NF952 (Fiil *et al* 1977) thi-1, pyrE60, argE3, his-4, proA2, thr-1, leuB6, mtl-1 xyl-5, ara-14, galK2, lacY1, rpsL31, supE44, cdd, gyrA, pyrG, recA1 (λcI857, S7, pyrG+, relA+)	CF956 (relA1 SpoT204)	0.2 mM phosphate. Supplements according to Davis *et al* 1980	glucose	0.38	65	radiolabeling, formic acid extraction, TLC
			CF955 (relA1 SpoT203)			0.43	42	
			CF954 (relA1 SpoT202)			0.52	32	
			CF953 (SpoT201)			0.63	18	
			CF952 (arg)			0.86	7	
			CF951 (relA1)			0.88	5	
	Schreiber *et al* 1991	K12 derivative	JM109 (recA1, Delta(lac-proAB), gyr96, thi, hsdR17, supE44, (F' traD36, proAB, lacIqZDeltaM15)) + pSM11 (cat. relA) (according to authors not relA1)	0.4 mM phosphate	glucose + amino acids (-Glu -Gln)	0.33	400	As Sarubbi *et al* 1988
						0.38	424	
						0.44	272	
						0.56	248	
						0.57	320	
						0.57	336	
						0.61	136	
						0.64	184	
						0.68	184	
						0.69	48	
						0.71	160	
						0.77	88	
						0.82	60	
						0.96	48	
						1.00	88	
						1.04	128	
						1.17	40	

Table S3.2: Data overview of basal ppGpp concentrations used in this chapter.

Figure	Study	Parent strain	Strain	Growth medium	Carbon source	Growth rate (1/h)	ppGpp (pmol/OD)	ppGpp quantification
3.2	Schreiber *et al* 1991	K12 derivative	JM109 (recA1, Delta(lac-proAB), gyr96, thi, hsdR17, supE44, (F' traD36, proAB, lacIqZDeltaM15)) + pSM11 (cat. relA) (according to authors not relA1)	0.4 mM phosphate	glucose + amino acids (-Glu -Gln)	1.29 1.29 1.29 1.35 1.42 1.50	40 56 72 24 24 24	As Sarubbi *et al* 1988
	Noga *et al* 2020	K12	NCM3722 pRelA	1.32 mM phosphate	glucose	0.31 0.64 0.82 1.00	175 78 70 30	1 ml sample, formic acid extraction, SPE, LCMS
	Zhu *et al* 2019		NCM3722 pMeshI	no phosphate added?	glycerol	0.60 0.38 0.30 0.18	75 45 28 15	2 ml sample, centrifuged for 0.5' at 4dC and washed once. Then formic acid extraction, SPE and UPLC-MS.
			NCM3722 pRelA	-	LB	0.25 0.80 1.25 1.70	150 50 25 20	
3.3	Poulsen *et al* 1987	K12 MC4100 (araD139, D(lac)U169, rpsL, thi)	S01792 (MC4100 carAB, guaB, galK)	AB medium (Clark and Maaloe 1967), thiamine, uridine, guanine (at 32 °C)	glucose + amino acids	1.5 1.5 0.79 0.88 0.85	 0.07* 0.01* 0.03*	radiolabeling, formic acid extraction, TLC
	Vogel *et al* 1991	B AS19 leu pyrB5 rel+	NF321 (Fiil *et al*, j. mol. biol 1972)	leucine, thiamine, 0.3 mM phosphate, uracil 20 ug/ml	glucose	1.30 1.18 0.92 0.82	44 26 23 15	radiolabeling, formic acid extraction, TLC

Table S3.2: Data overview of basal ppGpp concentrations used in this chapter.

Figure	Study	Parent strain	Strain	Growth medium	Carbon source	Growth rate (1/h)	ppGpp (pmol/OD)	ppGpp quantification
3.1	Buckstein *et al* 2008	K12	MG1655	1 mM phosphate, thymine	glycerol	0.50	180	50 ml sample, formic acid extraction, ion exchange chromatograhpy, dialysis, lyophilization, HPLC
					glucose	1	100	
					glucose + amino acids	2	48	

references

[1] N. C. E. Imholz, M. J. Noga, N. J. F. van den Broek, and G. Bokinsky. "Calibrating the bacterial growth rate speedometer: a re-evaluation of the relationship between basal ppGpp, growth, and RNA synthesis in *Escherichia coli*". In: *Frontiers in Microbiology* (2020). doi: 10.3389/fmicb.2020.574872.

[2] K. Johnsen, S. Molin, O. Karlstrom, and O. Maaloe. "Control of protein synthesis in *Escherichia coli*: analysis of an energy source shift-down". In: *Journal of Bacteriology* 131.1 (1977), pp. 18–29.

[3] U. Vogel, S. Pedersen, and K. A. J. F. Jensen. "An unusual correlation between ppGpp pool size and rate of ribosome synthesis during partial pyrimidine starvation of *Escherichia coli*". In: *Journal of Bacteriology* 173.3 (1991), pp. 1168–1174.

[4] M. A. Sorensen, K. F. Jensen, and S. Pedersen. "High Concentrations of ppGpp Decrease the RNA Chain Growth Rate: Implications for Protein Synthesis and Translational Fidelity During Amino Acid Starvation in *Escherichia coli*". In: *Journal of Molecular Biology* 236 (1994), pp. 441–454.

[5] P. Sanchez-Vazquez, C. N. Dewey, N. Kitten, W. Ross, and R. L. Gourse. "Genome-wide effects on *Escherichia coli* transcription from ppGpp binding to its two sites on RNA polymerase". In: *Proceedings of the National Academy of Sciences* (2019).

[6] J. J. Lemke, P. Sanchez-Vazquez, H. L. Burgos, G. Hedberg, W. Ross, and R. L. Gourse. "Direct regulation of *Escherichia coli* ribosomal protein promoters by the transcription factors ppGpp and DksA". In: *Proceedings of the National Academy of Sciences* 108.14 (2011), pp. 5712–5717.

[7] P. Edelmann and J. Gallant. "Mistranslation in *E. coli*". In: *Cell* 10.1 (1977), pp. 131–137. doi: 10.1016/0092-8674(77)90147-7.

[8] P. H. OFarrell. "The suppression of defective translation by ppGpp and its role in the stringent response". In: *Cell* 14.3 (1978), pp. 545–557. doi: 10.1016/0092-8674(78)90241-6.

[9] J. A. Gallant and D. Foley. "Stringent control of translational accuracy". In: *Regulation of macromolucular synthesis by low molecular weight mediators*. 1979.

[10] D. B. Dix and R. C. Thompson. "Elongation factor Tu-guanosine 3′-diphosphate 5′-diphosphate complex increases the fidelity of proofreading in protein biosynthesis: Mechanism for reducing translational errors induced by amino acid starvation". In: *Proceedings of the National Academy of Sciences* 83 (1986), pp. 2027–2031.

[11] A. L. Svitil, M. Cashel, and J. W. Zyskind. "Guanosine tetraphosphate inhibits protein synthesis *in vivo*". In: *The Journal of Biological Chemistry* 268.4 (1993), pp. 2307–2311. issn: 0021-9258.

[12] V. A. Mitkevich, A. Ermakov, A. A. Kulikova, S. Tankov, V. Shyp, A. Soosaar, T. Tenson, A. A. Makarov, M. Ehrenberg, and V. Hauryliuk. "Thermodynamic Characterization of ppGpp Binding to EF-G or IF2 and of Initiator tRNA Binding to Free IF2 in the Presence of GDP, GTP or ppGpp". In: *Journal of Molecular Biology* 402.5 (2010), pp. 838–846. doi: 10.1016/j.jmb.2010.08.016.

[13] K. Kihira, Y. Shimizu, Y. Shomura, N. Shibata, M. Kitamura, A. Nakagawa, T. Ueda, K. Ochi, and Y. Higuchi. "Crystal structure analysis of the translation factor RF3 (release factor 3)". In: *FEBS Letters* 586.20 (2012), pp. 3705–3709.

[14] J. Gallant, J. Irr, and M. Cashel. "The mechanism of amino acid control of guanylate and adenylate biosynthesis". In: *Journal of Biological Chemistry* 246.18 (1971), pp. 5812–5816.

[15] J. Hochstadt-Ozer and M. Cashel. "The Regulation of Purine Utilization in Bacteria. V. Inhibition of purine phosphoribosyltransferase activities and purine uptake in isolated membrane vesicles by guanosine tetraphosphate". In: *Journal of Biological Chemistry* 247 (1972), pp. 7067–7072.

[16] M. M. Stayton and H. J. Fromm. "Guanosine 5′-diphosphate-3′-diphosphate inhibition of adenylosuccinate synthetase". In: *Journal of Biological Chemistry* 254 (1979), pp. 2579–2581.

[17] C. C. Pao and B. T. Dyess. "Effect of unusual guanosine nucleotides on the activities of some *Escherichia coli* cellular enzymes". In: *Biochimica et Biophysica Acta* 677 (1981), pp. 358–362.

[18] B. Wang, P. Dai, D. Ding, A. D. Rosario, R. A. Grant, B. L. Pentelute, and M. T. Laub. "Affinity-based capture and identification of protein effectors of the growth regulator ppGpp". In: *Nature Chemical Biology* (2018). doi: 10.1038/s41589-018-0183-4.

[19] Y. Zhang, E. Zbornikova, D. Rejman, and K. Gerdes. "Novel (p)ppGpp Binding and Metabolizing Proteins of *Escherichia coli*". In: *mBio* 9.2 (2018), pp. 1–20.

[20] Y. E. Zhang, R. L. Baerentsen, T. Fuhrer, U. Sauer, K. Gerdes, and D. E. Brodersen. "(p)ppGpp Regulates a Bacterial Nucleosidase by an Allosteric Two-Domain Switch". In: *Molecular Cell* 74.6 (2019), pp. 1239–1249.

[21] D. P. Morton and S. M. Parsons. "Synergistic inhibition of ATP phosphoribosyltransferase by guanosine tetraphosphate and histidine". In: *Biochemical and Biophysical Research Communications* 74.1 (1977), pp. 172–177.

[22] M. R. Maurizi and F. Rasulova. "Degradation of Glutamate Dehydrogenase from *Escherichia coli*: Allosteric Regulation of Enzyme Stability". In: *Archives of Biochemistry and Biophysics* 397.2 (2002), pp. 206–216.

[23] U. Kanjee, I. Gutsche, S. Ramachandran, and W. A. Houry. "The enzymatic activities of the *Escherichia coli* basic aliphatic amino acid decarboxylases exhibit a pH zone of inhibition". In: *Biochemistry* 50 (2011), pp. 9388–9398.

[24] M. Taguchi, K. Izui, and H. Katsuki. "Activation of *Escherichia coli* phosphoenolpyruvate carboxylase by guanosine-5'-diphosphate-3'-diphosphate". In: *FEBS Letters* 77.2 (), pp. 270–272.

[25] M. Taguchi, K. Izui, and H. Katsuki. "Stringent control of glycolysis in *Escherichia coli*". In: *Biochemical and Biophysical Research Communications* 84.1 (1978), pp. 195–201.

[26] S. E. Polakis, R. B. Guchhait, and M. D. Lane. "Stringent control of fatty acid synthesis in *Escherichia coli*". In: *Journal of Biological Chemistry* 248.22 (1973), pp. 7957–7966.

[27] J. P. Stein and K. E. Bloch. "Inhibition of *E.coli* β-hydroxydecanoyl thioester dehydrase by ppGpp". In: *Biochemical and Biophysical Research Communications* 73.4 (1976), pp. 881–884.

[28] A. Spencer, E. Muller, J. E. Cronan, and T. A. Gross. "*relA* gene control of the synthesis of lipid A fatty acyl moieties". In: *Journal of Bacteriology* 130.1 (1977), pp. 114–117.

[29] R. J. Heath, S. Jackowski, and C. O. Rock. "Guanosine tetraphosphate inhibition of fatty acid and phospholipid synthesis in *Escherichia coli* is relieved by overexpression of glycerol-3-phosphate acyltransferase (*plsB*)". In: *Journal of Bacteriology* 269.42 (1994), pp. 26584–26590.

[30] M. Maciag, M. Kochanowska, R. Lyzen, G. Wegrzyn, and A. Szalewska-Palasz. "ppGpp inhibits the activity of *Escherichia coli* DnaG primase". In: *Plasmid* 63 (1 2010), pp. 61–67.

[31] R. U. Rymer, F. A. Solorio, A. K. Tehranchi, C. Chu, J. E. Corn, J. L. Keck, J. D. Wang, and J. M. Berger. "Binding Mechanism of Metal·NTP Substrates and Stringent-Response Alarmones to Bacterial DnaG-Type Primases". In: *Cell* 20.9 (2012), pp. 1478–1489.

[32] J. DeNapoli, A. K. Tehranchi, and J. D. Wang. "Dose-dependent reduction of replication elongation rate by (p)ppGpp in *Escherichia coli* and *Bacillus subtilis*". In: *Molecular Microbiology* 88.1 (2013), pp. 93–104.

[33] N. P. Fiil, B. M. Willumsen, J. D. Friesen, and K. V. Meyenburg. "Interaction of alleles of relA, relC and SpoT Genes in *Escherichia coli*: Analysis of the interconversion of GTP , ppGpp and pppGpp". In: *Molecular & General Genetics* 101 (1977), pp. 87–101.

[34] R. Harshman and H. Yamazaki. "MS I accumulation induced by sodium chloride". In: *Biochemistry* 11.4 (1972), pp. 615–618.

[35] J. Gallant, L. Palmer, and C. C. Pao. "Anomalous synthesis of ppGpp in growing cells". In: *Cell* 11.1 (1977), pp. 181–185. doi: 10.1016/0092-8674(77)90329-4.

[36] Z. D. Dalebroux, S. L. Svensson, E. C. Gaynor, and M. S. Swanson. "ppGpp Conjures Bacterial Virulence". In: *Microbiology and Molecular Biology Reviews* 74.2 (2010), pp. 171–199.

[37] J. K. Hobbs and A. B. Boraston. "(p)ppGpp and the Stringent Response: An Emerging Threat to Antibiotic Therapy". In: *ACS Infectious Diseases* 5.9 (2019), pp. 1505–1517.

[38] T. K. Wood and S. Song. "Forming and waking dormant cells: The ppGpp ribosome dimerization persister model". In: *Biofilm* 2 (2020), pp. 1–6.

[39] V. Hauryliuk, G. C. Atkinson, K. S. Murakami, T. Tenson, and K. Gerdes. "Recent functional insights into the role of (p)ppGpp in bacterial physiology". In: *Nature Reviews Microbiology* 13.5 (2015), pp. 298–309.

[40] R. Lazzarini, M. Cashel, and J. Gallant. "On the Regulation of Guanosine Tetraphosphate Levels in Stringent and Relaxed Strains of *Escherichia coli*". In: *Journal of Biological Chemistry* 246.14 (1971), pp. 4381–4385.

[41] Y. Sokawa, J. Sokawa, and Y. Kaziro. "Regulation of stable RNA synthesis and ppGpp levels in growing cells of *Escherichia coli*". In: *Cell* 5.1 (1975), pp. 69–74.

[42] J. Ryals, R. Little, and H. Bremer. "Control of ribosomal-RNA and transfer-RNA syntheses in *Escherichia coli* by guanosine tetraphosphate". In: *Journal of Bacteriology* 151.3 (1982), pp. 1261–1268.

[43] E. Sarubbi, K. E. Rudd, and M. Cashel. "Basal ppGpp level adjustment shown by new SpoT mutants affect steady state growth rates and *rrnA* ribosomal promoter regulation in *Escherichia coli*". In: *MGG Molecular & General Genetics* 213.2-3 (1988), pp. 214–222. doi: 10.1007/BF00339584.

[44] V. J. Hernandez and H. Bremer. "Guanosine tetraphosphate (ppGpp) dependence of the growth rate control of *rrnB* P1 promoter activity in *Escherichia coli*". In: *Journal of Biological Chemistry* 265.20 (1990), pp. 11605–11614.

[45] M. Zhu, M. Mori, T. Hwa, and X. Dai. "Disruption of transcription–translation coordination in *Escherichia coli* leads to premature transcriptional termination". In: *Nature Microbiology* (2019). doi: 10.1038/s41564-019-0543-1.

[46] W. Ross, P. Sanchez-Vazquez, A. Y. Chen, J. H. Lee, H. L. Burgos, and R. L. Gourse. "ppGpp binding to a site at the RNAP-DksA interface accounts for its dramatic effects on transcription initiation during the stringent response". In: *Molecular Cell* 62.6 (2016), pp. 811–823. doi: 10.1016/j.molcel.2016.04.029.

[47] R. Little, J. Ryals, and H. Bremer. "Physiological characterization of *Escherichia coli rpoB* mutants wit abnormal control of ribosome synthesis". In: *Journal of Bacteriology* 155.3 (1983), pp. 1162–1170.

[48] K. Potrykus, H. Murphy, N. Philippe, and M. Cashel. "ppGpp is the major source of growth rate control in *E. coli*". In: *Environmental Microbiology* 13.3 (2011), pp. 563–575.

[49] M. Scott, S. Klumpp, E. M. Mateescu, and T. Hwa. "Emergence of robust growth laws from optimal regulation of ribosome synthesis". In: *Molecular Systems Biology* 10.8 (2014), p. 747.

[50] E. Bosdriesz, D. Molenaar, B. Teusink, and F. J. Bruggeman. "How fast-growing bacteria robustly tune their ribosome concentration to approximate growth-rate maximization". In: *FEBS Journal* 282.10 (2015), pp. 2029–2044.

[51] M. F. Traxler, S. M. Summers, H. T. Nguyen, V. M. Zacharia, G. A. Hightower, J. T. Smith, and T. Conway. "The global, ppGpp-mediated stringent response to amino acid starvation in *Escherichia coli*". In: *Molecular Microbiology* 68.5 (2008), pp. 1128–1148.

[52] H. Bremer and P. P. Dennis. "Modulation of Chemical Composition and Other Parameters of the Cell at Different Exponential Growth Rates". In: *EcoSal Plus* 3.1 (2008). doi: 10.1128/ecosal.5.2.3.

[53] X. Dai, M. Zhu, M. Warren, R. Balakrishnan, V. Patsalo, and H. Okano. "Reduction of translating ribosomes enables *Escherichia coli* to maintain elongation rates during slow growth". In: *Nature Microbiology* (2016). doi: 10.1038/nmicrobiol.2016.231.

[54] S. H. J. Li, Z. Li, J. O. Park, C. G. King, J. D. Rabinowitz, N. S. Wingreen, and Z. Gitai. "*Escherichia coli* translation strategies differ across carbon, nitrogen and phosphorus limitation conditions". In: *Nature Microbiology* 3.8 (2018), pp. 939–947.

[55] Y. K. Kohanim, D. Levi, G. Jona, B. D. Towbin, A. Bren, and U. Alon. "A bacterial growth law out of steady state". In: *Cell Reports* 23.10 (2018), pp. 2891–2900.

[56] V. Varik, S. R. A. Oliveira, V. Hauryliuk, and T. Tenson. "HPLC-based quantification of bacterial housekeeping nucleotides and alarmone messengers ppGpp and pppGpp". In: *Scientific Reports* 7.1 (2017), pp. 1–12. doi: 10.1038/s41598-017-10988-6.

[57] H. Jin, Y. M. Lao, J. Zhou, H. J. Zhang, and Z. H. Cai. "A rapid UHPLC-HILIC method for algal guanosine 5′-diphosphate 3′-diphosphate (ppGpp) and the potential separation mechanism". In: *Journal of Chromatography B: Analytical Technologies in the Biomedical and Life Sciences* 1096.February (2018), pp. 143–153. doi: 10.1016/j.jchromb.2018.08.009.

[58] Y. Ihara, H. Ohta, and S. Masuda. "A highly sensitive quantification method for the accumulation of alarmone ppGpp in *Arabidopsis thaliana* using UPLC-ESI-qMS/MS". In: *Journal of Plant Research* 128.3 (2015), pp. 511–518. doi: 10.1007/s10265-015-0711-1.

[59] C. Patacq, N. Chaudet, and F. Letisse. "Absolute Quantification of ppGpp and pppGpp by Double-Spike Isotope Dilution Ion Chromatography-High-Resolution Mass Spectrometry". In: *Analytical Chemistry* 90.18 (2018), pp. 10715–10723. doi: 10.1021/acs.analchem.8b00829.

[60] J. Irr and J. Gallant. "The control of RNA synthesis in *Escherichia coli*. II. Stringent control of energy metabolism." In: *Journal of Biological Chemistry* 244.8 (1969), pp. 2233–2239.

[61] E. Baracchini, R. Glass, and H. Bremer. "Studies *in vivo* on *Escherichia coli* RNA polymerase mutants altered in the stringent response". In: *Molecular & General Genetics* 213 (1988), pp. 379–387.

[62] M. H. Buckstein, J. He, and H. Rubin. "Characterization of nucleotide pools as a function of physiological state in *Escherichia coli*". In: *Journal of Bacteriology* 190.2 (2008), pp. 718–726.

[63] E. Baracchini and H. Bremer. "Stringent and growth control of rRNA Synthesis in *Escherichia coli* are both mediated by ppGpp". In: *Journal of Biological Chemistry* 263.6 (1988), pp. 2597–2602.

[64] S. R. Khan and H. Yamazaki. "Inapparent correlation between guanosine tetraphosphate levels and RNA contents in *Escherichia coli*". In: *Biochemical and Biophysical Research Communications* 59.I (1974), pp. 125–132.

[65] G. Schreiber, S. Metzgers, E. Aizenman, S. Roza, M. Cashel, and G. Glaser. "Overexpression of the *relA* gene in *Escherichia coli*". In: *Journal of Biological Chemistry* 266.6 (1991), pp. 3760–3767.

[66] M. J. Noga, F. Buke, N. J. F. van den Broek, N. Imholz, N. Scherer, F. Yang, and G. Bokinsky. "Posttranslational Control of PlsB Is Sufficient To Coordinate Membrane Synthesis with Growth in *Escherichia coli*". In: *mBio* 11 (4 2020), e02703–19. doi: 10.1128/mBio.02703-19.

[67] N. P. Fiil and K. Von Meyenburg. "Accumulation and turnover of guanosine tetraphosphate in *Escherichia coli*". In: *Journal of Molecular Biology* 71 (1972), pp. 769–783.

[68] R. Furman, E. M. Danhart, M. NandyMazumdar, C. Yuan, M. P. Foster, and I. Artsimovitch. "pH Dependence of the Stress Regulator DksA". In: *PLOS ONE* 10.3 (2015), e0120746.

[69] J.-S. Kim, L. Liu, L. F. Fitzsimmons, Y. Wang, M. A. Crawford, M. Mastrogiovanni, M. Trujillo, J. K. A. Till, R. Radi, S. Dai, and A. Vázquez-Torres. "DksA–DnaJ redox interactions provide a signal for the activation of bacterial RNA polymerase". In: *Proceedings of the National Academy of Sciences* 115.50 (2018), E11780–E11789.

[70] D. Vinella, K. Potrykus, H. Murphy, and M. Cashel. "Effects on growth by changes of the balance between GreA, GreB, and DksA suggest mutual competition and functional redundancy in *Escherichia coli*". In: *Journal of Bacteriology* 194.2 (2012), pp. 261–273.

[71] S. Gopalkrishnan, W. Ross, A. Y. Chen, and R. L. Gourse. "TraR directly regulates transcription initiation by mimicking the combined effects of the global regulators DksA and ppGpp". In: *Proceedings of the National Academy of Sciences* 114.28 (2017), E5539–E5548.

[72] L. Fernández-Coll and M. Cashel. "Contributions of SpoT hydrolase, SpoT synthetase, and RelA synthetase to carbon source diauxic growth transitions in *Escherichia coli*". In: *Frontiers in Microbiology* 9.AUG (2018), pp. 1–13.

[73] P. Poulsen and K. F. Jensen. "Effect of UTP and GTP pools on attenuation at the *pyrE* gene of *Escherichia coli*". In: *Molecular and General Genetics* 208 (1987), pp. 152–158.

[74] M. Cashel and J. Gallant. "Two Compounds implicated in the Function of the RC Gene of *Escherichia coli*". In: *Nature* 221 (1969), pp. 838–841.

[75] J. Friesen, N. Fiil, and K. von Meyenburg. "Synthesis and turnover of basal level guanosine tetraphosphate in *Escherichia coli*". In: *Journal of Biological Chemistry* 250.1 (1975), pp. 304–309.

[76] M. T. Hansen, M. L. Pato, S. Molin, N. P. Fiil, and K. von Meyenburg. "Simple downshift and resulting lack of correlation between ppGpp pool size and ribonucleic acid accumulation". In: *Journal of Bacteriology* 122.2 (1975), pp. 585–591.

[77] W. Ross, C. E. Vrentas, P. Sanchez-Vazquez, T. Gaal, and R. L. Gourse. "The magic spot: A ppGpp binding site on *E. coli* RNA polymerase responsible for regulation of transcription initiation." In: *Molecular Cell* 50 (2013), pp. 420–429.

[78] K. D. Murphy and H. Bremer. "Control of *spoT*-dependent ppGpp synthesis and degradation in *Escherichia coli*". In: *Methods in Enzymology* 371 (2003), pp. 596–601.

[79] E. Lyons, M. Freeling, S. Kustu, and W. Inwood. "Using Genomic Sequencing for Classical Genetics in *E. coli* K12". In: *PLoS ONE* 6.2 (2011), e16717.

[80] S. D. Brown and S. Jun. "Complete Genome Sequence of *Escherichia coli* NCM3722". In: *Genome Announcements* 3.4 (Aug. 2015). doi: 10.1128/genomea.00879-15.

4

Suprabasal guanosine tetraphosphate (ppGpp) levels inhibit translation rates in *E. coli* through various targets

ppGpp is known as an alarmone, as upon various stresses, its concentration dramatically spikes, rearranging transcription of most genes due to its action on RNA polymerase in concert with DksA. Besides coordinating transcription, ppGpp has been reported to bind enzymes in several major metabolic pathways, including the synthesis of proteins. However, the precise regulatory role of ppGpp regarding translation has yet to be deciphered, as there is evidence both supporting and refuting an inhibition of translation by ppGpp. Both the lack of quantitative data about ppGpp, as well as the confounding effect of ppGpp on transcription currently hamper to settle this debate. Here, we have developed in vitro and in vivo approaches to titrate ppGpp in cellular systems where translation is uncoupled from transcription. Using a newly developed LC-MS method, we identify three concentration regions with different roles for ppGpp. At the so-called basal regime (up to $200\,\mathrm{pmol\,OD^{-1}}$*), ppGpp does not affect translation directly. At stringent response levels (above* $700\,\mathrm{pmol\,OD^{-1}}$*), ppGpp dramatically inhibits translation initiation and/or elongation. Interestingly, at intermediate concentrations, another mechanism is active as ppGpp limits the fraction of active ribosomes.*

This chapter has been submitted for publication as: N. C. E. Imholz, D. Foschepoth, C. Danelon, and G. Bokinsky. "Suprabasal guanosine tetraphosphate (ppGpp) levels reduce translation rates in *E. coli* by inhibiting various targets". In: (2020)

4.1. Introduction

The signaling molecule ppGpp is the major regulator of growth rate in *E. coli* [2]. It is best known for its direct interaction with RNA polymerase, which inhibits the synthesis of ribosomes and changes transcription of over 750 genes during response to stress [3]. During regular growth, low ppGpp concentrations inversely correlate with growth rate [4–6]. Albeit discovered nearly 50 years ago, it is still not clear what the exact effects are of these so-called basal ppGpp levels.

Besides RNA polymerase, 50 other targets of ppGpp have been reported that could play a role in the growth rate control of ppGpp, of which most are involved in protein synthesis [7, 8]. Protein synthesis consumes up to 40% of the total energy budget of the cell [9] and its output comprises 42-60% of the dry weight [10]. As translation is a costly process, it is reasonable that it is regulated at many points by a major signal such as ppGpp. Especially given the structural similarity between the energy carrier used to drive reactions (GTP) and ppGpp, it seems plausible that ppGpp could act as a competitive inhibitor of ribosome associated GTPases, as supported by several *in vitro* studies [7, 8, 11–13], though not all [14, 15].

However, previous studies have not been able to unambiguously demonstrate an effect of ppGpp towards protein synthesis. On one hand, *in vitro* studies showing interactions between ppGpp and IF2, EF-G and RF3, lack a direct *in vivo* confirmation. On the other hand, *in vivo* studies have had contradicting outcomes, concluding ppGpp only affects transcription and not translation [16–18], or inhibits both [19–23]. This is due to the difficulty of disentangling a possible effect of ppGpp on protein synthesis from other targets in the cell, such as RNA polymerase. In addition, quantification of ppGpp is tricky, and most studies infer effects of ppGpp by comparison of wild type, *relA*- and/or ppGpp-defective strains, which does not lead to a quantitative understanding of the physiological roles of ppGpp.

To settle this debate, we designed a series of *in vitro* and *in vivo* experiments in which the effects of ppGpp on transcription and translation were uncoupled and monitored independently. Combined with absolute quantitation of intracellular ppGpp concentrations, we show that at stringent concentrations above 700 pmol OD^{-1} ppGpp inhibits translation directly and post-translationally. At intermediate ppGpp levels, ranging from 300 to 700 pmol OD^{-1}, there is an inhibition of translation which however does not appear to affect translation initiation or elongation. Rather the active fraction of ribosomes has reduced. At even lower, basal ppGpp concentrations, ppGpp does not directly affect translation whatsoever, apart from its transcriptional control of RNA polymerase.

4.2. Materials and methods

4.2.1. PURE *in vitro* reactions

The PURE system consists of *E. coli* translation initiation factors, elongation factors and termination factors, ribosomes, aminoacyl tRNA synthetases and T7 phage RNA polymerase as well as all NTPs, amino acids and necessary cofactors [24, 25]. Addition of DNA will result in synthesis of the protein of interest. The exact amounts of all compounds are known, guaranteeing complete control over the system. The system was commercialized by GeneFrontier as PUREfrex.

The PUREfrex *in vitro* reactions were performed according to manufacturer's protocol and were kindly provided by Christophe Danelon. The plasmid carrying the YFP-Spinach sequence was also kindly provided by Christophe Danelon. The PCR of the YFP-Spinach construct (**Figure 4.1A**) including the T7 promoter and ribosomal binding site was performed according to van Nies *et al.* [26]. The compounds were pipetted in a mastermix in a specific order because deviations appeared to affect the results (**Table S4.2**). Peptidyl-tRNA hydrolase (PTH) was kindly provided by Anne Doerr and added at 2 µM. 19 µL of mastermix was transferred to a new tube to which 1 µL ppGpp (0, 2, 10 or 20 mM) was added. Subsequently 19 µL of these solutions were transferred to cuvettes (Hellma), closed with lid, and placed in a fluorescence spectrophotometer (Cary Eclipse from Varian) in a temperature-controlled holder set at 37 °C. The fluorescence signal for Spinach and YFP was recorded at respectively 460/502 and 515/528 nm, every 30 seconds for 500 minutes. The cuvettes were cleaned immediately after each experiment with successively 0.2 % Hellmanex, 1M KOH, nuclease-free water, 100 % EtOH, each incubating for 1 min in a bath sonicator with three nuclease-free water washes in between each solvent.

For data analysis, a linear curve was fitted to the initial part of the fluorescence traces. In the initial part of the curve no substrates are limiting yet, and the exponential increase of YFP can be approximated with a linear curve. Hereto, a Matlab script determined for each window of 10 min (20 data points) whether the trend was linear using a Durbin-Watson test. The slope of the earliest linear 10 min window was used as Spinach or YFP synthesis rate.

4.2.2. *In vitro* transcription and translation using cellular lysates

Experimental information

The protocol for cell free lysate preparation was based on Hansen *et al.* [27]. *E. coli* Rosetta2 was grown in 2YTPG broth at 37 °C. At OD 1.5 cells were centrifuged (3000 g 10 min, 4 °C) and the cell pellet suspended in ice-cold 20 % sucrose. After 10 min incubation on ice, cells were again centrifuged (same conditions), resuspended in ice-cold MQ (4 times pellet weight). Centrifugation, resuspension in MQ and 10 min incubation on ice was repeated once more, before two more washes with ice-cold MQ (1.5 x volume). The spheroplast pellet was then stored at −80 °C,

thawed and resuspend in ice-cold MQ (0.8 x volume). Cell lysis was performed using sonication (10 cycles of 10 s at 10 µm amplitude and 30 s on ice). The lysate was centrifuged at 30 000 g for 30 min at 4 °C, dialyzed 1 x against 50 % dialysis buffer (5 mM Tris, 30 mM potassium glutamate, 7 mM magnesium glutamate and 0.5 mM DTT) and 3 x against 100 % dialysis buffer (10 mM Tris, 60 mM potassium glutamate, 14 mM magnesium glutamate and 1 mM DTT).

The lysate *in vitro* transcription and translation reaction had a volume of 10 uL and contained 33 % v/v of the cell lysate and 66 % v/v reaction buffer, with a final concentration of 50 mM Hepes (pH 8.0), 1 mM UTP, 1 mM CTP, 3 mM ATP, 3 mM GTP, 0.66 mM spermidine, 0.5 mM cyclic adenosine monophosphate (cAMP), 0.22 mM nicotinamide adenine dinucleotide (NAD), 0.17 mM coenzyme A, 20 mM 3-phosphoglyceric acid (3-PGA), 0.045 mM folinic acid, 10 mM magnesium glutamate, 66 mM potassium glutamate and 20 µM DFHBI. The same DNA was used as in the PURE system, at a concentration of 2 nM. ppGpp was added last at a final concentration of 0 to 1 mM and right after the plates were sealed with transparent stickers. The reaction was monitored in black 384-well plates in a Tecan spectrophotometer at 37 °C, measuring fluorescence every 5 min at 460/503 nm (gain 120) and 506/540 nm (gain 100) for excitation/emission of respectively Spinach and YFP.

Data analysis

The same Matlab script was used as for the PURE data to find and fit the initial linear part of the fluorescence traces. For the kinetic model, the Michaelis-Menten model for mixed inhibition was used, which can be written as [28]:

$$\frac{1}{v_0} = \frac{[S](\frac{K_{ies}+[I]}{K_{ies}}) + K_M(\frac{K_{ie}+[I]}{K_{ie}})}{v_{max}[S]} \tag{4.1}$$

with S the substrate (GTP), I the inhibitor (ppGpp), v_0 the initial reaction rate, v_{max} the theoretical upper limit for the reaction rate, K_{ie} and K_{ies} the inhibition constants of the inhibitor by binding to free enzyme and enzyme-substrate complex respectively, K_M the Michaelis-Menten constant of the substrate. With $[S] \gg K_M$, this can be rewritten as either equation 4.2 or 4.3 for respectively the Lineweaver-Burk and Dixon plot:

$$\frac{1}{v_0} = \frac{1}{v_{max}}(1 + \frac{[I]}{K_{ies}}) + \frac{[I]}{v_{max}}\frac{K_M}{K_{ie}[S]} \tag{4.2}$$

$$\frac{1}{v_0} = \frac{1}{v_{max}} + \frac{1}{v_{max}}(\frac{1}{K_{ies}} + \frac{K_M}{K_{ie}[S]})[I] \tag{4.3}$$

The y-intercept of the Dixon plot ($1/v_0$ vs. [I]) allows to estimate v_{max}, which can be used in equation 4.2 to determine $\frac{K_M}{K_{ie}}$ from the slope of the Lineweaver-Burk plot

($1/v_0$ vs. $1/[S]$). Substituting $\frac{K_M}{K_{ie}}$ in the slope of the Dixon plot ultimately yields an estimate of K_{ies}. The values obtained for these parameters are given in **Table 4.1**. A K_M value of 0.05 mM^{-1} was used for translation based on K_M values of translation factors (see **Table 1.1** and Chapter 1). The K_M of T7 RNA polymerase for GTP is about 0.2 mM^{-1} [29, 30].

Table 4.1: Estimated parameters for mixed inhibition model of transcription and translation

	Slope Dixon plot (min (a.u. mM)$^{-1}$)		**y-intercept Dixon plot** (min a.u.$^{-1}$)			**Slope Lineweaver-Burk plot** (min (a.u. mM)$^{-1}$)		**y-intercept Lineweaver-Burk plot** (min a.u.$^{-1}$)	
GTP (mM)	YFP	Spinach	YFP	Spinach	ppGpp (mM)	YFP	spinach	YFP	spinach
1.5	0.2677	0.1174	0.2971	0.2033	0.0	0.0016	0.0037	0.3047	0.1965
3.0	0.2863	0.1083	0.2821	0.2038	0.5	0.2357	0.0747	0.3126	0.2208
4.5	0.3205	0.0332	0.2373	0.2018					
Average	0.2915	0.0863	0.2722	0.2030					

Model parameter	YFP	Spinach
v_{max} (a.u. min^{-1})	3.67	4.93
K_{ies} (mM^{-1})	3.60	17.86
K_M/K_{ie} (a.u.)	1.73	0.030
K_M (mM^{-1})	0.050	0.2

	slope Dixon plot according to model parameters	
GTP (mM)	YFP	spinach
1.5	0.3899	0.0155
3.0	0.2328	0.0134
4.5	0.1804	0.0127
Average	0.2677	0.0139

4.2.3. Bacterial strains, media and growth conditions

An overview of strains used is given in **Table S4.3**. To construct *E. coli* MG1655DE3, the λDE3 prophage was integrated in the chromosome of *E. coli* MG1655 using a λDE3 lysogenization kit (Novagen) according to manufacturer's protocol. P1 transduction was used to integrate the chromosomal RNA polymerase mutations of *E. coli* RLG14536 and RLG14537 (carrying *rpoC*1- and *rpoC*2- respectively) [31] into the chromosome of *E. coli* NCM3722. Hereto a protocol from the Bob Sauer lab [32] was used and mutations were confirmed by sequencing (Macrogen).

Cells were grown from single colonies in MOPS minimal medium (**Table S2.2**) with 0.2 % glucose ([33]) and if mentioned all amino acids (**Table S2.3**), in 250 mL culture flasks placed in a water bath (Grant Instruments Sub Aqua Pro) set at 37 °C on top of a magnetic stir plate (2 mag MIXdrive 1 Eco and MIXcontrol 20) with a 12 mm magnetic stir bar (VWR) set at 1200 rpm. Optical density was measured

at 600 nm using an Ultrospec 10 Cell Density Meter (GE Healthcare) to monitor growth.

4.2.4. Vectors for expression of RelA, GFP and Broccoli

All primers used can be found in **Table S4.4**. pET28c-2xBroccoli was obtained from Filonov *et al.* [34]. To construct pET28c-GFP, sfGFP was PCR amplified from pSB1C3 with inclusion of a strong RBS and SLiCEd [35] into the pET28c backbone using primers NI27 and NI24 for pSB1C3 and primers NI23 and NI20 for pET28c-2xBroccoli.

Plasmid pS101**-RelA*, received from Ferhat Buke, was constructed by replacing RFP on pBbS2k-RFP with a DNA sequence encoding the first 455 amino acids of the native MG1655 RelA gene. YFP fluorophore mVenus was fused to RelA* via a glycine-serine linker using restriction cloning.

In pSC101**-RelA*, *kan* was replaced by *amp* to generate pSC101**-RelA*-Amp by SLiCE using primers NI289/NI290 to amplify *amp* from pBbA5a-RFP and NI288/NI293 to amplify the backbone of pSC101**-RelA*. This was in order to combine pET28c-GFP or pET28c-2xBroccoli (both *kan*) with pSC101**-RelA*-Amp.

Subsequently the SC101** origin of pSC101**-RelA*-Amp was replaced by the 15A origin by SLiCE of the PCR of pSC101**-RelA*-Amp with primers NI294/NI295 and the PCR of the 15A origin of pBbA5a-RFP with primers NI291/NI292.

Finally, pJEx-RelA* was made by SLiCE of RelA*, which was amplified by PCR using primers NI332/NI335 and pSC101-RelA* as template, into the backbone of pTR-JExA1-RFP, which was PCR amplified using primers NI333/NI334.

4.2.5. *In vivo* synthesis of GFP and Broccoli

Overnight cultures of *E. coli* MG1655DE3 pSC101**-RelA*-Amp and pET28c-GFP or pET28c-2xBroccoli in MOPS 0.2 % glucose and 0.2 % casamino acids were diluted to OD 0.05 and grown in Nunc 96-well plates with lid (200 µL per well) in a Synergy HTX plate reader (BioTek) at 37 °C under continuous shaking (282 cpm, 3 mm amplitude). Absorbance at 600 nm and Broccoli or GFP fluorescence (excitation filter 485/20 and emission filter 516/20, gain 70) were measured every 5 min.

4.2.6. LacZ assays

LacZ assays were performed according to Griffith and Wolf [36] and Dai *et al.* [37]. Cells were grown as described in section 4.2.3 and at OD 0.3 the *lac* operon was induced with 5 mM isopropyl-β-D-thiogalactoside (IPTG) (Sigma). Right after induction 200 µL cell culture was added to 5 µL chloramphenicol (35 mg mL^{-1}) and immediately frozen in liquid nitrogen, every 15 s for 4 min. Samples were stored in

−20 °C. For the β-galactosidase assay, 75 µL thawed cells were added to 75 µL Z-buffer (60 mM Na_2HPO_4, 40 mM NaH_2PO_4, 10 mM KCl, 1 mM $MgSO_4$, pH 7.0, 50 mM β-mercaptoethanol) in a 96-well plate and incubated at room temperature for 5 min. Then 15 µL of freshly prepared 4-methylumbelliferyl-β-D-galactopyranoside (MUG) (2 mg mL^{-1} in dimethylsulfoxide, Sigma) was added and incubated for 1 h at room temperature. The reaction was stopped by adding 75 µL 1 M Na_2CO_3. Fluorescence was measured using a Synergy H1 plate reader (BioTek) at ex/em 365/450 nm.

The amount of LacZ initially increases exponentially with time, given that mRNA increases linearly (equations 4.4 and 4.5)[38]. Hence, a linear curve was fit to the square root of the signal corrected for signal at t_0: $\sqrt{\mathrm{Em}_{450}(t) - \mathrm{Em}_{450}(t_0)}$. To determine $\mathrm{Em}_{450}(t_0)$ the average of the first 4 samples was used. The intercept of the linear fit with the x-axis is the time needed to produce the first molecule of LacZ, T_{first}. The translation elongation rate in amino acids per second [aa s^{-1}] can then be calculated by dividing the length of LacZ (1024 amino acids) by T_{first}.

$$\frac{\mathrm{d[LacZ]}}{\mathrm{d}t} \backsim [mRNA] \backsim t \tag{4.4}$$

$$\mathrm{[LacZ]} \backsim t^2 \tag{4.5}$$

4.2.7. LC-MS analysis of *in vitro* transcription and translation reactions and *in vivo* ppGpp levels

As in Chapter 2.

4.3. Results

4.3.1. Translation is inhibited by ppGpp independently of transcription in cellular extracts.

Cellular extracts contain the whole cytoplasmic fraction of *E. coli*, including all possible translational targets of ppGpp, and pose therefore an interesting model to study transcription as well as translation. We programmed these cellular extracts with DNA encoding YFP as well as the fluorophore-activating RNA Spinach in order to distinguish effects on transcription from effects on translation (**Figure 4.1A**) [26]. To remove any effect of ppGpp on transcription, transcription is driven by the T7 phage RNA polymerase, present in the extract, which is known to be less sensitive to ppGpp [39]. **Figure 4.1B-C** show typical fluorescence traces of YFP and Spinach respectively. It can be observed that increasing concentrations of ppGpp reduce the synthesis of Spinach and YFP, yet the decrease in YFP synthesis is much larger.

To quantify the effect of ppGpp, linear slopes were fit to the initial, linear part of both curves as in this phase the composition of the reaction stays approximately constant. This was normalized to the slope of the condition with 0 mM ppGpp to compare the relative decrease of YFP and Spinach synthesis rate. Average inhibition for the YFP synthesis rates were 59 %±9 % whereas those of Spinach were 23 %±18 % at 4.5 mM GTP and 1.5 mM ppGpp (**Figure 4.1D-E**).

4.3.2. *In vitro* inhibition of translation by ppGpp is not merely competitive with GTP

As many proposed translational targets of ppGpp are GTPases, we hypothesized that the inhibition by ppGpp on translation would be competitive with regard to GTP. To test this hypothesis, we first verified the range of GTP concentration for GTP saturated YFP and Spinach synthesis in the cellular extracts, which was from 1.5 to 4.5 mM (Supplementary information and **Figure S4.1**). Within this range of GTP, we also varied ppGpp concentrations.

Assuming a single Michaelis-Menten dependence of ribosome associated GTPases on GTP, the inhibition by ppGpp can be quantified and a mode of inhibition can be inferred using a Dixon and Lineweaver-Burk plot, standard in biochemical analysis of modes of enzyme inhibition (explained in supplementary methods). The slopes and y-intercept of both plots allow to estimate the necessary parameters for a Michaelis-Menten (MM) model with mixed inhibition. We used a subset of data (26 traces, shown in **Figure S4.2A**) to derive these parameters for a mixed inhibition model (shown in **Figure S4.2B-C**).

Assuming a K_M for translation of 0.05 mM^{-1} (**Table 1.1**), the inhibitory constants for free enzyme and enzyme-substrate complex (K_{ie} and K_{ies}) were 0.029 mM^{-1} and 3.6 mM^{-1}. This indicates that the inhibitory mechanism is mainly competitive at ppGpp concentrations below 1 mM. Only at higher ppGpp concentrations the non-competitive term plays a significant role. In **Figure 4.1D** the MM model based on the calculated inhibition constants for ppGpp is overlaid on top of averaged data of in total 76 individual YFP traces. Using the same approach for Spinach transcription data, no MM model could be fitted nicely to the data as there is overall no significant inhibition by ppGpp (**Figure 4.1E**).

4.3.3. *In vivo* decoupling of transcription and translation confirms ppGpp inhibits translation directly

Given the observed reduction of transcription and particularly translation by ppGpp *in vitro*, our next step was to verify if this occurred *in vivo*. Hereto, we constructed a strain to monitor transcription and translation in a manner analogous to the cellular extract system (**Figure 4.2A**). The genetic constructs used were fluorophore-activating RNA Broccoli and GFP expressed with the T7 promoter in *E.*

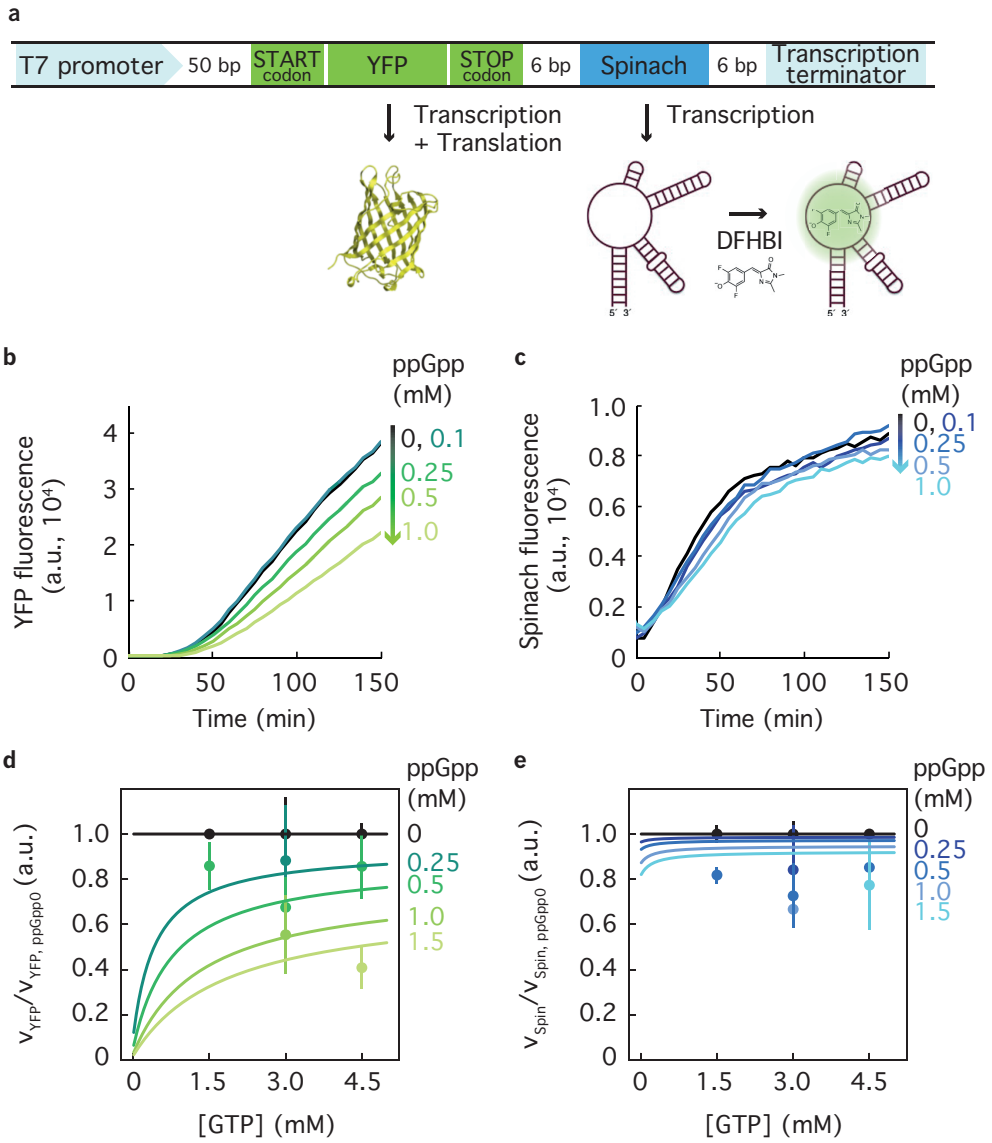

Figure 4.1: Kinetic analysis of transcription and translation in *E. coli* cellular extracts. A) The YFP-Spinach DNA template used in extract reactions. The Spinach aptamer forms a fluorescent complex with DFHBI. Adapted from van Nies *et al.* [26]. B) Exemplary YFP and C) Spinach fluorescence traces at various ppGpp concentrations. Slopes of the initial linear increase of the curves were used to determine synthesis rates (materials and methods). D,E) Based on a subset of YFP and Spinach traces, a mixed inhibition model was developed (materials and methods), here overlaid with the average and standard deviation of all acquired YFP and Spinach traces (Table S4.1 for number of traces for each condition). v_{YFP}: synthesis rate of YFP, v_{Spin}: synthesis rate of Spinach, ppGpp0: at 0 mM ppGpp.

coli MG1655DE3, a strain which expresses the T7 RNA polymerase. Due to overlapping excitation/emission spectra, Broccoli and GFP were expressed in separate strains. Constitutively active RelA (RelA*) was expressed with varying induction levels to set a range of intracellular ppGpp concentrations, with a corresponding reduction in growth rate (**Figure 4.2A**).

A difficulty however, with actively growing *E. coli*, is that induction of RelA will eventually adjust the number of ribosomes, which might confound an observation of direct inhibition of translation by ppGpp. To uncouple the potential direct effects of ppGpp on translation from the indirect transcriptional effects on ribosome number, ribosomal inhibitors or hibernation factors, rifampicin was added immediately after induction of GFP. Rifampicin specifically inhibits *E. coli* and not T7 RNA polymerase [40].

Both transcription and translation were monitored by expressing fluorescent RNA and protein respectively. The increase in fluorescence signal is a direct measure of the transcription or translation rate. Example fluorescence traces are presented in **Figure 4.2B**. As shown in **Figure 4.2C** the Broccoli synthesis rate remains within a narrow band of about 20% for all conditions, independent of the degree of RelA* induction. However, the rate of GFP synthesis decreases with RelA* induction by $39\,\% \pm 7\,\%$ at $8\,\mathrm{ng\,mL^{-1}}$ aTc. This indicates that not ribosome number or active transcription by RNA polymerase is limiting translation, but another ppGpp related mechanism. However, this effect was only significantly observed when induced RelA* caused a growth rate reduction of about $37\,\% \pm 11\,\%$.

4.3.4. Stringent ppGpp concentrations inhibit translation elongation and/or initiation

Having established that growth limiting concentrations of ppGpp directly inhibit translation *in vitro* and *in vivo*, we aimed at elucidating at which exact concentrations and to which degrees ppGpp affects translation. Does the inhibition also occur below ppGpp levels observed during stress response? Hereto, we titrated ppGpp *in vivo* using both low and high copy number RelA* plasmids, and quantified the ppGpp concentration using LC-MS. In this range of ppGpp concentrations, we determined the translation rate using well-known LacZ assays (**Figure 4.3A**). LacZ assays are used to measure translation elongation rates (k_{elong}) and to estimate which fraction of the total ribosome number are actively translating.

The moment the LacZ signal starts to increase after induction corresponds to the time needed to synthesize the first molecule of LacZ of 1024 amino acids, T_{first} (indicated in **Figure 4.3A**). More specifically, this lag phase before detection of the first LacZ includes the time needed for transcription (T_{TRX}), translation initiation (T_{init}) and translation elongation (the length of the protein divided by the actual elongation rate k_{elong}) as in equation 4.6 [37]. Given that transcription of LacZ is not affected by the stringent response *in vivo* [3], we expect only the rate of translation initiation and elongation to potentially be affected by ppGpp. The time

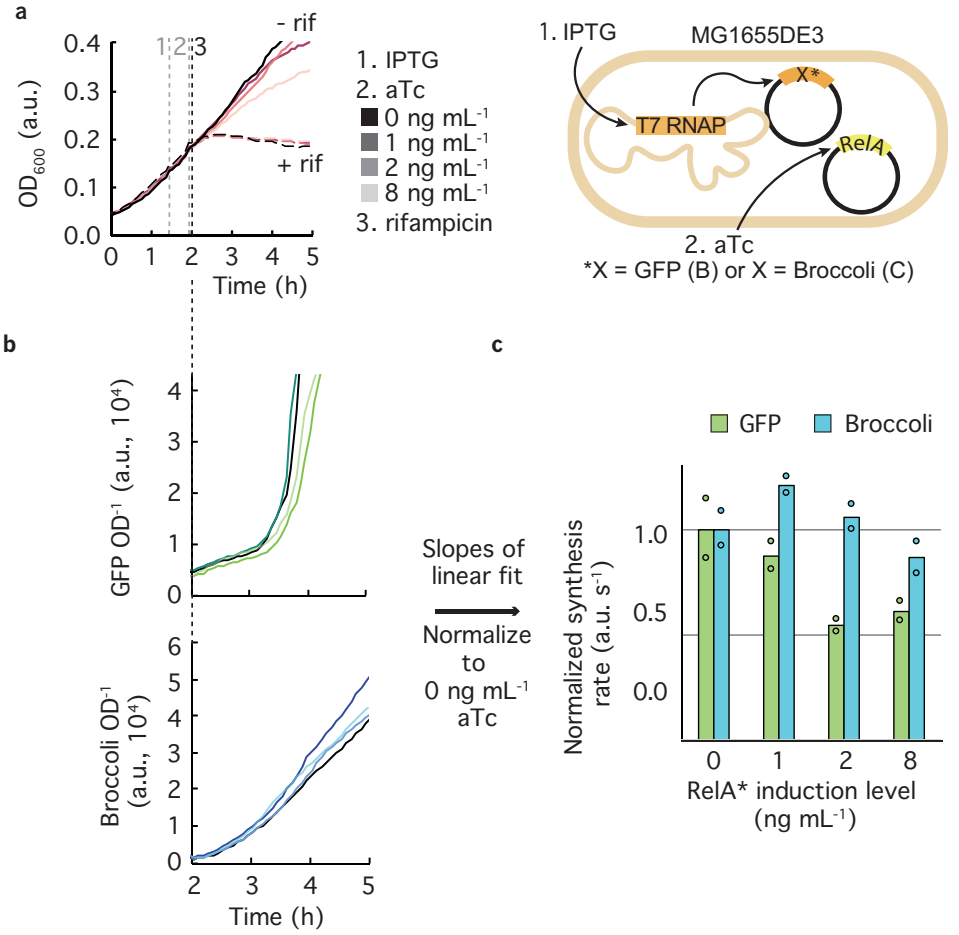

Figure 4.2: The GFP synthesis rate decreases *in vivo* due to RelA expression. A) Set-up of the experiment. *E. coli* MG1655DE3 expresses 2 plasmids: one carrying IPTG-inducible GFP or Broccoli and the other anhydrous tetracycline (aTc) inducible RelA*. Cells growing in MOPS medium with 0.2 % glucose and 0.2 % casamino acids were induced with 1 mM IPTG at 1h25 (1) to induce GFP or Broccoli expression. At 1h55 (2) they were induced with various aTc concentrations to establish a range of intracellular ppGpp levels. At 2h00 half the wells received 200 µg mL^{-1} rifampicin. B) Fluorescence traces of GFP or Broccoli. C) From the fluorescence traces the GFP and Broccoli synthesis rates were determined by fitting linear slopes to the region between 3.5-4 h for GFP and 3-5 h for Broccoli. The slopes of the fits were then normalized the slope of the wells not expressing RelA (no aTc added). Bars represent the average of 2 replicates (shown as dots) per condition.

required to translate the protein including transcription and translation initiation can be calculated as the length of the protein divided by the TIER (Translation Initiation and Elongation Rate, in aa s^{-1}) (equation 4.7).

$$T_{first} = T_{TRX} + T_{init} + \frac{1024aa}{k_{elong}} \tag{4.6}$$

$$T_{first} = \frac{1024aa}{TIER} \tag{4.7}$$

LacZ assays were performed with *E. coli* NCM3722 grown in glucose medium while RelA* was induced to various degrees to get a range of ppGpp levels, covering both basal as well as stringent levels. LacZ assays were performed right before (0 min), 5 min and 10 min after RelA* induction. The TIER was determined at these ppGpp concentrations (**Figure 4.3B**). In glucose medium, the elongation and initiation rates do not vary significantly at basal levels. Only at a ppGpp level of 689 ± 66 pmol OD^{-1} the TIER decreases to about 8 aa s^{-1}, similar to that of stationary phase [37].

4.3.5. Suprabasal ppGpp concentrations reduce the fraction of active ribosomes

We noticed that the slope of the LacZ assays showed a different behaviour than the TIER: they were inhibited relatively more. The slopes of the LacZ assays are with exception of one tested condition (a 23 ± 6 % reduction at 87 ± 46 pmol OD^{-1}) not inhibited by ppGpp below 200 pmol OD^{-1}. Above that however there is a consistent reduction in slope up to 57 ± 6 % at 689 ± 66 pmol OD^{-1} (**Figure 4.3C**).

As shown by Dai *et al.* [37], addition of antibiotics that inhibit the active fraction of ribosomes decreases the slope of the LacZ assay without adjusting the translation initiation or elongation rate. Whereas the T_{first} represents the time needed to synthesize a single lacZ, the slope of the LacZ assay represent the rate of total accumulation of LacZ. The total synthesis of LacZ can be written as equation 4.8,

$$\frac{d[LacZ]}{dt} \backsim N.f_A.TIER, \tag{4.8}$$

in which f_A is the fraction of ribosomes that is actively translating LacZ and N the total number of ribosomes. The fraction of active ribosomes is affected by release factors, RMF, HPF and any other protein involved in the recycling or hibernation of ribosomes. Transcription of some of these factors is controlled by ppGpp. N is determined by synthesis rate of ribosomal RNA and proteins by RNA polymerase, which is known to be directly controlled by ppGpp.

Given that the LacZ slope is inhibited relatively more by ppGpp than the TIER (**Figure 4.3D**), this means that the active fraction and/or total number of ribosomes has decreased. A decrease in total ribosome number would not be surprising given the well-known transcriptional inhibition of rRNA by ppGpp. A decrease in active fraction is also very plausible given that ppGpp controls transcription of certain proteins involved in this term, such as RMF and HPF. However, it is also possible that ppGpp via post-translational regulation directly affects proteins such as RF3.

To decipher whether transcriptional regulation by ppGpp affects LacZ synthesis rates, we repeated the LacZ assays with *E. coli* strains carrying mutations in RNA polymerase rendering it insensitive to ppGpp. Hereto, the mutations discovered by Ross *et al.* [31] were transferred to *E. coli* NCM3722 using P1 phage transduction, resulting in strains with either a mutation in ppGpp binding site 1 (*rpoC*1-) or ppGpp binding site 2 (*rpoC*2-). Unfortunately, we could not transfer both mutations *rpoC*1- and 2- mutations to our model strain NCM3722. Due to the presence of a chromosomal tetracycline resistance marker, the aTc-inducible RelA* plasmid was replaced by the Jungle Express system, which is induced with crystal violet. In addition, glucose amino acids medium or LB was used instead of glucose minimal medium in order to avoid the*rpoC*2- would show reduced translation because of an impaired capacity to synthesize amino acids without ppGpp.

Switching from medium without to medium with amino acids resulted for the wild type in a different response to RelA* induction. Although in glucose medium there was still active translation at maximal induction, in medium with amino acids this resulted in a complete arrest of translation as no LacZ was detectable (TER below 4 aa s^{-1}) (**Figure 4.3E,F**). This was the case with both aTc and crystal violet induced RelA* expression. It appears that stringent ppGpp levels completely shut off translation of LacZ. The same response was obtained in the *rpoC*1- and 2- mutants, indicating that the arrest on translation by ppGpp is not due to a direct effect of ppGpp on RNA polymerase (**Figure 4.3E,F** and **Figure S4.3**).

With this new induction system, we sought for an inducer concentration that would cause a relatively higher decrease in LacZ slope than TIER in the wild type. This point was found at 75 nM crystal violet (**Figure 4.3F,G**). However, for unknown reasons, the TIER was lower in the WT than the mutant, which we believe shows the mutant has some aberrant transcription or translation of LacZ. This was confirmed by the observation that even without induction of RelA, the absolute slopes of the LacZ (sampled at the same OD) was significantly less than the wild type (**Figure S4.3**), indicating the mutant has a lower total number of ribosomes, or lower fraction of active ribosomes.

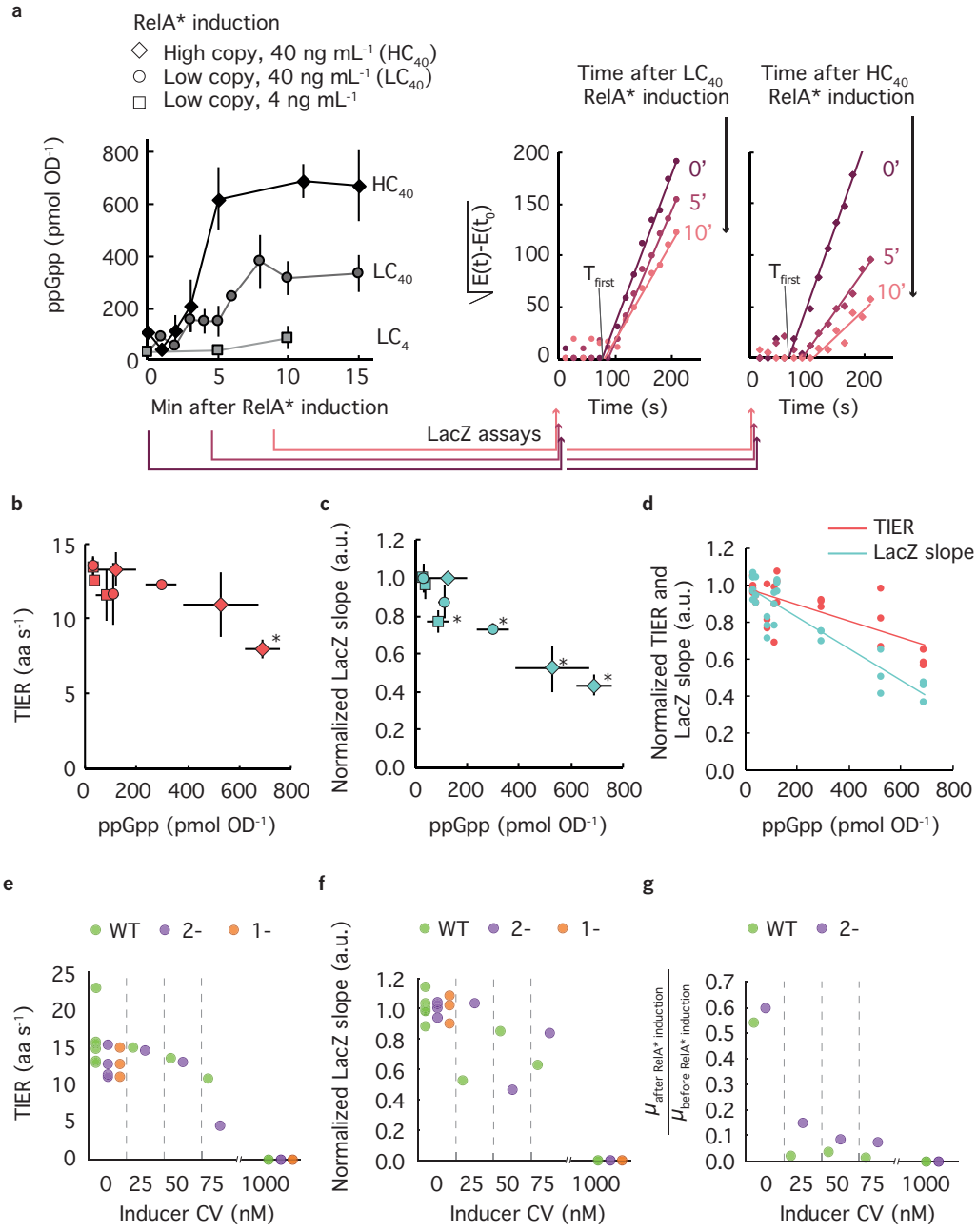
a
RelA* induction
High copy, 40 ng mL-1 (HC40)
Low copy, 40 ng mL-1 (LC40)
Low copy, 4 ng mL-1
ppGpp (pmol OD-1)
HC40
LC40
LC4
Min after RelA* induction
Time after LC40 RelA* induction
Time after HC40 RelA* induction
√E(t)-E(t0)
Tfirst
0'
5'
10'
Time (s)
LacZ assays
b
TIER (aa s-1)
ppGpp (pmol OD-1)
c
Normalized LacZ slope (a.u.)
d
TIER
LacZ slope
Normalized TIER and LacZ slope (a.u.)
e
WT
2-
1-
Inducer CV (nM)
f
g
μafter RelA* induction / μbefore RelA* induction

Figure 4.3: Stringent ppGpp levels reduce translation initiation and elongation rates as well as total LacZ translation rates. **A**) Overview of the experimental approach: RelA* was induced with 4 or 40 ng mL^{-1} anhydrous tetracycline from low copy (LC) or high copy (HC) plasmids, at which LacZ assays were performed as indicated by the colored arrows. **B, C**) Translation initiation and elongation rates (TIER) (B) and LacZ slopes (C) of NCM3722 wild type grown in glucose medium with induction of RelA*. **D**) TIER and LacZ slope were normalized to 0 ng mL^{-1} induction of RelA* and this was plotted as a function of ppGpp. Data points represent biological replicates. **E, F**) TIER (E) and LacZ slopes (F) of NCM3722 wild type (WT) and *rpoC2*- and 1- mutants grown in glucose amino acids or LB medium in response to various inducer (crystal violet, CV) concentrations. Data points represent biological replicates. **G**) Decrease in growth rate of NCM3722 WT and *rpoC2*- mutant after RelA* induction, growing in LB medium. Errors bars represent the standard deviation of three biological replicates. *P-value < 0.05 for two-tailed t-test comparing to 0 ng mL^{-1} induction of the same condition.

4.3.6. The PURE system shows inhibition of IF2, EF-G and RF3 are sufficient to explain the *in vivo* observed inhibition of translation by ppGpp

To finally understand if purely a post-translational regulation of IF2, EF-G and RF3 by ppGpp could explain the reduced translation rates, without a potential effect of any proteins regulating ribosome activity that are transcriptionally regulated by ppGpp, we used the highly controllable PURE system. The PURE system consists of all the minimal components required to allow *in vitro* transcription and translation. Transcription is again driven by the T7 phage RNA polymerase, known to be less sensitive to ppGpp [39]. The only proteins related to translation consist out of initiation factors IF1, IF2 and IF3, elongation factors EF-G, EF-Tu and EF-Ts, release factors RF1, RF2 and RF3, ribosome recycling factor [25] and peptidyl-tRNA hydrolase (PTH).

We programmed PURE systems with the same DNA used in the cellular extracts, encoding YFP as well as the fluorophore-activating RNA Spinach, and varied the ppGpp concentration. **Figure 4.4A,B** shows model traces of both the YFP and Spinach signals as the PURE reaction proceeds. At increasing ppGpp concentrations, the accumulation of YFP is reduced by 50% $\pm$ 10 %, although there might also be an inhibitory effect on Spinach synthesis (19% $\pm$ 13 % inhibition at 1 mM ppGpp, **Figure 4.4C**). At the ppGpp/GTP ratios observed during steady-state growth (1/25 [41], here 0.1 mM ppGpp), translation is inhibited no more than by 12 % $\pm$ 12 %.

The results of this assay are quantitatively consistent with the *in vitro* transcription and translation rates in cellular extracts (**Figure 4.1D**), as well as the *in vivo* reduction of LacZ synthesis rates (**Figure 4.3C**). Although this does not guarantee that IF2, EF-G and RF3 are the only *in vivo* post-translational targets of ppGpp regarding translation, they appear sufficient to implement a system in the cell to adjust

protein synthesis rates to the various ppGpp levels that occur under stress.

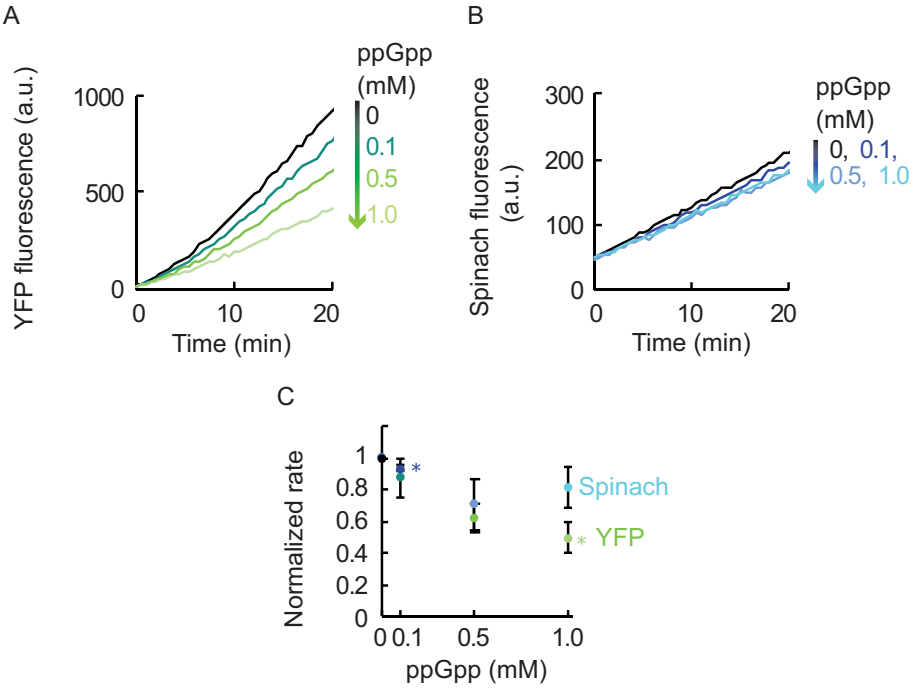

Figure 4.4: ppGpp inhibits translation in the PURE system, containing only IF2, EF-G and RF3 as known ppGpp targets. A) and B) Exemplary kinetic traces of YFP (A) and Spinach (B) fluorescence of a PURE system inhibited with ppGpp. C) YFP and Spinach synthesis rates were determined by the slope of a linear curve fitted to the fluorescence traces (see materials and methods), which were subsequently normalized to the slope of the 0 mM ppGpp trace. Error bars represent standard deviation of normalized slopes of 3 experiments. *P-value < 0.05 of two-tailed t-test compared to 0 mM ppGpp.

4.4. Discussion

The various intracellular targets of the signaling molecule ppGpp have been extensively studied. For both transcription and translation, it is unclear at exactly which concentrations ppGpp affects either and under which conditions. Mechanistically it has been shown that ppGpp binds to RNA polymerase and that stringent levels orchestrate transcription of virtually all genes in *E. coli* [3, 31]. The effect on translation however remains elusive. Various studies have determined or suggested interactions between ppGpp and EF-Tu, EF-G, IF-2, RMF and several other proteins involved in translation [7, 8, 11–13, 21, 22, 37, 42]. However, these either lack *in vivo* relevance or accurate quantification of ppGpp, which is essential given that the

activity of ppGpp is concentration dependent and can vary between three orders of magnitude. Here, we have quantified the effect of ppGpp on translation in several *in vitro* and *in vivo* systems, in which a potential inhibition of ppGpp on translation was uncoupled from its transcriptional regulation.

In both PURE and cell extract systems translation rates were inhibited for about 50 % at 1 mM ppGpp, which *in vivo* corresponds to stringent levels [7, 41]. The slightly reduced transcription in these systems indicates that T7 RNA polymerase is much less sensitive to ppGpp than *E. coli* RNA polymerase, which aligns with earlier studies [39]. These *in vitro* data suggest that stringent ppGpp levels not only inhibit translation by inhibiting ribosome synthesis, but also by directly affecting the translation reaction itself or the recycling of ribosomes.

We confirmed these results *in vivo* using fluorescent reporters for transcription and translation, as well as LacZ assays, at various ppGpp levels set by RelA induction. The usage of T7 RNA polymerase allowed to detect direct effects of ppGpp on the translation system without the well-known inhibition of ribosome synthesis. The fluorescent reporters confirmed the *in vitro* results that low induction of RelA has no significant effect on translation.

In the LacZ assays, the effects of ppGpp show a keen dependence on concentration, both regarding translation initiation and elongation rate and total LacZ translation rate (LacZ slope). Specifically, at concentrations below 200 pmol OD^{-1}, we do not detect any direct effects of ppGpp on translation. We observe that artificially setting ppGpp to higher but still basal levels (0-130 pmol OD^{-1}, see section 1.6.1) does not significantly decrease the TIER.

Dai *et al.* [37] showed that during steady growth in various media (and thus in basal ppGpp regime) the transcription of LacZ mRNA and translation initiation times do not vary, but that the translation elongation rate decreases at lower growth rates as well as the fraction of active ribosomes. The apparent discrepancy can be explained as follows: in Dai *et al.* [37], the basal ppGpp concentration was varied by adjusting the composition of the medium. We only varied ppGpp levels by titrating expression of RelA*. This means that the variation in translation elongation rate and active ribosome fraction in [37] is probably only due to a transcriptional effect of ppGpp on proteins involved in ribosome hibernation or rescuing of stalled ribosomes, and not a post-translational effect of IF-2.

At concentrations above 700 pmol OD^{-1}, we observe an immediate drop in TIER, consistent with *in vitro* experiments. This demonstrates stringent ppGpp inhibits translation initiation and/or elongation factors post-translationally. Between 300 pmol OD^{-1} and 700 pmol OD^{-1}, we observe more complex effects: the TIER is not significantly affected, but the total LacZ translation rate is, with a 25% reduction at 300 pmol OD^{-1}. The fact that total LacZ translation rate is inhibited at lower ppGpp concentrations than the TIER, suggests that either the number of ribosomes or their activity is affected. Potential post-translational targets could be RF3 [13] or one of

the many enzymes involved in releasing stalled ribosomes or ribosome recycling [9].

In order to untangle post-translational from transcriptional effects of ppGpp in the 300-700 pmol OD^{-1} regime, LacZ assays with RNA polymerase mutants insensitive to ppGpp were performed [31]. Unfortunately, it appeared removal of ppGpp binding site 2 on RNA polymerase leads to a decreased capacity for translation. It can however be assumed for the wild-type strain that the total number of ribosomes or proteins that affect the active fraction did not significantly alter within the 5 or 10 min after RelA induction, when the LacZ assays were performed. Then indeed a post-translational target for ppGpp must be present in this concentration regime. Yet, this requires verification.

A kinetic model of transcription and translation in cellular extracts suggests competitive inhibition with regard to GTP dominates, although the inhibition mechanism could be mixed with allosteric regulation. This is consistent with the observed inhibition in the PURE system. Here, the only translation related factors are the initiation, elongation and release factors, as well as ribosome recycling factor (RRF) [25] and peptidyl-tRNA hydrolase (PTH). IF2, EF-G and RF3 have been reported to be inhibited by ppGpp and all competitive with regard to GTP [12, 13]. The overlap between *in vivo* and *in vitro* data suggests inhibition of these three factors could be sufficient to explain the inhibition of translation by ppGpp.

On the other hand, Zhang *et al.* [8] discovered multiple additional proteins involved in ribosome biogenesis and translation in *E. coli* that are binding ppGpp: RsgA, HlfX, Der, ObgE, Era and LepA. The binding was always competitive with GTP and GDP with affinity constants in the low micromolar range for ppGpp and GDP, and about 10-fold higher for GTP (10-30 µM). Even though the affinity constants for ppGpp suggest that ppGpp could inhibit these GTPases at basal levels during steady state growth, the much higher intracellular concentrations of both GTP (estimates between 1.1 and 4.9 mM [41, 43]) could overcome this, depending on the Michaelis-Menten constant (K_M) of the target. For example, the K_M of EF-G for GTP was estimated to be 0.22 µM [44]. Applying Michaelis-Menten kinetics then indicates that it is practically unlikely for ppGpp to significantly inhibit EF-G (e.g. GTP would have to decrease 10-fold and ppGpp 1000-fold). IF2 on the contrary has a K_M of 30 µM, which combined with a 2.8 µM K_d [12] results in an IC_{50} of 100 µM ppGpp at 1.1 mM GTP or 455 µM ppGpp at 4.9 mM GTP. A kinetic analysis of IF2 hence confirms that it could be inhibited *in vivo* by ppGpp. Unfortunately, biochemical data are missing for RF3.

In conclusion, in this study we have shown ppGpp has multiple roles in regulating translation. Besides the more characterized effects on transcription and the well-known effect on ribosome synthesis, our data suggest ppGpp inhibits translation initiation and/or elongation factors, as well as factors involved in recycling of ribosomes. In particular IF2 and RF3 are very likely directly targeted by ppGpp. The relative importance of the various roles of ppGpp is concentration dependent

and dependent on the conditions the cell is in. At *in vivo* concentrations up to 200 pmol OD^{-1}, ppGpp appears to have no post-translational effect on translation.

4.5. Acknowledgements

We would like to thank David Foschepoth for providing the cellular extracts and very useful discussions. We also would like to thank Anne Doerr for useful discussions and technical assistance with the PURE system. We would like to thank Christophe Danelon for providing the PURE system and useful discussions. Finally, we would like to thank Misha Klein for very useful discussions.

4.6. Supplementary information

4.6.1. Optimization of the DNA and GTP concentration in cellular lysates

More DNA increases RNA synthesis, which is one substrate of the translation machinery, yet simultaneously more transcription decreases the NTP pool needed for aminoacyl-tRNA and translation itself. In **Figure S4.4** the absolute Spinach and YFP synthesis rates for various DNA concentrations are shown as a function of added ppGpp concentration. The experiment was performed twice. At 0.5 nM DNA there was no detectable signal of Spinach, indicating the DNA concentration was too low. Given that there was still detection of YFP this indicates that YFP detection is more efficient than Spinach and/or that one mRNA molecule is translated several times. The difference of the values between the two experiments is likely due to maintenance of the spectrophotometer. The trends are however the same: 1) at high DNA concentration (10 nM) the Spinach signal increases, whereas the YFP signal decreases. Apparently, the higher amount of RNA does not increase YFP production, hence RNA is not rate-limiting for translation. Likely the higher amount of transcription uses the resources ATP and GTP needed for translation. At 2 nM Spinach synthesis rates are lower than at 10 nM, which indicates that 2 nM DNA is rate-limiting for T7 RNA polymerase. At 0.5 nM DNA translation rates are on average decreasing compared to higher DNA concentrations, showing that at this DNA concentration DNA – and hence RNA- is rate-limiting for the ribosome. At 2 nM translation rates were the highest, which means that ATP and GTP were not limiting. We therefore assume that ribosomes are at their maximal rate and that RNA is not limiting. Interestingly, the increase in Spinach and concomitant decrease in YFP synthesis rate at 10 nM DNA compared to 2 nM also indicates that in the lysate reaction the T7 RNA polymerase is not halting the ribosome, as well as that the ribosome is not pushing T7 RNA polymerase forward. If there is some direct coupling between T7 RNA polymerase and the ribosome, it would only be for a non-detectable fraction of T7 RNA polymerase or ribosomes. 2) At the used DNA concentrations, the Spinach transcription rates are not inhibited by ppGpp (at 10 nM DNA) or less than translation rates (at 2 nM DNA). For optimal YFP and Spinach synthesis, 2 nM DNA was used in further experiments as this had the best YFP signal and also sufficient Spinach signal.

Transcription and translation rates were not significantly affected by GTP concentration, apart from one experiment in which 3 or 4.5 mM GTP resulted in a higher initial translation rate than lower or higher GTP concentrations (**Figure S4.1**). This means that at all concentrations tested in **Figure 4.1** GTP was not limiting. This is particularly important because it has been shown that limiting nucleotides in *in vitro* transcription translation systems favours transcription over translation [45], which is an artefact we wanted to prevent.

4.6.2. Supplementary figures and tables

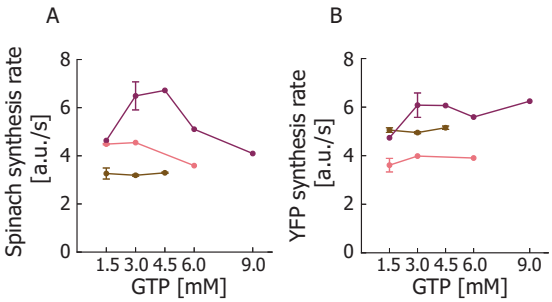

Figure S4.1: Absolute transcription (A) and translation (B) rates of lysate reactions at various GTP concentrations. The results are from 3 individual experiments.

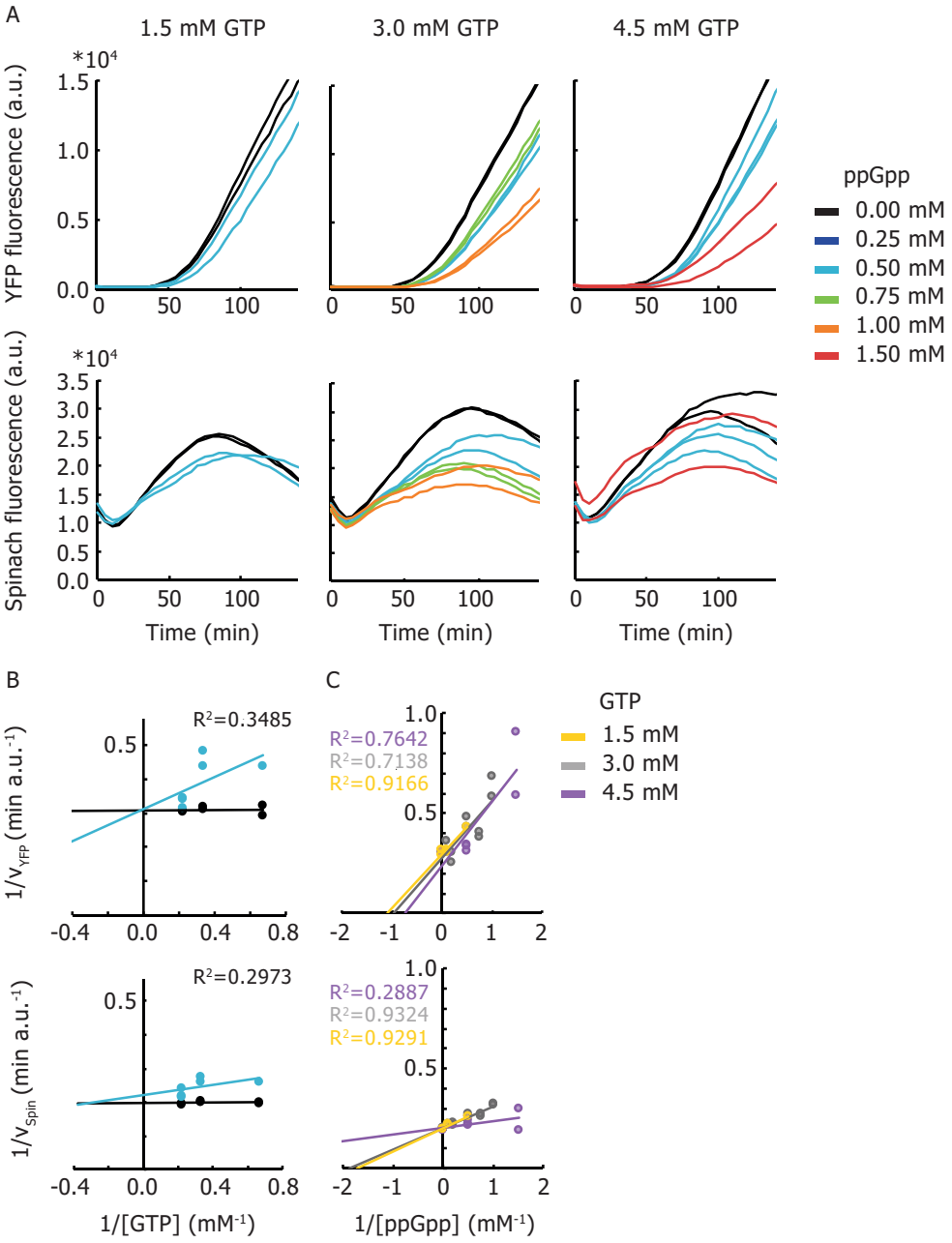

Figure S4.2: Development of a mixed inhibition model of translation by ppGpp. a) Set of YFP and Spinach traces of cellular extracts with varying GTP and ppGpp concentrations. b) and c): Data of a) was used for Lineweaver-Burk (b) and Dixon plots (c).

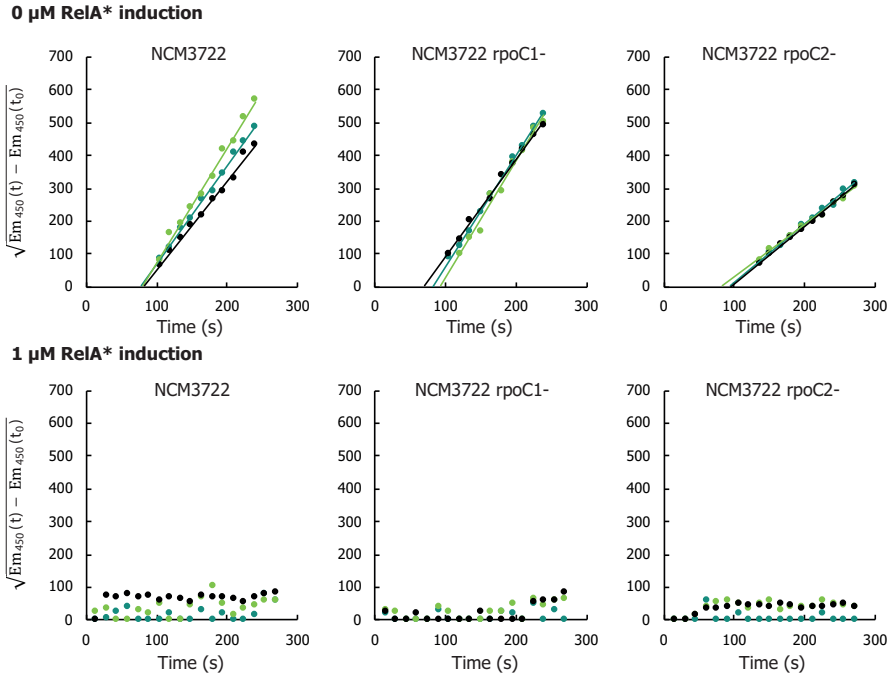

Figure S4.3: LacZ assay of NCM3722, NCM3722 *rpoC*1- and NCM3722 *rpoC*2- in glucose amino acids medium. All strains have no detectable LacZ synthesis after induction of RelA* with 1 µM crystal violet. Different colors represent biological replicates.

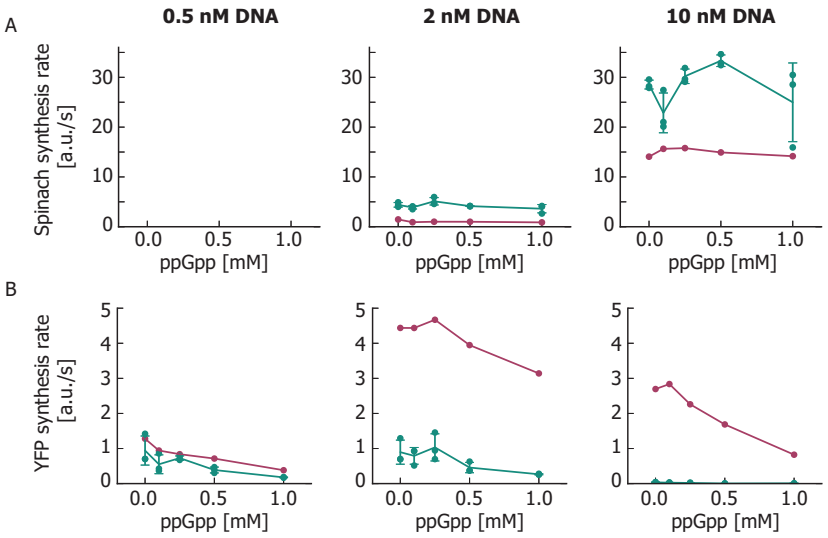

Figure S4.4: Optimization of DNA concentration and titration of ppGpp in the lysate *in vitro* transcription (A) and translation (B) reactions.

Table S4.1: Number of traces used for each condition in Figure 4.1D-E.

ppGpp (mM)	GTP (mM) 1.5	3.0	4.5	total
0.00	5	15	3	23
0.25		14		14
0.50	3	15	3	21
1.00		15		15
1.50			3	3
total	8	59	9	76

Table S4.2: PURE *in vitro* reaction assembly

Compound, in order of pipetting	Final concentration in cuvette
PURExpress feeding mix (2X)	1X
PURExpress enzyme mix (20X)	1X
PURExpress ribosomes (20X)	1X
DFHBI [400 µM]	20 µM
PTH [2 µM]	0.1 µM
DNA	4.5 ng µL^{-1}
MQ	–
ppGpp	0 to 1 mM

Table S4.3: Strains and plasmids used in this chapter.

Strain	Description	Source
E. coli DH5α	Used for cloning and plasmid amplification	Invitrogen
E. coli Rosetta2	F- *ompT hsdSB*(r_B- m_B-) *gal dcm*	Novagen
E. coli RLG14536	MG1655 rpoZΔ2-5-kan rpoC R362A R417A K615A-tetAR (1-2+)	Richard Gourse [31]
E. coli RLG14537	MG1655 rpoZ(WT)-kan rpoC N680A K681A –tetAR (1+2-)	Richard Gourse [31]
E. coli NCM3722	Wild type	CGSC 12355
E. coli NCM3722 *rpoC*1-	NCM3722 rpoC R362A R417A K615A tetAR (1-2+)	This work
E. coli NCM3722 *rpoC*2-	NCM3722 rpoC N680A K681A tetAR (1+2-)	This work
E. coli MG1655	Wild type	DSMZ 18039
E. coli MG1655DE3	MG1655 with prophage λDE3 with T7 RNA polymerase	This work
Plasmid		
pBbA5a-RFP	15A origin, *amp*, *lacUV5* promoter, RFP.	Addgene
pBbS2k-RFP	SC101** origin, *kan*, Tet promoter, RFP.	Addgene
pSC101**-RelA*	Expression of $RelA_{1-455}$-Gly-Ser-mVenus from tetracycline inducible promoter. Also carries *tetR* and *kan*	Ferhat Buke
pSC101**-RelA*-Amp	pSC101**-RelA* with *kan* replaced by *amp*	This work
p15A-RelA*	pSC101**-RelA*-Amp with the SC101** origin replaced by the 15A origin	This work
pTR-JExA1-RFP	Expression of RFP using the Jungle Express[46] expression system. Carries SC101 origin and *kan*.	[46]
pJEx-RelA*	pTR-JExA1-RFP with RFP replaced by *relA**	This work
pSB1C3	Carries sfGFP.	iGEM
pET28c-2xBroccoli	Broccoli dimer expressed from T7 promoter, *kan*.	[34]
pET28c-GFP	sfGFP expressed from T7 promoter, *kan*.	This work

Table S4.4: Primers used in this work.

Primer name	Sequence
NI20	CGGCATGGATGAGCTTTATAAGTAATAacgaaaggaagctg agttgg
NI23	CTCCTTTTGACATCTAGTATTTCTCCTCTTTAATCCTATAG TGAGTCGTATTAATTTCGC
NI24	CAACTCAGCTTCCTTTCGTTATTACTTATAAAGCTCATC CATGCC
NI27	GACTCACTATAGGattaaagaggagaaatactagATGTCAAA AGGAGAAGAGCTG
NI288	agaaaaataaacaaataggggttccgcggcgaaacgatcctcatcc
NI289	ttaccaatgcttaatcagtgagg
NI290	cgcggaaccctatttg
NI291	tttccataggctccgc
NI292	ggctgacttcaggtgctac
NI293	aggtgcctcactgattaagcattggtaagcgggactctgggg
NI294	tcaaatgtagcacctgaagtcagccgcttggattctcaccaataaaaaac
NI295	gcttgtcaggggggcggagcctatggaaacctaggtataaacgcaga aagg
NI332	gatcttttaagaaggagatatacatatggttgcggtaagaagtg
NI333	cacttcttaccgcaaccatatgtatatctccttcttaaaagatc
NI334	catggacgagctgtacaagtaaggatccaaactcgagtaag
NI335	gatccttactcgagtttggatccttacttg

references

[1] N. C. E. Imholz, D. Foschepoth, C. Danelon, and G. Bokinsky. "Suprabasal guanosine tetraphosphate (ppGpp) levels reduce translation rates in *E. coli* by inhibiting various targets". In: (2020).

[2] K. Potrykus, H. Murphy, N. Philippe, and M. Cashel. "ppGpp is the major source of growth rate control in *E. coli*". In: *Environmental Microbiology* 13.3 (2011), pp. 563–575.

[3] P. Sanchez-Vazquez, C. N. Dewey, N. Kitten, W. Ross, and R. L. Gourse. "Genome-wide effects on *Escherichia coli* transcription from ppGpp binding to its two sites on RNA polymerase". In: *Proceedings of the National Academy of Sciences* (2019).

[4] R. Lazzarini, M. Cashel, and J. Gallant. "On the Regulation of Guanosine Tetraphosphate Levels in Stringent and Relaxed Strains of *Escherichia coli*". In: *Journal of Biological Chemistry* 246.14 (1971), pp. 4381–4385.

[5] Y. Sokawa, J. Sokawa, and Y. Kaziro. "Regulation of stable RNA synthesis and ppGpp levels in growing cells of *Escherichia coli*". In: *Cell* 5.1 (1975), pp. 69–74.

[6] J. Ryals, R. Little, and H. Bremer. "Control of ribosomal-RNA and transfer-RNA syntheses in *Escherichia coli* by guanosine tetraphosphate". In: *Journal of Bacteriology* 151.3 (1982), pp. 1261–1268.

[7] B. Wang, P. Dai, D. Ding, A. D. Rosario, R. A. Grant, B. L. Pentelute, and M. T. Laub. "Affinity-based capture and identification of protein effectors of the growth regulator ppGpp". In: *Nature Chemical Biology* (2018). doi: 10.1038/s41589-018-0183-4.

[8] Y. Zhang, E. Zbornikova, D. Rejman, and K. Gerdes. "Novel (p)ppGpp Binding and Metabolizing Proteins of *Escherichia coli*". In: *mBio* 9.2 (2018), pp. 1–20.

[9] D. N. Wilson and K. H. Nierhaus. "The Weird and Wonderful World of Bacterial Ribosome Regulation". In: *Critical Reviews in Biochemistry and Molecular Biology* 42.3 (2007), pp. 187–219.

[10] H. Bremer and P. P. Dennis. "Modulation of Chemical Composition and Other Parameters of the Cell at Different Exponential Growth Rates". In: *EcoSal Plus* 3.1 (2008). doi: 10.1128/ecosal.5.2.3.

[11] P. Milon, E. Tischenko, J. Tomsic, E. Caserta, G. Folkers, A. La Teana, M. V. Rodnina, C. L. Pon, R. Boelens, and C. O. Gualerzi. "The nucleotide-binding site of bacterial translation initiation factor 2 (IF2) as a metabolic sensor". In: *Proceedings of the National Academy of Sciences* 103.38 (2006), pp. 13962–13967.

[12] V. A. Mitkevich, A. Ermakov, A. A. Kulikova, S. Tankov, V. Shyp, A. Soosaar, T. Tenson, A. A. Makarov, M. Ehrenberg, and V. Hauryliuk. "Thermodynamic Characterization of ppGpp Binding to EF-G or IF2 and of Initiator tRNA Binding to Free IF2 in the Presence of GDP, GTP or ppGpp". In: *Journal of Molecular Biology* 402.5 (2010), pp. 838–846. doi: 10.1016/j.jmb.2010.08.016.

[13] K. Kihira, Y. Shimizu, Y. Shomura, N. Shibata, M. Kitamura, A. Nakagawa, T. Ueda, K. Ochi, and Y. Higuchi. "Crystal structure analysis of the translation factor RF3 (release factor 3)". In: *FEBS Letters* 586.20 (2012), pp. 3705–3709.

[14] E. Hamel and M. Cashel. "Guanine nucleotides in protein synthesis". In: *Archives of Biochemistry and Biophysics* 162.1 (1974), pp. 293–300.

[15] A. M. Rojas and M. Ehrenberg. "How does ppGpp affect translational accuracy in the stringent response?" In: *Biochimie* 73.5 (1991), pp. 599–605. doi: 10.1016/0300-9084(91)90028-Y.

[16] K. Johnsen, S. Molin, O. Karlstrom, and O. Maaloe. "Control of protein synthesis in *Escherichia coli*: analysis of an energy source shift-down". In: *Journal of Bacteriology* 131.1 (1977), pp. 18–29.

[17] U. Vogel and K. F. Jensen. "Effects of guanosine 3',5'-bisdiphosphate (ppGpp) on rate of transcription elongation in isoleucine-starved Escherichia coli". In: *Journal of Biological Chemistry* 269.23 (1994), pp. 16236–16241. issn: 00219258.

[18] M. A. Sorensen, K. F. Jensen, and S. Pedersen. "High Concentrations of ppGpp Decrease the RNA Chain Growth Rate: Implications for Protein Synthesis and Translational Fidelity During Amino Acid Starvation in *Escherichia coli*". In: *Journal of Molecular Biology* 236 (1994), pp. 441–454.

[19] J. Gallant, L. Palmer, and C. C. Pao. "Anomalous synthesis of ppGpp in growing cells". In: *Cell* 11.1 (1977), pp. 181–185. doi: 10.1016/0092-8674(77)90329-4.

[20] P. Edelmann and J. Gallant. "Mistranslation in *E. coli*". In: *Cell* 10.1 (1977), pp. 131–137. doi: 10.1016/0092-8674(77)90147-7.

[21] P. H. OFarrell. "The suppression of defective translation by ppGpp and its role in the stringent response". In: *Cell* 14.3 (1978), pp. 545–557. doi: 10.1016/0092-8674(78)90241-6.

[22] D. B. Dix and R. C. Thompson. "Elongation factor Tu-guanosine 3'-diphosphate 5'-diphosphate complex increases the fidelity of proofreading in protein biosynthesis: Mechanism for reducing translational errors induced by amino acid starvation". In: *Proceedings of the National Academy of Sciences* 83 (1986), pp. 2027–2031.

[23] A. L. Svitil, M. Cashel, and J. W. Zyskind. "Guanosine tetraphosphate inhibits protein synthesis *in vivo*". In: *The Journal of Biological Chemistry* 268.4 (1993), pp. 2307–2311. issn: 0021-9258.

[24] Y. Shimizu, A. Inoue, Y. Tomari, T. Suzuki, T. Yokogawa, K. Nishikawa, and T. Ueda. "Cell-free translation reconstituted with purified components". In: *Nature Biotechnology* 19.August (2001), pp. 751–755.

[25] Y. Shimizu, T. Kanamori, and T. Ueda. "Protein synthesis by pure translation systems". In: *Methods* 36.3 (2005), pp. 299–304. doi: 10.1016/j.ymeth.2005.04.006.

[26] P. van Nies, Z. Nourian, M. Kok, J. Moeskops, J. M. Poolman, R. Eelkema, J. H. V. Esch, Y. Kuruma, T. Ueda, and C. Danelon. "Unbiased Tracking of the Progression of mRNA and Protein Synthesis in Bulk and inside Lipid Vesicles". In: (2013), pp. 1–24.

[27] M. M. K. Hansen, L. H. H. Meijer, E. Spruijt, R. J. M. Maas, M. V. Rosquelles, J. Groen, H. A. Heus, and W. T. S. Huck. "Macromolecular crowding creates heterogeneous environments of gene expression in picolitre droplets". In: *Nature Nanotechnology* 11 (2015), p. 191. url: https://doi.org/10.1038/nnano.2015.243.

[28] B. T. Burlingham and T. S. Widlanski. "An intuitive look at the relationship of Ki and IC50: a more general use for the dixon plot". In: *Concepts in Biochemistry* 80.2 (2003), p. 2.

[29] P. Thomen, P. J. Lopez, and F. Heslot. "Unravelling the Mechanism of RNA-Polymerase Forward Motion by Using Mechanical Force". In: *Physical Review Letters* 94.12 (2005). doi: 10.1103/PhysRevLett.94.128102.

[30] D. Patra, E. M. Lafer, and R. Sousa. "Isolation and characterization of mutant bacteriophage T7 RNA polymerases". In: *Journal of Molecular Biology* 224.2 (1992), pp. 307–318.

[31] W. Ross, P. Sanchez-Vazquez, A. Y. Chen, J. H. Lee, H. L. Burgos, and R. L. Gourse. "ppGpp binding to a site at the RNAP-DksA interface accounts for its dramatic effects on transcription initiation during the stringent response". In: *Molecular Cell* 62.6 (2016), pp. 811–823. doi: 10.1016/j.molcel.2016.04.029.

[32] S. Moore. *Sauer: P1vir phage transduction*. Ed. by OpenWetWare. 2011. url: https://openwetware.org/wiki/Sauer:P1vir_phage_transduction.

[33] F. C. Neidhardt, P. L. Bloch, and D. F. Smith. "Culture Medium for Enterobacteria". In: *Journal of Bacteriology* 119.3 (1974), pp. 736–747.

[34] G. S. Filonov, J. D. Moon, N. Svensen, and S. R. Jaffrey. "Broccoli: rapid selection of an RNA mimic of green fluorescent protein by fluorescence-based selection and directed evolution". In: *Journal of the American Chemical Society* 136.46 (2014), pp. 16299–308. doi: 10.1021/ja508478x.

[35] Y. Zhang, U. Werling, and W. Edelmann. "Seamless Ligation Cloning Extract (SLiCE) Cloning Method". In: *Methods Molecular Biology* 1116 (2014), pp. 235–244. doi: 10.1007/978-1-62703-764-8.

[36] K. L. Griffith and R. E. Wolf. "Measuring Beta-Galactosidase Activity in Bacteria: Cell Growth, Permeabilization, and Enzyme Assays in 96-Well Arrays". In: *Biochemical and Biophysical Research Communications* 290.1 (2002), pp. 397–402. doi: 10.1006/bbrc.2001.6152.

[37] X. Dai, M. Zhu, M. Warren, R. Balakrishnan, V. Patsalo, and H. Okano. "Reduction of translating ribosomes enables *Escherichia coli* to maintain elongation rates during slow growth". In: *Nature Microbiology* (2016). doi: 10.1038/nmicrobiol.2016.231.

[38] R. Schleif, W. Hess, S. Finkelstein, and D. Ellis. "Induction Kinetics of the L-Arabinose Operon of *Escherichia coli*". In: 115.1 (1973), pp. 9–14.

[39] M. Yamagishi, J. Cole, M. Nomura, F. W. Studier, and J. Dunn. "Stringent control in *Escherichia coli* applies also to transcription by T7 RNA polymerase". In: *Journal of Biological Chemistry* 262.9 (1987), pp. 242–3940–3943. doi: 10.1038/newbio240242a0.

[40] M. Chamberlin and J. Ring. "Characterization of T7-specific Ribonucleic Acid Polymerase II. Inhibitors of the enzyme and their application to the study of the enzymatic reaction". In: *Journal of Biological Chemistry* 248 (1973), pp. 2245–2250.

[41] V. Varik, S. R. A. Oliveira, V. Hauryliuk, and T. Tenson. "HPLC-based quantification of bacterial housekeeping nucleotides and alarmone messengers ppGpp and pppGpp". In: *Scientific Reports* 7.1 (2017), pp. 1–12. doi: 10.1038/s41598-017-10988-6.

[42] T. K. Wood and S. Song. "Forming and waking dormant cells: The ppGpp ribosome dimerization persister model". In: *Biofilm* 2 (2020), pp. 1–6.

[43] B. D. Bennett, E. H. Kimball, M. Goa, R. Osterhout, S. J. Van Dien, and J. D. Rabinowitz. "Absolute metabolite concentrations and implied enzyme active site occupancy in *Escherichia coli*". In: *Nature Chemical Biology* 5.8 (2009), pp. 593–599.

[44] W. Mohr D. adn Wintermeyer and M. V. Rodnina. "Arginines 29 and 59 of elongation factor G are important for GTP hydrolysis or translocation on the ribosome". In: *The EMBO Journal* 19.13 (2000), pp. 3458–3464.

[45] D. J. Foschepoth. "Towards a synthetic metabolism: exploitation of synthetic and natural nucleotide synthesis pathways for in vitro gene expression". PhD thesis. Radboud Universiteit Nijmegen, 2017.

[46] T. L. Ruegg, J. H. Pereira, J. C. Chen, A. DeGiovanni, P. Novichkov, V. K. Mutalik, G. P. Tomaleri, S. W. Singer, N. J. Hillson, B. A. Simmons, P. D. Adams, and M. P. Thelen. "Jungle Express is a versatile repressor system for tight transcriptional control". In: *Nature Communications* 9.1 (2018), pp. 1–13. doi: 10.1038/s41467-018-05857-3.

5

An *in vitro* study of SpoT binding partners

SpoT, together with RelA, is responsible for the coordination of intracellular ppGpp levels with extracellular conditions. Being the sole enzyme capable of both synthesizing and hydrolyzing ppGpp, SpoT is behind the inverse correlation of so-called basal ppGpp levels with growth rate. As such, understanding what regulates SpoT activity holds the key to understanding bacterial growth rate control. Yet, despite decades of research, what molecular mechanism determines its catalytic activity remains a mystery. A few proteins such as acyl carrier protein (ACP) and the small GTPase ObgE have been reported to interact with SpoT and ACP was hypothesized to lock SpoT in hydrolysis mode. In this chapter, ACP was purified and an in vitro assay was developed to study how the hydrolysis activity of semi-purified SpoT responds to ACP. In contrast with a previous study, a concentration of $1\,\mathrm{mg\,mL^{-1}}$ *holo-ACP inhibited SpoT hydrolysis by* $70\,\%$*. SpoT mutation S587N, believed to abolish the interaction with ACP, was no longer inhibited by holo-ACP, thereby confirming holo-ACP inhibits SpoT hydrolysis. For ObgE no effect on SpoT hydrolysis activity was detected. Considering the in vivo concentration of ACP, as well as possible competition with other proteins interacting with SpoT, it seems unlikely holo-ACP influences SpoT activity in other conditions than during extreme stresses that significantly increase the intracellular holo-ACP level. Therefore, what regulates SpoT activity during steady-state growth, remains to be discovered.*

5.1. Introduction

At this point, the reader has read extensively about the importance of (p)ppGpp as a signaling molecule in *E. coli*, guiding the cell through all kinds of stresses and environmental adaptations, besides having an unknown role in steady-state growth rate control. However, (p)ppGpp is merely the effector of decisions imposed by the enzymes that synthesize and degrade it. RelA and SpoT are in fact the enzymes that adjust (p)ppGpp to environmental cues (**Figure 5.1**). Although RelA is essential for appropriate response to amino acid limitation, it still is not vital: RelA deletion mutants grow in a variety of conditions. SpoT on the contrary cannot be removed from the chromosome[1] and possesses ultimate control over ppGpp as it is able to both synthesize and hydrolyze (p)ppGpp.

In contrast to RelA, (p)ppGpp synthesis by SpoT is activated by a broad range of conditions, some of which shown in **Figure 5.2**. These include fatty acid starvation [2], carbon limitation [3–6], iron limitation [7], phosphate limitation [4], inhibition of ATP synthesis [6] and nutrient upshifts [8]. SpoT even responds to combined starvation for multiple amino acids [6]. Finally, RelA deletion mutants have shown that SpoT can single-handedly synthesize ppGpp levels correlating with growth rate [4, 9, 10]. Thus, SpoT on its own ascertains an appropriate (p)ppGpp response to nearly all environmental changes *E. coli* is faced with.

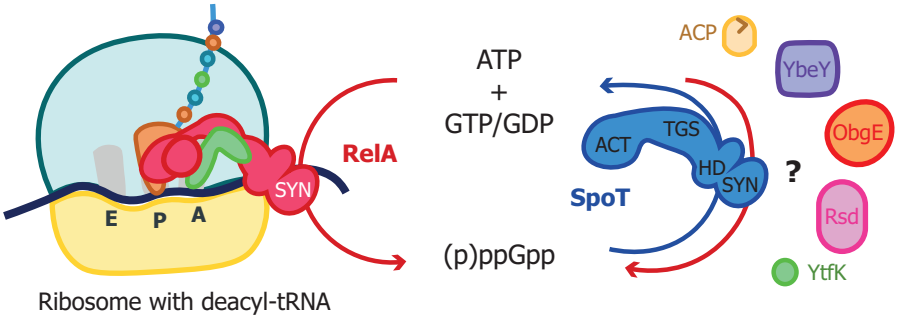

Figure 5.1: RelA and SpoT together determine ppGpp levels, yet only SpoT is essential. SpoT has both hydrolysis and synthesis capacity, whereas RelA can only synthesize ppGpp. For RelA it is clear which molecular mechanism activates it: the interaction with a formerly translating ribosome, stalled due to the binding of a deacylated tRNA in its A-site. For SpoT however, it is barely known which mechanisms drive it to synthesis or hydrolysis of ppGpp.

[1] SpoT can be deleted together with RelA. The double knock-out however grows only in a very limited set of conditions [1].

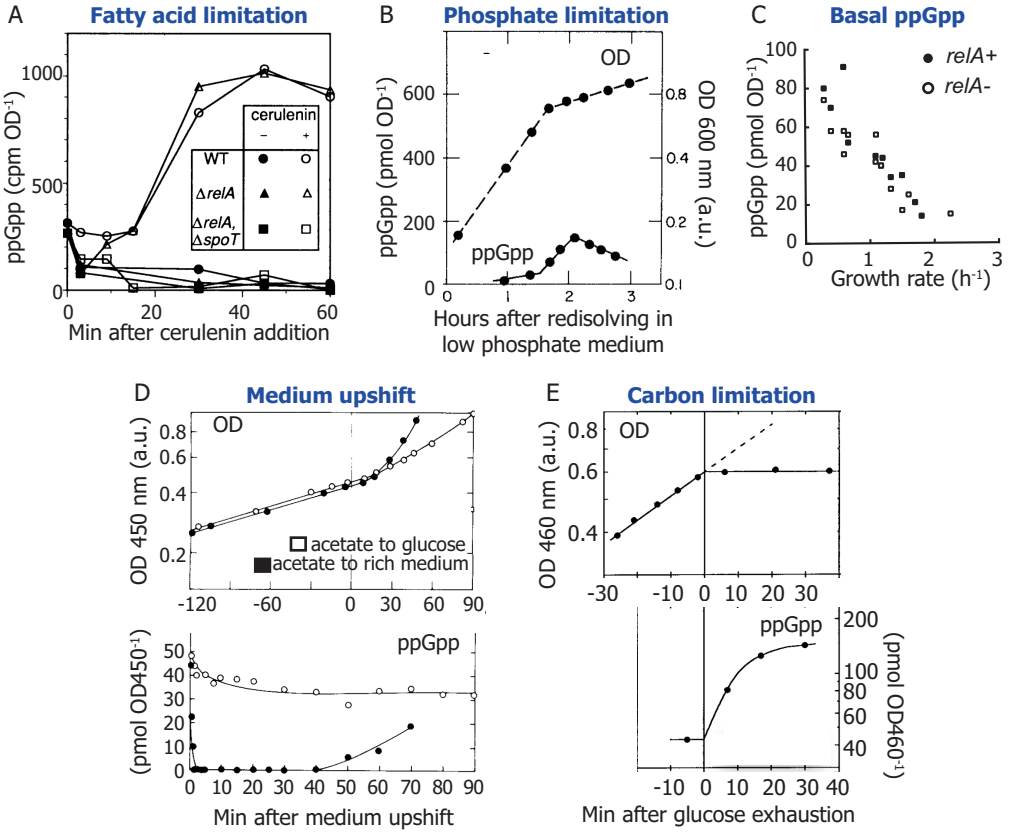

Figure 5.2: A selection of ppGpp responses effected by SpoT only. By comparing Δ*relA* and wild-type strains, the role of SpoT in determining ppGpp levels becomes clear. A) Cerulenin addition inhibits fatty acid synthesis, which rapidly increases due to SpoT. Data from [2]. B) Δ*relA* cells growing on low-phosphate medium eventually cease growth, with a concomitant SpoT-dependent increase in ppGpp. Data from [4]. C) SpoT is behind the correlation between basal ppGpp and growth rate. Data from [4, 9, 10]. D) Depending on the type of medium improvement (supporting faster growth), the ppGpp levels decrease in Δ*relA*. 'Rich medium' contains glucose, 19 amino acids, thiamine, hypoxanthine. Data from [8]. E) Δ*relA* cells growing on low-glucose medium eventually cease growth, with a concomitant SpoT-dependent increase in ppGpp. Data from [6].

This raises the fascinating question how a single enzyme is able to integrate such a vast amount of information. Somehow the state of fatty acid, carbon, phosphate, iron metabolism is *sensed* by SpoT and the catalytic activity of SpoT is *adapted accordingly*. The question hence diverges into two sub-questions. The first addresses what is sensed by SpoT. Is there some kind of protein, metabolite or signaling molecule that represents metabolism as a whole? Or is SpoT combining multiple intracellular cues representing individual metabolic pathways? The second ques-

tion aims at a structural understanding of SpoT. SpoT contains several regulatory and catalytic domains: how do these influence one another? Is SpoT by default hydrolyzing (p)ppGpp and in need of activation in order to synthesize it? Or does it require a cue for both hydrolysis and synthesis? Unfortunately, very little is known about the relative amounts of hydrolysis and synthesis rates (**Table 5.1**.)

Currently none of these questions can be answered with certainty, and for good reasons. The fact that single SpoT knock-outs are not viable, that tag-free SpoT purification has not been achieved[2] and that *in vitro* synthesis of ppGpp by SpoT has still not been observed, all demonstrate that both *in vivo* and *in vitro* classic assays to investigate enzymes are difficult and possibly not applicable to SpoT.

Fortunately, perseverant scientists have used pull-down assays, bacterial-two-hybrid assays and genetic screens to identify potential interaction partners of SpoT. This way a frighteningly long list of proteins that might interact with SpoT has been drawn up. For some of these, subsequent studies have (somewhat) substantiated the interaction, yet leaving question marks regarding the *in vivo* function of the interaction. These include the interaction between SpoT and YbeY, ObgE, ACP, Rsd and YtfK (discussed in detail in section 1.3.3). When this project was started, only ACP and ObgE were mentioned in several studies to (potentially) interact with SpoT. Therefore, the aim of this chapter was to study the effect of these on the catalytic activity of SpoT.

SpoT and ACP

Acyl carrier protein (ACP) is a cofactor in fatty acid synthesis (FAS), lipid A and lipoic aid synthesis, quorum sensing, bioluminescence and toxin activation [18]. ACP carries fatty acid chains to numerous enzymes involved in these pathways. It is only 9 kDa, but one of the most abundant proteins in the cell with 60 000 molecules/cell

[2]The first to purify (untagged?) full-length SpoT since the first attempts in 1977 [11–13] has been Mechold *et al.* [14]. Unfortunately, it is not possible to trace back exactly which SpoT construct and overexpressing strain were used, as this (and other papers) refer to unpublished data [15, 16]. Recently, Lee, Park, and Seok [17] purified GST-tagged SpoT.

Table 5.1: Currently known activity of *E. coli* SpoT in various growth conditions.

Growth condition	Synthesis	Hydrolysis	Net ppGpp
Multiple amino acid deprivation [6]	increase	decrease	increase
Glucose starvation [6]	decrease	decrease	increase
Inhibition ATP synthase with azide [6]	increase	decrease	increase
Glucose addition to glucose starved cells [6]	?	increase	decrease
Cerulenin addition (fatty acid starvation) [2]	?	?	increase
Glucose-lactose diauxic shift [5]	?	?	decrease
Medium shift-up [8]	?	?	decrease

during exponential growth [19]. It consists out of four α-helices that create a pocket where the whole acyl chain or only part of it is buried, depending on the length of the acyl-chain [18]. The attached acyl-chain can thus dramatically alter the properties of ACP. Since there are dozens of fatty acids and its intermediates in the cell, ACP actually encompasses a family of molecules, also called ACP species.

The interaction between SpoT and ACP is not very well characterized. Several studies have demonstrated the interaction by purifying ACP and co-purifying SpoT with it or vice versa [20–22].The interaction takes place via the TGS domain of SpoT and helix II of ACP [22, 23]. Battesti and Bouveret [22] discovered several point mutants of SpoT that were presumably no longer able to interact with ACP and showed a different ppGpp response to cerulenin, an inhibitor of fatty acid synthesis [18]. More specifically, whereas wild-type SpoT synthesizes ppGpp upon cerulenin treatment [2], the SpoT mutants did not, indicating the ACP-SpoT interaction is necessary for the cell to sense the blockage of fatty acid synthesis and synthesize ppGpp. Although it is not known which ACP-species bind to SpoT and during which conditions, preliminary data based on pull-downs after cerulenin treatment or glucose starvation suggest that the SpoT-ACP interaction is stable in these conditions. This implies ACP might be permanently bound to SpoT [22]. This led to a model in which SpoT by default binds ACP, keeping SpoT in a basal hydrolysis state corresponding to basal ppGpp levels. When the cell becomes starved for carbon or fatty acids the proportions of ACP species change, which would be sensed by SpoT and provoke a transition from hydrolysis to synthesis state.

SpoT and ObgE

Another protein that has been claimed to interact with SpoT in several bacterial species is ObgE or CgtA. ObgE is a mysterious GTP hydrolase, to which numerous functions have been ascribed based on various diverging studies, related to DNA replication [24–26], ribosome maturation [27], stress response and ppGpp signaling [28]. ObgE is vital for *E. coli* and cannot be knocked-out [29]. At the genetic level, ObgE is part of an operon including ribosomal proteins L21 and L27 and is regulated by DksA and ppGpp, as are ribosomes [30]. This is why it is present in concentrations similar to ribosomes, high during exponential growth and low during stationary phase [26]. Also at the protein level there is a link with ribosomes: several studies have observed ObgE in ribosomal fractions [31]. During purification of ObgE, several proteins co-purified, including CsdA/DeaD, a helicase part of the 30S ribosomal assembly, and SpoT. The interaction with SpoT was confirmed with a yeast-two-hybrid assay. Sato *et al.* [27] however did not detect SpoT in a pull down of ObgE. Jiang *et al.* [32] studied the association of both ObgE and SpoT in ribosomal fractions. Specifically, ObgE binds 30S and mainly 50S ribosomes [32, 33], which is not affected by ppGpp, as the binding is similar for wild type and $ppGpp^0$ strains. SpoT is also mainly ribosome associated, both 50S and 30S fractions. However, in stationary phase and stress situations (such as serine or glucose starvation by serine hydroxamate or α-methylglucoside respectively) SpoT

was detected in the not ribosome bound state. Thus, the ribosomal binding patterns of ObgE and SpoT do not completely overlap, and ObgE does not need SpoT to interact with the ribosomal fractions.

Hypothesis and goals of this chapter

In a still obscure way, some or all of these interactions allow SpoT to set ppGpp levels such that they correlate with the growth rate of the cell. The ACP-SpoT interaction presents a possible explanation. The ratios of the different ACP species are likely to vary with the flux through the fatty acid synthesis pathway, as with a higher flux, the usage of precursors increases. The growth rate directly depends on the flux of the fatty acid pathway, as fatty acids are part of phospholipids which are put in the membrane of the growing cell. Given that ACP interacts with SpoT, it was hypothesized that SpoT senses the flux through the fatty acid synthesis pathway. A decrease in flux would cause a decrease in acylated ACP, downregulating the ppGpp hydrolase activity of SpoT [34, 35].

Prior studies in our lab have quantified the various ACP species in different steady-state growth rates to determine whether the hypothesis that ACP species could correlate with the rate of fatty acid synthesis or growth rate is plausible. Indeed, some species varied with growth rate (**Figure 5.3A**). To pinpoint exactly which ACP species were the most likely to control SpoT activity, ACP-pools were quantified in stress conditions known to change SpoT activity. These include addition of the antibiotic cerulenin [36] (**Figure 5.3B**), diauxic shift in a RelA- strain (**Figure 5.3C**) and response to chloramphenicol and medium upshift [37]. From these it was clear that there is a large variation in the ratios of the various ACP species in different conditions. For example, when *E. coli* MG1655 grows in glucose and casamino acids, the most abundant ACP species are holo-ACP (32%), the saturated acyl-ACPs up to C14 (17%) and hydroxylated acyl-ACPs (10%). C16-ACP only counts for 1%, acetyl- and malonyl-ACP for 3% and all unsaturated ACPs for 2%. Ketoacyl-ACPs were not detected due to low abundance.

Interestingly, inhibition of fatty acid synthesis by cerulenin (**Figure 5.3B**) caused an immediate decrease in holo-ACP to about 8% and hydroxylacyl and unsaturated acyl-ACPs to less than 1% each. Concomitantly, all saturated acyl-ACP's increase dramatically to 64% of the pool. The fact that the relative increase of some ACP species is larger than the decrease of others insinuates that an increased fraction of the cellular ACPs has been devoted to fatty acid biosynthesis or that the cell has synthesized more ACP. Despite this extensive data-set, there was no specific ACP species of which the quantity consistently correlated with activity of SpoT. In other words, it does not appear that a single ACP species can promote ppGpp synthesis or hydrolysis of SpoT.

To determine which ACP species interact with SpoT *in vivo* is difficult because it is impossible to completely control the levels of each individual ACP species and because of their scope. *In vitro* using purified SpoT, one could assess the effect of the

individual ACP species on SpoT, which was the aim of this chapter. This required overcoming several major challenges, including 1) purifying SpoT (despite decades of research there was no published protocol for this) and ACP; 2) synthesizing the different ACP species, which requires expensive substrates and which is difficult to obtain in the high concentrations that mimic the cell's cytoplasm; and 3) measuring SpoT activity by quantifying ppGpp with a newly developed LC-MS method. For these reasons, the goal was not (yet) to biochemically characterize SpoT by determining the k_{cat}, K_i of ACP inhibition, hydrolysis mechanism, etcetera. Instead we were aiming at a qualitative understanding of the interaction between SpoT and ACPs. A second aim of this chapter was to confirm or refute the interaction between ObgE and SpoT and determine whether ObgE affects SpoT activity.

5.2. Materials and methods

5.2.1. Strains and plasmids

A list of strains and plasmids used can be found in **Table S5.1**. All primers were obtained from IDT DNA. pSpoT allows expression of a CBP N-terminal tagged *E. coli* SpoT. It was kindly provided by Mattia Cerri. To obtain it, *spoT* was PCR amplified from MG1655 genomic DNA using primers MC29032016SpotF and MC29032016SpotR (**Table S5.2**). The CBP tag, a spacer region and a sequence overlapping with *spoT* was purchased as a single fragment (MC31032016CBPSPOTsy) from IDT, which was PCR amplified with primers MC29032016CBPSynF and MC29032016CBPSynR. The two PCR products were then SOE-ed together and subsequently digested with BglII and XhoI. To create pSpoT, this was ligated in a vector containing the pSC101** origin of replication and *kanR* marker.

Point mutations were introduced into pSpoT by overlap extension PCR (annealing temperature 70 °C) using primers as listed in **Table S5.2**. PCRs were digested with DpnI (3 h at 37 °C, then 5 min at 80 °C) and then directly transformed into *E. coli* DH5α. Plasmids were sequenced to confirm the presence of the point mutations before transformation into MG1655.

For pObgE construction, *obgE* was amplified from genomic MG1655 DNA using primers NI275 and NI276 and placed between the NdeI and BamHI sites in pET28a (Novagen), appending a thrombin-cleavable N- terminal His6-tag to ObgE. For construction of pACP (performed by Marek Noga), containing thrombin-cleavable N-terminally His6-tagged ACP, *acpP* was amplified from *E. coli* MG1655 genomic DNA with primers MN01 and MN02 (**Table S5.2**). Further the protocol was identical to that of pObgE.

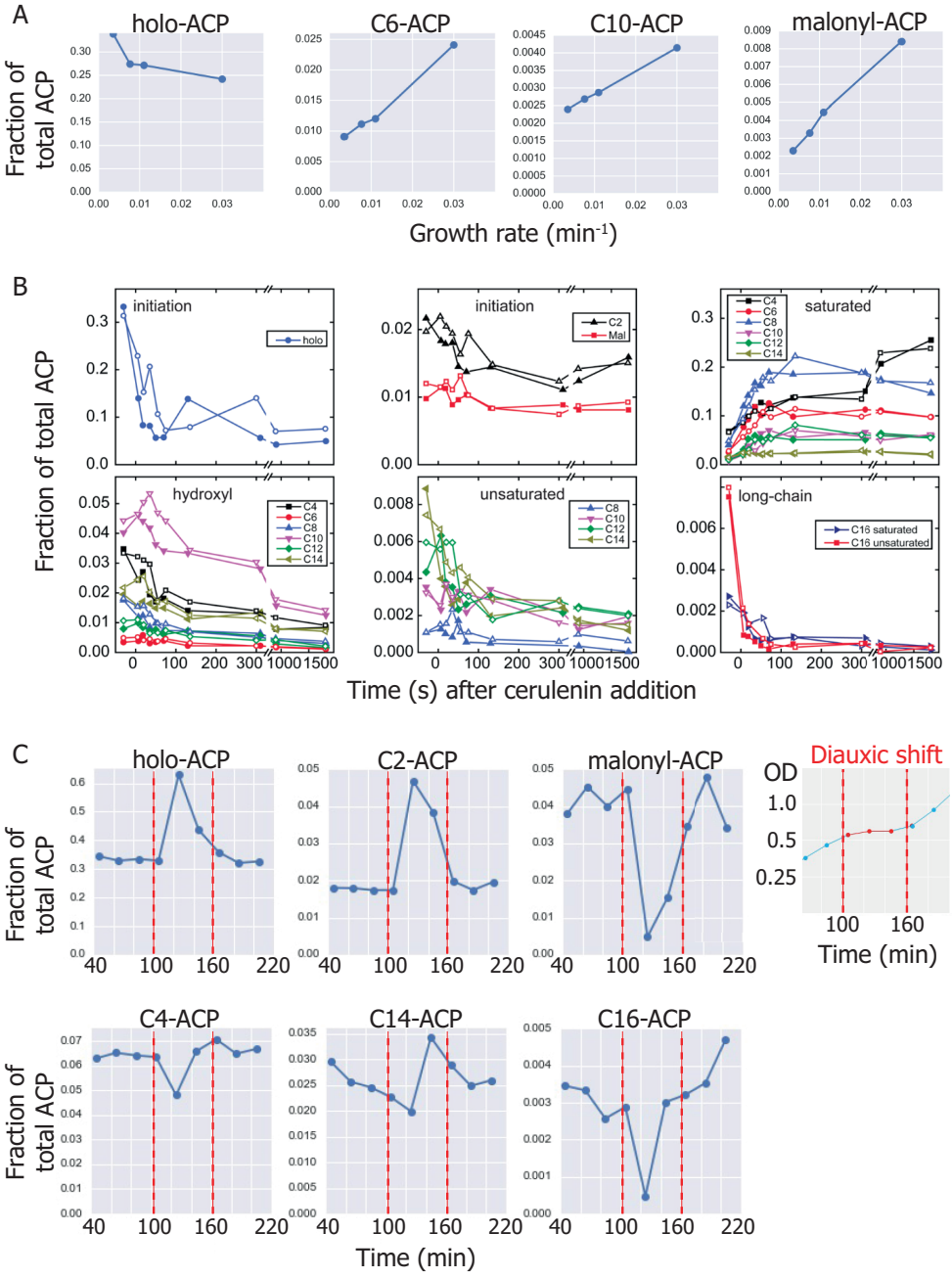
A
holo-ACP
C6-ACP
C10-ACP
malonyl-ACP
Fraction of total ACP
Growth rate (min-1)
B
initiation
holo
initiation
C2
Mal
saturated
C4
C6
C8
C10
C12
C14
hydroxyl
unsaturated
long-chain
C16 saturated
C16 unsaturated
Fraction of total ACP
Time (s) after cerulenin addition
C
holo-ACP
C2-ACP
malonyl-ACP
Diauxic shift
OD
Time (min)
C4-ACP
C14-ACP
C16-ACP
Fraction of total ACP
Time (min)

Figure 5.3: Variation of ACP pools due to cerulenin addition, in various growth rates and during glucose-lactose diauxic shift. A) The fraction of several ACP species (anti)correlates with the growth rate. B) Immediately after cerulenin addition, the ACP species fraction change. Data from Noga *et al.* [36]. C) Evolution of several ACP species during growth on MOPS medium containing 0.04% glucose and 0.2% lactose. At the onset of growth arrest during the transition from glucose to lactose, ACP species change significantly. The peaks during the transition coincide with the ppGpp response (Chapter 2). Data of A) and C) were obtained by Mattia Cerri [37].

5.2.2. Preparation SpoT lysates

This protocol is based on Battesti and Bouveret [22]. An overnight culture of MG1655 with pSC101-CBP-SpoT or pSC101-CBP-SpoT$_{mutant}$ was diluted 1:50 in LB with antibiotics (kanamycin 25 µg mL^{-1}), 25 mL per final sample. Cells were grown at 250 rpm and 37 °C to an optical density of 0.3 and induced with 50 ng mL^{-1} anhydrous tetracycline. When the cells reached an OD between 2 and 3, they were centrifuged at 4000 g, 4 °C for 20 min. Supernatant was discarded and the pellet washed with 1/10 volume of the culture using ice cold binding buffer (binding buffer 1 high salts or BB1-HS: 10 mM Tris-HCl pH 8.0, 150 mM NaCl, 1 mM Mg-acetate, 2 mM $CaCl_2$, 100 µM $MnCl_2$). Centrifugation was repeated and supernatant discarded. Pellets were resuspended in 0.5 mL binding buffer per 25 mL original culture, pooled and sonicated on ice for 30 min (continuously 5 sec on and 5 sec off with 40 % amplitude). Lysates were centrifuged for 30 min at 27 000 g and 4 °C. Hereafter, the supernatant could be stored at −80 °C after addition of 0.5 mL 50 % glycerol per mL of supernatant (aliquoted in 1.5 mL aliquots). Lysates could be kept at −80 °C for at least 4 months without losing activity. Option 2: Lysates were kept on ice without glycerol addition and used right away in next step.

5.2.3. Preparation of SpoT beads

For one pull-down sample, 25 µL of calmodulin sepharose beads (GE Healthcare) were used. E.g. if the total assay needed 12 samples, 12*25 µL or 300 µL calmodulin beads were prepared. Beads were washed 3 times with 1 mL binding buffer (binding buffer 1 low salts or BB1-LS: 10 mM Tris-HCl pH 8.0, 15 mM NaCl, 1 mM Mg-acetate, 2 mM $CaCl_2$, 100 µM $MnCl_2$, final pH 8.0) by centrifuging at 500 rpm at 4 °C for 30 sec, discarding supernatant, resuspending in BB1-LS and vortexing. SpoT lysates were added to beads, such that 300 mL culture was used for 300 µL beads, followed by incubation at 4 °C while gently tumbling for 2.5 h to 3 h. Incubation times of 24 h resulted in lower SpoT activity. Hereafter, the beads were washed 6 times with 5 mL BB1-LS, again by centrifuging 500 rpm for 30 sec at 4 °C, removing supernatant, resuspending, and vortexing. Removal of supernatant was done by decantation and for the final step with a pipette to make sure all beads were at the bottom of the recipient. This bead-residue was finally resuspended in the same

volume as the initial bead volume used (e.g.300 µL for 12 samples). SpoT beads were analyzed with SDS-PAGE using 4–20% Mini-Protean TGX stain-free protein gels (Bio-Rad), which were subsequently stained with Coomassie Blue (BioSafe by Bio-Rad).

5.2.4. ppGpp hydrolysis/synthesis assay (with purified ACP)

For a single assay 25 µL prepared beads was briefly centrifuged at 500 rpm. The supernatant was removed such that only beads were left, and this was resuspended in 19 µL binding buffer (with or without ACP). In case ACP was present, the beads (and control without ACP) were incubated at 4 °C for 90 min while gently tumbling. After, this was put at 37 °C for a few minutes. Once at 37 °C, at 0 min 1 µL of ppGpp stock to a final concentration of 150 µM (unless mentioned otherwise) was added. For each time point, the beads were centrifuged briefly in a table centrifuge and 1 µL supernatant was added to 19 µL quenching solution (50 % methanol, 30 % acetonitrile, 20 % water, containing ^{13}C internal standard) and put on ice. The content was determined with LC-MS.

5.2.5. LC-MS measurements of nucleotides

2 µL of the quenched supernatant was injected onto a cHILIC column as in chapter 2 to analyze ppGpp, GMP, GDP, GTP, AMP, ADP and ATP levels. Concentrations were determined using calibration curves based on standards of 0, 10, 20, 50, 100 and 200 µM. The LOD was calculated as the limit of the blank (LOB) + 1.645 * $SD_{10\,\mu M}$, in which LOB = $mean_{blank}$ + 1.645 * SD_{blank} [38] (SD, standard deviation).

5.2.6. Buffer optimization

Binding buffer 1 (BB1) [22] was compared to binding buffer 2 (BB2-HS) from Heinemeyer and Richter [11], which contained 10 mM Tris-HCl, 2 mM $MnCl_2$, 25 mM NH_4 – acetate, 200 mM Na-acetate, 2 mM dithiothreitol, 2 mM $CaCl_2$, final pH 7.55. The low salt variant of this buffer was BB2-LS (10 mM Tris-HCl, 2 mM $MnCl_2$, 2.5 mM NH_4 – acetate, 20 mM Na-acetate, 2 mM dithiothreitol (DTT), 2 mM $CaCl_2$, final pH 7.7. In case ACP was added to SpoT, 2 mM or 4 mM DTT was added to the buffer (incl. to the control without ACP added). Before the assay, the beads were incubated with ACP for 70 to 90 min at 4 °C while gently tumbling.

5.2.7. Purification of ACP

BL21 pACP was grown in terrific broth (TB) with 50 µg mL^{-1} kanamycin at 230 rpm and 37 °C until an OD between 0.9 and 1.3, induced with 750 µM IPTG and then put at 18 °C for 19 h. Cells were pelleted (6700 g, 20 min, 4 °C), supernatant discarded

and washed with 50 mL phosphate-buffered saline (1.37 M NaCl, 27 mM KCl, 100 mM Na_2HPO_4, 18 mM KH_2PO_4, pH 7.4) (original culture 500 mL). Cells were pelleted again and dissolved in 15 mL resuspension buffer (150 mM Tris-HCl pH 7.5, 150 mM NaCl, 10 % glycerol). Cells were sonicated on ice with a tip sonicator (3 min at 40 % , 1 sec on 2 sec off) and lysate was centrifuged at 14 000 g for 35 min at 4 °C. The supernatant was put on a column containing 4 mL Ni-NTA beads (Thermo Fisher) that were pre-washed with resuspension buffer. The column with supernatant was incubated at 4 °C while tumbling for 3 h. The column was uncapped and lysate flow through collected (unbound fraction). The column was washed with 10 mL resuspension buffer and then with 5 mL wash buffer (150 mM NaCl, 20 mM Tris-HCl pH 7.5). Column was capped, and 1.9 mg thrombin (40-300 U mg^{-1}) dissolved in 2 mL wash buffer was added to the column to remove the His-tag from ACP. After 2.5 days of incubation (tumbling) at 4 °C, the eluate was collected. 8 mL wash buffer was added and the flow through was collected in 1 mL fractions. Finally, 5 mL elution buffer (300 mM imidazole, 20 mM Tris-HCl pH 7.5, 150 mM NaCl) was added and 1 mL fractions collected to remove all ACP from the column. Fractions were kept at 4 °C and analysed using SDS-PAGE. The column was washed with 15 mL bead regeneration buffer (20 mM 2-(N-morpholine)-ethanesulfonic acid (MOPS), 0.1 M NaCl, pH 5.0), 15 mL MQ and beads were resuspended in 4 mL 20 % ethanol and kept at 4 °C.

Because ACP has a pI of 4.1, it is possible to further purify ACP by precipitating it at pH 4.1, as most other proteins will still be in solution. ACP containing fractions were first centrifuged 10 min 4 °C at 15 000 g to remove precipitate. Supernatant was added 1:1 to 200 mM formate buffer (pH 3.69). After intense vortexing the sample was centrifuged again and supernatant removed. The pellet was redissolved in 100 µL 20 mM $KHPO_4$ buffer (pH 7.2). The concentrated ACP samples were further purified into holo-ACP and apo-ACP fractions using high performance liquid chromatography (HPLC). The column used was a Zorbax 300SB-C8 with mobile phases A 0.1 % trifluoroacetic acid (TFA) and B 0.08 % TFA in acetonitrile (100 µL injection volume). Fractions corresponding to holo- or apo-ACP were collected, and these were verified to be holo-/apo-ACP with LC-MS using the same column. For LC-MS, mobile phase A was 25 mM formic acid and mobile phase 25 mM formic acid in acetonitrile. The LC-MS method was as in [36]. The HPLC fractions containing holo- or apo-ACP were pooled, frozen in liquid nitrogen and lyophilized (−40 °C, < 1 mbar). Lyophilized ACP was redissolved in BB1-LS with 2 mM DTT. This redissolved ACP had a pH of about 5.5 due to traces of TFA, which was via titration determined to be about 0.05%. To remove this TFA, ACP was twice precipitated with formate buffer and resuspended in BB1-LS.

5.2.8. SpoT-ObgE binding assay

Purification of ObgE was based on Feng *et al.* [39] with adjustments. *E. coli* BL21DE3 pObgE was grown in 1 L LB with antibiotics, 37 °C and 250 rpm, until and OD600 of 0.6. After induction with 1 mM IPTG, cells continued growing for 5 h

at 30 °C. Subsequently, cells were centrifuged (4000 rpm, 10 min), resuspended in lysis buffer (20 mM Tris-HCl, pH 7.5, 500 mM NaCl, 50 mM imidazole) and sonicated. Hereafter, the lysate was centrifugated (15 000 rpm for 30 min). In the SpoT-binding assay with ObgE, 200 µL ObgE lysate or ObgE lysis buffer was added to a SpoT-beads sample and incubated overnight at 4 °C while gently tumbling. Next day, the beads samples were washed three times with SpoT binding buffer 1 (low salts) before performing a ppGpp hydrolysis assay as described above. Presence of ObgE in the lysate and on the SpoT-beads was verified with SDS-PAGE.

5.2.9. Proteomics method to analyze pulled down SpoT, ACP and ObgE

Protein standards to develop proteomics method

For standards, ACP and SpoT were purified as mentioned above. ObgE was further purified from the lysate as follows. ObgE lysate was loaded onto a column with 4 mL Ni-NTA beads pre-equilibrated with lysis buffer. The column was washed with 20 mL lysis buffer and eluted with 10 mL elution buffer (20 mM Tris-HCl, pH 7.5, 500 mM NaCl, 500 mM imidazole). Eluted fractions were spin-filtered to remove buffer. Skyline was used to *in silico* digest the proteins and generate transitions based on the Uniprot protein sequence.

Preparation of isotopically labeled internal standards

E. coli MG1655 pSpoT and *E. coli* BL21DE3 pObgE were grown in 0.2 % glucose MOPS minimal medium with necessary antibiotics and $^{15}NH_4Cl$ as sole nitrogen source. These cells were grown, SpoT and ObgE overexpressed, harvested and lysed as their respective protocols above. The lysates were used as internal standard for the relative quantitation of SpoT, ObgE and ACP in bead-samples. There was no need to overexpress ACP as the cellular concentration is ample to easily detect ACP in lysates.

Protein precipitation and digestion

A SpoT-beads sample (containing ^{14}N proteins) was centrifugated and all supernatant removed. Beads were redissolved in 50 µL elution buffer (same as binding buffer but with 2 mM EGTA instead of Ca^{2+}), sonicated and centrifugated. To the supernatant 50 µL of both ^{15}N-labeled lysates of cells overexpressing SpoT or ObgE was added.

To precipitate the proteins, the following solutions were added with intense vortexing in between: 1) 400 µL methanol, 2) 100 µL chloroform, 3) 300 µL LC-MS grade water. The samples were centrifuged (1 min, 15 000 rpm, 4 °C) and the upper layer was carefully removed. After addition of another 300 µL methanol and vortexing,

samples were centrifuged again (10 min, 15 000 rpm, 4 °C). The total supernatant was removed and (invisible) pellets dried in a vacuum centrifuge for 30 min without heating. The proteins were solubilized in 50 µL protease buffer (50 mM ammonium bicarbonate pH 7.8, 1 mM $CaCl_2$, 0.2 % ProteaseMax (Promega)) with vigorous vortexing and sonication for 10 min. Hereafter 5 µL of 50 mM DTT was added and again vortexed. Then, 15 µL of freshly prepared 50 mM iodoacetamide (in 200 mM ammonium bicarbonate) was added and incubated at room temperature in the dark for 30 min. Hereafter, 4 µL Trypsin Gold (Promega) solution (1 µg µL^{-1} in 50 mM acetic acid) was added, the sample vortexed, briefly centrifuged and incubated overnight at 37 °C. The digestion was stopped the next day by addition of 5 µL 10 % TFA. After 5 min of incubation at room temperature, the samples were centrifuged (10 min, 15 000 rpm, 4 °C). Supernatant was stored at 4 °C before analysis with LC-MS.

Quantification of SpoT, ObgE and ACP with LC-MS

The LC-MS system was identical to the one in chapter 2. The column compartment was set at 40 °C. 5 µL sample was injected for analysis on an Acquity UPLC CSH130 C18 column (1.7 µm particle size, 2.1 mm ID, 50 mm length, Waters). Chromatographic separation was performed using a binary gradient by mixing mobile phase A (25 mM ammonium formate) and B (25 mM ammonium formate in acetonitrile) at a flow rate of 0.6 mL/ min. First mobile phase B increased from 2 to 25 % in 10 min, then from 25 to 40 % in 2 min and finally from 40 to 80 % in 0.5 min followed by a 0.5 min hold and a 4 min re-equilibration under initial conditions before the next injection. The mass spectrometer was operating in dynamic MRM mode with positive polarity using the transitions of **Table S5.3**. Fragmentor voltage was set to 130 for all traces. An acquisition time filter of 0.035 min was applied to the data.

LC-MS data analysis

LC-MS data files were processed with Skyline or MassHunter to integrate peak areas. Peak areas for each compound were divided by peak area of the matching ^{15}N-labeled internal standard.

5.3. Results

5.3.1. SpoT purification

To confirm SpoT was pulled down from the cells, the SpoT beads were analyzed using SDS-PAGE (**Figure 5.4**). As a control a MG1655 lysate without overexpression of SpoT was used. When comparing the control with lysate in which SpoT was overexpressed, there is one clear new band slightly above 75 kDa, consistent with 83 kDa of CBP-SpoT. Therefore SpoT was pulled-down although various other proteins were co-purified with it. In particular there are 3 bands visible around 50 kDa.

Given that in the lysate without overexpressed SpoT these are also present, these proteins likely bind non-specifically to the beads, and not SpoT. The band around 15 kDa is possibly calmodulin, which has a mass of 16.8 kDa (UniProt).

For ideal control of experimental conditions, SpoT should be eluted from the beads and further purified as other proteins that might interfere in the assay also bound to the calmodulin beads. SpoT was eluted from the beads using binding buffer 2 (high salt) with 2 mM EGTA instead of $CaCl_2$. Without Ca^{2+}, the CBP tag will no longer bind to the calmodulin beads and hence release SpoT. However, when ppGpp hydrolysis activity was tested, there was no significant decrease in ppGpp or increase in GDP (**Figure 5.5**).

EGTA, although often referred to as a Ca^{2+}-specific chelator, in fact also chelates other cations. The logarithmic stability constants for Ca^{2+} and Mn^{2+} are 11.0 and 12.3 respectively [40], indicating the affinity for Mn^{2+} is about 10-fold higher than Ca^{2+}. It was shown experimentally that although equimolar amounts of EGTA and Ca^{2+} (at pH 7.3) lead to complete complexation, equimolar addition of Mn^{2+} effectively replaces over 90 % of the Ca^{2+} in the Ca^{2+}-$EGTA^{4-}$ complexes [40]. Bearing this in mind, it seems more likely that the EGTA removed the Mn^{2+} necessary for the hydrolysis activity of SpoT instead of the Ca^{2+} [11, 12]. Another potential explanation for the lost activity of eluted SpoT, is that the release from the beads somehow affected its folding, in particular the relative orientation of the catalytic domains, which affects SpoT activity [14].

Given that when SpoT attached to the beads exhibited detectable ppGpp hydrolysis, it was decided to not further complete the purification as it was deemed not absolutely vital for our goal, which was to detect a potential interaction between ACP and SpoT. Therefore SpoT activity was further studied while attached to the calmodulin beads.

5.3.2. Purification of ACP and *in vitro* synthesis of ACP species

An overview of the ACP purification are presented in **Figure 5.6A**. The purification of ACP using UPLC was expected to result in two peaks, one for holo-ACP and one for apo-ACP, as these are the most abundant species in the cell during ACP overexpression. There were however various peaks, most often two for apo-ACP and four for holo-ACP (**Figure 5.6B**). Urea-PAGE analysis of these peaks indicated the left peak of apo-ACP contained pure apo-ACP (**Figure 5.6C lane 4**), whereas the right peak also contained other unknown protein(s) (Figure 5.6C **lane 3**). These other proteins however could not be washed away using ACP-precipitation as they precipitated together with apo-ACP (the mysterious protein is not present in the supernatant, Figure 5.6C **lane 2**). Unfortunately, the precipitation of ACP is not very efficient as about half the apo-ACP is lost in the supernatant (**lane 2**). The four holo-ACP peaks contained different relative amounts holo-ACP and dimerized holo-ACP, and occasionally apo-ACP (Figure 5.6C **lanes 6-8**). The fractions containing only holo-ACP were pooled into the final holo-ACP solution used in SpoT hydrolysis

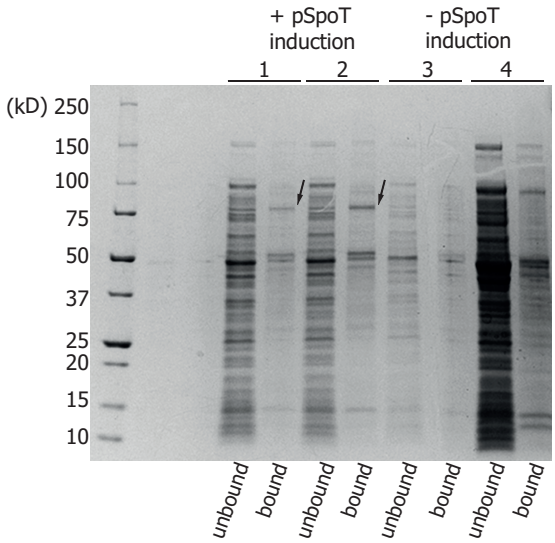

Figure 5.4: SDS-PAGE of SpoT purification with calmodulin beads. Four bead samples were analyzed for their bound and unbound fractions. Bead samples 1 and 2 were pull downs of MG1655 pSpoT lysate with SpoT overexpressed, whereas samples 3 and 4 are pull downs of MG1655 lysate. The arrows indicate the band corresponding to SpoT.

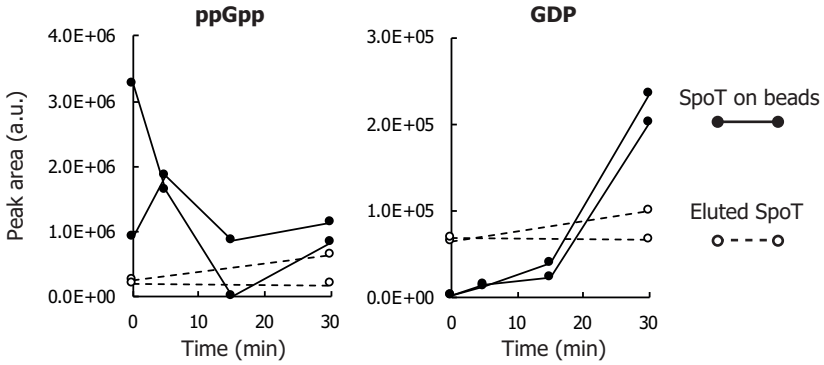

Figure 5.5: ppGpp hydrolysis activity of eluted SpoT. The SpoT pulldown and ppGpp hydrolysis activity test were performed in BB2-HS. Before eluting SpoT, the activity of SpoT was tested (black curve). Since there were no internal standards, there is a high variability in the data (e.g. ppGpp signal at 0 min). However the GDP signal clearly increases, indicating SpoT is active. SpoT was eluted from the exact same beads with BB2-HS containing EGTA. GDP levels do not increase significantly, indicating SpoT has reduced activity compared to SpoT bound to the beads.

assays (Figure 5.6C **lane 5**, dissolved in BB1-LS 2 mM DTT). **Figure 5.6D** shows the results of the *in vitro* synthesis of C4-ACP and C8-ACP. In the given conditions, the conversion of apo-ACP (1 mg mL^{-1}) to C4 or C8-ACP is complete as there is no apo-ACP detectable in the samples of C4 and C8-ACP. However, there was a significant loss of C8-ACP after precipitation to remove SFP synthase (C8* in Figure 5.6D).

5.3.3. Optimization of sample preparation for ppGpp and GDP measurements

In order to asses *in vitro* SpoT activity, it was necessary to absolutely quantify ppGpp and GDP, respectively the substrate and product in case of ppGpp hydrolysis. For absolute quantification of compounds using LC-MS, an internal standard (IS) is vital. Without IS, LC-MS analysis can add a significant error to a measurement as there can be various sources of variation between samples even within a single measurement batch: the injection volume, the ionization efficiency, the degree of in-source degradation and the detection. This is illustrated by the preliminary test of SpoT activity in **Figure 5.5**. To compensate for all these errors, it is common to use an internal standard identical for all samples, existing of the compounds of interest but isotopically labeled, such as ^{13}C or ^{15}N. These are chemically the same as the unlabeled compound and hence will behave the same in the MS and undergo the same sources of error. Therefore, the quenching solution was dried ^{13}C *E. coli* lysate dissolved in 50 % methanol, 30 % acetonitrile, 20 % MQ. **Figure 5.7** shows that using the ratio of ^{12}C/^{13}C for quantitation improves the variability between samples and allows to make an accurate calibration curve for GDP and ppGpp. Each time the LC-MS was used, a calibration curve of both ppGpp and GDP was measured in order to quantify GDP and ppGpp in the samples of that run. The average limit of detection (LOD) was 3.5 µM $\pm$ 1.4 µM for GDP and 7.1 µM $\pm$ 3.0 µM for ppGpp (see methods).

5.3.4. Optimization and assessment of *in vitro* SpoT activity

Buffers for SpoT activity

Several buffers were screened to improve the *in vitro* activity of SpoT. Both the buffers used for the preparation of the lysate, and for the actual hydrolysis of ppGpp were varied. Buffers used for protein purification contain high salt concentrations to reduce interactions between the protein of interest and other proteins in the cell, allowing a higher degree of purity. The buffers tested were based on a protocol by Battesti and Bouveret [22] and Heinemeyer and Richter [11], and will be called respectively binding buffer 1 high salt and binding buffer 2 high salt. (BB1-HS, BB2-HS). However, the buffer used to test the activity of the protein of interest needs to contain all necessary cofactors, and mimic the conditions of the cell. Since the substrate and product of the reaction in our case are measured with LC-MS, the

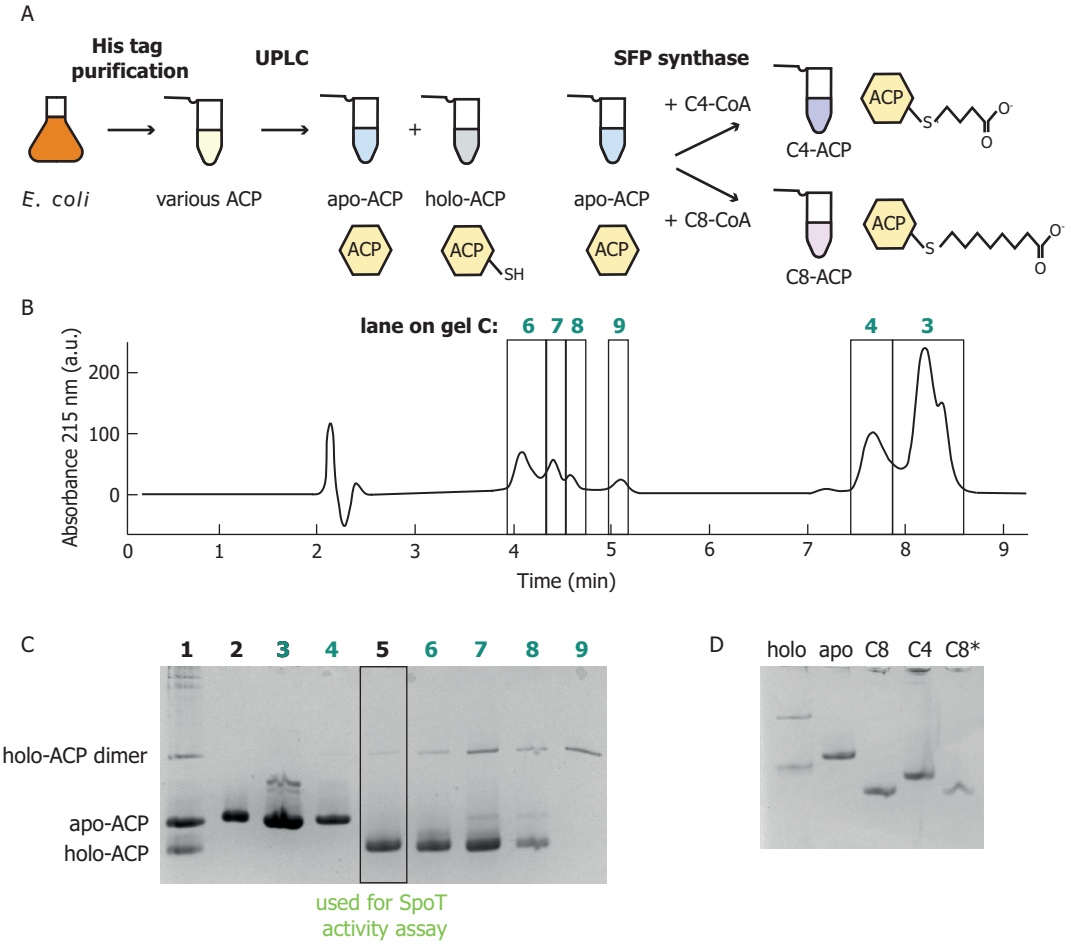

Figure 5.6: Holo-ACP purification and *in vitro* synthesis of ACP species. A) Overview of the purification and *in vitro* modification of ACP species. B) Chromatogram of UPLC purification of ACP (absorbance at 215 nm). After 4 min holo-ACP elutes and after 7.5 min apo-ACP. The various peaks were analyzed using urea-PAGE (C). C) Lane 1: Eluted ACP after His-tag purification, sample that was used for UPLC; lanes 2-9: see text. D) Urea-PAGE of purified holo-ACP (lane 1) and apo-ACP (1 mg mL^{-1}, lane 2), and *in vitro* synthesized C8-ACP (lane 3) and C4-ACP (lane 4) using apo-ACP, SFP synthase and C8-CoA or C4-CoA respectively. Lane 5 represents C8-ACP after one round of precipitation and redissolving in order to remove SFP synthase. There is a significant loss of C8-ACP. The upper band in lane 1 represents dimers of holo-ACP.

buffer also has to be MS compatible, so preferably preventing the formation of adducts that are not measured and preventing ion suppression (ions in the sample hinder efficient ionization of the compounds of interest). Moreover, the high salt concentrations in the purification buffers could impede interactions between SpoT and other proteins. Therefore, the buffers tested were again of [22] and [11], but with lower salt concentration and were called BB1-LS and BB2-LS (low salt).

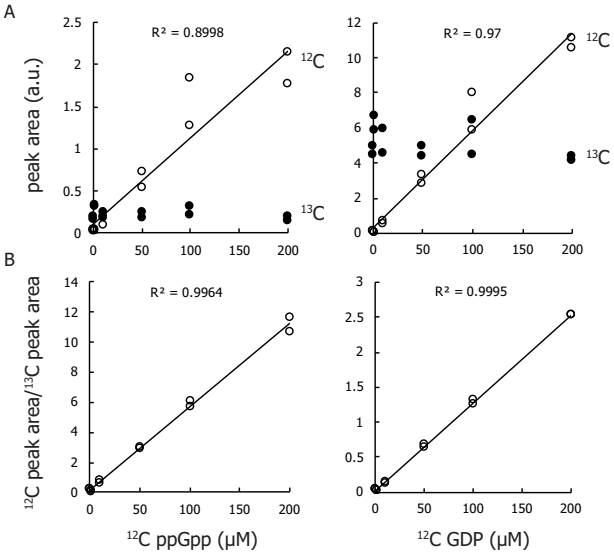

Figure 5.7: Calibration curves of ppGpp and GDP for *in vitro* SpoT activity assays. ^{12}C ppGpp and GDP standards were diluted in BB1-HS, containing ^{13}C labeled internal standards. A) Peak areas of ^{12}C and ^{13}C ppGpp and GDP of the calibration samples. B) The ratio of ^{12}C/^{13}C results in a more precise calibration curve. Samples were injected twice, using cHILIC method (chapter 2).

When comparing SpoT beads that were prepared in BB1-HS, the hydrolysis happens just as efficiently in BB1-LS and BB2-LS (**Figure 5.8**), as in both cases GDP levels increase already after 1 min, reaching saturation after 2 min. However, SpoT beads prepared in BB2-HS appear less active in hydrolyzing ppGpp. This could be because the lysate was prepared a few months before the lysate prepared in BB1-HS. It could also be that the buffer simply does not allow for SpoT activity as much, or that the specific salts in the buffer do (not) prevent interaction between SpoT and other proteins that inhibit/promote SpoT hydrolysis activity. However, during the optimization of the assay, in some experiments BB2 seemed better than BB1 and vice versa. In the end, BB1 was selected as the optimal buffer for purification (HS) and *in vitro* activity assays (LS).

Assuming that the substrate (ppGpp) is present in saturating amounts ($S >> K_M$ in equation 5.1), the hydrolysis rate v_{max} by SpoT can be estimated by the slope of initial linear part of the hydrolysis curves. The activity of CBP-SpoT in buffer BB2-LS

might be higher than in BB1-LS, although this was only apparent from the GDP and not the ppGpp curve (**Figure 5.9**).

$$v = \frac{dP}{dt} = \frac{v_{\max} * S}{K_M + S} \tag{5.1}$$

However, the hydrolysis rates can only be compared between SpoT-bead samples of a single purification batch. Given that $v_{\max} = k_{cat} * E$, with E the amount of enzyme, the hydrolysis rate depends on the amount of SpoT attached to the bead, which can vary from one purification round to another.

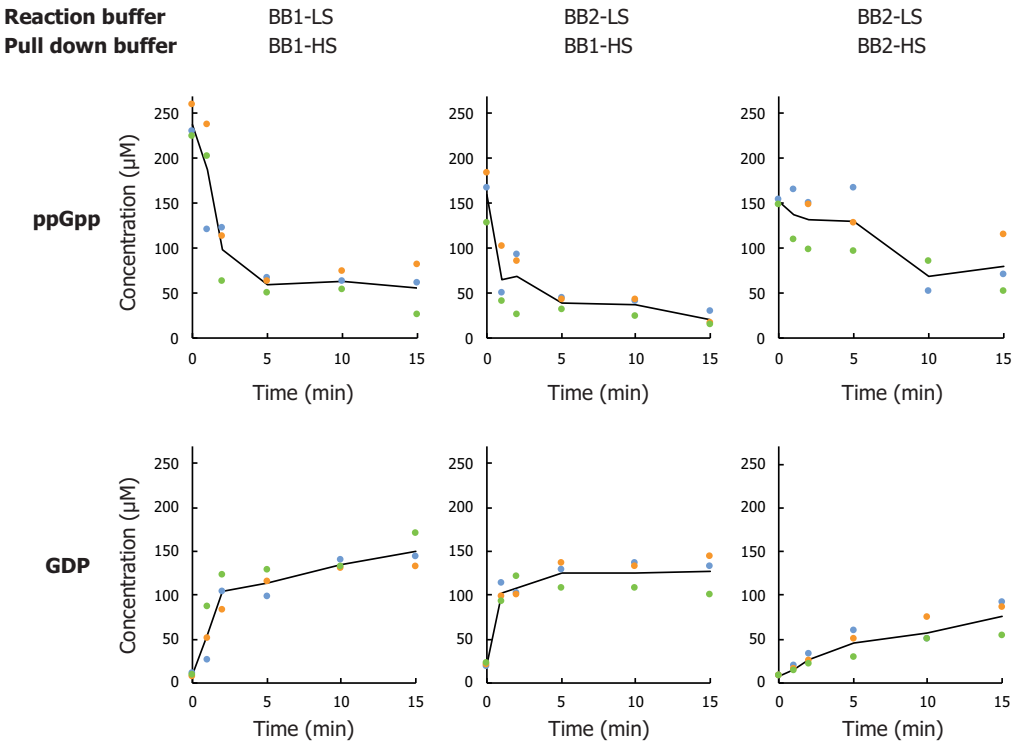

Figure 5.8: Buffer optimization for *in vitro* ppGpp hydrolysis by SpoT. SpoT was pulled down in either BB1-HS or BB2-HS. SpoT beads were eventually washed and resuspended in BB1-LS or BB2-LS. A) Curves of decreasing ppGpp and B) increasing GDP due to hydrolysis activity of SpoT. The curves are the average of three replicates (shown as coloured circles) originating from one SpoT purification batch.

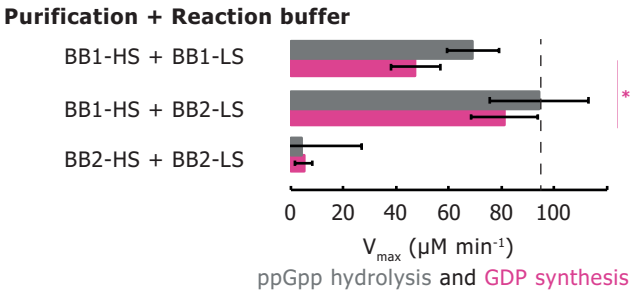

Figure 5.9: ppGpp hydrolysis rates of SpoT in the different buffers. V_{max} was calculated based on the initial linear part of the curves of figure 5.8. *P < 0.05 of a two-tailed t-test.

Activity of SpoT with holo-ACP and apo-ACP

To determine whether interaction with ACP affects the activity of SpoT, ACP was purified into holo-ACP and apo-ACP. These ACP species were added to SpoT-beads and incubated for 90 min to allow a potential interaction between ACP and SpoT to occur. Although apo-ACP does not accumulate in the cell, its interaction with SpoT was also assessed as a comparison to the other ACPs. If an interaction between SpoT and ACP is specific for certain acyl chains, it was assumed that apo-ACP would interact less with SpoT. As shown in **Figure 5.10**, holo-ACP addition had a dramatic effect on ppGpp hydrolysis by SpoT. Addition of 2 mg mL^{-1} holo-ACP completely abolished SpoT activity (**Figure 5.11**). Apo-ACP also inhibited ppGpp hydrolysis, although not as effectively as holo-ACP. As a comparison, the intracellular concentration of ACP is 0.73 mg mL^{-1} [3]. During steady state growth in glucose the fraction of ACP that is holo-ACP is about 0.35, or 0.25 mg mL^{-1}.

The other known enzymatic activity of SpoT, (p)ppGpp synthesis, has never been reported *in vitro* [16]. Possibly some interaction with other proteins or a cellular signal is necessary to convert SpoT from hydrolysis to synthesis state. Nevertheless, it was verified if the assay used for hydrolysis could allow ppGpp synthesis (**Figure 5.10**). SpoT on its own did not synthesize ppGpp from ATP and GDP, which is no surprise given that its default mode is hydrolysis. Holo-ACP could however potentially change the activity towards synthesis, as it inhibits hydrolysis. Therefore, SpoT's activity after incubation with holo-ACP was determined in presence of ATP and GTP (**Figure 5.12**). The decrease in ATP could be due to the presence of kinases that non-specifically bound to the beads, as there was a mild increase in ADP (data not shown). However, no synthesis of pppGpp (or ppGpp) was detected.

[3] According to Rock and Cronan [19] the number of ACP molecules per cell is 60 000. Dividing by Avogadro's constant this results in $9.96*10^{-20}$ mol per cell. Given that the molecular weight of ACP is 9 kDa and that the volume of *E. coli* during exponential growth on glucose is 1.22 fL [41], that results in an ACP concentration of 82 μM or 0.73 mg mL^{-1}.

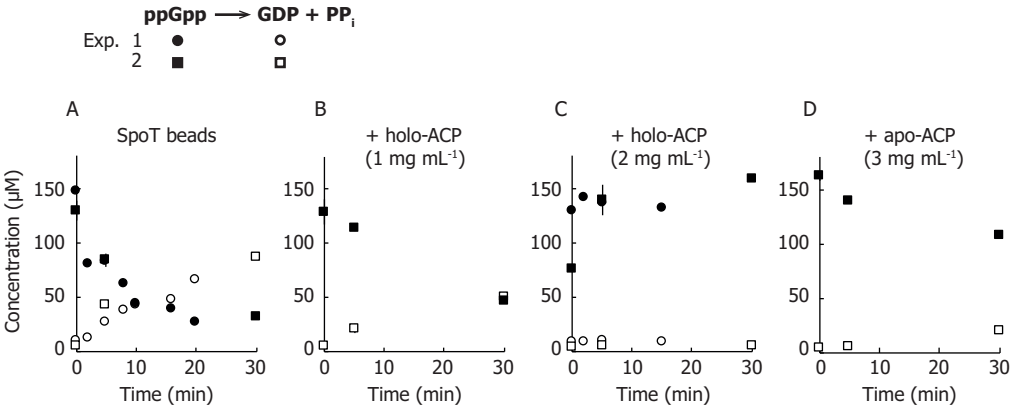

Figure 5.10: *In vitro* ppGpp hydrolysis of SpoT is inhibited by holo-ACP or apo-ACP. SpoT-beads were incubated with 0 (A), 1 (B) and 2 mg mL^{-1} (C) holo-ACP or 3 mg mL^{-1} apo-ACP and tested for ppGpp hydrolysis. The two experiments were performed with different batches of both SpoT and purified ACP. For exp. 1 ACP was dissolved in BB1-LS with 4 mM DTT, and for exp. 2 BB1-LS with 2 mM DTT.

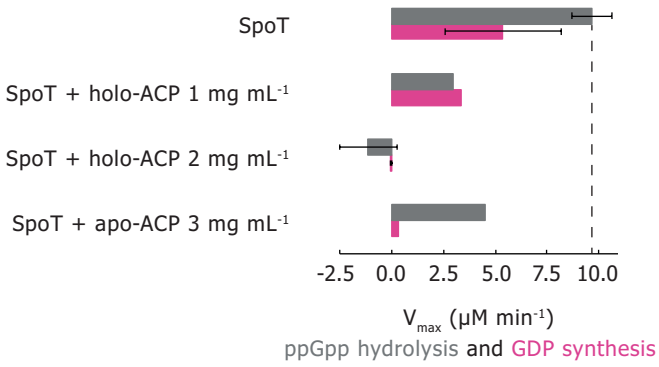

Figure 5.11: ppGpp hydrolysis rates of SpoT beads, with and without ACP. The initial linear part of the curves of Figure 5.10 were used to calculate V_{max}.

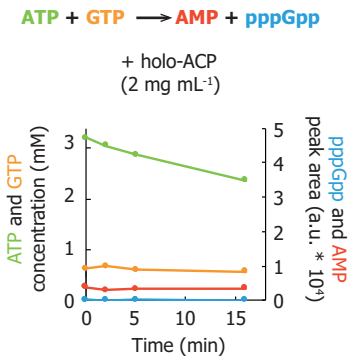

Figure 5.12: Holo-ACP does not induce pppGpp synthesis by SpoT *in vitro*. The reaction contained SpoT beads with 2 mg mL^{-1} holo-ACP, 3 mM ATP and 0.8 mM GTP.

ppGpp hydrolysis and synthesis activity of SpoT mutants

Having established *in vitro* degradation of ppGpp, we also aimed at studying the synthesis activity of SpoT. Many point mutants have been discovered which cause different phenotypes and hence give clues about when and how SpoT is active. In **Table 5.2**, a brief overview is given of some of these. We hypothesized that mutants with impaired hydrolysis activity might be more likely to exhibit synthesis activity, or that it would be easier to detect synthesis in these mutants. Therefore, each of these mutants was overexpressed, extracted with a pull-down assay and tested for ppGpp hydrolysis activity.

Not all mutants behaved exactly as reported in literature. As expected, for both SpoT H72A and T78I no GDP was detectable after 15 min, suggesting they no longer possess the capacity to hydrolyze ppGpp (**Figure 5.13A,B**). Although SpoT R140C is also known to be hydrolysis inactive, SpoT R140C exhibited decreased but not absent hydrolysis activity (25 µM GDP after 15 min, significantly above the LOD) (**Figure 5.13C**). For SpoT H255Y it was assumed it would no longer hydrolyze or

Table 5.2: SpoT mutants and their activity based on literature and the pull-down assay.

SpoT mutant	Reported activity	Result pull-down assay
H72A	No hydrolysis [42]	Confirmed
T78I (SpoT202)	No hydrolysis [43, 44]	Confirmed
R140C (SpoT203)	No hydrolysis [43, 44]	Confirmed (or low rate)
H255Y	No hydrolysis or more synthesis [44]	Hydrolysis
A404E	No interaction ACP [22]	No hydrolysis
S587N	No interaction ACP [22]	Confirmed

have increased ppGpp synthesis activity. It still hydrolyzed ppGpp (**Figure 5.13D**), which implies that it might show increased ppGpp synthesis activity. Therefore this and mutants T78I, R140C and A404E were also tested for ppGpp synthesis activity by adding 3.5 mM ATP and 0.5 mM GTP to active beads, however for none an increase in pppGpp was observed (data not shown). In theory it might be possible that some point mutants are not expressed well and therefore show no activity. Currently a proteomics method to quantify the amount of (mutant) SpoT on the beads is being developed (**Figure 5.14** for preliminary data).

The paper that first reported interaction between ACP and SpoT also identified residues within SpoT that might be responsible for the interaction [22]. In order to confirm that the observed reduced hydrolysis activity upon incubation with ACP was definitely due to ACP, these mutants were pulled down and hydrolysis activity was tested with and without holo-ACP. SpoT A404E shows impaired hydrolysis activity as it only synthesized 16 µM GDP after 15 min, which might explain why Battesti and Bouveret [22] identified it as not binding ACP (**Figure 5.13E**). SpoT S587N however still hydrolyzes ppGpp, even in the presence of 15 mg mL^{-1} apo-ACP and holo-ACP (before UPLC separation, about 20 % holo-ACP) (**Figure 5.13F-G**). Wild-type SpoT no longer hydrolyzes ppGpp when incubated with holo-ACP or apo-ACP. This is consistent with SpoT S587N no longer interacting with ACP and holo-ACP possibly inhibiting SpoT hydrolysis activity.

Activity of SpoT with ObgE

As ObgE has also been reported to be a binding partner of SpoT, ObgE was over-expressed, and the lysate containing elevated levels of ObgE added to SpoT beads. After overnight incubation, beads contained elevated levels of a close to 50 kDa protein (**Figure 5.15A**), presumably ObgE. A few other low kDa proteins also were pulled down, which are possible binding partners of ObgE. The presence of ObgE however did not affect hydrolysis of ppGpp (**Figure 5.15B**).

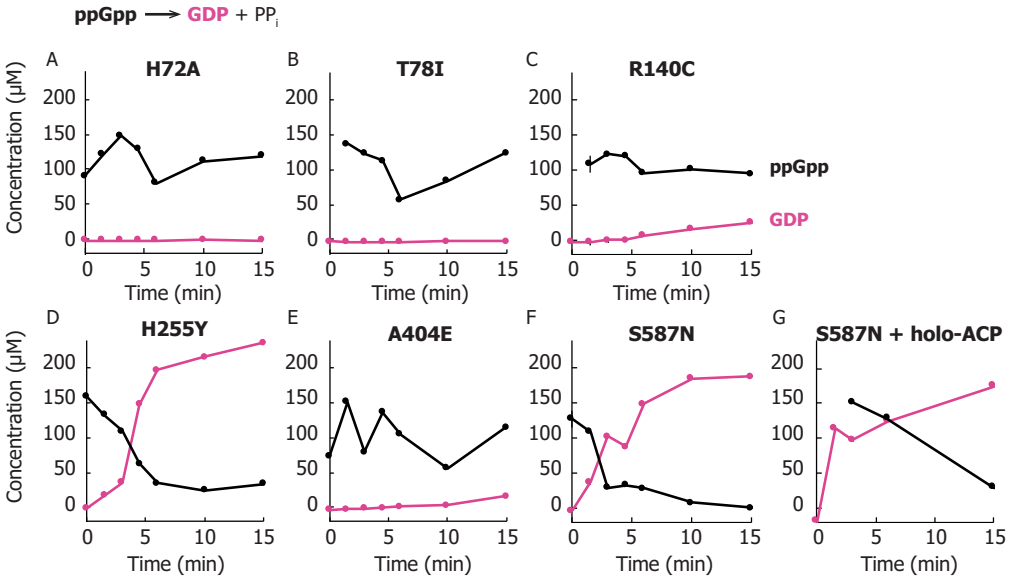

Figure 5.13: *In vitro* activity of SpoT mutants used in other studies. A-F: ppGpp hydrolysis curves of pulled down SpoT mutants H72A (A), T78I (B), R140C (C), H255Y (D), A404E (E) and S587N (F). S587N was also tested for ppGpp hydrolysis activity in the presence of holo-ACP (G). The concentration of DTT was 4 mM.

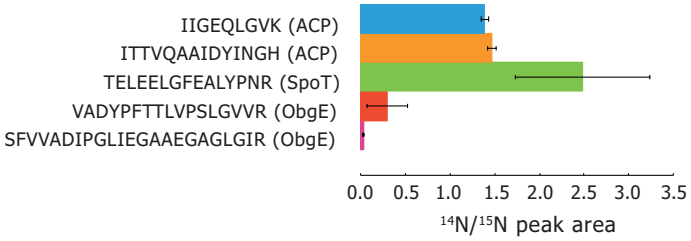

Figure 5.14: Detection of pulled down SpoT, ACP and ObgE with proteomics allows relative quantification of these proteins in different bead samples. SpoT bead samples (^{14}N) were mixed with equal amounts of ^{15}N labeled lysate of *E. coli* overexpressing ObgE as an internal standard to correct for technical variation. These were digested with Trypsin and analyzed with LC-MS. The 5 peptides shown represent those with the highest signal for the proteins of interest. The ratio of ^{14}N to ^{15}N represents the variety in the amount of protein in different bead samples. Here, 3 bead samples were analyzed, which showed ACP is present about equally in the different samples, there is quite some bead-to-bead variation in SpoT, and ObgE is not present above background noise.

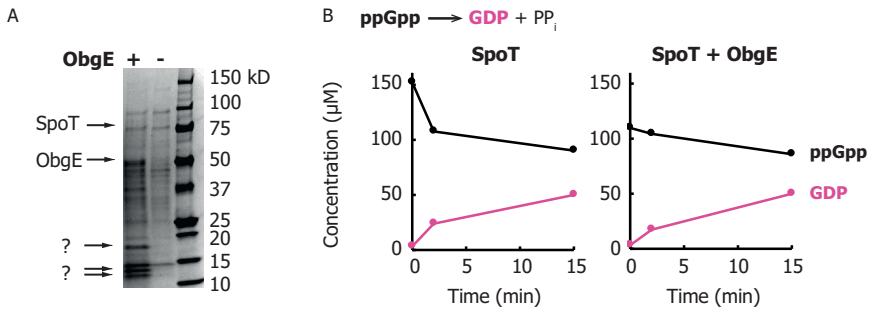

Figure 5.15: *In vitro* hydrolysis activity of SpoT is unaffected by ObgE. A) SDS-PAGE of SpoT beads incubated with lysate of ObgE overexpressing cells (+ObgE) or binding buffer (-ObgE). B) The same SpoT beads were tested for ppGpp hydrolysis.

5.4. Discussion

SpoT is a mysterious enzyme known to be responsible for the correlation between basal ppGpp levels and growth rate in *E. coli*. Despite decades of research, very little is known about what steers its activity towards hydrolysis or synthesis of ppGpp. The aim of this chapter was to uncover more about the potential interactions between SpoT and other proteins, given that in literature several are mentioned. Although the interaction between SpoT and ACP is most reported, only once the nature and function of the interaction have been investigated in more depth [22]. This led to the hypothesis that SpoT might sense the flux through the fatty acid synthesis pathway by interacting with the various ACP species differently. More specifically, ACP would bind to SpoT C-terminally and lock it in hydrolysis mode. When the cell would starve for carbon or fatty acids, the proportions within the pool of ACP species would change, provoking a transition from hydrolysis to synthesis mode.

Here we developed an *in vitro* assay to analyze the catalytic activity of SpoT, and how this activity changes in response to other proteins.

5.4.1. Is the ACP-SpoT interaction an *in vitro* artefact?

As previously observed, ACP was pulled down together with SpoT given that the proteomics method could detect ACP on SpoT-beads. It is possible however that the interaction is established via a disulphide bridge between the terminal sulfhydryl group of the phosphopantetheine arm of ACP and one of the eight cysteine residues of SpoT, that could form when the cell lyses and the intracellular reducing environment is exposed. Hence the question: is the ACP-SpoT interaction an *in vitro* artefact?

To prevent the formation of disulphide bridges, SpoT hydrolysis assays were performed in the presence of the reducing agent DTT. The concentration of DTT (2 or 4 mM) was equal to or higher than concentrations used in purifications of ACP (2 mM [45], 1 mM [46]), or in assays used to demonstrate an interaction based on disulphide bridges [20]. Specifically,2 mM DTT was sufficient to abolish the interaction between ACP and IscS, indicating they interact via a disulphide bridge [20]. In our experiment, at 2 mM DTT the majority of holo-ACP was not in dimerized as shown with urea-PAGE. In addition, even in the presence of 4 mM DTT, we observed consistent inhibition of SpoT hydrolysis by holo-ACP. Therefore, it is unlikely that the SpoT-ACP interaction is an artefact caused by disulphide bridge formation.

5.4.2. Is the ACP-SpoT interaction relevant *in vivo*?

Still, can we be certain that a direct interaction between (holo-)ACP and SpoT caused the decreased hydrolysis activity? There are several observations that support this. First, addition of ACP inhibited *in vitro* hydrolysis of ppGpp by SpoT in a concentration dependent manner. Interestingly both holo-ACP and apo-ACP could inhibit hydrolysis, although holo-ACP about twice as effectively. In bacterial two hybrid assays Battesti and Bouveret [22] observed that ACP without the phosphopantetheine arm (mutation S36T) interacted about 8-fold less with SpoT compared to wild-type ACP, similar to our data. However, apo-ACP is not detectable in the cell unless CoA synthesis is inhibited in the presence of amino acids, a situation that is likely not physiologically relevant [47]. Therefore, the inhibition of hydrolysis by apo-ACP might not be relevant *in vivo*.

Second, a SpoT mutant (S587N) presumed to not bind ACP [22], showed a ppGpp hydrolysis activity unaffected by the presence of ACP. The hydrolysis activity of SpoT S587N without ACP was however similar to that of wild-type SpoT. This indicates that either mutation S587N locks SpoT in hydrolysis mode, or that ACP effectively no longer can inhibit SpoT. Given that S587N is still able to synthesize ppGpp *in vivo* [22], it appears SpoT S587N is not 'stuck' in hydrolysis mode. This suggests that ACP indeed inhibits hydrolysis by directly interacting with SpoT. Unfortunately, the other reported mutation to abolish an interaction between ACP and SpoT (A404E) was barely hydrolyzing ppGpp in our assay. The original study discovering the mutation reported lower *in vivo* synthesis activity of strains carrying SpoT A404E [48]. Apparently, this mutation affects both synthesis and hydrolysis activities, which is also in line with the complementation assays performed by [22].

The question still remains whether the holo-ACP interaction with SpoT has high enough affinity to occur *in vivo*. A holo-ACP concentration of 1 mg mL^{-1} inhibited SpoT by 70 %, yet during steady-state growth the holo-ACP concentration is estimated at 0.26 mg mL^{-1}. During glucose-lactose diauxic shift, however, this rises to 0.48 mg mL^{-1} which could significantly reduce SpoT hydrolysis of ppGpp. Admittedly, in neither conditions holo-ACP could completely shut off ppGpp hydrolysis. Future experiments, started in this chapter, should decipher the effect of other ACP

species on SpoT. Potentially, the combined action of several or all ACP species has more effect.

5.4.3. SpoT mutants

Although the activity assay so far could only analyze hydrolysis activity by SpoT, it could confirm and also refute the activity of several SpoT mutants used in *in vivo* experiments. For example, SpoT T88I and R140C, known as *SpoT202* and *SpoT203*, have reduced hydrolysis activities, consistent with the higher basal ppGpp levels *in vivo* [43]. SpoT A404E was presumed to not interact with ACP, and based on complementation assays still able to hydrolyze ppGpp as the mutation S587N [22]. However, the hydrolysis activity of A404E was significantly less, similar to mutation R140C (*SpoT203*). It is possible therefore that not the abolished interaction with ACP, but simply the damaged activity of SpoT is responsible for the altered growth observed in complementation assays [22].

5.4.4. SpoT-ObgE interaction

Although our results confirm ObgE is pulled down with SpoT and they therefore likely interact, preliminary data did not show an effect of ObgE on the hydrolysis activity of SpoT. Jiang *et al.* [32] yet did not observe an overlap in the presence of ObgE and SpoT in ribosomal fractions, implying that their interactions is weak or not. Also the screen of Butland *et al.* [21] did not detect ObgE, neither did Sato *et al.* [27]. It should be noted though that none of these pull-downs detected (or mentioned) YbeY, YtfK and Rsd. Pull-downs appear to be on one hand sensitive to false positives (as whole complexes might imply direct interactions that do not occur *in vivo*) and the other hand prone to false negatives, as weak interactions might not be detected, or as some interactions might be affected depending on the specific properties of the purification buffer.

5.4.5. Towards a model for regulation of SpoT activity

The relatively weak interaction between holo-ACP and SpoT is coherent with the current view that SpoT by default constantly hydrolyzes ppGpp. As soon as the pool changes towards increased fractions of long-chain fatty acids, holo-ACP would be replaced, allowing SpoT to hydrolyze more ppGpp. A complicating factor is that ACP potentially competes with other regulatory proteins, such as Rsd, which was recently discovered to also bind SpoT at the TGS domain but activate ppGpp hydrolysis [17].

Whether an interaction with (holo-)ACP alone could be overcome by Rsd depends on its affinity for SpoT and its cellular concentration. Given that an approximately two-fold increase in hydrolysis activity was obtained in the presence of 0.52 mg mL^{-1}

Rsd [17], the interaction with Rsd is not orders of magnitude higher than the one with holo-ACP. The intracellular concentration of Rsd is 3000 molecules/cell during exponential growth, and 6000 during stationary phase, of which parts are interacting with RpoD and HPr [49]. ACP concentrations are at the very least 10-fold higher. Bearing all this in mind, it is questionable whether the Rsd-SpoT interaction is relevant *in vivo*. Moreover, the little *in vivo* evidence to demonstrate the effect of Rsd on SpoT consists of ppGpp measurements normalized to GTP, which was not constant (supplementary material of [17]). The absolute ppGpp concentrations might not be significantly affected by Rsd.

At first sight the relative decrease in holo-ACP and increase in ppGpp levels after cerulenin addition are not in line with the result that holo-ACP inhibits hydrolysis by SpoT. The decrease in holo-ACP would allow more hydrolysis to occur and hence ppGpp levels to go down. However, this could be explained if the influence of holo-ACP is overcome by another allosteric regulator, such as YtfK. YtfK binds at another site on SpoT and is known to be responsible for the increase in ppGpp during fatty acid and phosphate starvation [50].

When the current data about ACP, Rsd and YtfK are pieced together, it becomes clear that although their individual interactions with SpoT sometimes have counterintuitive outcomes, their combined interactions do not contradict the response of SpoT to certain stresses (**Table 5.3**). Based on the different domains of SpoT interacting with ACP, Rsd and YtfK, it is possible YtfK binds independently, and that the activities of ACP and Rsd balance each other out. For all these binding partners mutations are known that modify the interaction with SpoT [17, 22, 50]. It would be interesting to combine these mutations *in vivo* during the conditions in table 5.3 to verify if some interactions dominate over or compete with others. Measuring proteins levels of (mutant) Rsd, ACP species and YtfK combined with the actual ppGpp levels should reveal more precisely which interaction(s) contribute to synthesis or hydrolysis mode and under which conditions.

It still has to be investigated what the effect is of other ACPs, but given that YtfK also affects basal level [50], it is unlikely that merely the ratios of ACPs – although there are correlations with the growth rate – are the determinants of SpoT activity during steady state growth. Considering that even more proteins such as YbeY might be involved, it appears that the activity of SpoT is determined by a plethora of interactions that together regulate SpoT, according to the plethora of conditions the cell can be in.

5.5. Acknowledgements

I would like to thank Niels van den Broek for help with developing the proteomics method. I would like to thank Niels van de Broek and Marek Noga for support with the ACP purification.

Table 5.3: Model of SpoT activity based on current knowledge of interaction with proteins Rsd, YtfK and holo-ACP. PEP: phosphoenolpyruvate, Pyr: pyruvate, HPr-P: phosphorylated HPr. Holo-ACP fractions were obtained from Noga *et al.* [36] and Mattia Cerri [37] (Figure 5.3). In the illustrations SpoT and the different domains are represented as in Figure 1.3. The domain names depictured in white are active. *The PEP/pyruvate ratio determines the phosphorylation state of HPr, which affects Rsd binding to SpoT. In fatty acid starvation, the concentration of pyruvate decreases [51], hence the PEP/pyruvate ratio is presumed to increase. **Under phosphate starvation the flux to PEP and pyruvate decreases, or the flux to pyruvate increases, depending on the growth rate [52], therefore it is assumed here that the PEP/pyruvate ratio decreases.

***In vivo* condition**	**Rsd interaction**	**YtfK interaction**	**holo-ACP fraction**	**(Net) SpoT activity**	**Illustration**
Fatty acid starvation/ cerulenin	PEP/Pyr ↑*, HPr-P releases Rsd, which promotes hydrolysis.	promotes ppGpp synthesis.	is only 0.05. SpoT not inhibited.	ppGpp synthesis. YtfK interaction dominates.	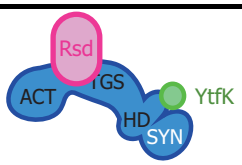
Phosphate starvation	PEP/Pyr ↓**, HPr binds Rsd.	promotes ppGpp synthesis.	?	ppGpp synthesis. YtfK interaction dominates.	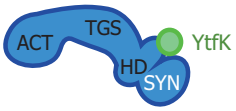
Glucose-lactose diauxic shift	HPr-P releases Rsd. Rsd promotes hydrolysis.	?	increases up to 0.65. holo-ACP inhibits hydrolysis.	ppGpp synthesis. Holo-ACP outcompetes Rsd.	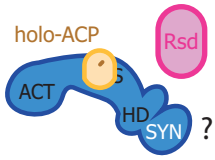
Basal growth in glucose medium	HPr binds Rsd.	promotes ppGpp synthesis.	is 0.35. holo-ACP could mildly inhibit hydrolysis.	basal ppGpp synthesis. Synthesis/ hydrolysis is balanced by YtfK and holo-ACP.	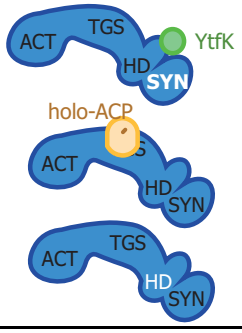

5.6. Supplementary information

Table S5.1: List of strains and plasmids used in this chapter.

E. coli strain	Description	Source
DH5α	Used for cloning and plasmid amplification	Invitrogen
BL21DE3	Used for ObgE and ACP purification	Invitrogen
MG1655	Used for purification of SpoT and SpoT mutants	DSMZ 18039
Plasmid	**Description**	**Source**
pET28a	Empty expression vector with IPTG-inducible T7 promoter, *KanR*	Novagen
pSpoT	SpoT C-terminally fused to calmodulin binding protein expressed from Tet promoter. SC101**, *KanR*, *TetR*	Mattia Cerri
pSpoT-T78I	pSpoT with SpoT mutated as T78I	This work
pSpoT-R140C	pSpoT with SpoT mutated as R140C	This work
pSpoT-D293A	pSpoT with SpoT mutated as D293A	This work
pSpoT-H255Y	pSpoT with SpoT mutated as H255Y	This work
pSpoT-S587N	pSpoT with SpoT mutated as S587N	This work
pSpoT-A404E	pSpoT with SpoT mutated as A404E	This work
pSpoT-H72A	pSpoT with SpoT mutated as H72A	This work
pACP	pET28a-ACP (*KanR*)	Marek Noga
pObgE	pET28a-ObgE (*KanR*)	This work

Table S5.2: List of primers and oligonucleotides used in this chapter.

Primer	Sequence
MC29032016SpotF	TTGTATCTGTTTGAAAGCCTG
MC29032016SpotR	TTACTCGAGTTAGGATCCTTAATTTCGGTTTCGGG
MC31032016CBPSPOTsy	AAAAGATCTCCATGGAACTAAAGAGAAGATGGAAA AAGAATTTCATAGCCGTCTCAGCAGCCAACCGCTT TAAGAAAATCTCATCCTCCGGGGCACTTGTCGAGT CGACTCTAGAATTCTTGTATCTGTTTGAAAGCCTG AATCAACTGATTCAAACCTACCTGCCGGAAGACCA AATCAAGCGTCTGCGGCAGGCGTATCTCGTTGCAC GTGATGCTCACGAGGGGCAAACACGTTCAAGCGGT GAACCCTATATCACGCACCCGGTAGCGGTTGCCTG CATTCTGGCCGAGATGAAACTCGACTATGAAACGC TGATGGCGGCGCTGCTGCATGACGTGATTGAAGAT ACTCCCGCCACCTACCAGGATATGGAACAGCTTTT TGGTAAAAGCGTCGCCGAGCTGGTAGAGGGGGTGT CGAAACTTGATAAACTCAAGTTCCGCGATAAGAAAG AGGCGCAGGCCGAAAACTTTCGCAAGATGATTATG
MC29032016CBPSynF	AAAAGATCTCCATGGAACTAAAG
MC29032016CBPSynR	CATAATCATCTTGCGAAGTT
NI239-SpoT-T78I-for	GATTGAAGATATTCCCGCCACCTACCAGGATATGG
NI240-SpoT-T78I-rev	GGAATATCTTCAATCACGTCATGCAGCAGC
NI241-SpoT-R140C-for	CTTGCCGACTGTACCCACAACATGCGCACGC
NI242-SpoT-R140C-rev	GGGTACAGTCGGCAAGTTTGATGAGGATGACGC
NI243-SpoT-D293A-for	GTGAAAGCCTATATCGCCATTCCAAAAGCGAACGGC
NI244-SpoT-D293A-rev	GCGATATAGCCTTTCACGCGGCCCGGACG
NI245-SpoT-H255Y-for	GCGTTTTTACTCGATCATGGACATCTACGCTTTCCG
NI246-SpoT-H255Y-rev	CATGATCGAATGAAAACGCTGCTCTTTGAGCACC
NI247-SpoT-A404E-for	CGGTGAAACGCCCGTCGACTTCGCTTATGC
NI248-SpoT-A404E-rev	CGGGCGTTTCACCGGCAGGCAGCTCGAC
NI249-SpoT-S587-for	GTCAACCCCGGTAAAGGTCTGGTGATCCAC
NI250-SpoT-S587N-rev	CTTTACCGGGGTTGACGTGGGCGATAATCG
NI251-SpoT-H72A-for	GCGGCGCTGCTGGCTGACGTGATTGAAG
NI252-SpoT-H72A-rev	GCCAGCAGCGCCGCCATCAGCGTTTCATAGTCG
NI275-ObgE-for	GCGGATCCTTAACGCTTGTAAATGAACTCAAC
NI276-ObgE-rev	GCCATATGATGAAGTTTGTTGATGAAGCATC
MN01	GCGCTCCATATGATGAGCACTATCGAAGAACGCGTT AAGAAAATTATCGGCG
MN02	GCGCTCGGATCCTTACGCCTGGTGGCCGTTGATGTAAT CAATG

Table S5.3: List of transitions used in the LC-MS method for the analysis of SpoT, ObgE and ACP. RT: retention time (min).

Protein	Peptide	14N or 15N	precursor ion	product ion	RT*	Collision energy
SpoT	TELEELGFEALYPNR	14N	890.9	386.2	9.7	28.6
			890.9	549.3		
		15N	900.4	393.2		
			900.4	557.3		
ObgE	VADYYPFTTLVPSLGVVR	14N	917.5	727.4	10.9	29.4
			917.5	826.5		
			917.5	1385.8		
		15N	929.0	740.4		
			929.0	840.5		
			929.0	1404.8		
	SFVVADIPGLIEGAAEGAGLGIR	14N	738.1	643.4	11.9	21.8
			738.1	515.3		
		15N	747.7	653.4		
			747.7	523.3		
ACP	IIGEQLGVK	14N	478.8	730.4	4.8	15.8
			478.8	227.1		
		15N	484.3	739.4		
			484.3	229.1		
	ITTVQAAIDYINGHQA	14N	857.9	917.4	9.1	27.6
			857.9	1101.5		
		15N	868.4	929.4		
			868.4	1115.4		

references

[1] K. Potrykus, H. Murphy, N. Philippe, and M. Cashel. "ppGpp is the major source of growth rate control in *E. coli*". In: *Environmental Microbiology* 13.3 (2011), pp. 563–575.

[2] M. Seyfzadeh, J. Keener, and M. Nomura. "SpoT-dependent accumulation of guanosine tetraphosphate in response to fatty acid starvation in *Escherichia coli*". In: *Proceedings of the National Academy of Sciences* 90.23 (1993), pp. 11004–11008.

[3] R. B. Harshman and H. Yamazaki. "Formation of ppGpp in a relaxed and stringent strain of *Escherichia coli* during diauxie lag". In: *Biochemistry* 10.21 (1971), pp. 3980–3982.

[4] R. Lazzarini, M. Cashel, and J. Gallant. "On the Regulation of Guanosine Tetraphosphate Levels in Stringent and Relaxed Strains of *Escherichia coli*". In: *Journal of Biological Chemistry* 246.14 (1971), pp. 4381–4385.

[5] R. M. Winslow. "A consequence of the *rel* gene during a glucose to lactate downshift in *Escherichia coli*. The rates of ribonucleic acid synthesis." In: *The Journal of Biological Chemistry* 246.15 (1971), pp. 4872–4877.

[6] K. D. Murray and H. Bremer. "Control of *spoT*-dependent ppGpp synthesis and degradation in *Escherichia coli*". In: *Journal of Molecular Biology* 259 (1996), pp. 41–57.

[7] D. Vinella, C. Albrecht, M. Cashel, and R. D'Ari. "Iron limitation induces SpoT-dependent accumulation of ppGpp in *Escherichia coli*". In: *Molecular Microbiology* 56.4 (2005), pp. 958–970.

[8] J. Friesen, N. Fiil, and K. von Meyenburg. "Synthesis and turnover of basal level guanosine tetraphosphate in *Escherichia coli*". In: *Journal of Biological Chemistry* 250.1 (1975), pp. 304–309.

[9] Y. Sokawa, J. Sokawa, and Y. Kaziro. "Regulation of stable RNA synthesis and ppGpp levels in growing cells of *Escherichia coli*". In: *Cell* 5.1 (1975), pp. 69–74.

[10] J. Ryals, R. Little, and H. Bremer. "Control of ribosomal-RNA and transfer-RNA syntheses in *Escherichia coli* by guanosine tetraphosphate". In: *Journal of Bacteriology* 151.3 (1982), pp. 1261–1268.

[11] E. Heinemeyer and D. Richter. "*In vitro* degradation of guanosine tetraphosphate (ppGpp) by an enzyme associated with the ribosomal fraction from *Escherichia coli*". In: *FEBS letters* 84.2 (1977), pp. 357–361.

[12] J. Sy. "*In vitro* degradation of guanosine 5'-diphosphate, 3'-diphosphate". In: *Proceedings of the National Academy of Sciences* 74.12 (1977), pp. 5529–5533.

[13] G. An, G. Justesen, R. F. Watsen, and J. D. Friesen. "Cloning the *spoT* gene of *Escherichia coli*: identification of the *spoT* gene product". In: *Journal of Bacteriology* 137.3 (1979), pp. 1100–1110.

[14] U. Mechold, M. Cashel, K. Steiner, D. Gentry, and H. Malke. "Functional analysis of a *relA/spoT* gene homolog from *Streptococcus equisimilis*". In: *Journal of Bacteriology* 178.5 (1996), pp. 1401–1411.

[15] D. R. Gentry and M. Cashel. "Cellular localization of the *Escherichia coli* SpoT protein". In: *Journal of Bacteriology* 177.13 (1995), pp. 3890–3893.

[16] D. R. Gentry and M. Cashel. "Mutational analysis of the *Escherichia coli spoT* gene identifies distinct but overlapping regions involved in ppGpp synthesis and degradation". In: *Molecular Microbiology* 19.6 (1996), pp. 1373–1384.

[17] J.-W. Lee, Y.-H. Park, and Y.-J. Seok. "Rsd balances (p)ppGpp level by stimulating the hydrolase activity of SpoT during carbon source downshift in *Escherichia coli*". In: *Proceedings of the National Academy of Sciences* 115.29 (2018), pp. 6845–6854.

[18] D. I. Chan and H. J. Vogel. "Current understanding of fatty acid biosynthesis and the acyl carrier protein". In: *The Biochemical journal* 430.1 (2010), pp. 1–19. doi: 10.1042/BJ20100462.

[19] C. O. Rock and J. E. Cronan. "*Escherichia coli* as a model for the regulation of dissociable (type II) fatty acid biosynthesis". In: *Biochimica et Biophysica Acta (BBA) - Lipids and Lipid Metabolism* 1302.1 (1996), pp. 1–16. doi: 10.1016/0005-2760(96)00056-2.

[20] D. Gully, D. Moinier, L. Loiseau, and E. Bouveret. "New partners of acyl carrier protein detected in *Escherichia coli* by tandem affinity purification". In: *FEBS Letters* 548.1-3 (2003), pp. 90–96. doi: 10.1016/S0014-5793(03)00746-4.

[21] G. Butland, J. M. Peregrin-Alvarez, J. Li, W. Yang, X. Yang, V. Canadien, A. Starostine, D. Richards, B. Beattie, N. Krogan, M. Davey, J. Parkinson, J. Greenblatt, and A. Emili. "Interaction network containing conserved and essential protein complexes in *Escherichia coli*". In: *Nature* 433.7025 (2005), pp. 531–537. doi: 10.1038/nature03239.

[22] A. Battesti and E. Bouveret. "Acyl carrier protein/SpoT interaction, the switch linking SpoT-dependent stress response to fatty acid metabolism". In: *Molecular Microbiology* 62.4 (2006), pp. 1048–1063. doi: 10.1111/j.1365-2958.2006.05442.x.

[23] S. Angelini, L. My, and E. Bouveret. "Disrupting the acyl carrier protein/SpoT interaction *in vivo*: Identification of ACP residues involved in the interaction and consequence on growth". In: *PLoS ONE* 7.4 (2012). doi: 10.1371/journal.pone.0036111.

[24] R. Dutkiewicz, M. Slominska, G. Wegrzyn, and A. Czyz. "Overexpression of the cgtA (yhbZ, obgE) gene, coding for an essential GTP-binding protein, impairs the regulation of chromosomal functions in *Escherichia coli*". In: *Current Microbiology* 45.6 (2002), pp. 440–445.

[25] J. J. Foti, J. Schienda, V. A. Sutera, and S. T. Lovett. "A bacterial G protein-mediated response to replication arrest". In: *Molecular Cell* 17.4 (2005), pp. 549–560.

[26] G. Kobayashi, S. Moriya, and C. Wada. "Deficiency of essential GTP-binding protein ObgE in *Escherichia coli* inhibits chromosome partition". In: *Molecular Microbiology* 41.5 (2001), pp. 1037–1051.

[27] A. Sato, G. Kobayashi, H. Hayashi, H. Yoshida, A. Wada, M. Maeda, S. Hiraga, K. Takeyasu, and C. Wada. "The GTP binding protein Obg homolog ObgE is involved in ribosome maturation". In: *Genes to Cells* 10.5 (2005), pp. 393–408.

[28] N. S. Persky, D. J. Ferullo, D. L. Cooper, H. R. Moore, and S. T. Lovett. "The ObgE/CgtA GTPase influences the stringent response to amino acid starvation in *Escherichia coli*". In: *Molecular Microbiology* 73.2 (2009), pp. 253–266.

[29] L. Dewachter, N. Verstraeten, M. Jennes, T. Verbeelen, J. Biboy, D. Monteyne, D. Perez-Morga, K. J. Verstrepen, W. Vollmer, M. Fauvart, and J. Michiels. "A mutant isoform of ObgE causes cell death by interfering with cell division". In: *Frontiers in Microbiology* 8 (2017), pp. 1–12.

[30] R. Maouche, H. L. Burgos, L. My, J. P. Viala, R. L. Gourse, and E. Bouveret. "Coexpression of *Escherichia coli* obgE, encoding the evolutionarily conserved obg GTPase, with ribosomal proteins L21 and L27". In: *Journal of Bacteriology* 198.13 (2016), pp. 1857–1867.

[31] P. Wout, K. Pu, S. M. Sullivan, V. Reese, S. Zhou, B. Lin, and J. R. Maddock. "The *Escherichia coli* GTPase CgtAE cofractionates with the 50S ribosomal subunit and interacts with SpoT, a ppGpp synthetase/hydrolase". In: *Journal of Bacteriology* 186.16 (2004), pp. 5249–5257.

[32] M. Jiang, S. M. Sullivan, P. K. Wout, and J. R. Maddock. "G-protein control of the ribosome-associated stress response protein SpoT". In: *Journal of Bacteriology* 189.17 (2007), pp. 6140–6147.

[33] M. Jiang, K. Datta, A. Walker, J. Strahler, P. Bagamasbad, P. C. Andrews, and J. R. Maddock. "The *Escherichia coli* GTPase CgtAE is involved in late steps of large ribosome assembly". In: *Journal of Bacteriology* 188.19 (2006), pp. 6757–6770.

[34] K. Potrykus and M. Cashel. "(p)ppGpp: Still Magical?" In: *Annual Review of Microbiology* 62.1 (2008), pp. 35–51.

[35] A. Pokhilko. "Monitoring of nutrient limitation in growing *E . coli* : a mathematical model of a ppGpp-based biosensor". In: (2017), pp. 1–10.

[36] M. J. Noga, M. Cerri, N. Imholz, P. Tulinski, and G. Bokinsky. "Mass-Spectrometry-Based Quantification of Protein-Bound Fatty Acid Synthesis Intermediates from *Escherichia coli*". In: *Journal of proteome research* 15 (2016), pp. 3617–3623.

[37] M. Cerri. "Growth rate sensing in *Escherichia coli*. The link between fatty acid synthesis and growth regulation." TU Delft, 2016, pp. 1–122.

[38] D. A. Armbruster and T. Pry. "Limit of blank, limit of detection and limit of quantitation". In: *The Clinical Biochemist Reviews* 29 (2008), S49–S52.

[39] B. Feng, C. S. Mandava, Q. Guo, J. Wang, W. Cao, N. Li, Y. Zhang, Y. Zhang, Z. Wang, J. Wu, S. Sanyal, J. Lei, and N. Gao. "Structural and Functional Insights into the Mode of Action of a Universally Conserved Obg GTPase". In: *PLoS Biology* 12.5 (2014), pp. 1–14. doi: 10.1371/journal.pbio.1001866.

[40] B. A. Bulos and B. Sacktor. "Determination of the concentration of free Ca^{2+} in the presence of magnesium (or manganese) and chelating effectors of the NAD^+-linked isocitrate dehydrogenase". In: *Analytical Biochemistry* 95 (1979), pp. 62–72.

[41] V. Varik, S. R. A. Oliveira, V. Hauryliuk, and T. Tenson. "HPLC-based quantification of bacterial housekeeping nucleotides and alarmone messengers ppGpp and pppGpp". In: *Scientific Reports* 7.1 (2017), pp. 1–12. doi: 10.1038/s41598-017-10988-6.

[42] D. Sun, G. Lee, J. H. Lee, H.-Y. Kim, H.-W. Rhee, S.-Y. Park, K.-J. Kim, Y. Kim, B. Y. Kim, J.-I. Hong, C. Park, H. E. Choy, J. H. Kim, Y. H. Jeon, and J. Chung. "A metazoan ortholog of SpoT hydrolyzes ppGpp and functions in starvation responses." In: *Nature structural & molecular biology* 17.10 (2010), pp. 1188–94.

[43] E. Sarubbi, K. E. Rudd, and M. Cashel. "Basal ppGpp level adjustment shown by new SpoT mutants affect steady state growth rates and *rrnA* ribosomal promoter regulation in *Escherichia coli*". In: *MGG Molecular & General Genetics* 213.2-3 (1988), pp. 214–222. doi: 10.1007/BF00339584.

[44] B. Spira, X. Hu, and T. Ferenci. "Strain variation in ppGpp concentration and RpoS levels in laboratory strains of *Escherichia coli* K-12". In: *Microbiology* 154.9 (2008), pp. 2887–2895.

[45] R. B. Hill, K. R. MacKenzie, J. M. Flanagan, J. E. Cronan, and J. H. Prestegard. "Overexpression, purification, and characterization of *Escherichia coli* acyl carrier protein and two mutant proteins". In: *Protein Expression and Purification* 6 (1995), pp. 394–400.

[46] N. M. Kosa, R. W. Haushalter, A. R. Smith, and M. D. Burkart. "Reversible labeling of native and fusion-protein motifs". In: *Nature Methods* 9.10 (2012), pp. 981–984.

[47] D. H. Keating and Y. A. N. Zhang. "The Apparent Coupling between Synthesis and Posttranslational Modification of *Escherichia coli* Acyl Carrier Protein Is Due to Inhibition of Amino Acid Biosynthesis". In: 178.9 (1996), pp. 2662–2667.

[48] J. Johansson, C. Balsalobre, S. Wang, J. Urbonaviciene, D. Jun Jin, B. Sondén, and B. E. Uhlin. "Nucleoid Proteins Stimulate Stringently Controlled Bacterial Promoters". In: *Cell* 102.4 (2000), pp. 475–485.

[49] S. E. Piper, J. E. Mitchell, D. J. Lee, and S. J. W. Busby. "A global view of *Escherichia coli* Rsd protein and its interactions". In: *Molecular BioSystems* 5 (2009), pp. 1943–1947.

[50] E. Germain, P. Guiraud, D. Byrne, B. Douzi, M. Djendli, and E. Maisonneuve. "YtfK activates the stringent response by triggering the alarmone synthetase SpoT in *Escherichia coli*". In: *Nature Communications* 10.1 (2019), pp. 1–12.

[51] A. K. Sinha, K. S. Winther, M. Roghanian, and K. Gerdes. "Fatty acid starvation activates RelA by depleting lysine precursor pyruvate". In: *Molecular Microbiology* 112.4 (2019), pp. 1339–1349.

[52] M. Dauner, T. Storni, and U. Sauer. "*Bacillus subtilis* Metabolism and Energetics in Carbon-Limited and Excess-Carbon Chemostat Culture". In: *Journal of Bacteriology* 183.24 (2001), pp. 7308–7317.

6

Conclusion and outlook

Bacteria impact our daily lives in numerous ways, and are vital (or detrimental) to our health and planet. This thesis aimed at improving our understanding of what is vital to bacteria: the signaling molecule guanosine tetraphosphate (ppGpp). Despite its early discovery 50 years ago - and a very active research field today, many aspects of its role in microbial physiology have remained obscure.

Put together, chapters 1-4 discuss a long list of literature and experiments showing intracellular enzymes are being regulated (or not) by ppGpp. One important target is RNA polymerase, although many others are metabolic enzymes. Its various targets in the cell have also varying affinities for ppGpp, and are likely co-regulated by other molecules, with concentrations depending on growth rate and environmental conditions. Untangling this complex network of *which molecule* regulates *which enzyme*, under *which condition* and *to which degree*, will only be possible with accurate quantitation of ppGpp, and other key metabolites such as ATP and GTP.

Therefore, the first goal of this thesis was to accurately quantify ppGpp in bacterial cultures in various (changing) environmental conditions. This required low sampling volumes, and hence an increased sensitivity compared to other methods available. The LC-MS method developed in chapter 2 eventually was successful and could be applied to more accurately map the dynamics of ppGpp in a range of conditions, a necessity for a deeper understanding of ppGpp signaling. In particular the absolute (not relative) quantitation of ppGpp is important to compare data among publications and to build on to other researchers' findings.

The improved method provided the means to study the behavior of *basal* ppGpp: low ppGpp concentrations occurring in *E. coli* growing at steady-state in conditions supporting various growth rates (chapter 3). These levels have been claimed to be responsible for determining bacterial growth rate - a very interesting finding also from an engineering or medical point of view. Control over ppGpp might be used as a tool to steer bacterial production away from growth, or to improve the

design of antibiotics. Growth rate control by ppGpp is believed to occur via its regulation of RNA polymerase. However, numerous examples of growth conditions and perturbations exist where basal ppGpp concentrations do not correlate with growth rate, implying ppGpp is not 'all mighty' in controlling growth. Especially RNA polymerase mutants with reduced affinity for ppGpp, show RNA levels surprisingly close to wild-type cells. Does this mean transcriptional regulation by ppGpp is not as important as we thought? Are there additional transcription factors competing with ppGpp?

The aim of chapter 4 was to disentangle the transcriptional regulation from that of other enzymes, in particular involved in protein synthesis. ppGpp indeed appears to directly inhibit protein synthesis besides controlling the synthesis rates of ribosomes, albeit only at high concentrations of ppGpp. As such, the potential direct inhibition of translation or ribosome-associated factors is probably not relevant at basal ppGpp concentrations. The direct inhibition of translation is therefore unlikely to contribute to the steady-state growth rate control by ppGpp.

In order to determine the exact role of ppGpp on regulating transcription, translation and metabolism, these aspects of cellular physiology have to ideally be simultaneously studied, as they also affect one another. Transcription and protein synthesis determine the capacity of a cell to synthesize more molecules (metabolites) at a certain rate, whereas metabolism provides the actual substrates to fuel (and regulate) transcription and protein synthesis. By regulating both, ppGpp could hold all the keys to regulate the cell. Whether it actually does, is a question future research might answer through the use of transcriptomics, proteomics and metabolomics combined with computational models.

On a different note, elucidating the regulation of SpoT still is (one of) the main challenge(s) in the ppGpp field. Given the multitude of potential interactions reported, *in vitro* activity screening will be important to validate these. The developed pull-down assays suggest that ACP might regulate SpoT in a different way from expected based on *in vivo* results. Still, validation is necessary, and hopefully chapter 5 will be a useful starting point for future researchers.

Acknowledgements

I would like to thank my committee members for their time and effort in reading my thesis, their scientific interest, and their very useful feedback. I would like to thank my promoter Marileen for her care for the Bionanoscience department.

Greg, I want to thank you for giving me the opportunity of starting a project in your at the time very young lab. Although the original ingenious idea of a biosensor turned out to be very tricky, soon the seedling of this project grew into a large plant with many ramifications. (That reminds we, we never tried to measure ppGpp in plants...) I am also very grateful for your never subsiding trust in me. You were always willing to invest in every course, conference or material I asked for, a generosity some PhD students can only dream of.

Helena, my wonderful lab mate! The best moments of my PhD were without doubt the ones where we were dancing in the lab (SAP!), chilling in the office (t... out!), eating falafel in the BN corner, tae-boing or whatever crazy things we were up to. Your confidence and resilience deeply inspired me. The last year I missed your vibrant personality. Ferhat, thank you for always offering a hand to help and being friendly and calm. You were (and are) the rock of the lab.

Marek, thank you for your help with the LC-MS. Niels, thank you for all the help with setting up the crazy methods in our lab, and for the fun conversations. You've saved my life more than once. Elena, it was great having an experienced, wise and compassionate postdoc in the lab. Thank you for all your support. Nikki, thank you for the help with MS, happy you joined our group. Flora, especially in the final stage of my PhD I'm grateful you were there. Your warmth and humour brightened my day. Eve, girl, we've had so much fun being silly and sassy in the lab. It was a great joy sharing a lab with you.

I thank my students Ana, Mirte, David and Thomas for all their interest and excitement they brought to their projects. Félicia, Jared, Margot, Otto, Maya, your presence greatly added to the fun-factor of the lab! Thanks for all the laughs. Mattia, it seemed you already were a PhD student while doing your masters' project, and it was hard to see you go! Thanks for all the interesting conversations.

I am truly blessed with the paranymphs I have by my side. Alicia, joder, you're the bread to my butter. Words fail me to describe how happy I am for having met you. Thank you for all the hilarious moments. Please never stop making mess upped movies and recordings (which I never erase f.y.i.). Becca, you're so genuinely caring, empathetic and wise. You've brought me so much comfort in the tough later

years of my PhD. I loved all the cocktails and coffees we've had talking about this crazy experience we will both have gone through! I can't wait to visit you and Jochem in New Zealand.

A very special thanks to my dear friend Misha. Thank you for taking the effort of carefully reading my scribbles and providing feedback about models and manuscripts. Thank you for listening to my struggles. I've learned a lot from you.

Any PhD in BN would be nowhere without its great support staff. Sacha, thank you for your sincere interest, and always being ready to help out. Suzanne, thank you for taking care of things (probably more than we're aware of) efficiently. Erwin, thank you for all your help with the radio lab. Jérémie, thank you for teaching me the ins and outs of microscopes. Anne, thank you for your help with protein gels and in vitro expression. Esengul, thanks for your advice with cloning. Pawel, thank you for your help with the HPLC and your PCR tricks. Ramon, thanks for always showing a friendly face and helping out in the lab. Thanks to all our secretaries, Jolijn, Dijana, Amanda, Nadine and others for making our lives easier.

BN is truly filled with numerous kind and unique people and I am grateful for all the support I've received from them. Jonás, thanks for showing me your obscenely small toilet. Also, the ppGpp-FtsZ microscopy experiment was fun! Dave the Rave, stay awesome and raving to ABBA. Sam, thanks for sharing your musical talent with me. Anthony, thank you for bringing humour and poetry to BN. I still enjoy your well-crafted emails. Benjamin, thanks for making BN a fitter place. I will not forget those self-defence classes! Dominik, thanks for getting me to run. Paulien, thanks for sharing with me your in vitro experience. Jochem, thanks for the always cheerful, fun talks. Patrick, thanks for your interesting facts and unique humour. Fede, thank you for caring about the social and cultural life in BN. Fayezeh, I don't think I've ever met someone more generous. Thank you for the great dinners and trip together, and instigating me to finish my goals (now done ;)). Hirad, thank you for always being a friendly lab mate. Keep the SAP going. Thanks to the best postdoc-duo ever, Mathijs and Louis. That first office will always be the most awesome ever (including the occasional mandarin choking). Mathijs, Brahms blijft 't beste. Louis, thank you for all the supergezellige baking and cooking moments. A big thanks to the BN babes for those ladies' nights, Mathia, Laura, Lisa, Viktorija and Stefanie.

I'd like to thank Marije for being the driving force behind Casimir, and always bearing the PhD's best interest in mind. Thanks to the Casimir platform, Kirsten, Koen, Gesa, Marcos, Robbie and Guoji, for aspiring to improve the life of PhDs, and for the fun meetings.

A special thanks to Rosemarijn, for her marvellous insights and experience with intervision. Tatiana, Susana, Melika, Vilborg, Sixue, Eduardo, I really enjoyed our meetings.

A dirtynerdy thanks to the splendid little clan of Ali, Rolandje, Jo and Mehr. Can't wait for our next adventure. Sokken sokken sokken sokken sokken!

Merel, I always enjoy our times together. Thank you for sharing those lunches, coffees, yoga sessions and occasional salsa dances.

Jeroen, you are a fabulous friend. Thanks for all the amazing food, booty-shaking salsa and crazy laughs. A big thanks to the whole SoSalsa club, Diego, Chi, Marijn, Rick, Rudy, Diewertje, Madusha, and many others for the great moments we all share when dancing together.

Mariya, my passion for science started with the awesome project I did with you, in which we kicked some ass! Thank you for your guidance before, during and for sure also after my PhD.

Ines, Lise, Dorien, Jolien, it is always great to have the bio-engineering babes together. Thank you for your friendship.

Hannelaure and Gerben, your visits to Delft have been amongst the highlights of my PhD. Thank you for the great moments together.

Lieve Sophie, my oldest, loyal friend. Thank you for always being there.

My cutiepie Benootje! Thank you for those amazing trips, filled with 'lekkar ete' and laughter. No matter the distance, I know I always have my bestie on my side.

My dear mother, we have been through a rollercoaster together over the last few years, yet have come out of it stronger. Thank you for your everlasting care and support, you are my rock. Pap, thank you for all your support. Mauriceke, thank you for being yourself no matter what. Thank you for your (sometimes surprising) wisdom and (never surprising) *mafdoenerij*, both very inspirational. I'm proud to be your little sister.

Mehr'joonam, I am so grateful of your love and support over these years. You bring color and joy to my life. Let's continue to build a home together, whatever exotic destination life brings us next.

Curriculum Vitæ

Nicole Imholz

25-02-1993	Born in Voorburg, The Netherlands.

Education

2004–2010	Secundary education Sint-Albertuscollege Haasrode, Belgium
2010–2015	B. Sc. Bioscience Engineering M. Sc. Biomolecular Engineering and Bionanotechnology KU Leuven Leuven, Belgium
2012–2013	ERASMUS exchange study Universidade Técnica de Lisboa Lisbon, Portugal
2015–2020	Ph. D. Research Department of Bionanoscience, Delft University of Technology Delft, The Netherlands *Thesis:* A quantitative analysis of growth regulation by ppGpp in *E. coli* *Supervisor:* dr. G. Bokinsky *Promotor:* Prof. dr. M. Dogterom *Co-Promotor:* dr. G. Bokinsky

Awards

2015	Best Master's thesis of 2015 Bioscience Engineering VBI, Alumni Association Faculty of Bioscience Engineering

List of Publications

- **Imholz, N. C. E.**, D. Foschepoth, C. Danelon, and G. Bokinsky. "Suprabasal guanosine tetraphosphate (ppGpp) levels reduce translation rates in *E. coli* by inhibiting various targets". In: (2020). *Submitted.*
- **Imholz, N. C. E.**, M. J. Noga, N. J. F. van den Broek, and G. Bokinsky. "Calibrating the bacterial growth rate speedometer: a re-evaluation of the relationship between basal ppGpp, growth, and RNA synthesis in *Escherichia coli*". In: *Frontiers in Microbiology* (2020). doi: 10.3389/fmicb.2020.574872
- M. J. Noga, F. Buke, N. J. F. van den Broek, **N. Imholz**, N. Scherer, F. Yang, and G. Bokinsky. "Posttranslational Control of PlsB Is Sufficient To Coordinate Membrane Synthesis with Growth in *Escherichia coli*". In: *mBio* 11 (4 2020), e02703–19. doi: 10.1128/mBio.02703-19
- M. J. Noga, M. Cerri, **N. Imholz**, P. Tulinski, and G. Bokinsky. "Mass-Spectrometry-Based Quantification of Protein-Bound Fatty Acid Synthesis Intermediates from *Escherichia coli*". In: *Journal of proteome research* 15 (2016), pp. 3617–3623
- S. Malik, M. I. Petrova, **N. C. E. Imholz**, T. L. A. Verhoeven, S. Noppen, E. J. M. Van Damme, S. Liekens, J. Balzarini, D. Schols, J. Vanderleyden, and S. Lebeer. "High mannose-specific lectin Msl mediates key interactions of the vaginal *Lactobacillus plantarum* isolate CMPG5300". In: *Scientific Reports* 6.1 (2016)
- M. I. Petrova, **N. C. E. Imholz**, T. L. A. Verhoeven, J. Balzarini, E. J. M. Van Damme, D. Schols, J. Vanderleyden, and S. Lebeer. "Lectin-Like Molecules of *Lactobacillus rhamnosus* GG Inhibit Pathogenic *Escherichia coli* and *Salmonella* Biofilm Formation". In: *PLOS ONE* 11.8 (2016). doi: 10.1371/journal.pone.0161337
- M. I. Petrova, E. Lievens, S. Malik, **N. Imholz**, and S. Lebeer. "*Lactobacillus* species as biomarkers and agents that can promote various aspects of vaginal health". In: *Frontiers in Physiology* 6 (2015)